

EFFECTS OF METHYLMERCURY IN THE DOPAMINE SYNTHESIZING
PHEOCHROMOCYTOMA PC12 CELL LINE

By

Chelsea Tate Tiernan

A DISSERTATION

Submitted to
Michigan State University
in partial fulfillment of the requirements
for the degree of

Neuroscience – Doctor of Philosophy

2013

ABSTRACT

EFFECTS OF METHYLMERCURY IN THE DOPAMINE SYNTHESIZING PHEOCHROMOCYTOMA PC12 CELL LINE

By

Chelsea Tate Tiernan

Methylmercury (MeHg) is a potent bioaccumulative neurotoxicant that targets discrete neuronal populations, including the nigrostriatal dopamine (NSDA) neuronal system. Epidemiological evidence has implicated chronic exposure to MeHg as an environmental risk factor for Parkinson disease (PD), and experimental analyses using *in vivo* animal and *in vitro* cell culture models have demonstrated that acute exposure to MeHg alters DA homeostasis, including release, reuptake, and metabolism. The purpose of the studies described in this dissertation is to characterize MeHg-induced changes in DA synthesis, release, reuptake, and metabolism, and to investigate mechanisms by which MeHg exerts its neurotoxic effects in the pheochromocytoma (PC12) cell line.

MeHg causes a concentration- and time-dependent increase in DA release. Higher concentrations (5 μ M) are associated with an increased incidence of cell death at later time points (60-120 min). However 2 μ M MeHg induces DA release by 60 min without altering cell viability. Thus this concentration and time-point was selected to examine other indices of DA homeostasis. MeHg-induced DA release is abolished by inhibition of vesicular exocytosis with reserpine, but not inhibition of membrane transport with desipramine. A role for synthesis in MeHg-induced DA release was indicated by an increase in the concentration of intracellular DA and the rate of decline of intracellular DA following acute treatment with the tyrosine hydroxylase (TH) inhibitor α -methyltyrosine (AMT). MeHg stimulates DA synthesis indicated by an increase in DOPA accumulation following

treatment with the DOPA decarboxylase inhibitor NSD-1015. This is supported by the observation that MeHg elevates phosphorylation of TH at serine residue 40, without altering the total amount of TH. Moreover, MeHg-induced DA release is dependent upon DA synthesis because pre-treatment with AMT abolishes MeHg-induced DA release.

MeHg induces aberrant DA metabolism. Intracellular concentrations of DOPAC are decreased, while intracellular concentrations of the intermediate metabolites DOPAL and DOPET are increased. This metabolomic profile suggests that MeHg inhibits the oxidation of DOPAL to DOPAC and thus inhibits aldehyde dehydrogenase (ALDH). MeHg does not directly impair ALDH activity. Instead, inhibition may be indirect because MeHg inhibits mitochondrial respiration and ATP synthesis, and decreases availability of the ALDH cofactor nicotinamide adenine dinucleotide (NAD).

To assess the roles of extracellular and intracellular calcium (Ca^{2+}) in altered DA release and metabolism, undifferentiated PC12 cells were exposed to MeHg in both the absence and presence of extracellular and/or intracellular Ca^{2+} . Removal of intracellular but not extracellular Ca^{2+} attenuates MeHg-induced DA release. MeHg-impaired DA metabolism is not influenced by chelation of either Ca^{2+} source.

The present findings are consistent with the following conclusions: 1) MeHg-induced DA release is dependent upon DA synthesis and vesicular exocytosis, 2) MeHg impairs DA metabolism by indirectly inhibiting ALDH, 3) release of Ca^{2+} from intracellular stores triggers MeHg-induced DA release, and 4) aberrant DA metabolism is not affected by changes in intracellular Ca^{2+} homeostasis.

ACKNOWLEDGEMENTS

Completing this dissertation has been a long, arduous journey, and I would not have succeeded without the love, support, and guidance of many people. First and foremost, I express my deepest gratitude to my advisors Drs. Keith Lookingland and John Goudreau. Keith, thank you for always being optimistic and supportive. Thank you for honing my writing and critical thinking skills, and thank you for fostering my passion to teach. Your dedication to your students is inspirational, and your encouragement over the years has been essential to my success. John, thank you for all of your ideas. Your expertise and advice with writing, networking, brainstorming, and presentations have been invaluable. I also owe an immense debt of gratitude to Dr. William Atchison, committee member and co-investigator. Thank you for providing me with an opportunity to continue my education. Thank you for inspiring me to pursue science outreach and education. And thank you for the many sunny trips to Puerto Rico. Your continued assistance and guidance is inestimable. To my committee members Drs. Kyle Miller and Peter Cobbett, thank for the many meetings, conversations, and assistance. Your presence has enriched my graduate school experience.

A number of faculty members at MSU and my previous academic institutions, Western State Colorado University and Roaring Fork High School, have also provided crucial support for my education. I thank Dr. Lynwood Clemens for allowing me to assist in his Integrative Neurobiology course, and to use that experience as part of my Certification in College Teaching. I thank Dr. Charles Patrick Stark for my first research experience and for encouraging me to attend graduate school. May you find peace in your next adventure. I

thank Mrs. Wendy Boland and Mrs. Laura French who first inspired me to become a life-long learner, recognized my true talents and passions in science, and quietly challenged me to pursue my dreams.

I sincerely thank my fellow GoudLooking laboratory members, past and present. The collaborative, fun, and sometimes shocking environment has been a true pleasure. Special thanks to Dr. Bahareh Behrouz, Dr. Sam Pappas, Dr. Matt Benskey, (almost Dr.) Tyrell Simkins, and Hae-young Hwang. I thank my undergraduate technicians, Ethan Edwin, María Bernard, and Ninotchka Del Valle. Your dedication and hard work has helped make this dissertation a success. I wish you luck in the coming years as you all begin your graduate studies.

I thank my many friends who have been so loving and supportive over the years. However there are two people who I would like to thank especially. Chelsea Hutch, I know there is absolutely no way on Earth I would have made it through this gauntlet without you by my side every step of the way. Thank you for the late night runs to Tasty Twist and the marathons of Dexter. Matt Benskey, it is difficult for me to find words to express my gratitude for your love and encouragement. Without your intellectual and emotional support, I would be lost. Thank you for instilling confidence in me. Thank you for not accepting anything less than the very best from me. And most importantly, thank you for helping me learn how to relax and enjoy a beautiful sunset.

Last, but certainly not least, I would like to thank my amazing, extended, and incredibly understanding family. To my brother Zeke Tiernan, thank you for reminding me what true endurance is. I can't wait to cheer you on during your next 100 miles! To my brother Alex Tiernan, thank you for reminding me that life is for living. Your love and

support has always been one of the greatest blessings in my life. And to my parents Edward Tiernan and Carrie Katsis thank you. Dad, I don't think a father has ever been so proud of his daughter. Your constant love is a treasure I will carry with me always. Thank you for encouraging me to complete this educational endeavor and thank you for taking an active interest in my research. I love you forever, I love you for always, and long as I'm living, your baby I'll be. Mom, thank you for being patient, even when your life was chaotic, and thank you for being understanding, even when my problems were ridiculous. I am eternally grateful for the love and friendship that we share. Thank for being the eccentric, beautiful, and passionate woman you are. To you both, I am so blessed. I can only hope to be the kinds of parents you are some day. Thank you!

TABLE OF CONTENTS

LIST OF TABLES.....xii

LIST OF FIGURES.....xiii

KEY TO ABBREVIATIONS.....xvi

Chapter 1. General Introduction.....1

 1.1. Statement of Purpose.....1

 1.2. Methylmercury.....3

 1.3. Neurotoxicity of MeHg.....6

 1.4. Molecular mechanisms of MeHg-mediated neurotoxicity7

 1.5. Parkinson’s disease.....10

 1.6. Epidemiological evidence of MeHg as an environmental risk factor for PD.....11

 1.7. Dopamine.....13

 1.7.1. DA synthesis.....15

 1.7.2. DA storage.....16

 1.7.3. DA release and activation of DA receptors.....17

 1.7.4. DA reuptake.....17

 1.7.5. DA metabolism.....18

 1.8. Effects of MeHg on DA neuronal homeostasis.....20

 1.8.1. MeHg targeting of DA synthesis.....20

 1.8.2. MeHg targeting of DA release.....21

 1.8.3. MeHg targeting of DA reuptake.....22

 1.8.4. MeHg targeting of DA metabolism.....23

 1.9. Pheochromocytoma 12 (PC12) cell line.....24

 1.9.1. PC12 cell morphology.....25

 1.9.2. PC12 cell neurochemistry.....26

 1.9.3. PC12 cell VGCC subtype expression.....29

 1.9.4. Differences between undifferentiated PC12 cells and DA neurons.....30

 1.9.5. Effects of MeHg in PC12 cells.....31

 1.10. Summary.....32

 1.11. Thesis objective.....33

Chapter 2. General Materials and Methods.....35

 2.1. Culture of PC12 cells.....35

 2.2. Chemicals and solutions.....37

 2.3. Neurochemical analyses.....41

 2.3.1. Calculation of rate constant.....41

 2.3.2. Synthesis of DOPAL standard.....42

 2.4. Cell viability.....46

 2.5. Western blot analysis of TH.....48

 2.6. Mitochondrial bioenergetics.....49

2.6.1. XF24 assay medium.....	49
2.6.2. Test compounds.....	49
2.6.3. Extracellular flux (XF) analysis.....	51
2.6.4. XF bioenergetics assay.....	54
2.6.5. XF24 drug exposure.....	55
2.6.6. XF24 optimization of experimental conditions.....	55
2.7. ALDH enzyme kinetics assay.....	61
2.8. NADH/NAD quantification.....	64
2.9. Measurement of fura-2 fluorescent change.....	66
2.10. Statistical analyses.....	67
Chapter 3. The role of <i>de novo</i> catecholamine synthesis in mediating MeHg-induced vesicular DA release.....	68
3.1. Introduction.....	68
3.2. Methods.....	70
3.2.1. Chemicals.....	70
3.2.2. Chemical treatment.....	70
3.2.3. Neurochemistry.....	70
3.2.4. Western blot analysis.....	71
3.2.5. Cell viability.....	71
3.2.6. Statistical analysis.....	72
3.3. Results.....	72
3.3.1. MeHg increases spontaneous DA release in a concentration- and time-dependent manner.....	72
3.3.2. Spontaneous MeHg-mediated DA release requires a functional vesicular, but not membrane, transporter.....	78
3.3.3. MeHg-mediated DA release is associated with increased intracellular DA concentrations and utilization of DA stores.....	80
3.3.4. MeHg-mediated DA release is associated with <i>de novo</i> DA synthesis and increased TH enzymatic activity.....	83
3.4. Discussion.....	87
3.4.1. MeHg-induced DA release.....	87
3.4.2. Vesicular transport, but not membrane transport contributes to MeHg-induced DA release.....	88
3.4.3. Evidence for a role of <i>de novo</i> DA synthesis in MeHg-induced DA release.....	90
Chapter 4. The roles of mitochondria and associated catabolic enzyme function in MeHg-impaired DA metabolism.....	92
4.1. Introduction.....	92
4.2. Methods.....	97
4.2.1. Chemicals.....	97
4.2.2. Chemical treatment.....	97
4.2.3. Neurochemistry.....	97
4.2.4. ALDH2 enzyme kinetics assay.....	98
4.2.5. Mitochondrial bioenergetics.....	98

4.2.6. NADH/NAD quantification.....	99
4.2.7 Statistical analysis.....	99
4.3. Results.....	100
4.3.1. MeHg impairs DA metabolism, shunting DA along an alternative metabolic pathway.....	100
4.3.2. Selective inhibition of ALDH with daidzin impairs DA metabolism in a manner similar to MeHg.....	105
4.3.3. Daidzin and rotenone impair DA metabolism in a manner that resembles MeHg.....	108
4.3.4. ALDH activity is not directly altered by MeHg.....	110
4.3.5. MeHg impairs mitochondrial function and decreases availability of the ALDH cofactor NAD.....	113
4.4. Discussion.....	119
4.4.1. The DA metabolomic profile induced by MeHg.....	119
4.4.2. Comparative effects of MeHg, daidzin, and rotenone on DA metabolism.....	121
4.4.3. Evidence for a role of mitochondrial dysfunction rather than direct ALDH inhibition in MeHg-impaired DA metabolism.....	122
4.4.4. Consequences of decreased NAD(H) following MeHg exposure.....	124
4.4.5. Potential biological effects of MeHg-impaired DA metabolism.....	126
4.4.6. Summary.....	127

Chapter 5. The role of extracellular Ca²⁺ in MeHg-induced alterations in DA release and metabolism.....	129
5.1. Introduction.....	129
5.1.1. Neurotransmitter release and VGCCs.....	129
5.1.2. Mitochondrial function and DA metabolism.....	131
5.2. Methods.....	133
5.2.1. Chemicals.....	133
5.2.2. Chemical treatment.....	134
5.2.3. Neurochemistry.....	134
5.2.4. Mitochondrial bioenergetics.....	134
5.2.5. Statistical analysis.....	135
5.3. Results.....	135
5.3.1. Spontaneous MeHg-mediated DA release is partially dependent upon the presence of extracellular Ca ²⁺ , but not Ca ²⁺ influx through VGCCs.....	135
5.3.2. Extracellular Ca ²⁺ stimulates mitochondrial bioenergetics, but does not contribute to MeHg-induced mitochondrial dysfunction or aberrant DA metabolism.....	140
5.4. Discussion.....	146
5.4.1. Role of extracellular Ca ²⁺ in spontaneous and MeHg-mediated DA release.....	147
5.4.2. Role of VGCCs in spontaneous and MeHg-mediated DA release.....	148

5.4.3. Role of extracellular Ca ²⁺ in mitochondrial bioenergetics and targeting by MeHg.....	149
5.4.4. Role of extracellular Ca ²⁺ in basal and MeHg-impaired DA metabolism.....	152
5.4.5. Summary.....	143

Chapter 6. The role of intracellular Ca²⁺ in MeHg-induced alterations in DA release and metabolism.....

6.1. Introduction.....	154
6.1.1. Regulation of intracellular Ca ²⁺	154
6.1.2. Effects of MeHg on intracellular Ca ²⁺ homeostasis.....	156
6.1.3. Effects of MeHg on DA release and metabolism.....	157
6.2. Methods.....	158
6.2.1. Chemicals.....	158
6.2.2. Treatment for neurochemistry and mitochondrial bioenergetics.....	158
6.2.3. Neurochemistry.....	159
6.2.4. Mitochondrial bioenergetics.....	159
6.2.5. Measurement of fura-2 fluorescent change.....	160
6.2.6. Statistical analysis.....	160
6.3. Results.....	160
6.3.1. MeHg-induced DA release is dependent upon the presence of intracellular Ca ²⁺	160
6.3.2. Intracellular Ca ²⁺ is essential for the maintenance of mitochondrial bioenergetics.....	166
6.3.3. Aberrant DA metabolism induced by MeHg is not dependent upon intracellular Ca ²⁺	170
6.4. Discussion.....	172
6.4.1. Role of intracellular Ca ²⁺ in spontaneous and MeHg-mediated DA release.....	172
6.4.2. Role of intracellular Ca ²⁺ in mitochondrial bioenergetics.....	175
6.4.3. Role of intracellular Ca ²⁺ in basal and MeHg-impaired DA metabolism.....	176
6.4.4. Summary.....	178

Chapter 7. General Discussion and Concluding Remarks.....

7.1. Role of Ca ²⁺ in MeHg-induced activation of DA synthesis.....	179
7.2. Role of Ca ²⁺ in MeHg-induced vesicular exocytosis.....	181
7.3. Collaborative relationship between extracellular and intracellular Ca ²⁺ pools.....	182
7.4. Aberrant DA metabolism induced by MeHg.....	185
7.5. Pathways by which MeHg targets DA neurons.....	188

7.6. Factors influencing sensitivity of DA-synthesizing cells to MeHg.....	191
7.7. Biological and clinical relevance to PD.....	193
7.8. Concluding Remarks.....	197
REFERENCES.....	198

LIST OF TABLES

Table 1.1. Catecholaminergic and cholinergic neurotransmitter content and enzyme activity in undifferentiated and differentiated PC12 cells28

Table 2.1. Summary of drug actions.....40

Table 2.2. Dilutions of test compounds for XF24 measurements of mitochondrial bioenergetics.....50

LIST OF FIGURES

Figure 1.1. Global mercury (Hg) cycle.....	5
Figure 1.2. The molecular structure of dopamine (3-hydroxytyramine).....	14
Figure 1.3. DA synthesis, release, and metabolism.....	19
Figure 2.1. Representative brightfield images of pheochromocytoma (PC12) cells in culture (passage 16)	36
Figure 2.2. High performance liquid chromatography (HPLC) chromatographs.....	44
Figure 2.3. Synthesis of DOPAL standard.....	45
Figure 2.4. Hoechst/ propidium iodide fluorescent stain for cell viability in PC12 cells.....	47
Figure 2.5. Mitochondrial Stress Test using the XF24 Analyzer	53
Figure 2.6. XF24 cell density optimization.....	58
Figure 2.7. XF24 assay medium optimization.....	59
Figure 2.8. XF24 FCCP titration.....	60
Figure 2.9. ALDH assay substrate optimization.....	63
Figure 2.10. Sample volume titration for NADH/NAD quantification.....	65
Figure 3.1. Concentration-response and time-course effects of MeHg on extracellular DA concentrations.....	74
Figure 3.2. Concentration-response and time-course effects of MeHg on cell viability.....	75
Figure 3.3. Representative images of cell viability	76
Figure 3.4. Effects of DA storage depletion and reuptake transporter inhibition on MeHg-induced DA release.....	79
Figure 3.5. Effect of MeHg on intracellular DA concentrations.....	81
Figure 3.6. Effect of MeHg on DA storage utilization.....	82
Figure 3.7. Effect of TH inhibition on MeHg-induced DA release.....	84

Figure 3.8. Effect of DOPA decarboxylase inhibition on TH enzymatic activity.....	85
Figure 3.9. Effect of MeHg on TH expression.....	86
Figure 4.1. Diagram depicting DA metabolic pathways.....	96
Figure 4.2. MeHg shunts DA metabolism along the reductive metabolic pathway.....	102
Figure 4.3. Percentage changes in the relative amounts of DA metabolites induced by MeHg.....	104
Figure 4.4. Concentration-response effects of the ALDH inhibitor daidzin on concentrations of intracellular metabolites.	106
Figure 4.5. Time-course effects of the ALDH inhibitor daidzin on concentrations of intracellular metabolites.....	107
Figure 4.6. Comparative effects of MeHg, daidzin, and rotenone on concentrations of intracellular metabolites.....	109
Figure 4.7. Comparative effects of MeHg, daidzin, and rotenone on ALDH activity.....	111
Figure 4.8. Concentration-response effects of MeHg on ALDH activity <i>ex vitro</i>	112
Figure 4.9. Comparative effects of MeHg, daidzin, and rotenone on mitochondrial bioenergetics.....	114
Figure 4.10. Quantification of changes in mitochondrial bioenergetics induced by MeHg, daidzin, or rotenone	115
Figure 4.11. Effect of MeHg on the production of NAD(H).....	117
Figure 5.1. Extracellular Ca ²⁺ does not contribute to MeHg-induced DA release.....	137
Figure 5.2. Spontaneous activation of VGCCs does not contribute to MeHg-induced DA release.....	139
Figure 5.3. Changes in mitochondrial bioenergetics induced by MeHg in the absence or presence of extracellular Ca ²⁺	142
Figure 5.4. Quantification of changes in mitochondrial bioenergetics induced by MeHg in the absence or presence of extracellular Ca ²⁺	143

Figure 5.5. Effect of MeHg in the absence or presence of extracellular Ca^{2+} on concentrations of intracellular metabolites.	145
Figure 6.1. Intracellular Ca^{2+} partially contributes to MeHg-induced DA release.....	163
Figure 6.2. Representative traces showing changes in the ratio of fura-2 intensity.....	165
Figure 6.3. Changes in mitochondrial bioenergetics induced by MeHg in absence or presence of either intracellular or extracellular Ca^{2+}	167
Figure 6.4. Quantification of changes in mitochondrial bioenergetics induced by MeHg in absence or presence of either intracellular or extracellular Ca^{2+}	168
Figure 6.5. Effect of MeHg in the absence or presence of intracellular and/or extracellular Ca^{2+} on intracellular concentrations of DOPAC and DOPET.....	171
Figure 7.1. Proposed model identifying molecular targets of MeHg toxicity in DA-synthesizing cells.	190

KEY TO ABBREVIATIONS

0-Ca ²⁺ HBS	Calcium-free HEPES-buffered saline
ACh	Acetylcholine
ALDH	Aldehyde dehydrogenase
AMT	α -methyltyrosine
AR	Aldehyde/ aldose reductase
ATP	Adenosine triphosphate
Ca ²⁺	Calcium
CaM-MPK	Ca ²⁺ /calmodulin-dependent multiprotein kinase
CAT	Choline acetyltransferase
DA	Dopamine
DAT	Dopamine transporter
D β H	Dopamine beta-hydroxylase
DDC	DOPA decarboxylase
DMI	Desipramine
DOPA	3,4-dihydroxyphenylalanine
DOPAC	3,4-dihydroxyphenylacetic acid
DOPAL	3,4-dihydroxyphenylacetaldehyde
DOPET	3,4-dihydroxyphenylethanol
ETC	Electron transport chain
FCCP	Carbonyl cyanide 4-(trifluoromethoxy)phenylhydrazone
HEPES	4-(2-hydroxyethyl)-1-piperazineethanesulfonic acid

HBS	HEPES-buffered saline
Hg	Mercury
IP ₃	Inositol 1,4,5-triphosphate
MAO	Monoamine oxidase
MeHg	Methylmercury
NAD	Nicotinamide adenine dinucleotide, oxidized
NADH	Nicotinamide adenine dinucleotide, reduced
NE	Norepinephrine
NET	Norepinephrine transporter
NSDA	Nigrostriatal dopamine
O ₂	Oxygen
OCR	Oxygen consumption rate
PCB	Polychlorinated biphenyl
PD	Parkinson disease
PKC	Ca ²⁺ /phospholipid-dependent protein kinase
pTH Ser40	Phosphorylated tyrosine hydroxylase at serine 40
ROS	Reactive oxygen species
SER	Smooth endoplasmic reticulum
TH	Tyrosine hydroxylase
VGCC	Voltage-gated calcium channel
VMAT	Vesicular monoamine transporter
XF	Extracellular flux

Chapter 1. General Introduction

1.1. Statement of Purpose

Methylmercury (MeHg) is a potent, bioaccumulative neurotoxicant linked to severe neurological dysfunction in humans. Discrete neuronal populations are selectively susceptible to the neurotoxic effects of MeHg, including the nigrostriatal dopamine (NSDA) pathway. Degeneration of NSDA neurons contributes to the onset of Parkinson disease (PD). Epidemiological evidence suggests that prolonged exposure to MeHg in human populations that consume large amounts of MeHg-contaminated marine food increases the incidence of PD. Furthermore, *in vitro* analyses and animals studies have concluded that MeHg alters DA neuronal homeostasis and induces selective DA cytotoxicity.

While it is clear that MeHg impairs DA neuronal function, the mechanisms by which MeHg targets processes in DA-synthesizing cells including synthesis, release, and metabolism remain unclear. Because MeHg cytotoxicity is generally associated with perturbation of intracellular calcium (Ca^{2+}) homeostasis and mitochondrial dysfunction, experiments were performed to identify the contributions of these molecular mechanisms to altered DA homeostasis using DA-synthesizing pheochromocytoma 12 (PC12) cells.

The overall aim of the research described in this dissertation is two-fold: 1) to characterize MeHg-induced changes in DA synthesis, release and metabolism in undifferentiated PC12 cells, and 2) examine the contributions of Ca^{2+} and mitochondrial dysfunction to these changes. The underlying hypothesis of these studies is that MeHg-induced increase in intracellular Ca^{2+} mediates changes in DA synthesis and release,

whereas MeHg-induced mitochondrial dysfunction mediates changes in DA metabolism. Evaluation of this hypothesis will elucidate mechanisms by which MeHg targets processes intrinsic to DA neurons thereby predisposing them to degeneration. These studies will provide a platform to develop novel targets of neuroprotective therapies for treating MeHg intoxication and PD.

1.2. Methylmercury

Methylmercury (MeHg) is composed of a methyl group (CH₃) bonded to a mercuric ion (Hg²⁺), which produces a monovalent charged cation with enhanced lipophilicity. It is produced from elemental mercury through both natural and industrial processes (Figure 1.1; Bhan and Sarkar, 2005). Mercury is released naturally during degassing of the Earth's crust, volcano emissions, and soil erosion. Human sources of elemental mercury include coal-burning, waste combustion, mercury mining, and mercury-containing fungicide use. Once released, mercury resides in the atmosphere as a vapor, where it is slowly oxidized to inorganic mercury by ozone (Morel et al., 1998). This more water-soluble form of mercury is deposited on the Earth's surface by rainwater and filters into aquatic ecosystems. The majority of oxidized mercury is reduced back to the vapor state and returns to the atmosphere, but aquatic microorganisms methylate a portion of inorganic mercurous salts to form MeHg (Clarkson, 1998).

MeHg *biomagnifies* in aquatic food chains, meaning that the concentration increases in aquatic organisms of each successive trophic level (i.e. increasing concentrations from algae, to zooplankton, to forager fish, to predatory marine animals). Additionally, aquatic animals accumulate and retain MeHg in their bodies, through a process called *bioaccumulation*. As a result of these two factors, MeHg reaches high concentrations in upper trophic level marine animals, such as shark, pilot whale, swordfish, and albacore tuna (WHO, 1990).

Marine predators are a component of the human diet, and in some cases provide the primary source of protein, vitamins, and minerals. As such, government agencies are

concerned about the potential public health risk associated with consumption of MeHg-contaminated marine food. For example, the Environmental Protection Agency (EPA) estimates the average MeHg concentration in marine animals consumed by adults in the general U.S. population is 157 $\mu\text{g}/\text{kg}$ (EPA, 2001). The oral reference dose, or the maximum acceptable oral dose, for MeHg is 0.1 $\mu\text{g}/\text{kg}/\text{day}$ (EPA, 2001). Therefore the consumption of 200 g (7oz.) of fish containing 157 $\mu\text{g}/\text{kg}$ MeHg would result in the intake of 31.4 μg MeHg, a concentration well above the recommended daily reference dose. Although studies investigating the adverse consequences of fish-consumption in adult populations have produced largely negative results (Haxton et al., 1979; Turner et al., 1980; Valciukas et al., 1986; Weil et al., 2005), there is concern about chronic, low-concentration consumption (WHO, 1990), as MeHg is known to produce severe neurotoxic effects in humans. Additionally, the issue of superimposition of MeHg-induced neurodegeneration as a function of age is a concern (Weiss et al., 2002; Landrigan et al., 2005; Monnet-Tschudi et al., 2006).

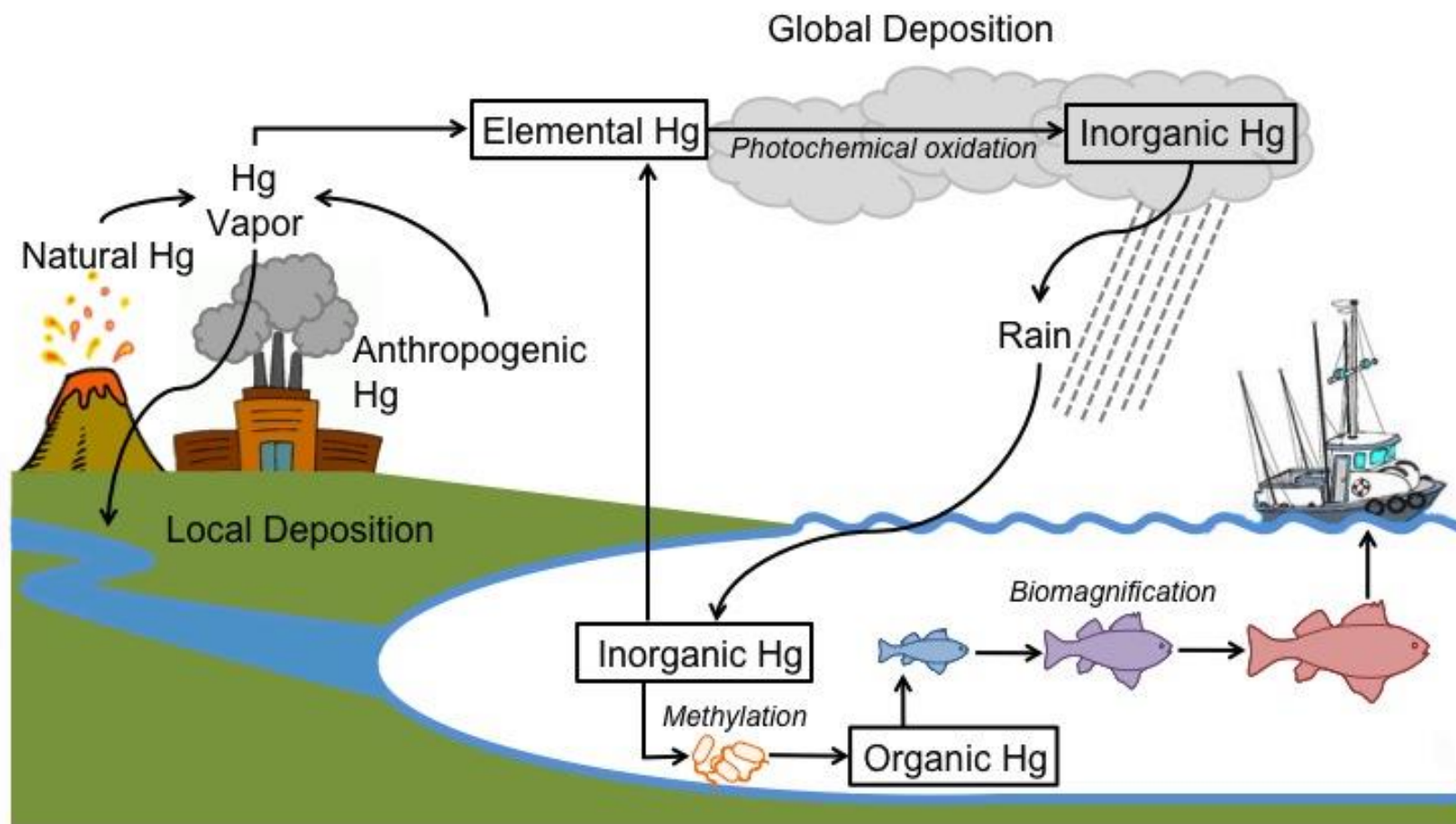


Figure 1.1. Global mercury (Hg) cycle. Hg is released from both natural and anthropogenic sources and for the most part enters the atmosphere as a vapor in its elemental state. It is oxidized to a more soluble inorganic form and deposited by rainwater into aquatic ecosystems. Here inorganic Hg can be methylated by microorganisms to form organic Hg, including MeHg. Due to its lipophilicity, organic Hg biomagnifies in aquatic food chains, reaching high concentrations in large predatory fish that are consumed by humans. For interpretation of the references to color in this and all other figures, the reader is referred to the electronic version of this dissertation. (Adapted from Tewalt et al., 2001)

1.3. Neurotoxicity of MeHg

MeHg pollution and consequent human intoxication was first documented in Minamata Bay in Kumamoto Prefecture, Japan between 1953-1956 (Takeuchi et al., 1962). Two additional large-scale outbreaks occurred in Niigata, Japan in the mid 1960's (Eto, 1997) and Iraq during the early 1970's (Bakir et al., 1973). Several other isolated incidences of MeHg intoxication have also been documented in the last half century (Hunter et al., 1940; Hunter and Russell, 1954; Davis et al., 1994; Nierenberg et al., 1998). Despite differences in source, concentration, and duration of exposure, signs and symptoms of MeHg intoxication and targeted brain regions were similar in all cases.

Primary signs of MeHg exposure are neurological dysfunctions characterized by ataxia, paresthesia, auditory and visual deficits, and dysarthria (Hunter et al., 1940; Amin-Zaki et al., 1978; Fukuda et al., 1999). Autopsies of brains of affected individuals show a unique and characteristic distribution of pathological features that correlate with clinical signs. In the cerebral cortex, lesions are found in the calcarine cortex of the occipital lobe, primarily along the calcarine fissure (Hunter and Russell, 1954; Takeuchi et al., 1962). Less severe lesions have also been observed in the precentral, postcentral, and temporal cortices (Eto, 1997). In the cerebellum, lesions appear deeper in the hemispheres (Hunter and Russell, 1954). The cerebellar granule cell population is most affected, while the adjacent Purkinje cells are relatively spared (Takeuchi et al., 1962).

The basis of selective sensitivity of certain neuronal cell populations to MeHg toxicity is not well understood, and very few comparative analyses have investigated this differential susceptibility. Perhaps the most well studied populations have been the cerebellar granule and adjacent Purkinje cells. As compared to Purkinje cells, granule cells

may be more susceptible to MeHg because of an inability to regulate intracellular divalent cations (Edwards et al., 2005). The resistance observed in Purkinje cells could be due to the expression of the Ca²⁺-binding protein, calbindin D28K (Kadowaki et al., 1993; Amenta et al., 1994), or possibly the differential expression of voltage-gated Ca²⁺ channel (VGCC) subtypes (Hillman et al., 1991; Randall and Tsien, 1995; Tanaka et al., 1995).

1.4. Molecular mechanisms of MeHg-mediated neurotoxicity

Cytotoxicity following MeHg exposure can occur by either apoptosis or necrosis (Kunimoto, 1994; Castoldi et al., 2000). The intensity of the insult is the critical factor in the time-to-onset and the mode of cell death initiated. High concentrations of MeHg (5-10µM) induce immediate necrotic death, whereas low concentrations (≤2.5µM) cause delayed apoptosis (Castoldi et al., 2000). Primary molecular mechanisms responsible for MeHg-induced cytotoxicity are still unclear, however disrupted intracellular calcium (Ca²⁺) homeostasis, impaired mitochondrial function, and inhibition of protein function due the toxicant's affinity for sulfhydryl groups have all been implicated (Atchison and Hare, 1994; Castoldi et al., 2001; Sanfeliu et al., 2003).

MeHg increases intracellular Ca²⁺ concentrations in several neuronal cell types, including cerebellar neurons (Sarafian, 1993; Marty and Atchison, 1997; Edwards et al., 2005), immature primary neuronal cultures (Mundy and Freudenrich, 2000), and immortalized neuroblastoma cells (Hare et al., 1993; Hare and Atchison, 1995a). The rise in intracellular Ca²⁺ proceeds in a biphasic manner with temporally and kinetically distinct

phases (Denny et al., 1993; Marty and Atchison, 1997). First, Ca^{2+} is mobilized from intracellular stores, including the smooth endoplasmic reticulum (SER) and mitochondria. MeHg induces an initial release of Ca^{2+} from an inositol 1,4,5-triphosphate (IP_3)-sensitive pool in the SER, which is buffered by the mitochondria, only to be released again after opening of the mitochondrial permeability transition pore (Hare and Atchison, 1995a; Limke and Atchison, 2002; Limke et al., 2003). During the second phase, extracellular Ca^{2+} enters the cell. This phase is mediated in part by VGCCs, as inhibition of these channels delays the onset of the second phase (Marty and Atchison, 1997). Elevated intracellular Ca^{2+} is thought to contribute to MeHg-mediated cell death because buffering intracellular Ca^{2+} with chelators or treatment with VGCC blockers attenuates MeHg-induced cell death in cerebellar granule cells (Marty and Atchison, 1998). Furthermore, VGCC block with the L-type VGCC antagonist flunarizine prevents the appearance of neurological signs in rats treated with MeHg (Sakamoto et al., 1996).

MeHg accumulates in mitochondria (Yoshino et al., 1966; Sone et al., 1977) leading to a variety of detrimental effects, including inhibition of mitochondrial respiration and adenosine triphosphate (ATP) production (Sone et al., 1977; Levesque and Atchison, 1991), generation of reactive oxygen species (ROS) (LeBel et al., 1990; Yee and Choi, 1994; Dreiem and Seegal, 2007), and dysregulation of mitochondrial Ca^{2+} buffering (Levesque and Atchison, 1991; Dreiem and Seegal, 2007). Mitochondrial Ca^{2+} dysregulation is likely related to MeHg-induced collapse of the mitochondrial membrane potential (Bondy and McKee, 1991; Levesque and Atchison, 1991; Hare and Atchison, 1992; Dreiem et al., 2005).

This mitochondrial membrane depolarization results in inhibition of Ca^{2+} uptake by and induction of Ca^{2+} efflux from the mitochondria (Levesque and Atchison, 1991; Limke et al., 2003), ultimately contributing to the accumulation of Ca^{2+} in the cytoplasm. Inhibition of mitochondrial respiration by MeHg is due to direct interaction with respiratory enzyme complexes (Sone et al., 1977; Yee and Choi, 1996; Mori et al., 2011). This is thought to contribute to oxidative damage because ROS formation increases after direct stimulation of the ubiquinol:cytochrome c oxidoreductase complex (Complex III) of the electron transport chain (ETC) (Yee and Choi, 1996). Furthermore, MeHg-induced inhibition of the mitochondrial ETC and generation of ROS precipitates apoptosis by releasing cytochrome c into the cytoplasm (Mori et al., 2011) that initiates the apoptotic cell death cascade (Cai et al., 1998).

MeHg has a high affinity for thiol groups (Hughes, 1957; Sanfeliu et al., 2003). As a result, proteins containing cysteine or methionine residues are acutely susceptible to structural and functional modifications by MeHg. Indeed, MeHg inhibition of PKC *in vitro* is mimicked by other sulfhydryl blocking agents, including 5,5'-dithiobis-2-nitrobenzoic acid and *N*-ethylmaleimide (Inoue et al., 1988). Furthermore, it is hypothesized that the affinity of MeHg for sulfhydryl groups contributes to oxidative stress provoked by mitochondrial ROS formation. MeHg depletes glutathione (Yee and Choi, 1996; Gatti et al., 2004; Cuello et al., 2010) and reduces the activity of glutathione reductase and glutathione peroxidase (Franco et al., 2009; Cuello et al., 2010), likely by binding thiol groups present in the active sites of these enzymes. The concomitant rise in ROS following MeHg exposure would result in exacerbated oxidative stress and cell death.

Because MeHg targets multiple brain regions and many cellular functions, it has been hypothesized that progressive damage, throughout one's lifetime, contributes to the development of certain neurodegenerative diseases later in life (Monnet-Tschudi et al., 2006). In diseases associated with aging, such as Parkinson disease (PD), the rate of cell loss normally occurring during aging might be accelerated by chronic, low-level exposure to neurotoxicants (Weiss et al., 2002; Weiss, 2011).

1.5. Parkinson's disease

PD is a progressive neurodegenerative disorder affecting more than 850,000 people in the United States alone (Fahn, 2003; Landrigan et al., 2005). Clinical presentation is classically characterized by debilitating motor signs, including resting tremor, rigidity, bradykinesia, and postural instability (Dauer and Przedborski, 2003). The severity of motor symptoms is due to the progressive loss of nigrostriatal dopamine (NSDA) neurons (Fahn, 2003), which originate in the substantia nigra and project to the striatum.

Mechanisms of NSDA neuronal loss are multi-factorial, involving both genetic and environmental risk factors (Di Monte, 2003). In the past two decades, genetic approaches to studying neurodegenerative diseases have resulted in the discovery of 28 distinct chromosomal regions associated with PD (Klein and Westenberger, 2012). Most notably, these include the regions that contain the genes that encode α -synuclein, leucine-rich repeat kinase 2, parkin, and DJ-1. Mutations in these genes have been linked to heritable, monogenetic forms of PD. However, these familial cases account for only about 10% of all PD cases (Thomas and Beal, 2007). Most patients are diagnosed with sporadic PD, for which causes are multifaceted and relatively unknown.

The search for environmental factors that contribute to PD has been more difficult. Toxicant exposure can occur well before clinical manifestation, resulting in a “silent latent period” that can remain undetected for years (Weiss et al., 2002; Landrigan et al., 2005), and reduce the number of neurons below those needed to sustain function in the face of normal aging (Weiss et al., 2002; Landrigan et al., 2005). A more complete understanding of how exposure to particular harmful agents impacts the pathogenesis of PD has far-reaching implications, including determination of gene-environment interactions, as well as the identification of at-risk populations and the development of preventative therapeutic strategies for treatment in these populations.

1.6. Epidemiological evidence of MeHg as an environmental risk factor for PD

In the mammalian central nervous system, MeHg accumulates mainly in the cortex, striatum, cerebellum, brain stem, and spinal cord (Møller-Madsen, 1994). Accumulation in the striatum might impair proper basal ganglia function necessary to modulate voluntary movement, and contribute to the presentation of motor signs associated with MeHg intoxication. Additionally, this pattern of accumulation suggests that MeHg exposure plays a pathogenic role in the onset of PD (Monnet-Tschudi et al., 2006).

A number of epidemiological studies have been carried out to investigate the relationship between MeHg content and the prevalence of PD. The most well studied population resides in the Faroe Islands, an archipelago in the northern Atlantic Ocean. The Inuit population in the Faroe Islands is stable, demarcated, ethnically homogenous, and geographically isolated, making it well suited for epidemiological studies. Estimated age-adjusted prevalence of idiopathic PD on the Faroe Islands is approximately 183.3 per

100,000, which is two-fold higher than that in the island of Als, Denmark or Rogaland, Norway, two geographically proximal locations (Wermuth et al., 1997; 2000; 2008).

Genetic mutations are thought to play only a minimal role in the higher prevalence of PD in the Faroe Islands. Of the 100 Faroes patients diagnosed with PD in 2008, only six were diagnosed before the age of 50 (Wermuth et al., 2008). Additionally, only 33% of Faroese patients with PD reported other family members with symptoms of PD or parkinsonism (Wermuth et al., 2008). These statistics suggest that the majority of PD cases in the Faroe Islands are idiopathic. Given the geographical isolation on the islands, it is also plausible that a predisposition to PD could be due to mutations of relevant genes.

Mutations in two genes that encode proteins associated with biochemical defense against peroxidation (Collins and Neafsey, 2002), human hemochromatosis gene (HFE; Milman et al., 2005) and the cytochrome P450 gene, CYP2D6 (Halling et al., 2005), occur more frequently in Faroese than other Caucasian populations. However evidence suggests there is no association between mutations in these genes and PD (Halling et al., 2008).

The higher prevalence of PD in the Faroe Islands has been associated with chronic, lifetime exposure to neurotoxic contaminants present in pilot whale meat and blubber (Petersen et al., 2008a), including both MeHg and polychlorinated biphenyls (PCBs). Based on this epidemiological analysis it is impossible to discern individual contributions of each of these neurotoxicants. Both MeHg and PCBs affect DA function (Minnema et al., 1989; Kalisch and Racz, 1996; Choksi et al., 1997; Mariussen and Fonnum, 2001; Faro et al., 2002), and there is some evidence to suggest that the contaminants may act in synergy to increase the risk for PD (Bemis and Seegal, 1999). However, a case-control study in Singapore indicates a specific dose-response relationship between blood mercury levels

and idiopathic PD (Ngim and Devathasan, 1989), suggesting that MeHg may be capable of contributing to the etiology of PD independently of other neurotoxic contaminants, such as PCBs.

Regardless of whether MeHg acts alone or in concert with other chemicals to contribute to the development of PD, in order to understand the synergy of multiple neurotoxicants it is necessary to elucidate more completely how each targets specific neuronal processes individually. Hence, further efforts are needed to elucidate the role of MeHg toxicity in NSDA neuronal loss. To this end, research aimed at investigating mechanisms by which MeHg selectively targets processes within DA neurons (i.e. synthesis, release, reuptake, and metabolism) would contribute to an understanding of how MeHg exposure contributes to the etiology of PD.

1.7. Dopamine

DA (3-hydroxytyramine; Figure 1.2) is a catecholamine neurotransmitter synthesized from the dietary amino acid tyrosine. Populations of DA cell bodies originate in discrete cell groups in the olfactory bulb, diencephalon, and mesencephalon, with axons projecting throughout the cortex, striatum, nucleus accumbens, hypothalamus and spinal cord (Björklund and Dunnett, 2007). DA plays roles in many important physiological processes including reward, cognition, movement, pain modulation, and hormone secretion (Graybiel, 1990; Le Moal and Simon, 1991; Spanagel and Weiss, 1999; Lookingland and Moore, 2005; Pappas et al., 2011), as well as serving as the precursor for another brain catecholamine, norepinephrine (NE; Hornykiewicz, 1966).

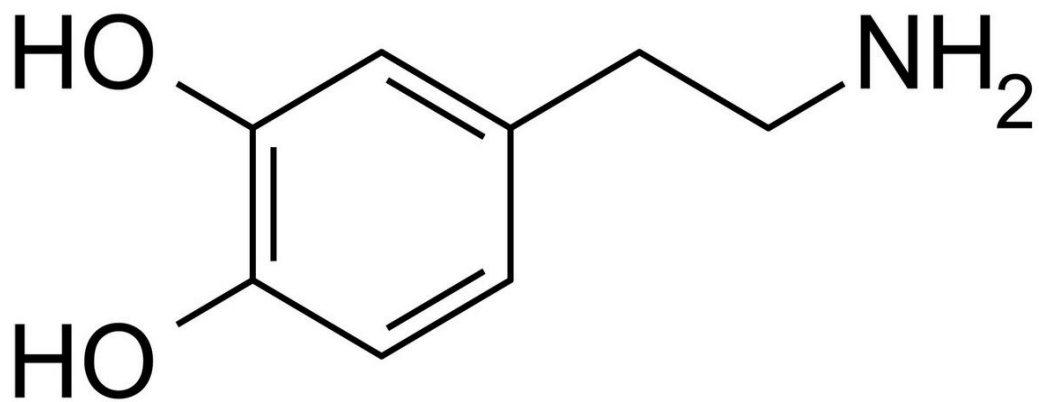


Figure 1.2. The molecular structure of dopamine (3-hydroxytyramine).

1.7.1. DA synthesis

The maintenance of DA homeostasis in the axon terminal, including synthesis, storage, release, reuptake and metabolism, is depicted in Figure 1.3. DA is synthesized from the dietary amino acid tyrosine, which is transported into the cell by the L-neutral amino acid transporter (Oxender and Christensen, 1963). The rate-limiting enzyme in DA synthesis, tyrosine hydroxylase (TH), converts tyrosine to 3,4-dihydroxyphenylalanine (DOPA; Levitt et al., 1965). Under physiological conditions, DOPA is not detectable in the neuron due to the high affinity and action of DOPA decarboxylase (DDC) that rapidly converts DOPA to DA (Blaschko, 1942).

Short-term regulation of DA synthesis is accomplished by changes in the phosphorylation state of TH (Kumer and Vrana, 1996). Phosphorylation of critical serine (Ser) residues (Ser19, -31, and -40) located on the N-terminus of the enzyme increase enzyme efficiency (Haycock, 1990; Daubner et al., 2011). The most important mechanism of TH activation is phosphorylation at Ser40, which decreases end-product feedback inhibition (Daubner et al., 1992; Ribeiro et al., 1992; Ramsey and Fitzpatrick, 1998). Phosphorylation of Ser19 and -31 have modest direct effects on TH activity, but increase the rate of Ser40 phosphorylation, thereby indirectly potentiating TH activity (Bevilaqua, 2001; Lehmann et al., 2006). A number of Ca^{2+} -dependent pathways mediate TH phosphorylation including Ca^{2+} /phospholipid-dependent protein kinase (PKC; Albert et al., 1984; Vulliet et al., 1985) and Ca^{2+} /calmodulin-dependent multiprotein kinase (CaM-MPK; Yamauchi and Fujisawa, 1981; Vulliet et al., 1984).

Dephosphorylation of TH is accomplished by two protein phosphatases (PP), 2A and 2C (Dunkley et al., 2004), both of which are capable of acting at Ser40 (Haavik et al., 1989; Bevilaqua et al., 2003). Studies have only begun to elucidate regulation of these phosphatases and mechanisms by which they dephosphorylate TH. Under physiological conditions, PP2A accounts for ~90% of TH phosphatase activity in rabbit corpus striatum (Haavik et al., 1989), and PP2C activity is approximately one third of this activity (Bevilaqua et al., 2003). However certain physiological conditions may favor PP2C activity, for example high Mg^{2+} levels (Bevilaqua et al., 2003). Chaperone proteins may also regulate PP2A and PP2C activity. The active form of PP2A requires the co-localization of three subunits, and chaperone proteins play a pivotal role in the formation of the active PP2A heterotrimer (Dobrowsky et al., 1993). One potential chaperone protein is α -synuclein, which shares physical and functional homology with the 14-3-3 family of cytosolic chaperones (Ostrerova et al., 1999). Studies indicate that α -synuclein overexpression in both MN9D and PC12 cells decreased pTH Ser40 phosphorylation by increasing PP2A activity (Peng, 2005).

1.7.2. DA storage

The majority of newly synthesized DA is packaged into synaptic vesicles by the vesicular monoamine transporter (VMAT) (Erickson et al., 1992). DA packaging requires energy to store a large amount of neurotransmitter in a small vesicular space at a high concentration. VMAT relies upon the pH and electrochemical gradient generated by a vesicular H^+/K^+ -ATPase. ATP is used to sequester protons creating a low intravesicular pH

under physiological conditions (Rudnick, 1998). As a result, VMAT can couple DA uptake to the release of protons down their chemiosmotic pH gradient (Johnson and Scarpa, 1979).

1.7.3. DA release and activation of DA receptors

Action potential-induced depolarization of the axon terminal causes DA to be released from the synapse via Ca^{2+} -dependent vesicular exocytosis (Rubin, 1970; Leslie et al., 1985). Released DA can bind either pre- or post-synaptic DA receptors. DA receptors are G-protein coupled receptors categorized as D1- or D2-like (Missale et al., 1998). D1-like receptors are present on the post-synaptic membrane, and elicit an excitatory response by stimulating adenylate cyclase (Monsma et al., 1990). Conversely, D2-like receptors have an inhibitory effect on adenylate cyclase (Onali et al., 1985). They are present pre- and post-synaptically, where they inhibit DA synthesis through end-product feedback inhibition (Nowycky and Roth, 1978), or modulate the excitability of post-synaptic neurons, respectively.

1.7.4. DA reuptake

To terminate the action of DA in the synaptic cleft, DA is recaptured by the DA transporter (DAT) located on the presynaptic membrane (Kilty et al., 1991; Shimada et al., 1991; Usdin et al., 1991). The driving force for DA reuptake by DAT is provided by the transport of two Na^+ and one Cl^- into the cell (Gu et al., 1994; Torres et al., 2003).

Recaptured DA may either be re-packaged into synaptic vesicles for subsequent release, or metabolized in an effort to maintain low levels of non-vesicular DA.

1.7.5. DA metabolism

The major metabolic pathway of DA is oxidative deamination by the mitochondrial enzyme monoamine oxidase (MAO) (Kopin, 1964) to the reactive, transient intermediate 3,4-dihydroxyphenylacetaldehyde (DOPAL). Aldehyde dehydrogenase (ALDH), a nicotinamide adenine dinucleotide (NAD)-dependent enzyme, rapidly oxidizes DOPAL to the inactive metabolite 3,4-dihydroxyphenylacetic acid (DOPAC) (Marchitti et al., 2008). Under some circumstances DOPAL is also reduced to 3,4-dihydroxyphenylethanol (DOPET) by aldehyde/ aldose reductase (AR) (Elsworth and Roth, 1997).

Impaired conversion of DA to DOPAC renders cells susceptible to a variety of toxic compounds. Cytosolic DA can be autooxidized, which results in the formation of DA-quinones and ROS (Graham, 1978; Graham et al., 1978; LaVoie and Hastings, 1999; 2002). Furthermore, DOPAL itself is a highly reactive intermediate, which readily forms adducts with many cellular components (Marchitti et al., 2007). Because alterations in normal metabolism can impair cellular integrity, it is essential for cells to maintain tight regulation of DA synthesis, storage, release, and metabolism.

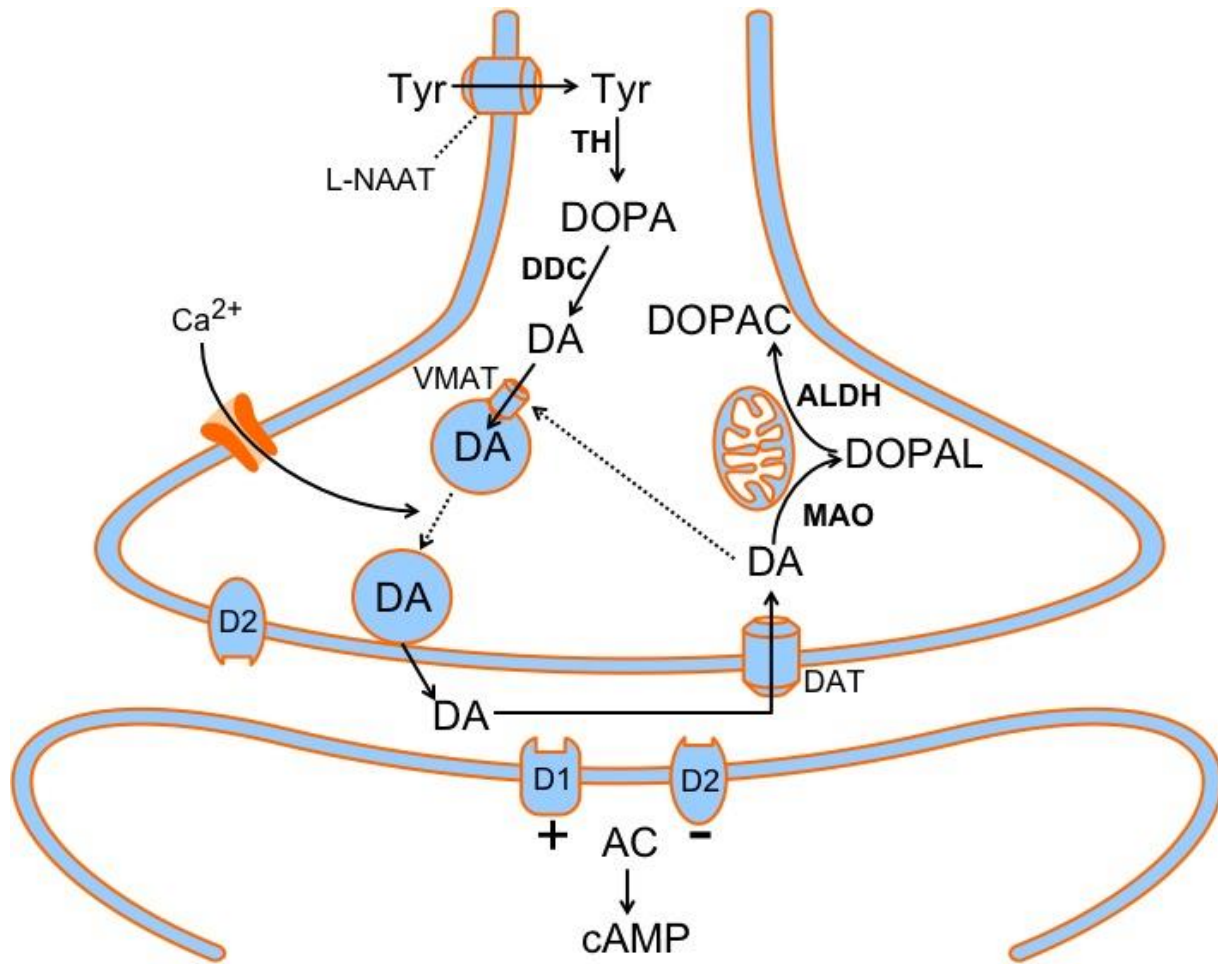


Figure 1.3. DA synthesis, release, and metabolism. Dietary tyrosine is hydroxylated to DOPA, which is rapidly decarboxylated to DA. DA is packaged into synaptic vesicles by VMAT, and is released from the synapse by depolarization-evoked, Ca^{2+} -dependent exocytosis. Once released, DA can bind pre- and post-synaptic D1 and D2 DA receptors to elicit either excitatory or inhibitory responses, depending on the type of receptor to which it binds and their subsequent effect on adenylate cyclase (AC) to generate cAMP. Termination of DA's action in the synapse is accomplished by reuptake through DAT. Recaptured DA can either be repackaged into synaptic vesicles or metabolized. DA metabolism proceeds in two steps, orchestrated by two mitochondrial-associated enzymes. First DA is deaminated by MAO to form DOPAL, and then DOPAL is oxidized by ALDH to form DOPAC. Tyr, tyrosine; L-NAAT, L-neutral amino acid transporter; TH, tyrosine hydroxylase; DOPA, dihydroxyphenylalanine; DDC, DOPA decarboxylase; DA, dopamine; VMAT, vesicular monoamine transporter; Ca^{2+} , calcium; D1, excitatory D1-like dopamine receptor; D2, inhibitory D2-like dopamine receptor; AC, adenylate cyclase; cAMP, cyclic adenosine monophosphate; DAT, dopamine transporter; MAO, monoamine oxidase; DOPAL, dihydroxyphenylacetaldehyde; ALDH, aldehyde dehydrogenase; DOPAC, dihydroxyphenylacetic acid.

1.8. Effects of MeHg on DA neuronal homeostasis

DA neurons are particularly sensitive to the toxic effects of MeHg. Exposure to nanomolar concentrations of the neurotoxicant selectively reduces the number of TH-positive neurons in murine embryonic stem cell cultures (Zimmer et al., 2011). Chronic, low-concentration exposure (1-2 μ M) to MeHg causes a significant loss of DA neurons in the nematode *Caenorhabditis elegans* (VanDuyn et al., 2010). Furthermore, MeHg impairs a variety of DA-specific bioprocesses in the cell, including synthesis, release, reuptake, and metabolism.

1.8.1. MeHg targeting of DA synthesis

Studies investigating effects of MeHg on DA synthesis have primarily measured changes in enzymatic activity of TH. Results are variable and inconsistent. Some studies report decreased TH activity following acute, high dose MeHg exposure in adult rats (Sharma et al., 1982; Kung et al., 1989). Others demonstrate no change in TH activity following either *in utero* or early postnatal exposure to acute, low doses of MeHg (Taylor and DiStefano, 1976; Bartolome et al., 1984). Omata et al. (1982) have suggested that MeHg stimulates TH activity during an early, asymptomatic phase of exposure to a high dose of MeHg in adult rats (days 5-10 of daily treatment). However, with the onset of neurological signs, 15 days into treatment, TH activity had returned to control rates. Discrepancies between these studies likely result from different exposure paradigms. As an additional caveat to the majority of these studies, TH activity was assessed in whole brain homogenates (Taylor and DiStefano, 1976; Omata et al., 1982; Sharma et al., 1982; Bartolome et al., 1984), which confounds interpretation of how MeHg selectively targets DA synthesis.

1.8.2. MeHg targeting of DA release

Spontaneous DA release increases following exposure to MeHg. This has been well documented in a variety of model systems, including ^3H -DA release from rat striatal synaptosomes (Minnema et al., 1989) and mouse striatal slices (McKay et al., 1986), as well as endogenous DA release from rat striatal synaptosomes (Dreiem et al., 2009), rat striatal punches (Bemis and Seegal, 1999), mouse striatal slices (Kalisch and Racz, 1996), and the striatum of conscious, free-moving rats (Faro et al., 1997; 1998; 2000; 2003; 2007). Mechanisms underlying MeHg-induced DA release, however, are not well characterized. While it is hypothesized that extracellular Ca^{2+} does not contribute (McKay et al., 1986; Minnema et al., 1989; Kalisch and Racz, 1996; Faro et al., 2002), a role for intracellular Ca^{2+} in MeHg-induced DA release has not been investigated. As MeHg is known to increase the concentration of cytosolic Ca^{2+} (Marty and Atchison, 1997) and intracellular Ca^{2+} contributes to MeHg-induced release of other neurotransmitters (Levesque and Atchison, 1987; 1988), this potential contribution is of interest. Only one study to date has specifically investigated mechanisms of MeHg-induced DA release. Faro et al. (2002) suggest that vesicular release is not involved, but instead attribute a role for DAT. However the authors could not discern whether MeHg was inhibiting DAT uptake or promoting a reversal of the transporter to release DA. Given the paucity of mechanistic studies, further investigation is needed to determine how MeHg targets the DA neuron to induce neurotransmitter release.

1.8.3. MeHg targeting of DA reuptake

The majority of studies investigating DA reuptake following exposure to MeHg have demonstrated inhibition of DAT activity (Komulainen and Tuomisto, 1982; Rajanna and Hobson, 1985; Bonnet et al., 1994; Dreiem et al., 2009; Zimmer et al., 2011). In these studies, ^3H uptake of DA or analogs with high affinity for DAT was assessed in striatal synaptosomes in the presence of MeHg. The IC_{50} , or concentration needed to inhibit 50% of transporter activity, was estimated at $2\mu\text{M}$ (Komulainen and Tuomisto, 1982; Bonnet et al., 1994; Dreiem et al., 2009). However, one study demonstrated inhibition at a much lower concentration (5nM) (Zimmer et al., 2011), while another found it to be much higher ($50\mu\text{M}$) (Rajanna and Hobson, 1985). In both cases, the discrepancy is likely due to the comparative sensitivity of the model system, mouse embryonic stem cells and whole brain homogenates, respectively.

While decreased DAT activity has been demonstrated in the majority of studies to date, a few have observed alternative effects. Bartolome et al. (1984) demonstrated a significant increase in ^3H -DA uptake in whole brain synaptosomes isolated from rat pups treated with MeHg *in utero*. Conversely, Komulainen et al. (1985) reported no change in ^3H -DA uptake in striatal synaptosomes isolated from rats treated with 10 mg/kg MeHg for one or five days *in vivo*. Interestingly, Komulainen and colleagues had previously demonstrated a decrease in DAT activity following *in vitro* exposure to MeHg (Komulainen and Tuomisto, 1982). It has been proposed that MeHg directly inhibits DAT by binding sulfhydryl groups present on the transporter (Bonnet et al., 1994; Dreiem and Seegal, 2007). If this is the case, the continued presence of MeHg may be necessary to inhibit DA

reuptake. However additional studies are needed to elucidate whether MeHg is inhibiting DAT and to determine how this inhibition may impact measurements of MeHg-induced DA release and metabolism.

1.8.4. MeHg targeting of DA metabolism

Effects of MeHg on DA metabolism have been assessed using two methods. Concentrations of the primary DA metabolite, DOPAC, have been measured by high-performance liquid chromatography (HPLC). *In vitro* analysis of striatal tissue or striatal synaptosomes has demonstrated that MeHg decreases DOPAC, and that this effect is concentration-dependent (Bemis and Seegal, 1999; Dreiem et al., 2009). These data suggest that MeHg inhibits DA metabolism.

Complementary to HPLC analyses, the activity of the enzyme that deaminates DA, MAO, has been measured by spectrophotometric or radiochemical assays. Results predominantly suggest that MeHg decreases MAO activity (Taylor and DiStefano, 1976; Chakrabarti et al., 1998; Beyrouy et al., 2006; Castoldi et al., 2006). The most powerful effect was reported by Chakrabarti et al. (1998), who demonstrated that MeHg causes a concentration-dependent decrease in MAO activity of rat synaptosomes isolated from the cortex, striatum, hypothalamus, hippocampus, brain stem, and cerebellum. The authors also observed decreased MAO activity in the same brain regions following *in vivo* treatment with an acute, high dose, but not an acute, intermediate dose of MeHg. Decreased MAO activity was also reported following *in utero* or neonatal treatment with MeHg (Taylor and DiStefano, 1976; Beyrouy et al., 2006; Castoldi et al., 2006), however these studies only demonstrate small decreases. Beyrouy et al. (2006) examined MAO activity in both male and female offspring

in five brain regions, and only demonstrated a decrease in the brainstem of female offspring of dams treated with a low dose of MeHg during gestation. Following a similar treatment paradigm, Castoldi et al. (2006) only reported a decrease in enzyme activity in the cerebellum of male offspring. Overall, these results support the conclusion that MeHg decreases DA metabolism, and suggest that it does so by targeting MAO. Because MAO is bound to the outer mitochondrial membrane (Schnaitman et al., 1967), MeHg-induced loss of mitochondrial membrane potential (Bondy and McKee, 1991; Hare and Atchison, 1992; InSug et al., 1997; Dreiem et al., 2005) could compromise enzyme activity.

However there is also one report of increased MAO activity in brain homogenates isolated from rats treated with 10 mg MeHg /kg/ day for 7 days (Omata et al., 1982). Discrepancies could be due to different experimental conditions, including methods of MeHg administration, animal age, or techniques used to measure MAO activity (e.g. substrate). These contradictory results and the lack of compelling evidence from multiple studies to support the conclusion that MeHg decreases MAO activity necessitate further investigation to determine if and how MeHg decreases DA metabolism.

1.9. Pheochromocytoma 12 (PC12) cell line

To investigate MeHg targeting of DA homeostasis, undifferentiated PC12 cells were chosen as the model system in the present series of experiments. The PC12 cell line is an immortalized, clonal cell line derived from a rat adrenal catecholamine-secreting pheochromocytoma (Greene and Tischler, 1976). Cultured under normal conditions, PC12 cells resemble adrenal chromaffin cells in morphology, physiology, and biochemistry. However, when cultured in the presence of nerve growth factor (NGF), PC12 cells exit the

cell cycle and differentiate to resemble sympathetic neurons. In both states PC12 cells synthesize, store, and release DA, NE, and acetylcholine (ACh). They also express a variety of ion channels and ligand-gated receptors. As such, PC12 cells represent a useful model for studying a plethora of cellular processes including neuronal differentiation, regulation and function of ion channels and membrane-bound receptors, and synthesis, storage and release of neurotransmitters. Accordingly, this cell line has been used in over 13,000 publications to date.

PC12 cells, in both their undifferentiated and differentiated states, are a valuable model system for studying DA neurochemistry and homeostasis (Greene and Rein, 1977a; Malagelada and Greene, 2011). They maintain all of the enzymes necessary for DA synthesis (i.e. TH, DDC) and metabolism (i.e. MAO, ALDH) (Greene and Tischler, 1976; Youdim et al., 1986; Robador et al., 2012), express high-affinity vesicular and membrane catecholamine transporters (Greene and Rein, 1977a; Friedrich and Bönisch, 1986), and release DA by both spontaneous and depolarization-evoked, Ca^{2+} -dependent, vesicular exocytosis (Greene and Tischler, 1976; Greene and Rein, 1977a; Ritchie, 1979; Wagner, 1985). However because of disparities in neurotransmitter content, enzyme activity, and cell morphology, undifferentiated and differentiated PC12 cells each provide unique advantages for studying DA synthesizing cells.

1.9.1. PC12 cell morphology

The most discernible difference between undifferentiated and differentiated PC12 cells is morphology. According to the original description of this cell line (Greene and Tischler, 1976), undifferentiated PC12 cells (Figure 2.1) are small, round, and tend to

clump in culture. Following treatment with NGF, cell multiplication ceases, and neuronal-like processes can be observed by 7 days. Over the course of days 7-22, the number, length, and density of processes increases until ~80% of cells have responded to NGF treatment. These neuronal-like processes, which most closely resemble primary sympathetic neuronal cultures (Chamley et al., 1972; Mains and Patterson, 1973), are fine, long, and branched, contain numerous varicosities, and form fascicles. The neuronal, post-mitotic phenotype of differentiated PC12 cells lends itself to studies of neuronal processes in DA neurons, including neuroprotection by growth factors in PD (Shimoke and Chiba, 2001; Salinas et al., 2003) and alteration of DA neurodevelopment and cell proliferation following exposure to toxicants (Parran et al., 2001; Chen et al., 2011). However, while DA neurons more closely resemble differentiated PC12 cells morphologically, disparities in the neurochemical profile suggest that undifferentiated PC12 cells are better suited for studies pertaining to DA homeostasis.

1.9.2. PC12 cell neurochemistry

The major differences induced by PC12 cell differentiation in content and activity of catecholaminergic and cholinergic neurotransmitters and enzymes are summarized in Table 1.1. The principal neurotransmitter in undifferentiated PC12 cells is DA, however measurable concentrations of NE and ACh are also present. Following differentiation, concentrations of DA and NE decrease by approximately 4- and 6-fold respectively (Greene and Tischler, 1976), while the concentration of ACh increases by approximately 4-fold (Greene and Rein, 1977b). Synthetic enzyme activity mirrors neurotransmitter content. The activity of catecholamine enzymes, including TH, DDC, and the NE synthetic enzyme DA

β -hydroxylase (D β H), decrease following differentiation (Greene and Tischler, 1976; Badoyannis et al., 1991), whereas the activity of enzymes necessary for ACh synthesis, including choline acetyltransferase (CAT), increase (Greene and Rein, 1977b).

Consequently, differentiated PC12 cells are more responsive to ACh, as compared to undifferentiated PC12 cells which are more responsive to DA (Dichter et al., 1977).

Because DA content and TH activity decrease profoundly with NGF treatment, DA homeostasis has been primarily characterized in undifferentiated PC12 cells. As in DA neurons, DA release in undifferentiated PC12 cells is coupled to synthesis, whereby newly synthesized DA is preferentially released (Greene and Rein, 1978). Furthermore, DA biosynthesis can be regulated acutely by TH phosphorylation (Tank et al., 1986) and factors such as high K⁺ and dibutyryl cyclic adenosine 3',5' monophosphoric acid (Greene and Rein, 1978), two agents demonstrated to mediate endogenous short-term DA synthesis in catecholaminergic tissue (Harris and Roth, 1971; Patrick and Barchas, 1976).

Table 1.1. Catecholaminergic and cholinergic neurotransmitter content and enzyme activity in undifferentiated and differentiated PC12 cells.

	Undifferentiated	Differentiated
NEUROTRANSMITTER CONTENT (nmol/mg protein)		
DA	16.6 ± 1.7 ¹	4.4 ± 0.4 ¹
NE	6.1 ± 6 ¹	1.5 ± 0.2 ¹
Epinephrine	< 0.15 ¹	< 0.15 ¹
ACh	1.3 ± 0.07 ²	5.6 ± 0.6 ²
ENZYME ACTIVITY (pmol/min/mg protein)		
TH	39 ± 5 ¹	10 ± 1 ¹
DDC	770 ± 99 ¹	130 ± 15 ¹
DβH	806 ± 84 ¹	161 ± 19 ¹
MAO-A	3.9 ± 0.4 ¹	N.D.
CAT	440 ± 17 ²	520 ± 20 ²

¹ Greene & Tischler. (1976) *Proc Natl Acad Sci (USA)*. 73: 2424-2428. ² Greene and Rein. (1977b) *Nature*. 268: 349-351. N.D. not determined. Prior to measuring neurotransmitter content and enzyme activity in differentiated state, PC12 cells were treated with 50mg/mL of NGF for 14 (catecholaminergic properties) or 22 (cholinergic properties) days.

1.9.3. PC12 cell VGCC subtype expression

One additional phenotypic change induced by NGF contributed to the selection of undifferentiated PC12 cells herein. The expression of VGCC subtypes is altered by PC12 cell differentiation (Shafer and Atchison, 1991a). Briefly, two VGCC subtypes have been primarily described in PC12 cells: the L- and N-subtypes (Takahashi et al., 1985; Janigro et al., 1989; Plummer et al., 1989; Reber et al., 1990). Biophysically, L- and N-type VGCCs are similar and activate at relatively depolarized membrane potentials; the L-type depolarizes at approximately -10mV and the N-type at approximately -20mV. These channel subtypes are most readily distinguished by pharmacological properties. The L-type VGCC is inhibited by dihydropyridine antagonists, whereas the N-type VGCC is sensitive to ω -conotoxin GVIA (Lacinová, 2005).

Undifferentiated PC12 cells predominately express L-type VGCCs (Janigro et al., 1989; Reber et al., 1990). However following treatment with NGF, there is a substantial increase in the expression of N-type VGCCs without a concomitant decrease in L-type VGCCs (Takahashi et al., 1985; Streit and Lux, 1987; Plummer et al., 1989; Usowicz et al., 1990). This difference is of importance presently because NSDA neurons express a high proportion of L-type VGCCs, which are used to maintain autonomous pacemaking activity (Nedergaard et al., 1993; Bonci et al., 1998; Chan et al., 2007). As such, the expression profile of VGCCs in undifferentiated PC12 cells more closely resembles that in NSDA neurons.

1.9.4. Differences between undifferentiated PC12 cells and DA neurons

While the neuronal phenotype of differentiated PC12 cells more closely parallels DA neuronal morphology, the neurochemical and protein expression profile of undifferentiated PC12 cells provides a more suitable model of DA synthesizing cells. For these reasons, undifferentiated PC12 cells were chosen for the studies presented in this dissertation. However there are a few important differences between undifferentiated PC12 cells and DA neurons. As described, PC12 cells synthesize and store two additional neurotransmitters, NE and ACh (Greene and Tischler, 1976; Greene and Rein, 1977a; 1977b). NE is stored alongside DA in large dense-core vesicles (Kishimoto et al., 2005), while ACh is stored in small clear-core vesicles that are observed most prominently in the differentiated state (Greene and Tischler, 1976; Liu et al., 2005). Because of the presence of these additional neurotransmitters, it is plausible that changes in DA homeostasis in undifferentiated PC12 cells might not directly reflect changes in DA neurons. However this seems unlikely considering the synthetic and degradatory pathways are essentially identical, and DA is the most prominent neurotransmitter in the undifferentiated state. The concentration of NE is much lower than that of DA, primarily because D β H requires reduced ascorbate as a cofactor, and in tissue culture medium the cofactor readily degrades (Greene and Rein, 1978). Additionally, in the undifferentiated state the concentration of ACh is relatively low as compared to DA.

Another major difference between undifferentiated PC12 cells and DA neurons is the process of DA reuptake. PC12 cells express the NE transporter (NET) as opposed to DAT (Greene and Rein, 1977a; Friedrich and Bönisch, 1986). However, NET and DAT are both members of a family of Na⁺- and Cl⁻-dependent carriers, and they have a sequence

homology of about 78%, with sequences being most similar in their transmembrane domains (Buck and Amara, 1995; Brüss et al., 1997). The major difference between these carriers is that while DAT requires two Na⁺ for transport, NET only requires one (Gu et al., 1994). Of importance is the affinity of NET for DA. Using kinetic assays of ³H-DA and ³H-NE uptake in the LLC-PK₁ cell line stably transfected with NET or DAT, Gu et al. (1994) found that while DAT and NET transport both catecholamines, DA was the preferred substrate for both transporters.

1.9.5. Effects of MeHg in PC12 cells

PC12 cells have been used as a model system to study the neurotoxic effects of MeHg. This work has primarily investigated cytotoxicity and MeHg targeting of VGCCs. In PC12 cells, as in other cell types, MeHg decreases cell viability in a concentration-dependent manner, dissipates the mitochondrial membrane potential, decreases ATP and glutathione production, and increases ROS formation (Parran et al., 2001; Gatti et al., 2004). Additionally, it has been demonstrated that MeHg decreases ⁴⁵Ca²⁺ influx in undifferentiated PC12 cells (Shafer et al., 1990). Inhibition of Ca²⁺ influx is complete at 250 μM, and mediated by disruption of VGCCs, not cytotoxicity, because no cell death was observed within the 1hr exposure paradigm. These authors went on to demonstrate that MeHg-mediated inhibition of VGCCs in PC12 cells is voltage-dependent, and occurs regardless of the state of the Ca²⁺ channel or membrane holding potential (Shafer and Atchison, 1991b).

1.10. Summary

MeHg is a potent environmental neurotoxicant, which produces severe pathological consequences in humans. Molecular mechanisms of MeHg-mediated neurotoxicity are still elusive, however perturbation of intracellular Ca^{2+} , mitochondrial dysfunction, and an affinity for thiol groups resulting in impaired protein function have been implicated. Despite relatively general neurotoxic effects, MeHg does not affect all cell types equally. DA neurons are one of the few cell types selectively susceptible to MeHg. Factors mediating this sensitivity are unknown, but could be related to unique processes in DA neurons that mediated the neurotransmitters synthesis, release, and metabolism. The experiments in this thesis were designed to investigate the susceptibility of DA neurons to MeHg-mediated toxicity using the immortalized clonal PC12 cell line.

1.11. Thesis Objective

The studies described in this dissertation were developed in order to test the central hypothesis that MeHg-induced increase in intracellular Ca^{2+} mediates changes in DA synthesis and release, whereas MeHg-induced mitochondrial dysfunction mediates changes in DA metabolism. The following specific aims and hypotheses were designed to test this central hypothesis.

a) Characterize the relationship between MeHg-induced DA synthesis and release in undifferentiated PC12 cells following exposure to MeHg.

Hypothesis: MeHg stimulates both DA synthesis and DA release. Activation of DA synthesis contributes to Ca^{2+} -dependent vesicular exocytosis.

b) Characterize the aberrant DA metabolomic profile in undifferentiated PC12 cells induced by MeHg, and examine direct and indirect factors mediating the inhibition of enzymes necessary for DA metabolism.

Hypothesis: MeHg impairs DA metabolism by inhibiting mitochondrial-associated enzymes that mediate its oxidative catabolism. These enzymes are inhibited indirectly as a result of mitochondrial dysfunction induced by the toxicant. Furthermore, inhibition of DA metabolism results in formation of aberrant toxic intermediates and compensatory up-regulation of an alternative reductive metabolic pathway.

c) Examine the contributions of extracellular and intracellular Ca²⁺ changes in DA release and metabolism induced by MeHg

Hypothesis: Intracellular, but not extracellular, Ca²⁺ mediates MeHg-induced DA release, whereas neither participate in MeHg-impaired DA metabolism.

The following chapters outline the research performed to address the above specific aims. The reader is referred to Chapter 2 for detailed methodology. Chapters 3-6 describe findings as they related to the central hypothesis and thesis objective. Chapter 7 provides a general discussion on the relevance and importance of this research as it relates to previous findings and information from the literature.

Chapter 2. General Materials and Methods

2.1. Culture of PC12 cells

Cell culture supplies, including RPMI-1640 medium, horse serum, trypsin, and penicillin-streptomycin, were purchased from GIBCO BRL (Grand Island, NY). Hyclone fetal bovine serum was purchased from Thermo Scientific (Logan, UT). PC12 cells (Gift of Dr. M.L. Contreras) were grown in RPMI-1640 medium supplemented with 10% (v/v) horse serum, 2.5% (v/v) fetal bovine serum, and 1% (v/v) penicillin-streptomycin (pH 7.3). Cultures were maintained in either 25-cm² or 75-cm² T-flasks in a humidified environment containing 5% CO₂ at 37°C. Culture medium was changed every 2-3 days. Every 4-5 days PC12 cultures were detached from the flasks with 0.25% (v/v) trypsin and sub-cultured at a density of 3x10⁵ cells/mL for a 5 day culture or 4x10⁵ cells/mL for a 4 day culture. All cultures were maintained at 80-90% confluence at the time of subculture. To maintain consistency from experiment to experiment, cells were used between passages 14-19 from our receipt. Experimental conditions were repeated in technical triplicate and experiments were replicated at least three times from separate cultures to minimize the risk of culture-specific confound. Representative brightfield images of PC12 cells (passage 16) in culture are depicted in Figure 2.1.

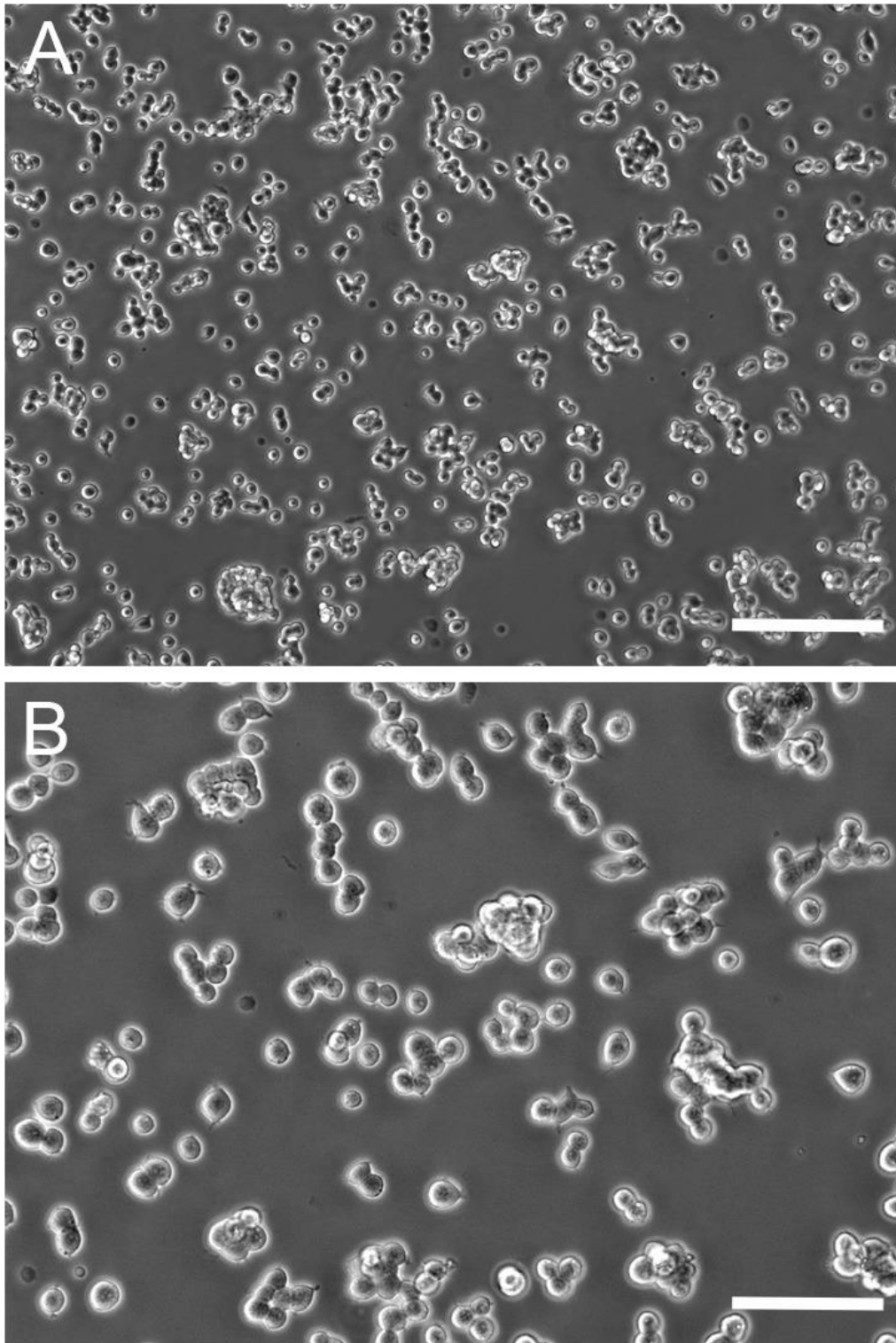


Figure 2.1. Representative brightfield images of pheochromocytoma (PC12) cells in culture (passage 16). Panel A) Low magnification. Scale bar = 200 μ m. Panel B) High magnification. Scale bar = 100 μ m.

2.2. Chemicals and solutions

The standard physiological saline used for extracellular solution was 4-(2-hydroxyethyl)-1-piperazineethanesulfonic acid (HEPES)-buffered saline (HBS), which contained (mM): 150 NaCl, 5 KCl, 2.4 CaCl₂, 1.6 MgSO₄, 20 HEPES, and 20 *d*-glucose (pH 7.3). The Ca²⁺-free buffer (0-Ca²⁺ HBS) had the same composition as HBS with the following exceptions (mM): 0 CaCl₂ and 0.02 ethylene glycol tetraacetic acid.

Methyl mercuric chloride (MeHg) was purchased from ICN Biochemicals Inc. (Aurora, OH). It was prepared as 10mM stock solution and stored for no more than 3 months at 4°C. On the day of each experiment, MeHg was diluted to working concentrations of 1, 2, or 5μM in HBS or 0-Ca²⁺ HBS.

Several pharmacological treatments were used to analyze distinct components of the DA biosynthetic and release pathways, VGCC function, and pathways of intracellular Ca²⁺ release. Concentrations were calculated as free-base. All chemicals were prepared fresh for each experiment. Table 2.1 summarizes the specific action of each chemical used.

α-Methyl-DL-tyrosine methyl ester hydrochloride (AMT; Sigma) was prepared in dH₂O as a 10mM stock solution and then diluted to a final concentration of 300μM either in culture medium for a 24 hr or 30 min pretreatment or in HBS for a 60 min co-treatment with 2μM MeHg.

Reserpine (Sigma) was dissolved in 100% DMSO as a 10mM stock solution and then diluted so the final concentration of DMSO was less than 0.05% (v/v). The 10mM stock was diluted to a final concentration of 50nM in either culture medium for a 3 hr pretreatment or in HBS for a 60 min co-treatment with 2 μ M MeHg.

Desipramine hydrochloride (DMI; Sigma) was prepared in dH₂O as a 10mM stock and then diluted to a final concentration of 1 μ M either in culture medium for a 15 min pretreatment or in HBS for a 60 min co-treatment with 2 μ M MeHg.

NSD-1015 (3-hydroxybenzylhydrazine; Sigma) was dissolved in dH₂O as a 1mM stock and then diluted to a final concentration of 10 μ M in HBS for a 60 min co-treatment with 2 μ M MeHg.

Daidzin (Sigma) was dissolved in 100% DMSO as stock solutions of 10mM and diluted so that the final concentration of DMSO was no more than 0.05% (v/v). The 10mM stock was diluted to a final concentration of 20 μ M in HBS for a 45 min treatment.

Rotenone (Sigma) was dissolved in 100% DMSO as stock solutions of 10mM and diluted so that the final concentration of DMSO was no more than 0.05% (v/v). The 10mM stock was diluted to a final concentration of 50nM in HBS for a 15 min treatment.

Nimodipine (Sigma) is light sensitive, and as such was protected from light during preparation and experimentation. It was dissolved in dH₂O as a 50mM stock solution, and then diluted to a final concentration of 2μM either in culture medium for a 15 min pretreatment or HBS for a 60 min co-treatment with 2μM MeHg.

Cadmium chloride (Sigma) was prepared in dH₂O as a 20mM stock solution and then diluted to a final concentration of 200μM either in culture medium for a 15 min pretreatment or HBS for a 60 min co-treatment with 2μM MeHg.

BAPTA/AM (1,2-Bis(2-aminophenoxy)ethane-N,N,N',N'-tetraacetic acid tetrakis(acetoxymethyl ester; Calbiochem) was dissolved in 100% DMSO as a 10mM stock solution and diluted to a final concentration of 50μM in HBS for a 30 min pretreatment and then a 60 min co-treatment with 2μM MeHg in either HBS or 0-Ca²⁺ HBS .

Table 2.1. Summary of drug actions.

Drugs	Action	Reference	Source
α -methyl-DL-tyrosine	TH inhibitor	(Spector et al., 1965)	Sigma
Reserpine	VMAT inhibitor; “vesicular depleter”	(Drukarch et al., 1996)	Sigma
Desipramine	NET inhibitor	(Brüss et al., 1997)	Sigma
NSD-1015	DDC inhibitor	(Carlsson et al., 1972)	Sigma
Daidzin	ALDH inhibitor	(Keung and Vallee, 1993)	Sigma
Rotenone	Complex I inhibitor of the mitochondrial ETC	(Lamensdorf et al., 2000a)	Sigma
Nimodipine	L-type VGCC inhibitor	(Neal et al., 2010)	Sigma
Cadmium	Non-specific VGCC inhibitor	(Taylor et al., 2000)	Sigma
BAPTA/AM	Intracellular Ca ²⁺ chelator	(Mahata et al., 2011)	Calbiochem

2.3. Neurochemical analyses

PC12 cells were seeded in 6-well plates (9.5cm²) coated with poly-D-lysine at a density of 6x10⁵ cells/mL (total volume of 2mL/well) 48 hr prior to pharmacological and/or toxicant treatment. At experiment termination, treatment medium was collected and acidified (1:1) with ice-cold tissue buffer (0.1M phosphate-citrate buffer containing 15% methanol (v/v), pH 2.5) for analysis of extracellular DA content. Cells were rinsed once with 1mL ice-cold phosphate buffered saline, harvested, and pelleted by centrifugation at 12,000 *g* for 5 min at 4°C. After centrifugation, the supernatant was removed and replaced with 100µL of ice-cold tissue buffer.

The content of DA and its metabolites in the treatment medium and supernatant was determined by means of high-pressure liquid chromatography coupled with electrochemical detection (HPLC-ED) using a Water 515 HPLC pump (Waters Corp., Milford, MA) and an ESA Coulochem 5100A electrochemical detector with an oxidation potential of +0.4V. Neurochemical content was quantified by comparing peak height of each sample to peak heights of standards and normalized to mL per sample for extracellular measurements or mg protein for intracellular measurements as determined by the bicinchoninic acid (BCA) protein assay (Sigma). Figure 2.2 depicts HPLC chromatographs of extracellular and intracellular samples as compared to 500pg standards.

2.3.1. Calculation of rate constant

Releasable stores of transmitter in catecholamine secreting cells are maintained by end-product feedback regulation of the balance between vesicular release and *de novo*

synthesis dependent replenishment. The slope of decline (or rate constant) of intracellular DA following inhibition of synthesis represents a reliable, indirect measurement of release or DA storage utilization (Brodie et al., 1966). In the present study, the rate constant was calculated from intracellular DA concentrations after 90 min AMT treatment. The slope of the lines representing the difference between cells treated with 2 μ M MeHg alone or combined with 300 μ M AMT was calculated, and then compared to HBS-treated cells in the absence or presence of AMT.

2.3.2. Synthesis of DOPAL standard

DOPAL is an endogenous aldehyde resulting from the normal oxidative metabolism of DA by MAO. DOPAL standards are not commercially available, therefore in order to measure DOPAL by HPLC-ED it was necessary to synthesize a standard. DA was dissolved in phosphate buffer (140mM NaCl, 8.1mM Na₂HPO₄, 1.4mM KH₂PO₄, pH 7.5) to a final concentration of 1mM. Phosphate-buffered DA (750 μ l) was incubated in two 12x75 culture tubes at 37°C for 15 min. The reaction was started by adding 25 μ L MAO (10 U) to each of the two culture tubes and gently mixing. In order to determine the optimal incubation duration for experimental analysis of DOPAL, 50 μ L aliquots were withdrawn from the reaction at different time intervals (10, 15, 30, 45 or 60 min). The reaction in the tubes was stopped by adding 450 μ L of ice-cold tissue buffer. Samples were transferred to a 1.5mL centrifuge and centrifuged at 12,000 x g for 10 min. Supernatants were removed and placed into a fresh tube for HPLC-ED analysis of DA and DOPAL. Concentrations of DA were compared to 1ng standards of DA. Concentrations of DOPAL were determined by normalizing the DOPAL peak height to the amount of DA lost at each time point. Figure 2.3

illustrates the time-dependent synthesis of DOPAL correlated with the time-dependent decline in DA. Based on this analysis, the 45min incubation time-point was selected for experimental analysis of DOPAL concentrations.

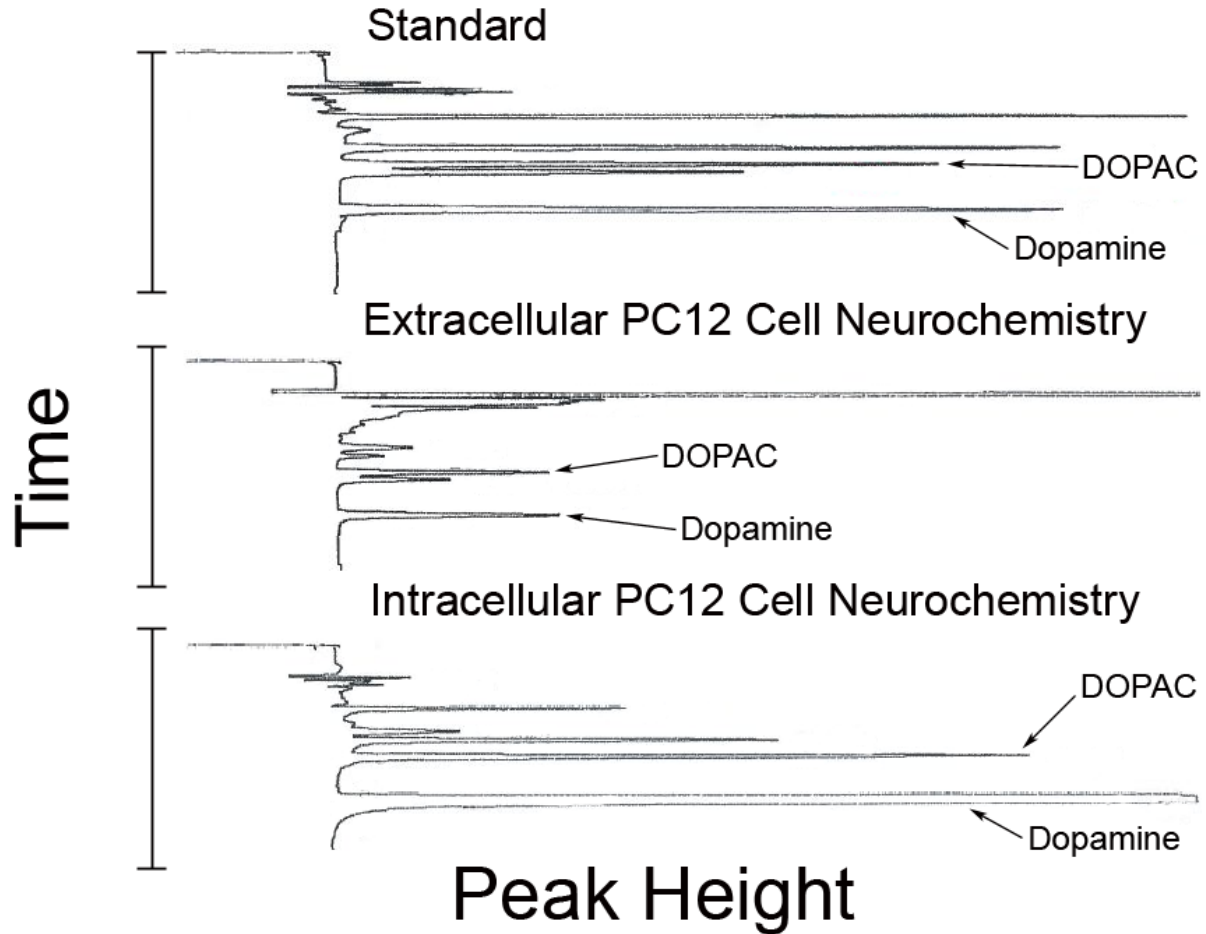


Figure 2.2. High performance liquid chromatography (HPLC) chromatographs. Extracellular (middle panel) and intracellular (lower panel) PC12 cell neurochemistry was compared to standard mixes (upper panel) containing 500pg NE, DOPET, DOPAC, DOPA, and DA. Comparison of the retention time allowed for determination of which neurochemicals were present in medium and cell samples. Peak height of samples was compared to peak height of standards to determine neurochemical content. Extracellular concentrations were normalized to mL per sample and expressed in ng/mL. Intracellular concentrations were normalized to protein content and expressed in ng/mg protein.

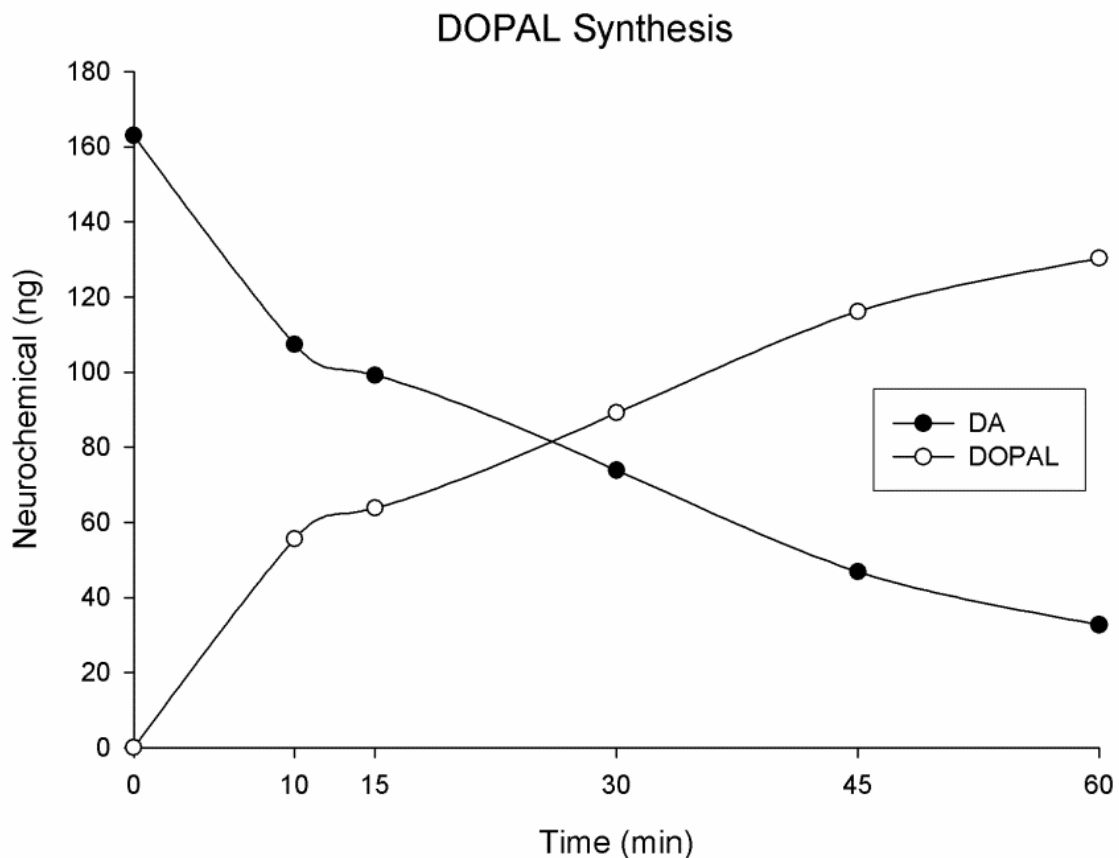


Figure 2.3. Synthesis of DOPAL standard. The rate of DOPAL formation (white circles) and DA depletion (black circles) after the incubation of DA (1.063 mM) with 10 U MAO. DA and DOPAL were measured by HPLC-ED. DA concentrations were determined by comparison with 163ng DA standards. Concentrations of DOPAL were determined by comparing DOPAL peak heights to the amount of DA decreased at each time point. Based on this analysis the 45 min incubation time-point was selected for experimental analysis of DOPAL concentrations.

2.4. Cell viability

PC12 cells were seeded in 96-well plates coated with poly-D-lysine at a density of 4×10^5 cells/mL 48 hr prior to treatment with HBS, 1, 2, or 5 μ M MeHg for 15, 30, 60 or 120 min. Hoechst 33342 (10 mg/mL) and propidium iodide (1 mg/mL) were diluted 1:10,000 in existing treatment medium. Cells were incubated in fluorophores at 37°C for 15 min prior to visualization on a Nikon Ellipse TE2000-U inverted microscope with diasopic illumination pillar (Nikon Instruments, Inc., Melville, NY) equipped with a T-FL EPO fluorescence attachment and X-Cite metal halide illumination system. DAPI (358nm/461nm) and rhodamine filters (610nm) were used for visualization. Images were acquired using MetaMorph image acquisition and analysis software (Molecular Devices, Sunnyvale, CA). One image was acquired per well, randomized and counted manually using a grid system. Viable cells had a blue-stained (Hoechst) nucleus, whereas non-viable cells had a high red (propidium iodide) fluorescence (Figure 2.4; Yuan et al., 2009). Each treatment was replicated in triplicate wells in three separate experiments.

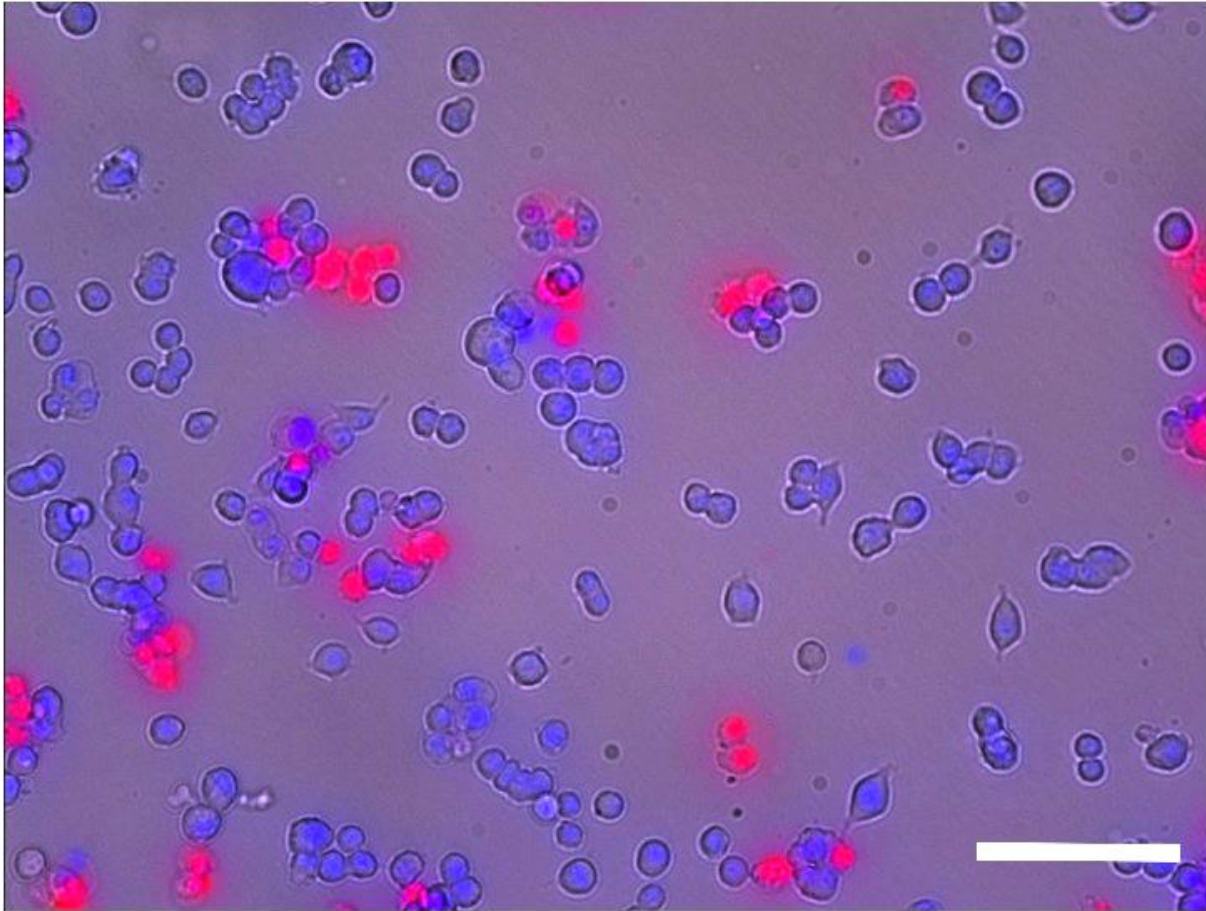


Figure 2.4. Hoechst/ propidium iodide fluorescent stain for cell viability in PC12 cells. Viable cells are stained with the membrane permeable blue-fluorescent dye, Hoechst 33342. The red-fluorescent dye, propidium iodide, is only permeant to cells with compromised membrane integrity, and thus stains dead cells. Scale bar = 200 μ m

2.5. Western blot analysis of TH

PC12 cells were seeded in 6-well plates coated with poly-D-lysine at a density of 6×10^5 cells/mL 48 hr prior to pharmacological and/or toxicant treatment. Following treatment, medium was aspirated and in some cases used for neurochemical analysis of extracellular DA content. Cells were rinsed once with 1mL ice-cold phosphate buffered saline, harvested, and pelleted by centrifugation at 12,000 *g* for 5 min at 4°C. Pellets were lysed with 50µL radio-immunoprecipitation assay (RIPA) buffer containing protease inhibitor (1:100) and phosphatase inhibitor (1:100). Protein content was determined by the bicinchoninic acid protein assay (Sigma).

Supernatant was prepared for Western blot analysis to quantify total and phosphorylated isoforms of TH. Equal amounts of protein (10-15µg) were separated on precast polyacrylamide gels (10% Bio-Rad, Hercules, CA, USA). Proteins were transferred to 0.45µm Immobulin-FL polyvinylidene fluoride (PVDFL) membranes (Millipore, Billerica, MA), incubated 1 hr in 5% skim milk (w/v) or bovine serum albumin blocking buffer and then reacted overnight with either rabbit anti-TH (1:5000; Chemicon, Billerica, MA), rabbit anti-TH Ser40 (1:1000, Cell Signaling, Danvers, MA), rabbit anti-TH serine-31 (1:1000; Chemicon, Temecula, CA, USA), rabbit anti-TH serine-19 (1:1000; Chemicon), or mouse anti-β-actin (1:2500; Cell Signaling) diluted in blocking buffer. Membranes were incubated with HRP-conjugated anti-rabbit or anti-mouse (1:5000; Cell Signaling) and bound antibodies were visualized using SuperSignal West Femto Chemiluminescent Substrate (Thermo Scientific, Rockford, IL) and the Odyssey Fc System (LiCor, Lincoln, NE). TH and phosphorylated TH bands were normalized to the β-actin signal to correct for variations in loading.

2.6. Mitochondrial bioenergetics

2.6.1. XF24 assay medium

RPMI-1640 (Sigma R1383-10X1L) was reconstituted in 1L-distilled water and supplemented with 2.5mM d-glucose. Assay medium was pHed to 7.4 and filter sterilized.

2.6.2. Test compounds

Sodium pyruvate, malic acid disodium salt, carbonyl cyanide 4-(trifluoromethoxy)phenylhydrazone (FCCP), and antimycin A were obtained from Sigma-Aldrich. Oligomycin A was obtained from Seahorse BioScience (Billerica, MA). Working concentrations of mitochondrial test compound were diluted from stock solutions in XF24 Assay Medium as described in Table 2.2.

Table 2.2. Dilutions of test compounds for XF24 measurements of mitochondrial bioenergetics.

Compound	Stock Conc.	Dilution	Working Conc.	Dilution	Final Conc.
Pyruvate	1M	20	50mM	10	5mM
Oligomycin A	2.5mM	227.27	11 μ M	11	1 μ M
FCCP	1mM	41.67	24 μ M	12	2 μ M
Antimycin A	1mM	76.9	13 μ M	13	1 μ M

2.6.3. Extracellular flux (XF) analysis.

The XF24 Extracellular Flux Analyzer (Seahorse Bioscience, Billerica, MA) is a fully integrated 24-well instrument that simultaneously measures the two major energy pathways of a cell—mitochondrial respiration and glycolysis. To examine respiration, the XF analyzer measures the rate at which oxygen (O₂) is consumed from the medium.

Glycolysis is quantified as the rate at which free protons are released and acidify the medium.

Each assay kit contains a cell culture plate and disposable biosensor cartridge. The bottom of the biosensor cartridge contains 24 pairs of two distinct fluorophores, one sensitive to O₂ and the other pH. Fiber-optic bundles insert themselves into the sleeves of the sensor cartridge, emit a light that excites the embedded fluorophores (O₂= 532nm, pH=470nm), and transmits the fluorophore emission signal (O₂=650nm, pH=530nm) to a set of photodetectors. Each cartridge is also equipped with four reagent delivery ports per well for dispensing testing agents at specified times during an assay.

The rates of oxygen consumption (OCR) and extracellular acidification are measured within a transient microchamber created in each of the 24 wells when the biosensor cartridge is lowered 200µm above the cells. During this time, analytes are measured every 22s until a 10% change in O₂ or pH is detected. The cartridge then rises, which allows the cells to restore medium to baseline.

At the beginning of each experiment, the biosensors are independently calibrated using an automated routine in the machine to determine the sensor gain based on sensory

output measured in a calibration reagent of known pH and O₂ concentration. Testing compounds are preloaded into the four injection ports and subsequently delivered pneumatically into the medium. Because XF measures are nondestructive, the real-time kinetic response of the same cell population can be measured repeatedly over time.

Experiments presented in Chapters 4-5 measured mitochondrial respiration under basal and stressed conditions. These conditions were created using an XF24 Mitochondrial Stress Test (Figure 2.5). Injection ports are loaded with oligomycin A, FCCP, and antimycin A. Basal respiration is measured first and then drugs are injected sequentially to measure OCR following inhibition of the ATP synthase, uncoupling of electron transporter and ATP synthesis, and inhibition of electron transport. Figure 2.5 describes how OCR measured under these conditions can be used to calculate four parameters of mitochondrial respiration: basal respiration, ATP turnover, proton leak, and maximum or spare respiration.

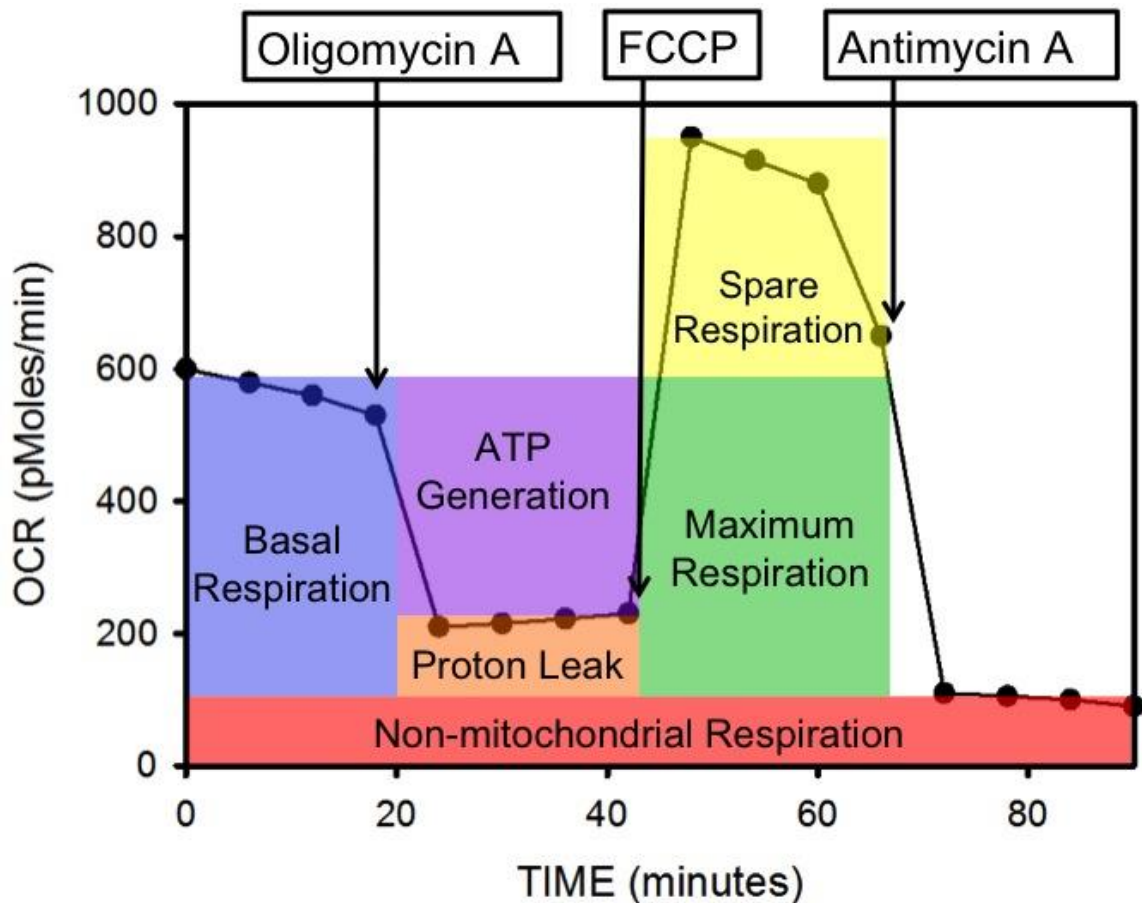


Figure 2.5. Mitochondrial Stress Test using the XF24 Analyzer. Sequential injections of specific mitochondrial inhibitors through the drug injection ports provide measurements of the 4 fundamental parameters of mitochondrial function: Basal Respiration (blue), ATP Turnover (purple), Proton Leak (orange), and Maximum or Spare Respiration (green and yellow). Oxygen consumption rate (OCR) is first measured under basal conditions (with or without the presence of a substrate, such as glucose or pyruvate), which provides a measurement of basal respiration. Oligomycin A is then injected to inhibit the ATP synthase, which prevents the phosphorylation of ADP to ATP. As a result, OCR decreases and the difference between Basal OCR and OCR following Oligomycin A is calculated as the rate at which ATP is generated. Oligomycin A does not reduce OCR to zero, and the remaining OCR is classified as Proton Leak, or the facilitated diffusion of protons into the mitochondrial matrix through an uncoupling protein present in the inner mitochondrial membrane. Oligomycin A is followed by an injection of the uncoupler FCCP, which acts as a mobile ion carrier, transporting protons across the inner mitochondrial membrane. Because FCCP disconnects electron transport from ATP generation, proton transport occurs at a maximal rate. The difference between OCR following FCCP and Basal OCR is calculated as Spare Respiration. This represents the amount of extra ATP that can be generated by oxidative phosphorylation in the face of a sudden increase in energy demand. Antimycin A is injected to inhibit the ETC at Complex III. This completely inhibits mitochondrial respiration. Remaining OCR is considered non-mitochondrial respiration, and is subtracted from all measurements to calculate accurately the parameters of mitochondrial respiration. Adapted from seahorsebio.com.

2.6.4. XF bioenergetics assay

PC12 cells were seeded in XF 24-well cell culture microplates (Seahorse Bioscience, Billerica, MA) coated with poly-D-lysine at a density of 7×10^5 cells in 100 μ L RPMI culture medium. The cell culture plate was incubated at 37°C/5% CO₂ for 1 h before 150 μ L of additional culture medium was added carefully to each well and cells were incubated at 37°C/5% CO₂ for 48 h.

The day before the experiment 1 mL of XF Calibrant solution (Seahorse Bioscience, Billerica, MA) was added to each well of the biosensor cartridge and incubated at 37°C/ no CO₂ overnight.

On the day of the experiment cells were treated with MeHg as described below. During cell equilibration, cartridge injection ports were loaded with testing compounds at working concentrations (Table 2.2), and then the biosensor cartridge was placed in the XF24 Flux Analyzer for automated calibration.

For the XF assay, the cell culture plate was placed in the calibrated XF24 Flux Analyzer. Baseline OCR (nM/min) and ECAR (milli-pH (mpH) units/min) were measured simultaneously 3 times. Between each rate measurement, assay medium was gently mixed by the XF24 Analyzer for 3-5 min to restore normal O₂ tension and pH in the microchamber surrounding the cells. Following baseline measurement, Ports A-D were sequentially injected (75 μ L) to reach testing compound final concentrations and the

medium was mixed for 3-5 min before OCR and ECAR were measured 3 times, as described for baseline measurements.

2.6.5. XF24 drug exposure

At the time of treatment, complete medium was aspirated and replaced with HBS or HBS containing 2 μ M MeHg, 50nM rotenone, or 20 μ M daidzin. In some experiments, cells were treated with 2 μ M MeHg in 0-Ca²⁺ HBS. Cells were incubated at 37°C/ 5% CO₂ for 60 min. To terminate drug exposure, treatment medium was aspirated, and cells were prepared for the XF Analyzer measurements. First, cells were rinsed with 1mL warmed XF24 assay medium, and then XF24 assay medium was brought to a final volume of 675 μ L. Cells were incubated at 37°C/no CO₂ for 1 hr to allow medium temperature and pH to equilibrate before the first measurements were made.

2.6.6. XF24 optimization of experimental conditions.

In order to measure accurately OCR as described in Methods Section 2.6.4, certain parameters were first optimized. These included cell plating density (Figure 2.6), assay medium composition (Figure 2.7), and FCCP concentration (Figure 2.8).

Because the O₂ biosensor takes a measurement from one small location within each well, plating densities that are too low or too high result in a variable distribution of cells along the bottom of the well and result in an inaccurate measurement of OCR. For this reason cells were seeded at densities between 40,000-90,000 cells/well and OCR was measured during a Mitochondrial Stress Test. As shown in Figure 2.6, the optimal density

was ~70,000 cells/well. At lower densities, basal OCR was too low and the maximum respiratory capacity was not pronounced. Although high densities (80,000-90,000 cells/well) had good basal OCR and a pronounced response to FCCP, there was some indication that once oxygen levels were depleted and measurements were terminated (as normal), oxygen levels were not able to return to baseline. This did not happen at 70,000 cells/well, so this density was chosen for future experiments.

Seahorse Biosciences provided best practices and basic protocol instructions for using their equipment with immortalized cell lines. One company suggestion is the use of their proprietary Dulbecco's Modified Eagle Medium (DMEM) for all XF24 assays. However PC12 cells are cultured in RPMI 1640 medium for growth, which contains different types and concentrations of amino acids, vitamins, and inorganic salts. Changing the medium just prior to intracellular measurements of mitochondrial respiration could dramatically alter cellular and respiratory activity. To determine which assay medium provided the most ideal experimental conditions, RPMI and DMEM assay media were compared (Figure 2.7).

In this experiment respiration substrates were also compared. Some RPMI medium was prepared with glucose as a substrate for the ETC, and some RPMI medium was prepared with galactose. Galactose was investigated as a potential substrate because PC12 cells have a very slow doubling time (~92 hrs) (Greene and Tischler, 1976). This suggests that the cells normally do not rely on oxidative phosphorylation, but instead are adapted to generate energy from glycolysis. This has been demonstrated to occur in many immortalized cell lines, and is referred to as the Crabtree effect (Rodríguez-Enríquez et al., 2001). It is possible to stimulate respiration in cancer cell lines by swapping glucose in the medium for galactose (Rossignol, 2004; Marroquin et al., 2007). Oxidation of galactose to

pyruvate by way of glycolysis yields no net ATP, which forces the cell to use oxidative phosphorylation to generate energy needed for survival. As shown in Figure 2.7, the optimal medium condition was RPMI 1640 medium with 2.5mM glucose present. Under these conditions, basal respiration was highest and FCCP produced a maximal response.

The last optimization experiment performed was an FCCP titration. The optimal concentration of this uncoupler must be determined to ensure maximum stimulation of uncoupled respiration without inhibiting respiration by using a concentration that is too high. Figure 2.8 illustrates the results of this titration; 2 μ M FCCP was chosen for future assays because this concentration maximally stimulated OCR without negatively altering oxygen consumption.

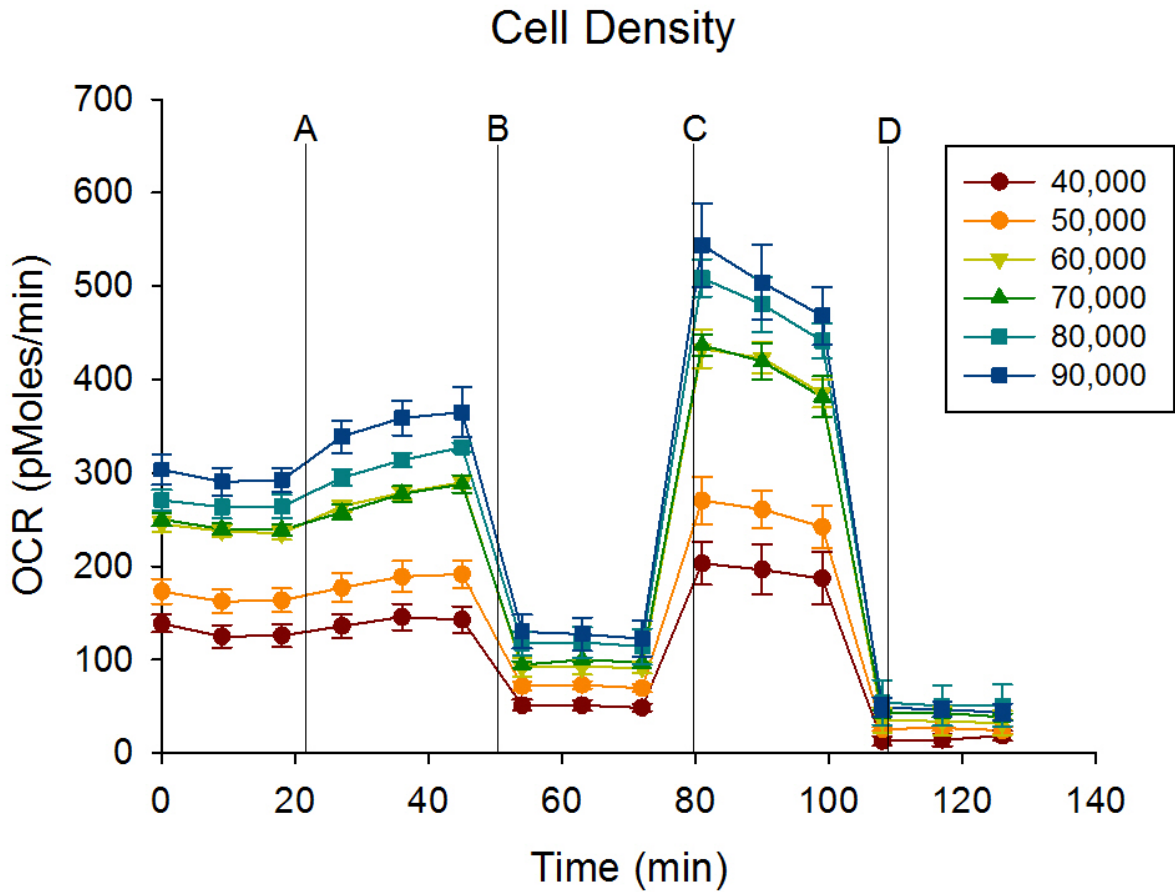


Figure 2.6. XF24 cell density optimization. Undifferentiated PC12 cells were plated at 40,000 (red), 50,000 (orange), 60,000 (light green), 70,000 (dark green), 80,000 (teal), or 90,000 (blue) cells/well. Bioenergetics were assessed using the Mitochondrial Stress Test: A) 50mM pyruvate, B) 1 μ M oligomycin A, C) 1 μ M FCCP, and D) 1 μ M antimycin A. Based on these data, a plating density of 70,000 cells/well was selected for future assays because basal OCR was high and cells responded well to FCCP with adequate oxygen levels within each well. These observations suggest that cells were plated at a density that was high enough to allow cell-cell interaction, but not too high as to result in cells growing on top of each other.

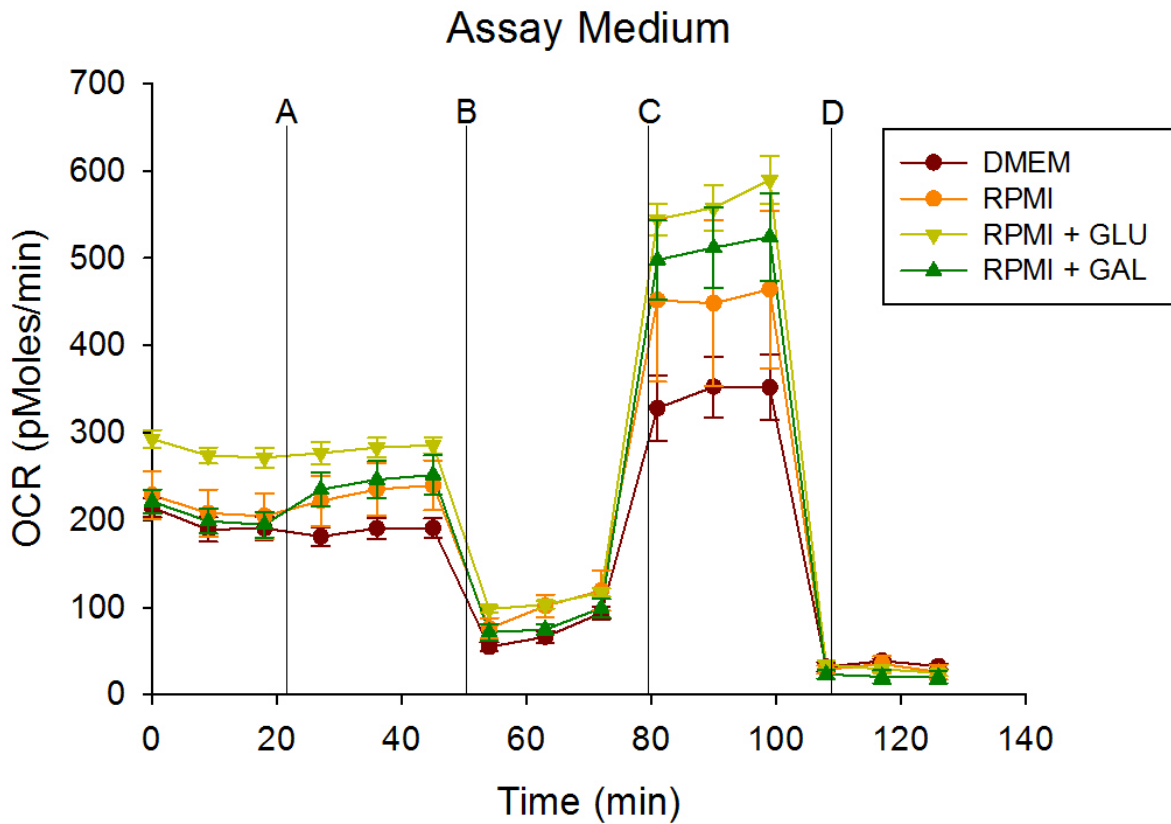


Figure 2.7. XF24 assay medium optimization. PC12 cells were seeded at a density of 70,000 cells/well and bioenergetics were assessed using the Mitochondrial Stress Test: A) 50mM pyruvate, B) 1 μ M oligomycin A, C) 1 μ M FCCP, and D) 1 μ M antimycin A. The assay was performed in either DMEM Assay Medium (red), RPMI 1640 Assay Medium (orange), RPMI 1640 + 2.5mM glucose (light green), or RPMI 1640 + 2.5mM galactose (dark green). Results demonstrate that RPMI 1640 + 2.5mM glucose was optimal.

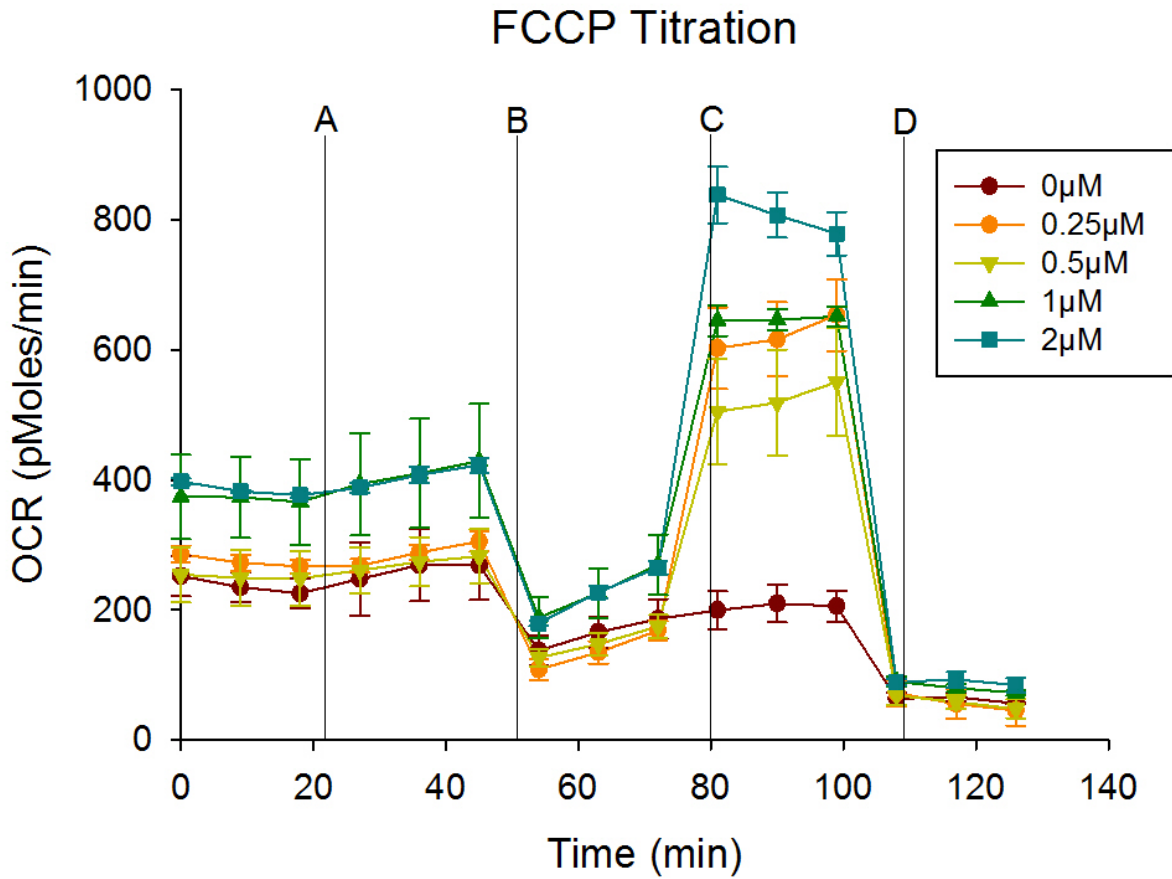


Figure 2.8. XF24 FCCP titration. PC12 cells were seeded at a density of 70,000 cells/well and bioenergetics were assessed using the Mitochondrial Stress Test: A) 50mM pyruvate, B) 1µM oligomycin A, and D) 1µM antimycin A. In port C FCCP was injected at concentrations of 0µM (red), 0.25µM (orange), 0.5µM (light green), 1µM (dark green), or 2µM (teal). Because 2µM FCCP produced maximum respiration without negatively altering oxygen consumption, this concentration was chosen for future experiments.

2.7. ALDH enzyme kinetics assay

PC12 cells were seeded in 6-well plates coated with poly-D-lysine at a density of 7×10^5 cells/mL and cultured for 24-48 h at 37°C/5% CO₂. At the time of treatment, growth medium was aspirated, replaced with HBS or HBS containing 2 μM MeHg, 50 nM rotenone, or 20 μM daidzin. Cells were incubated for 60 min with MeHg, 45 min with daidzin, or 15 min with rotenone at 37°C/5% CO₂. Following treatment, plates were centrifuged at 300 *g* for 5 min at 4°C. Treatment medium was aspirated and replaced with 150 μL homogenization buffer (0.1 M Tris-HCl, 10 mM DTT, 20% glycerol, and 1% Triton-X). Cells were scraped and then pelleted by centrifugation at 13,000 *g* for 8 min at 4°C. Protein concentration of supernatant was determined using the BCA protein assay (Sigma).

ALDH enzyme activity was determined spectrophotometrically by monitoring the reductive reaction of NAD to NADH at 340 nm using the Tecan Infinite® M1000 Pro microplate reader and Magellan data analysis software (Tecan Systems, Inc., San Jose, CA). Assays were carried out in 96-well plates containing 100 mM Tris-HCl buffer (pH 8.0) at 30°C. Two mM nicotinamide adenosine dinucleotide hydrate (NAD⁺; Sigma) and 100 μg PC12 cell lysate were added to the buffer. In some experiments, 2 μM MeHg, 50 nM rotenone, or 20 μM daidzin was added to the assay wells. To start the reaction, 10 mM propionaldehyde (Sigma) was added. Accumulation of NADH was recorded every 30 sec for 10 min. Substrate blanks (NAD + lysate) were run simultaneously and results were corrected for blank reactions. K_m was calculated using SigmaPlot 12.0 (SysStat Software, Inc., Point Richmond, CA, USA) and Michaelis–Menten kinetics were plotted to determine

the optimal concentration of substrate for future reactions (Figure 2.9). ALDH reaction rates were calculated as $\mu\text{mole NADH per min per mg protein}$.

Michaelis-Menten Kinetics

Substrate Inhibited

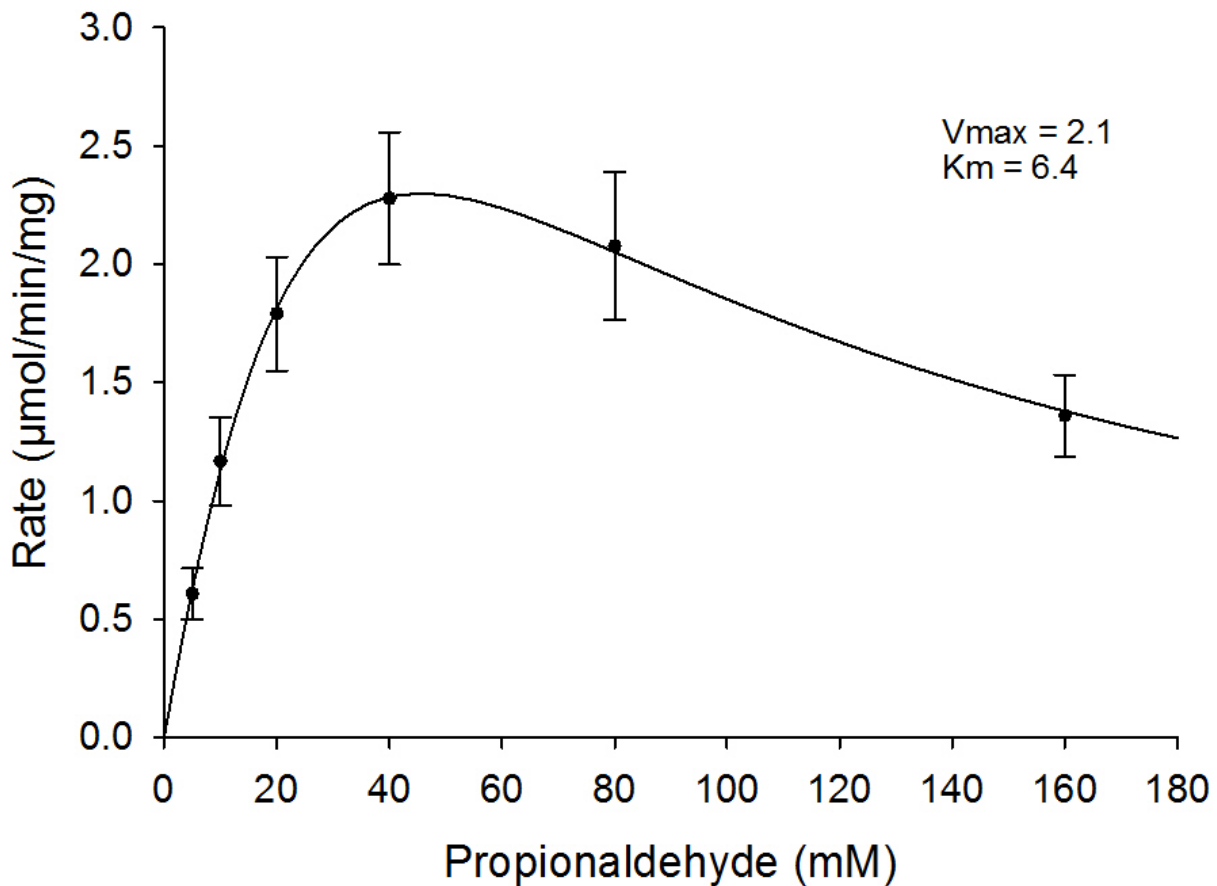


Figure 2.9. ALDH assay substrate optimization. In ALDH assays, propionaldehyde was used as the substrate. The K_m (concentration at which the reaction rate is half V_{max}) for propionaldehyde was determined. At concentration above 40mM, propionaldehyde inhibited ALDH activity. $V_{\text{max}} = 2.1\mu\text{mol}/\text{min}/\text{mg}$ protein and $K_m = 6.4\text{mM}$ propionaldehyde. Based on these results, 10mM propionaldehyde was selected for future experiments.

2.8. NADH/NAD quantification

PC12 cells were seeded in 6-well plates at 7×10^5 cells/mL and incubated at 37°C/5% CO₂ for 48 hr. At the time of treatment culture medium was aspirated and replaced with HBS for 60 min, 2µM MeHg in HBS for 60 min, or 50nM rotenone for 15 min. Following pharmacological exposure, treatment medium was aspirated, cells were washed once with cold PBS, and then pelleted by centrifugation at 10,000 *g* for 5 min at 4°C. NADH/NAD was extracted using 400µLNADH/NAD Extraction Buffer (Sigma) by two freeze/thaw cycles (20 min on dry ice followed by 10 min at room temperature). Samples were then vortexed for 10 sec and centrifuged for 10 min at 13,000 *g* to remove insoluble material. To quantify NAD, samples were measured as described below. For NADH measurements, 200µL was incubated at 60°C for 30 min before measurement.

A 96-well plate was loaded with 50µL sample (Figure 2.10) and 100µL Master Reaction Mix (NAD Cycling Buffer + NAD Cycling Enzyme; Sigma). Samples were incubated for 5 min to convert NAD to NADH, and then 10µL NADH Developer was added to each well. Samples were incubated for 1 hr at room temperature. Absorbance at 450nm was measured using spectrophotometry and the Tecan Infinite® M1000 Pro microplate reader with Magellan data analysis software (Tecan Systems, Inc., San Jose, CA). Average absorbance was compared to NADH standards to calculate the concentration of total NAD, total NADH, and the ratio of NAD:NADH.

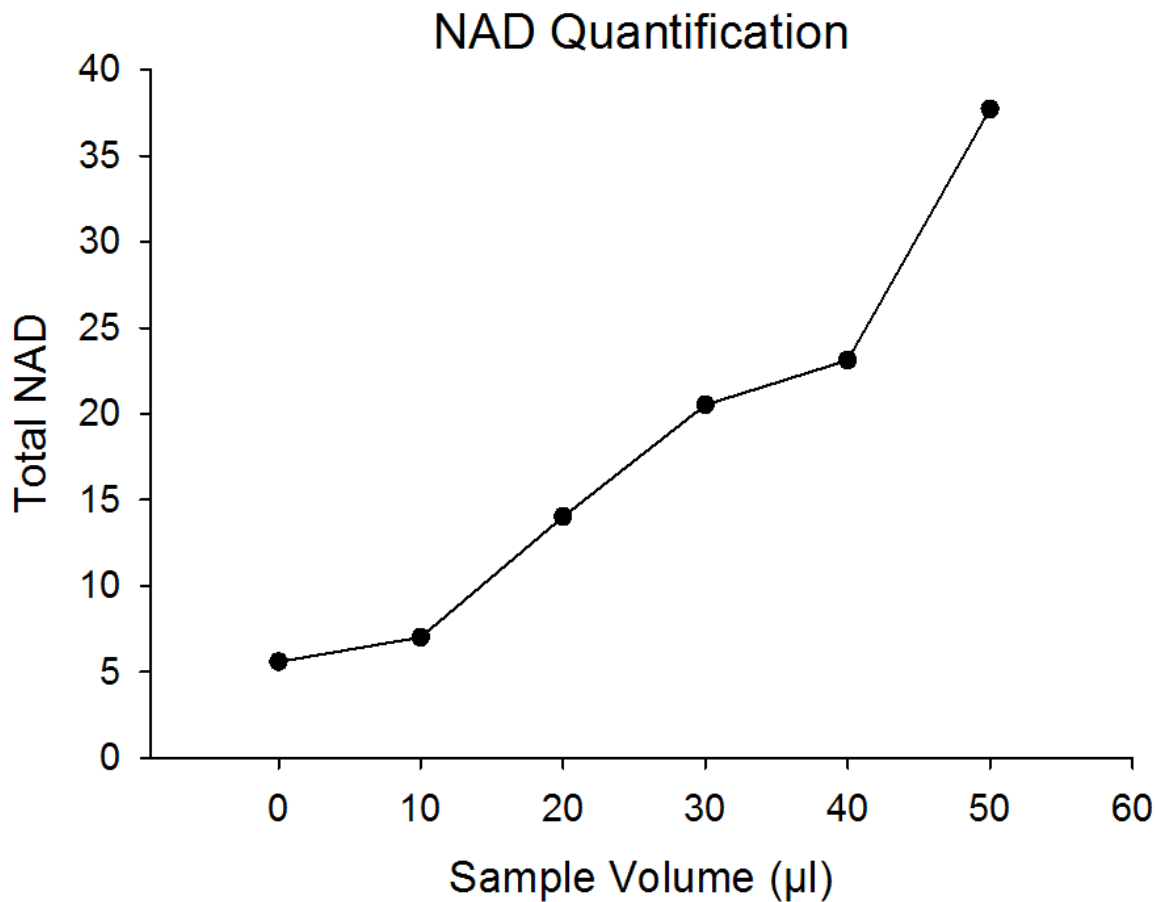


Figure 2.10. Sample volume titration for NADH/NAD quantification. NAD Cycling Enzyme was reacted with 0, 10, 20, 30, 40, or 50 µL cell lysate, and total NAD was quantified. Based on this optimization experiment, 50 µg lysate was selected as the volume for experimental analysis.

2.9. Measurement of fura-2 fluorescent change

Changes in the concentration of intracellular Ca^{2+} were monitored as changes in fluorescence of the ratiometric Ca^{2+} -indicating dye fura-2 using microfluorometric imaging. The perfusion buffer used in these experiments was always 0- Ca^{2+} HBS. PC12 cells were plated at 7×10^5 cells/mL on the upper surface of sterilized 25-mm diameter circular glass coverslips (Carolina Biological; Burlington, NC) in Petri dishes 24 hr prior to imaging. Cells were loaded with $2 \mu\text{M}$ fura-2 and $2 \mu\text{M}$ pluronic acid in RPMI culture medium and incubated in the absence or presence of $50 \mu\text{M}$ BAPTA/AM for 30 min at 37°C . After loading, the circular coverslip containing fura-2 loaded cells was mounted on an inverted microscope (Diaphot-TMD, Nikon, Toyko, Japan) and cells were perfused with 0- Ca^{2+} HBS containing $2 \mu\text{M}$ MeHg at 37°C . Digital fluorescent images were obtained using an IonOptix system (Milton, MA). Fura-2 fluorescence changes were monitored simultaneously in the soma of 10 cells within the same microscopic field. Data from these cells was used to visually analyze the time-to-onset of MeHg-induced changes in intracellular Ca^{2+} . These experiments were conducted to establish BAPTA/AM was chelating intracellular Ca^{2+} . Representative soma were selected to illustrate effects of 0- Ca^{2+} HBS and BAPTA/AM on MeHg-induced changes in intracellular Ca^{2+} .

2.10. Statistical analyses

SigmaPlot® software version 12.0 (SysStat Software, Inc., Point Richmond, CA) was used to make statistical comparisons among groups using unpaired t-test, one-, two-way ANOVA, or non-parametric alternatives as appropriate. If a significant difference was detected, *post hoc* analysis was followed by between-group comparisons using Tukey's test. Differences with a probability of error of less than 5% were considered statistically significant ($p < 0.05$).

Chapter 3. The role of *de novo* catecholamine synthesis in mediating MeHg-induced vesicular DA release

3.1. Introduction

Release of DA occurs predominantly by means of canonical Ca^{2+} -dependent vesicular exocytosis. In PC12 cells, DA is stored in large dense-core vesicles concentrated near the plasma membrane (Bauerfeind et al., 1993; Fornai et al., 2007), and released following cellular depolarization (Greene and Rein, 1977a; Kittner et al., 1987). Released DA is primarily recaptured by the NET in undifferentiated PC12 cells (Zhu and Hexum, 1992; Brüss et al., 1997). However certain cellular conditions, such as exposure to psychostimulant drugs (Sulzer et al., 1995), can reverse the transporter resulting in DA leakage into the synaptic cleft (Leviel, 2011).

DA release is, in part, regulated by DA synthesis. Once synthesized, DA inhibits TH activity by binding the catalytic site of the enzyme, and also by interfering with the interaction between TH and its cofactor, tetrahydrobiopterin (Kumer and Vrana, 1996; Dunkley et al., 2004). This end-product feedback inhibition decreases the rate of DA synthesis, and thus down-regulates DA release. Conversely, TH phosphorylation at critical Ser residues by a variety of protein kinases increases enzymatic activity (Daubner et al., 2011). Phosphorylation alters the conformation of DA-inhibited TH, which dissociates catecholamine from enzyme, and allows TH to return to its active state. The most important site of phosphorylation is at Ser residue 40 (Ser40), which directly increases TH activity (Daubner et al., 1992; Dunkley et al., 2004). Phosphorylation of other serine

resides, namely Ser19 and Ser31, serves to stabilize phosphorylation at Ser40 (pTH Ser40) (Royo et al., 2005).

MeHg stimulates spontaneous neurotransmitter release, but impairs depolarization-evoked transmitter release (Atchison and Narahashi, 1982; Atchison et al., 1984). This effect has been demonstrated in many neurotransmitter systems, including the dopaminergic system (Minnema et al., 1989). MeHg increases spontaneous DA release in a concentration-dependent manner through a presynaptic action (Kalisch and Racz, 1996; Faro et al., 2002; Dreiem et al., 2009; Tiernan et al., 2013).

Results of studies investigating the mechanisms underlying the stimulatory effects of MeHg on dopaminergic neuronal transmission have been inconsistent with respect to the underlying mechanisms responsible for MeHg-induced DA release. A role for DAT reversal has been proposed based on the finding that DAT inhibition or stimulation of transporter-mediated release produces an effect similar to that of MeHg alone (Faro et al., 2002). However, MeHg does not target DAT to induce release (Gassó et al., 2000), and may decrease transporter reuptake activity (Bonnet et al., 1994; Dreiem et al., 2009).

A role for vesicular exocytosis in MeHg-induced catecholamine release has been documented (Gassó et al., 2000), however non-vesicular DA release has also been described following MeHg exposure (Kalisch and Racz, 1996; Faro et al., 2002). Despite the coupling between neurotransmitter release and synthesis, no reports to date have investigated a potential role for DA synthesis in MeHg-mediated release. Therefore the goals of the present study were to: 1) identify pathways by which MeHg induces spontaneous DA release, differentiating between transporter-mediated and non-

transporter mediated release, and 2) examine the coupling between DA synthesis and MeHg-induced DA release.

3.2. Methods

3.2.1. Chemicals

MeHg (ICN Biochemicals), reserpine (Sigma), desipramine (DMI; Sigma), α -methyltyrosine (AMT; Sigma), and 3-hydroxybenzylhydrazine (NSD-1015; Sigma) were diluted from stock solutions in HBS. Drug solutions were diluted to final concentrations on the day of each experiment as described in General Methods Section 2.2.

3.2.2. Chemical treatment

PC12 cells were seeded at a density of 6×10^5 cells/mL in 6-well plates coated with poly-D-lysine 48 hr prior to treatment. To begin each experiment, culture medium was aspirated and replaced with HBS or HBS containing pharmacological treatment (with the exception of 24hr AMT pretreatment, which was prepared in RPMI-1640 culture medium). Cells were incubated at 37°C/5% CO₂ during treatment as described in General Methods Section 2.2.

3.2.3. Neurochemistry

At experiment termination, treatment medium was retained and acidified. Cells were rinsed, harvested, and pelleted by centrifugation. The content of DA and its precursor DOPA in the treatment medium and cell pellet were determined using HPLC-ED as

described in General Methods Section 2.3. Neurochemical concentrations were normalized to mL per sample for extracellular measurements or mg of protein for intracellular measurements as determined using the BCA protein assay (Sigma).

The rate constant was calculated from intracellular DA concentrations after 90 min AMT treatment as described in General Methods Section 2.3.1. The slope of the lines representing the difference between cells treated with 2 μ M MeHg alone or combined with 300 μ M AMT was calculated, and then compared to HBS-treated cells in the absence or presence of AMT.

3.2.4. Western blot analysis

At experiment termination, treatment medium was collected and analyzed as a positive control. Cells were rinsed once with 1 mL ice-cold phosphate buffered saline, harvested, and pelleted by centrifugation at 12,000 *g* for 5 min at 4°C. Pellets were lysed with 50 μ L radio-immunoprecipitation assay (RIPA) buffer containing protease inhibitor (1:100) and phosphatase inhibitor (1:100). Protein content was determined using the BCA protein assay (Sigma). Supernatant was prepared for Western blot analysis to quantify total and phosphorylated isoforms of TH as described in General Methods Section 2.5. TH and pTH Ser40 bands were normalized to the β -actin signal to correct for variations in loading.

3.2.5. Cell viability

PC12 cells were seeded in 96-well plates coated with poly-D-lysine at a density of 4×10^5 cells/mL 48 hr prior to treatment with HBS, 1, 2, or 5 μ M MeHg for 15, 30, 60 or 120

min. Hoechst 33342 (10 mg/mL) and propidium iodide (1 mg/mL) were diluted 1:10,000 in existing treatment medium. Cells were incubated in fluorophores at 37°C for 15 min prior to visualization. Image acquisition was as described in General Methods Section 2.4. Viable cells had a blue-stained (Hoechst) nucleus, whereas non-viable cells had a high intensity red (propidium iodide) fluorescence (Yuan et al., 2009).

3.2.6. Statistical analysis

SigmaPlot® software version 12.0 (SysStat Software, Inc., Point Richmond, CA) was used to make statistical comparisons among groups using unpaired t-test, one-, two-way ANOVA, or non-parametric alternatives as appropriate. If a significant difference was detected, *post hoc* between-group comparisons were performed using Tukey's test. Statistically significance was set at $p < 0.05$.

3.3. Results

3.3.1. MeHg increases spontaneous DA release in a concentration- and time-dependent manner

Measurements of DA in the medium reflect the balance between changes in DA release and transporter-mediated reuptake. DA was not detected in treatment medium in the absence of cells and any subsequent treatment-induced change in medium DA was, therefore, due to cellular DA release. In the absence of MeHg, the concentration of extracellular DA stabilized within the first 15 min, and remained at a steady state throughout the 120 min sampling period (Figure 3.1). MeHg caused both a concentration- and time-dependent increase in medium DA. At 1 μ M, MeHg did not significantly alter

extracellular DA accumulation, whereas 2 μM and 5 μM MeHg significantly increased the concentration of extracellular DA by 60 min and 30 min, respectively. These elevated levels were maintained for the duration of the experiment. The significant increase in extracellular DA concentrations induced by 5 μM MeHg at 60 and 120 min was associated with a significant incidence of cytotoxicity in a parallel set of cultures (Figures 3.2-3.3). Because 2 μM MeHg induced a significant increase in DA release by 60 min without inducing significant levels of cytotoxicity, this concentration and time point was selected for further analysis of release mechanisms.

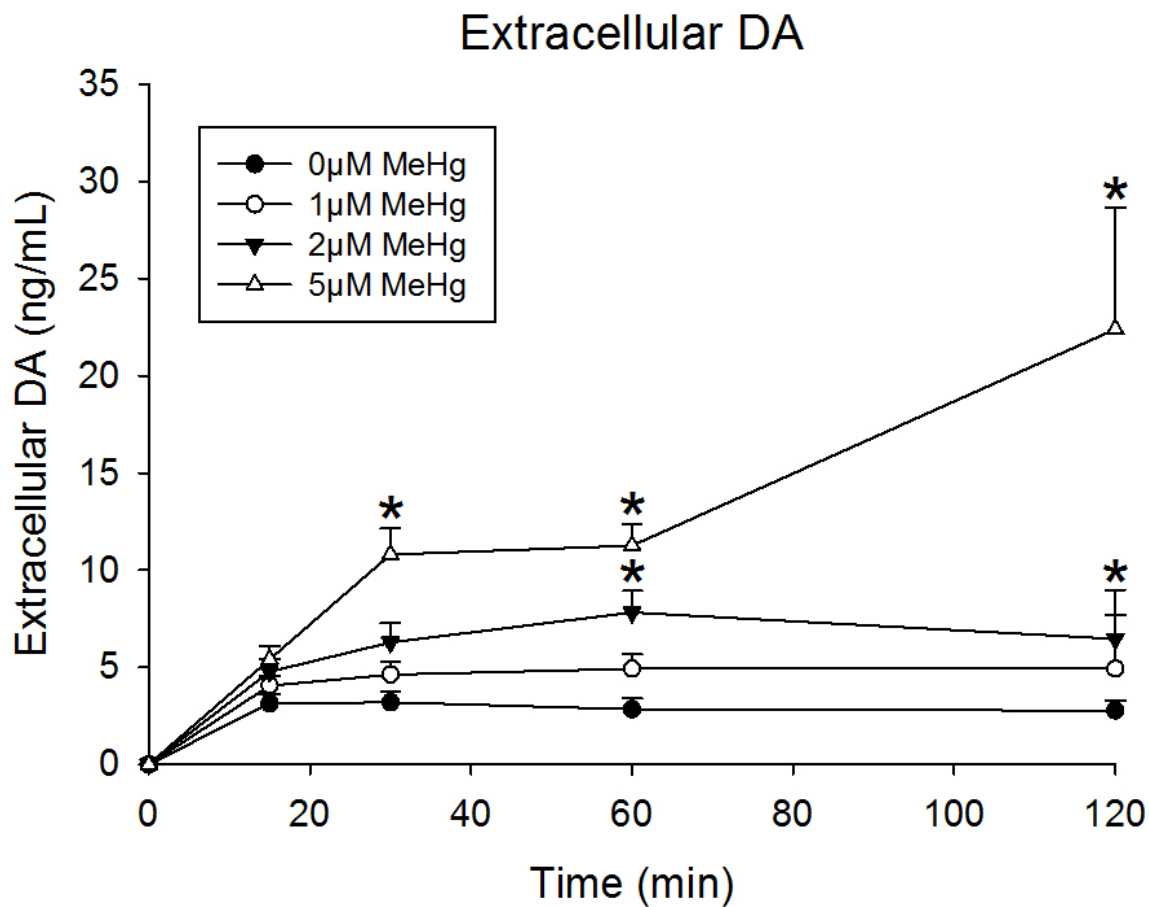


Figure 3.1. Concentration-response and time-course effects of MeHg on extracellular DA concentrations. Undifferentiated PC12 cells were treated with 0 μM (black circles), 1 μM (white circles), 2 μM (black triangles) or 5 μM (white triangles) MeHg in HBS for 15, 30, 60, or 120 min. The asterisk (*) indicates a value significantly different than 0 μM MeHg within a given time point ($p < 0.05$). Values are means + S.E.M. ($n = 3-4$, 3 replicates per n).

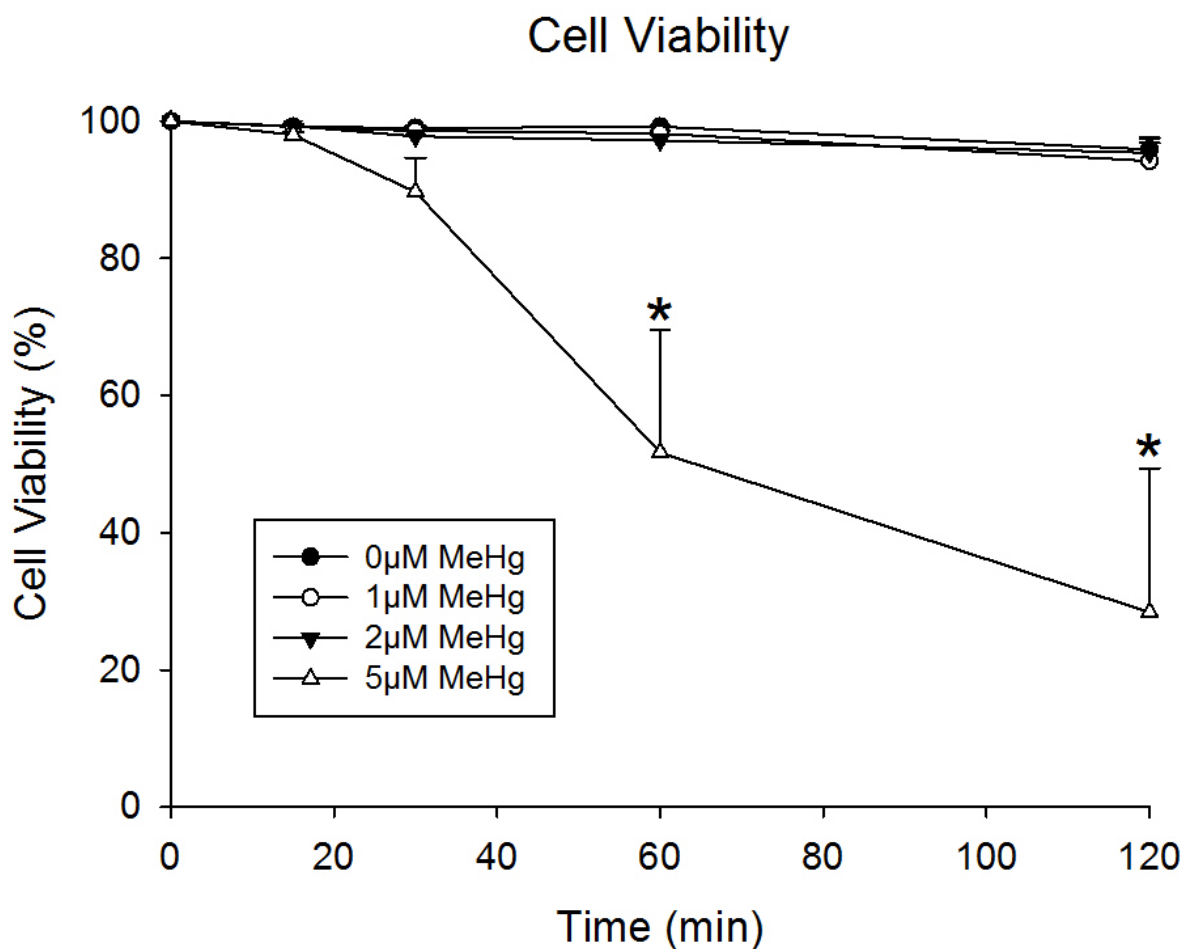


Figure 3.2. Concentration-response and time-course effects of MeHg on cell viability. Undifferentiated PC12 cells were exposed to 0µM (black circles), 1µM (white circles), 2µM (black triangles), or 5µM (white triangles) MeHg in HBS for 15, 30, 60, or 120 min. Following toxicant treatment, cultures were stained for viable (Hoechst 33342) and non-viable (propidium iodide) cells. The number of viable and non-viable cells was counted and expressed as percent live cells. The asterisk (*) indicates a value significantly different than 0 µM MeHg within a given time point ($p < 0.05$). Values are means + S.E.M ($n = 3$, 3 replicates per n).

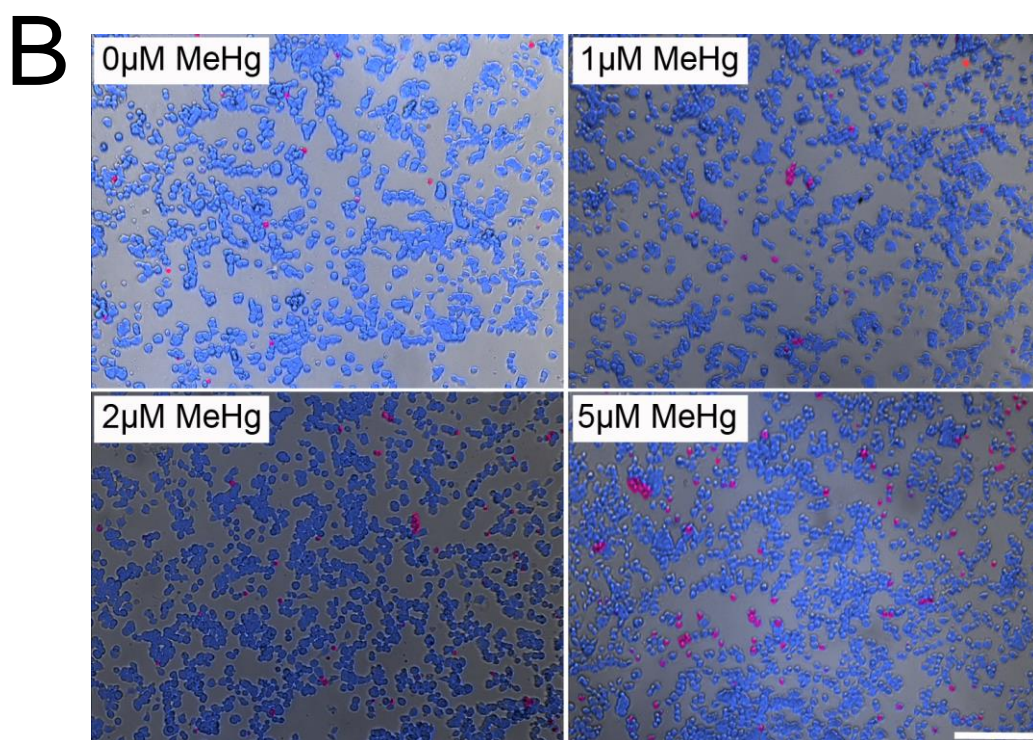
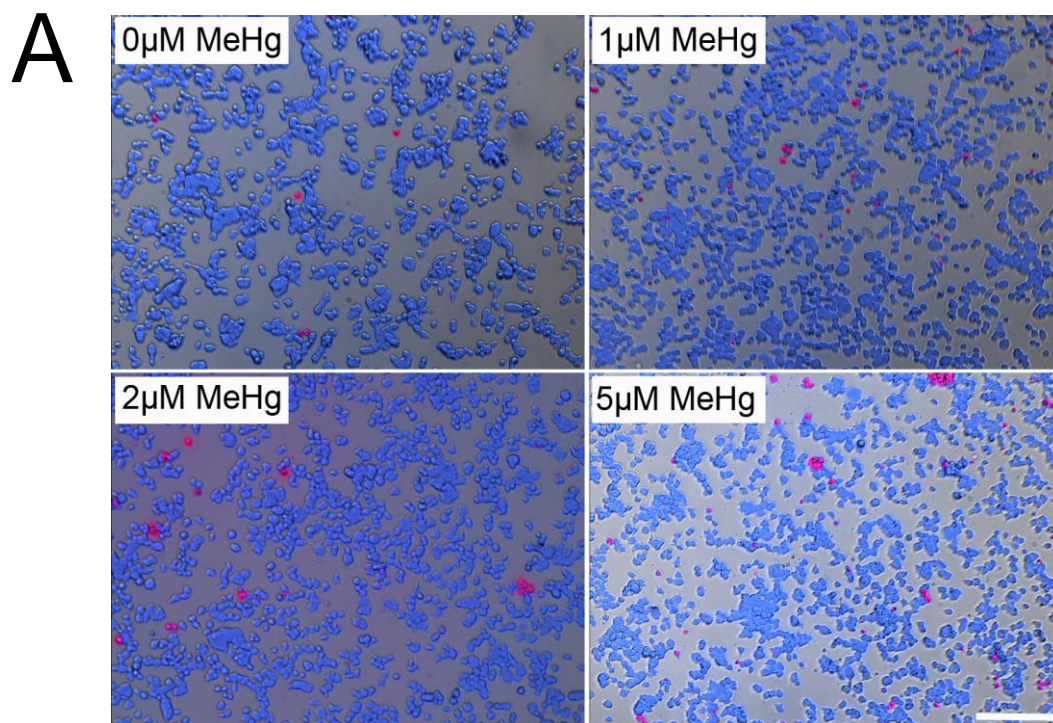
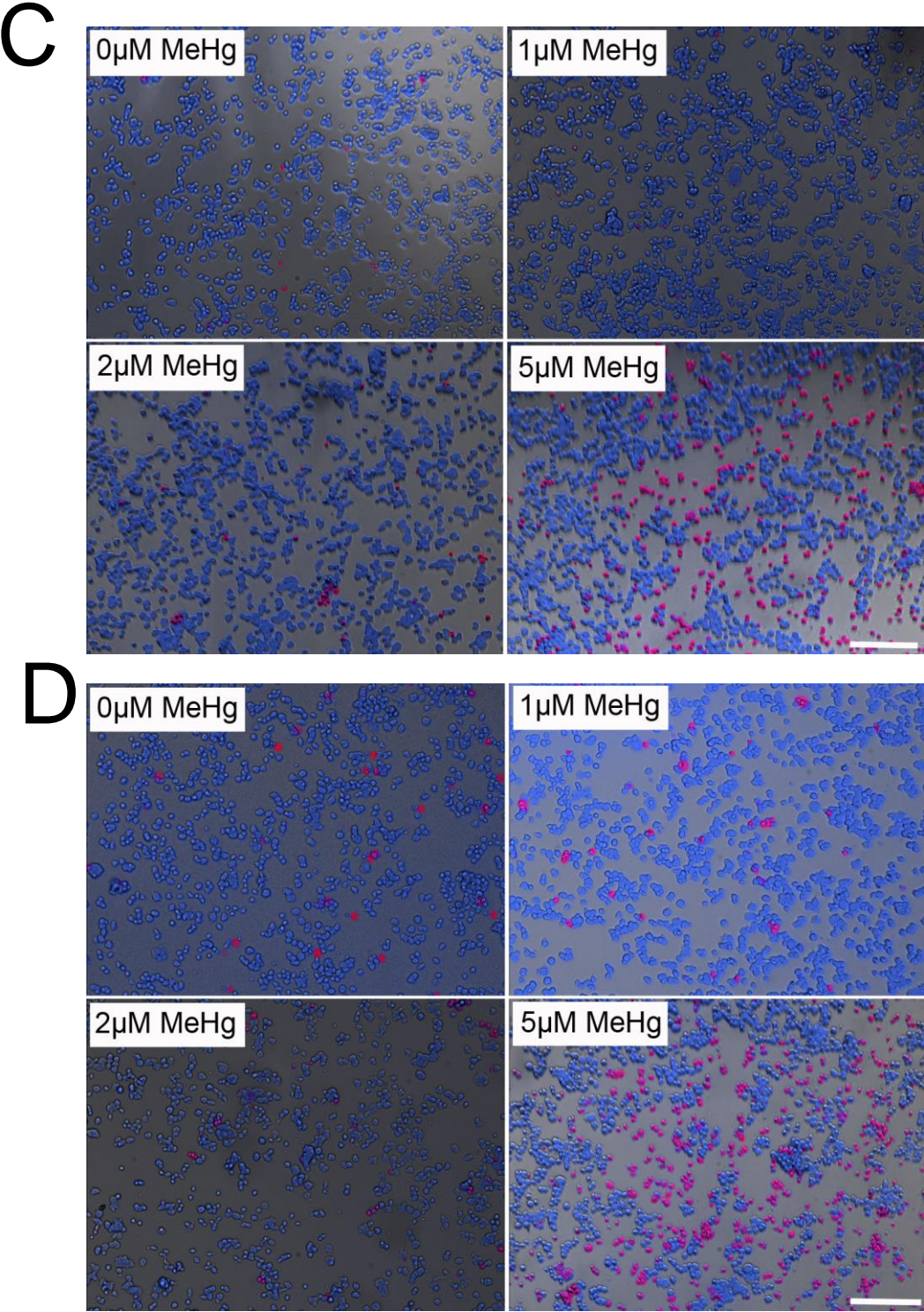


Figure 3.3. Representative images of cell viability. Undifferentiated PC12 cells were exposed to 0, 1, 2, or 5 μM MeHg in HBS for 15 (Panel A), 30 (Panel B), 60 (Panel C), or 120 (Panel D) min. Viable cells have a blue-stained (Hoechst) nucleus, whereas non-viable cells have an intense red (propidium iodide) fluorescence. Scale bar = 200 μm

Figure 3.3 cont'd



3.3.2. Spontaneous MeHg-mediated DA release requires a functional vesicular, but not membrane, transporter

To investigate the contributions of vesicular release and reuptake transporter activity in spontaneous MeHg-mediated DA release from PC12 cells, reserpine was used to inhibit the VMAT (Schuldiner et al., 1993) and DMI was used to block the NET (Brüss et al., 1997). Reserpine (50 nM) decreased spontaneous basal release and blocked the significant increase in extracellular DA induced by MeHg. In contrast, DMI had no significant effect on extracellular DA concentration ($p > 0.05$), but significantly augmented MeHg-induced DA release ($p < 0.05$; Figure 3.4A). However, while reserpine significantly attenuated the percentage change in extracellular DA induced by MeHg, DMI did not ($p > 0.05$, Figure 3.4B).

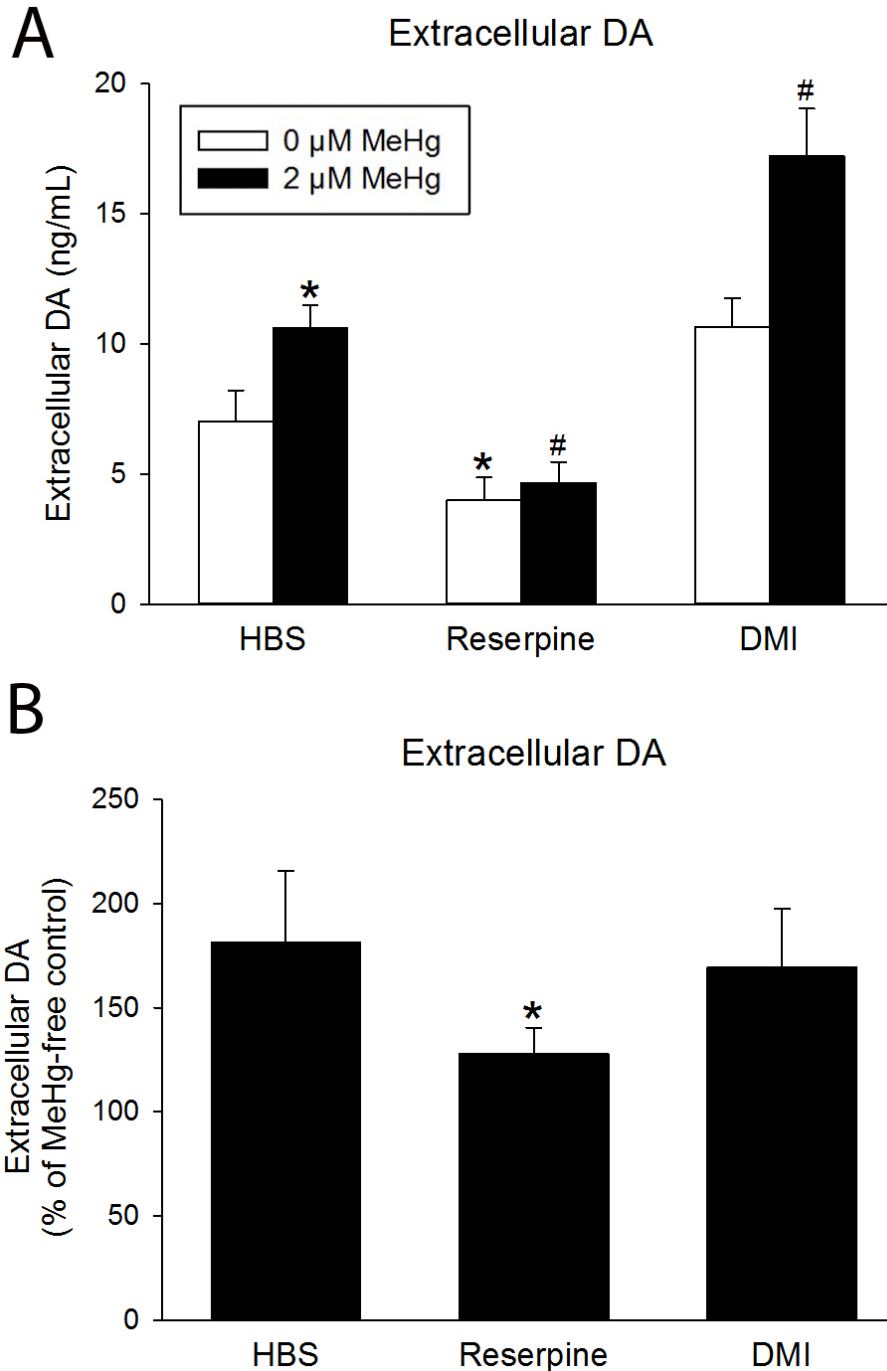


Figure 3.4. Effects of DA storage depletion and reuptake transporter inhibition on MeHg-induced DA release. Panel A) Concentrations of extracellular DA from undifferentiated PC12 cells preincubated with 50 nM reserpine for 60 min, 1 μ M DMI for 15 min, or vehicle in culture medium prior to co-treatment with 0 μ M (white bars) or 2 μ M (black bars) MeHg in HBS for 60 min. Panel B) The percentage change of extracellular DA after treatment with MeHg in cells treated with HBS, 50 nM reserpine, or 1 μ M DMI. The asterisk (*) indicates a value significantly different than HBS ($p \leq 0.05$). The hash (#) indicates a value significantly different than 2 μ M MeHg-HBS ($p \leq 0.05$). Values are means + S.E.M. ($n = 3$, 3 replicates per n).

3.3.3. MeHg-mediated DA release is associated with increased intracellular DA concentrations and utilization of DA stores

Spontaneous DA release induced by MeHg was associated with a significant increase in the concentration of intracellular DA (Figure 3.5). To determine if increased DA stores correlated with increased release, DA storage utilization was assessed using AMT (Brodie et al., 1966). The rate constant of decline of intracellular DA was significantly greater in MeHg-treated cells as compared to HBS-treated cells ($p < 0.05$), demonstrating that utilization of DA stores was significantly increased following MeHg exposure (Figure 3.6).

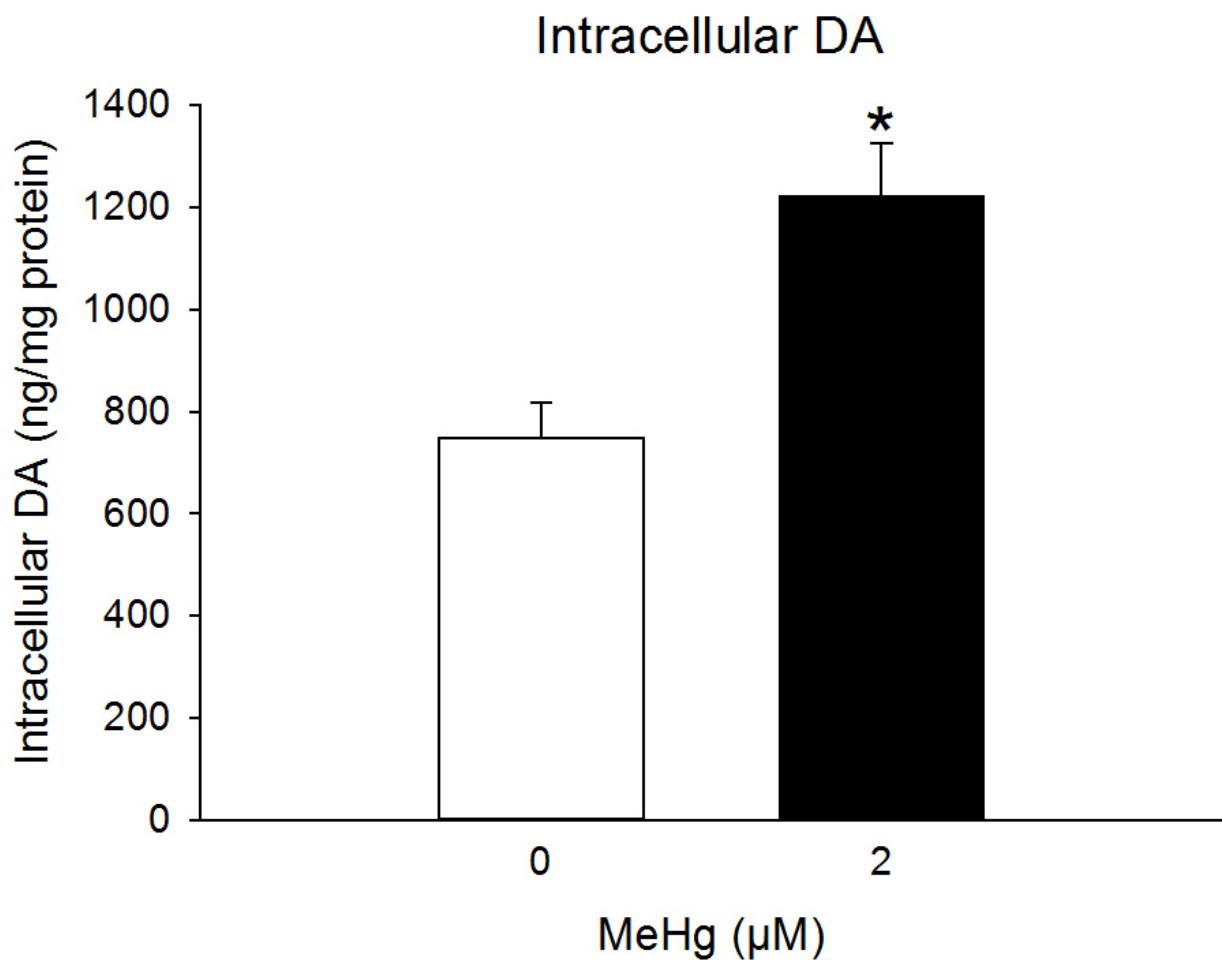


Figure 3.5. Effect of MeHg on intracellular DA concentrations. Undifferentiated PC12 cells were treated with either 0 µM (white bars) or 2 µM (black bars) MeHg in HBS for 60 min. The asterisk (*) indicates a significant difference from 0 µM MeHg ($p \leq 0.05$). Values are means + S.E.M. ($n = 3$, 3 replicates per n).

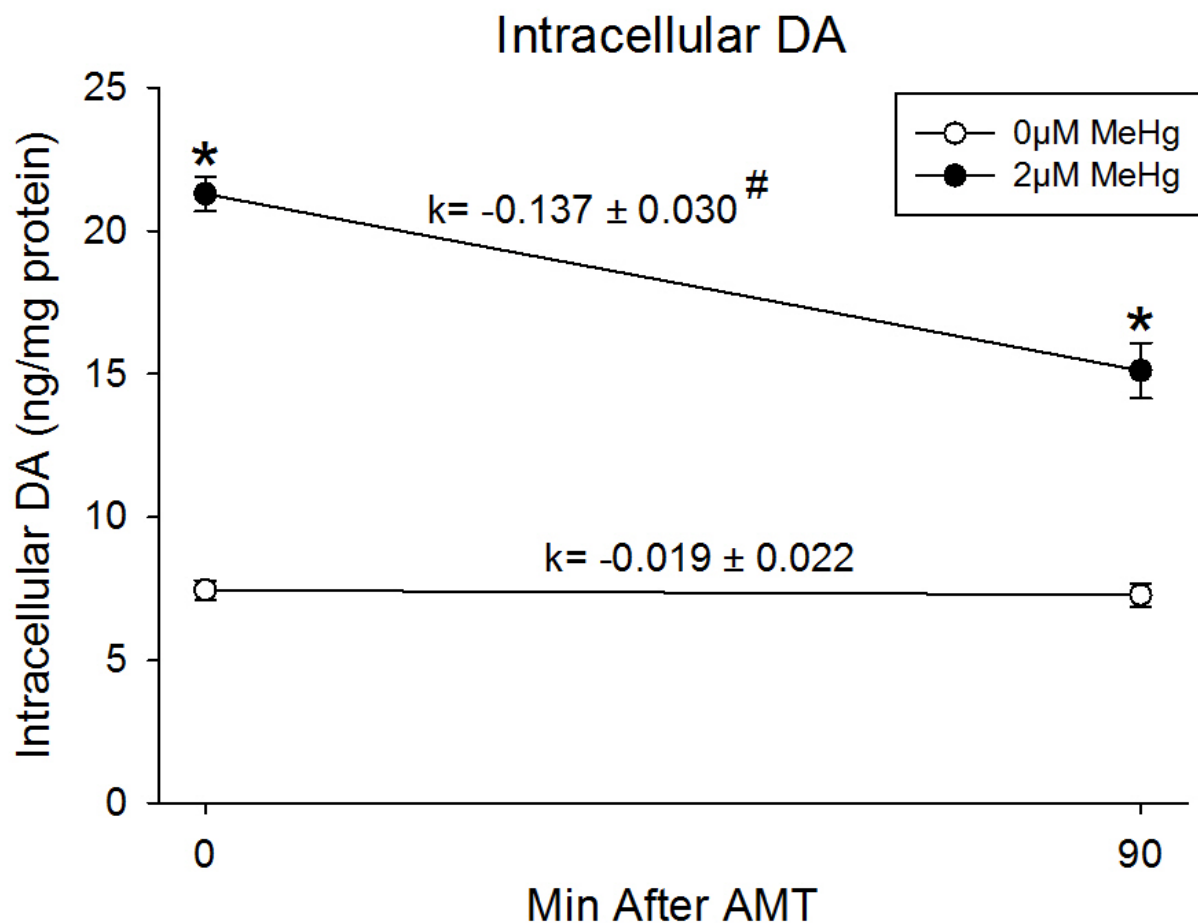


Figure 3.6. Effect of MeHg on DA storage utilization. Undifferentiated PC12 cells were preincubated with 300 μ M AMT or vehicle in culture medium for 30 min prior to treatment with either 0 μ M (white circles) or 2 μ M (black circles) MeHg in HBS in the absence or presence of 300 μ M AMT for 60 min. The rate constant (k) was calculated as the slope of the line between 0 and 90 min after AMT. The asterisk (*) indicates a value significantly different than 0 μ M MeHg within a given time point ($p \leq 0.05$). The hash (#) indicates a significant difference between rate constant values ($p \leq 0.05$). Values are means \pm S.E.M. ($n = 3$, 3 replicates per n).

3.3.4. MeHg-mediated DA release is associated with *de novo* DA synthesis and increased TH enzymatic activity

To examine the role of *de novo* DA synthesis in MeHg-mediated DA release, PC12 cells were treated with either the competitive TH inhibitor AMT (300 μ M) for 24 hr or the inhibitor of DOPA decarboxylase NSD-1015 (10 μ M) for 60 min. Complete inhibition of DA synthesis with AMT abolished the MeHg-mediated increase in extracellular DA concentrations, but did not alter basal DA release (Figure 3.7). The DA precursor DOPA was not detectable except in the presence of NSD-1015, after which its concentration was proportional to the rate of TH enzymatic activity. MeHg significantly increased the concentration of intracellular DOPA as compared to untreated cells (Figure 3.8). Western blot analysis of total and phosphorylated TH protein revealed that MeHg significantly increased the amount of pTH Ser40, without altering total TH protein (Figure 3.9).

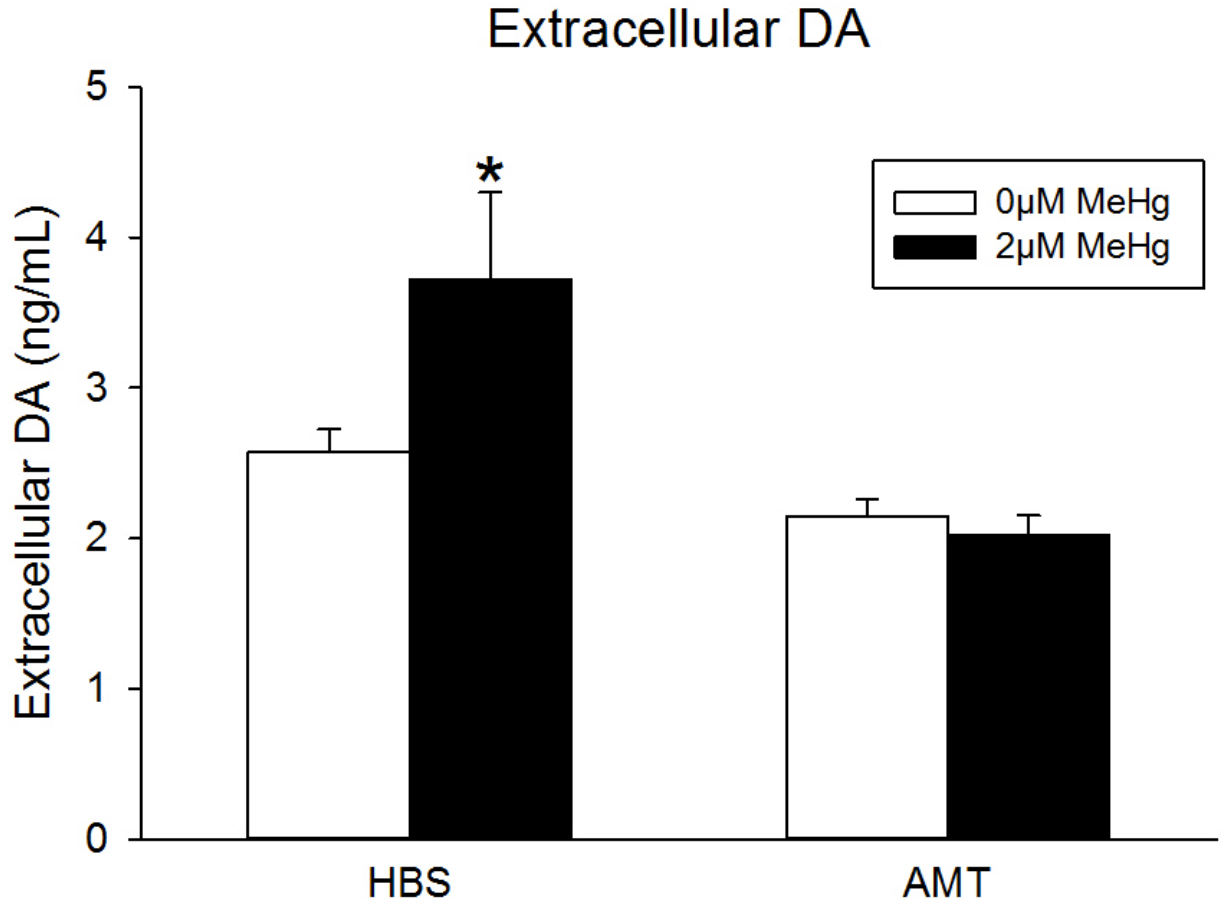


Figure 3.7. Effect of TH inhibition on MeHg-induced DA release. Undifferentiated PC12 cells were preincubated with 300 μ M AMT or vehicle in culture medium for 24 hr prior to co-treatment with either 0 μ M (white bars) or 2 μ M (black bars) MeHg in HBS for 60 min. The asterisk (*) indicates a value significantly different than 0 μ M MeHg-HBS ($p \leq 0.05$). Values are means + S.E.M. ($n = 3$, 3 replicates per n).

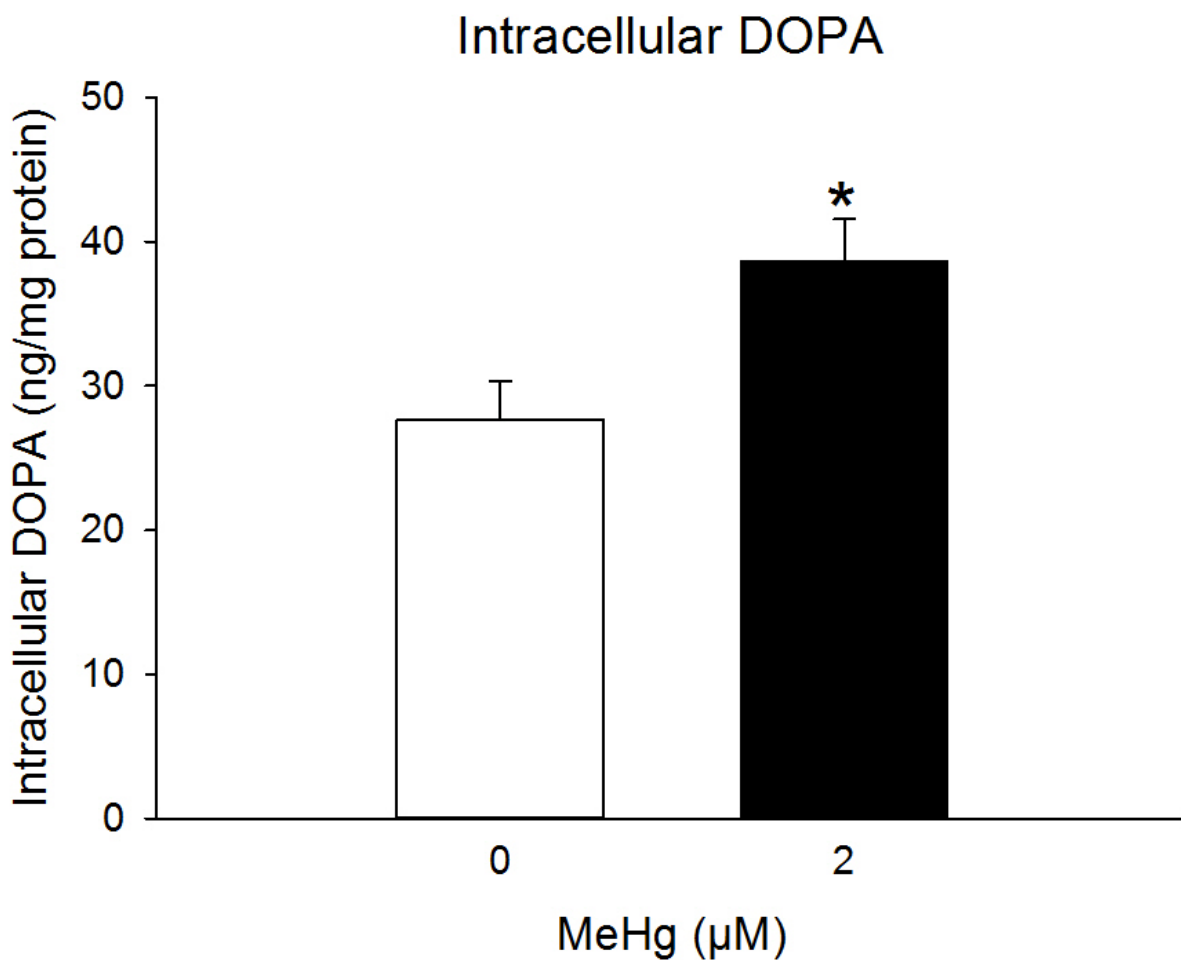


Figure 3.8. Effect of DOPA decarboxylase inhibition on TH enzymatic activity.

Undifferentiated PC12 cells were treated with 0 μM (white bars) or 2 μM (black bars) MeHg in HBS for 60 min, in the presence of 10 μM NSD-1015. DOPA accumulation was quantified using HPLC-ED as an index of TH enzymatic activity. The asterisk (*) indicates a significant difference between groups ($p \leq 0.05$). Values are means + S.E.M. ($n = 4, 3$ replicates per n).

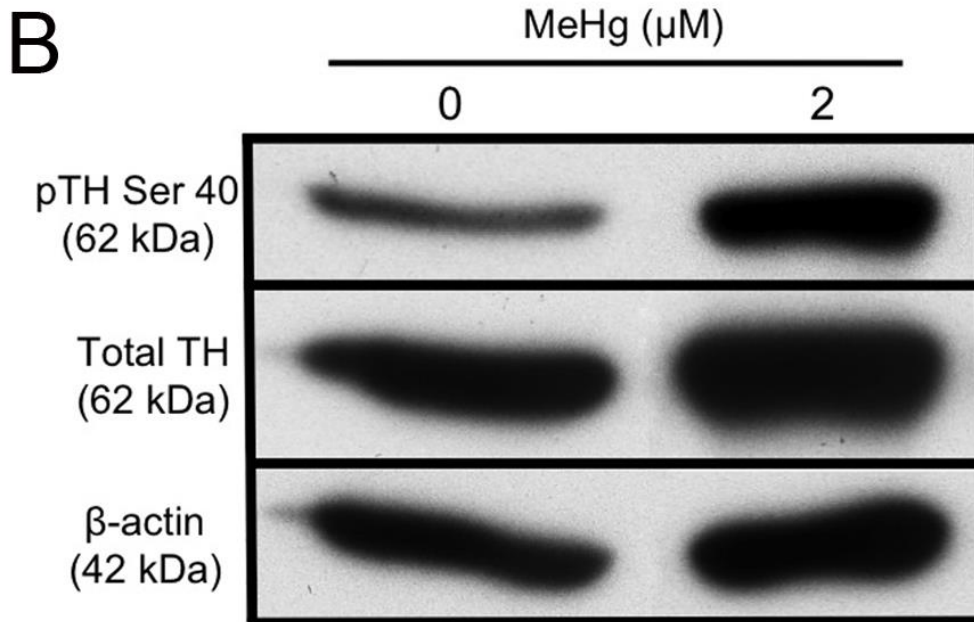
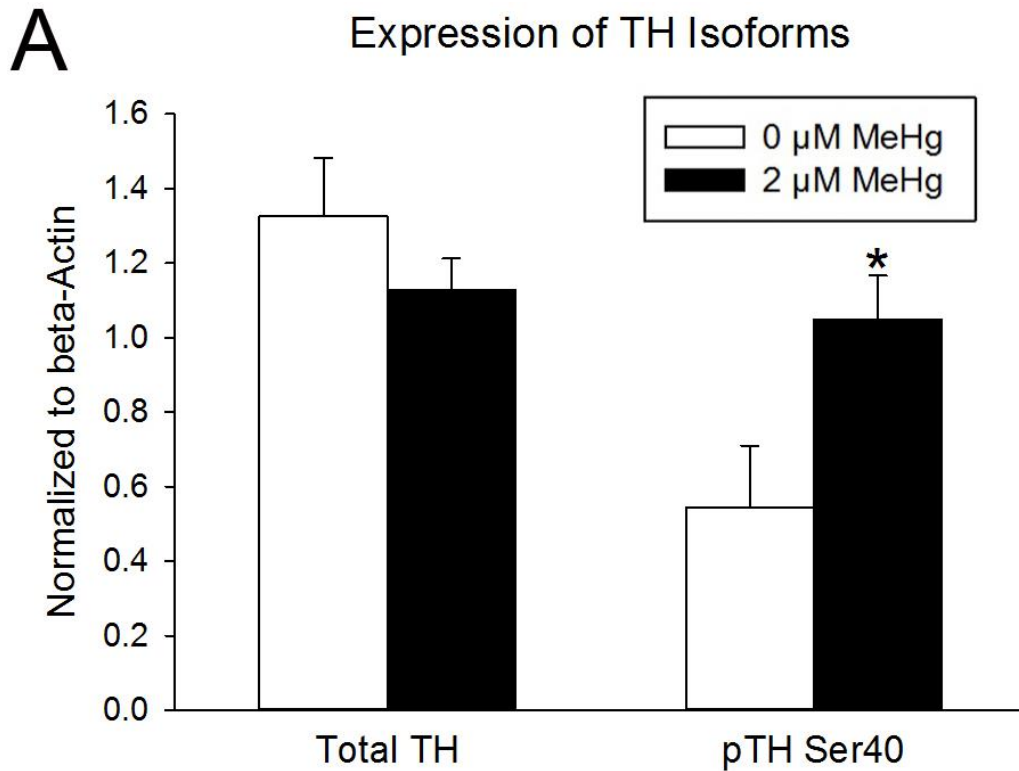


Figure 3.9. Effect of MeHg on TH expression. Panel A) Undifferentiated PC12 cells were treated with 0 μM (white bars) or 2 μM (black bars) MeHg in HBS for 60 min. Amounts of total TH and pTH Ser40 were quantified by Western blot and normalized to the level of expression of the housekeeping protein β -actin. The asterisk (*) indicates a significant difference between groups ($p \leq 0.05$). Values are means + S.E.M. ($n = 3$, 3 replicates per n). Panel B) Representative Western blot images for Total TH, pTH Ser40, and β -actin in cells treated with 0 μM or 2 μM MeHg.

3.4. Discussion

The present study contributes significantly to our understanding of mechanisms by which MeHg induces spontaneous DA release, in particular its interaction with the coupling between synthesis and vesicular exocytosis. These data are consistent with the following conclusions: 1) MeHg causes a concentration- and time-dependent increase in DA release from undifferentiated PC12 cells; 2) vesicular exocytosis, but not reuptake transporter activity, is responsible for both basal and MeHg-induced DA release; and 3) MeHg-induced DA release is dependent upon *de novo* DA synthesis and accelerated TH activity.

3.4.1. MeHg-induced DA release

Under basal conditions, DA release from PC12 cells is maintained at a steady state. During the first 15 min DA concentrations increased from 0 ng/mL to ~3 ng/mL, and then did not fluctuate significantly for the remainder of the experiment. The consistent level of extracellular DA in the medium likely reflects coupling between release and reuptake under basal conditions (Schmitz et al., 2003).

Increased DA release after exposure to MeHg has been well documented in other systems, including ³H-DA release from rat striatum (Minnema et al., 1989) and endogenous DA release from striatal synaptosomes (Dreiem et al., 2009), mouse striatal slices (Kalisch and Racz, 1996), and the striatum of conscious, free-moving rats (Faro et al., 2002). Results from the present study replicate these observations and demonstrate that MeHg-induced DA release is both concentration- and time-dependent. Low concentrations of MeHg (1 μM) do not alter DA release, however higher concentrations (2-5 μM) increase release. Furthermore, 5 μM MeHg increases DA release more rapidly than did 2 μM.

The increase in extracellular DA after exposure to 5 μM MeHg at 60 and 120 min was substantially higher than that observed at lower concentrations, but was more variable, and associated with an increased incidence of cell death. Exposure to 5 μM MeHg has previously been associated with rapid impairment of mitochondrial activity and membrane lysis consistent with necrotic cell death (Castoldi et al., 2000). Therefore it is hypothesized that as PC12 cells lyse, DA would be purged from the cell and increase its extracellular concentration above that expected in intact cells. DA released upon cell lysis would account for the sizable increase in extracellular DA and associated high variability. On the other hand, 2 μM MeHg increased DA release by 60 min, an effect not associated with cell death. The increase in DA release in the absence of cell death demonstrates that MeHg-induced DA release is associated with intracellular mechanisms unrelated to cell lysis. Ca^{2+} plays an essential role in neurotransmitter release and Ca^{2+} -dependent neurotransmitter release is a known target of MeHg toxicity (Atchison and Narahashi, 1982; Atchison, 1986; Yuan and Atchison, 2007). Therefore MeHg-induced Ca^{2+} signaling could be a primary site of action linking MeHg exposure to increased DA release.

3.4.2. Vesicular transport, but not membrane transport contributes to MeHg-induced DA release

Vesicular exocytosis and transporter-mediated reuptake are essential components of catecholamine release and recycling in PC12 cells (Lorang et al., 1994; Kishimoto et al., 2005; Fornai et al., 2007). In the present study, depletion of storage vesicles decreased basal release, confirming a role for vesicular stores in DA release from undifferentiated

PC12 cells. NET inhibition caused a small, although non-significant, increase in extracellular DA, likely due to inhibition of re-uptake of released DA.

Depletion of DA stores with reserpine abolishes MeHg-induced DA release. These data suggest that mobilization of vesicular DA stores contributes to the stimulatory effect of MeHg on DA release. A role for vesicular exocytosis in MeHg-induced catecholamine release is consistent with reports in the literature demonstrating that reserpine pretreatment blocks MeHg-induced ^3H -NE release from hippocampal slices (Gassó et al., 2000).

In the present study inhibition of the PC12 DA transporter NET increased DA release above that induced by MeHg alone. However the percentage change in extracellular DA after MeHg was comparable in control and DMI groups. This suggests that NET is functionally active, and does not contribute to the rise in extracellular DA following exposure to MeHg. In contrast, DAT transporter activity is reportedly decreased following exposure to MeHg (Bonnet et al., 1994; Dreiem et al., 2009), due to either a direct interaction between MeHg and the thiol group on DAT (Bonnet et al., 1994), or indirectly through inhibition of the Na^+/K^+ ATPase (Berg and Miles, 1979) or reduction of ATP needed to maintain the ion gradient used by the transporter (Torres et al., 2003; Gatti et al., 2004). In the present study it is possible that reuptake by the NET was partially inhibited by MeHg because addition of DMI to MeHg produced a larger increase in extracellular DA than either MeHg or DMI treatment alone.

3.4.3. Evidence for a role of de novo DA synthesis in MeHg-induced DA release

MeHg-induced DA release was accompanied by an increase in intracellular DA stores and acceleration of DA storage utilization. Increased DA stores could result from either stimulated DA synthesis and/or impaired DA metabolism. MeHg impairs DA metabolism; concentrations of the DA metabolites DOPAC and homovanillic acid are significantly decreased following exposure to MeHg (Chapter 4) (Dreiem et al., 2009). However, the increased rate of storage utilization following MeHg exposure also suggests a role for DA synthesis. Newly synthesized DA is preferentially released (Kopin, 1968), thus MeHg could also accelerate DA synthesis to increase DA release.

To elucidate the contribution of the DA biosynthetic pathway to the effects of MeHg, two pharmacological manipulations were employed. Inhibition of TH with AMT completely abolished MeHg-induced DA release. Indirect assessment of TH activity using NSD-1015 to block conversion of DOPA to DA suggests that MeHg stimulated TH activity; i.e., DOPA accumulation was increased following toxicant treatment. Western blot analysis confirmed that MeHg targets TH to increase DA synthesis. This effect is achieved by increasing phosphorylation of TH at Ser40, rather than altering the overall amount of enzyme present. These data demonstrates that MeHg targets TH activity, increasing the amount of newly synthesized DA available for release.

The mechanism by which MeHg targets TH phosphorylation to increase DA synthesis is unknown. One possible explanation is related to increased cytosolic Ca^{2+} following exposure to MeHg (Marty and Atchison, 1997). TH phosphorylation is mediated by Ca^{2+} -dependent protein kinases, including PKC (Albert et al., 1984; Vulliet et al., 1985)

and CaM-MPK (Yamauchi and Fujisawa, 1981; Vulliet et al., 1984). Activation of these phosphorylation pathways may be responsible for the observed increase in TH activity following exposure to MeHg. However, increased cytosolic Ca^{2+} could also inhibit the activity of protein phosphatase 2A or 2C (Bevilaqua et al., 2003), preventing TH dephosphorylation.

This is the first report demonstrating a stimulatory effect of acute MeHg exposure on TH activity that culminates in an increase in DA synthesis and consequently DA release. A previous report documented elevated TH activity in brain homogenates isolated from rats treated with MeHg for seven days (Omata et al., 1982), however the downstream consequences of MeHg-activated TH activity on catecholamine release were not studied. Results presented herein describe how MeHg targeting of the DA biosynthetic pathway contribute to MeHg-mediated DA release. This could be one mechanism by which MeHg induces cell-specific neurotoxicity. Decoupling of the regulation between biosynthesis and release, leading to an abnormally high level of extracellular DA, could disrupt the signal-to-noise ratio associated with normal neuronal activity-evoked release at the DA synapse.

Chapter 4. The roles of mitochondria and associated catabolic enzyme function in MeHg-impaired DA metabolism

4.1. Introduction

DA is metabolized in a two-step process. First, MAO catalyzes the oxidative deamination of DA to DOPAL. Second, this reactive intermediate metabolite either undergoes further oxidation mediated by ALDH to form the carboxylic acid DOPAC, or it is reduced by aldehyde/aldose reductase (AR) to form the alcohol DOPET (Eisenhofer, 2004; Meiser et al., 2013). These *oxidative* and *reductive* pathways of DA metabolism are illustrated in Figure 4.1. DA is predominately degraded along the *oxidative* metabolic pathway due to the absence of a β -hydroxyl group. This is contrast to the other catecholamines, NE and epinephrine, which contain a β -hydroxyl group, and are preferentially degraded along the *reductive* pathway (Duncan and Sourkes, 1974; Turner et al., 1974; Kawamura et al., 2002).

Tight regulation of DA metabolism is necessary because both cytosolic DA and DOPAL can be cytotoxic (Graham, 1978; Graham et al., 1978; Rees et al., 2009). Cytosolic DA undergoes autooxidation in the presence of molecular oxygen to form either a quinone or semiquinone (Graham, 1978; Kalyanaraman et al., 1985; Lévy and Bodell, 1993). These reactive species can covalently bind cellular proteins and DNA (Graham et al., 1978). Similarly, DOPAL has been reported to form adducts with protein amino acids, and to cross-link proteins and DNA (Nair et al., 1986; Nilsson and Tottmar, 1987; Nadkarni and Sayre, 1995; Brooks and Theruvathu, 2005; Rees et al., 2009). Subsequent biological effects of DA and aldehyde adducts could contribute to inactivation of enzymes (Chio and Tappel,

1969), depletion of antioxidant systems (Esterbauer et al., 1975), and altered signal transduction (Leonarduzzi et al., 2004), gene expression (Kumagai et al., 2000), and DNA repair (Feng et al., 2004). Indeed, the specific vulnerability and death of DA neurons in PD is hypothesized to involve the accumulation of these toxic compounds that are selectively produced in DA neurons (Li et al., 2001; Burke et al., 2003).

Dysfunction of *oxidative DA metabolism at the level of* either MAO or ALDH could contribute to oxidative stress and cytotoxicity associated with DA autooxidation and DOPAL adduct formation. MAO is localized on the outer mitochondrial membrane (Schnaitman et al., 1967), and is covalently bound to a flavin adenine dinucleotide molecule, which is used as a cofactor (Youdim et al., 2006). MAO catalyzes the oxidative deamination of a number of biogenic amines, including DA, NE, epinephrine, and serotonin (Shih et al., 1999; Nagatsu, 2004). In the case of DA, the reaction produces the corresponding aldehyde (i.e., DOPAL), hydrogen peroxide, and ammonia.

The ALDH superfamily includes enzymes that catalyze the NAD(P)⁺-dependent oxidation of a wide variety of aldehydes into their corresponding carboxylic acids. There are 19 known human ALDH proteins found in all subcellular regions, including the cytosol, mitochondria, endoplasmic reticulum, and nucleus (Marchitti et al., 2008). While ALDH enzymes are distributed widely throughout different tissues in the body, they display distinct substrate selectivity. In DA metabolism, two isozymes, ALDH1A1 and ALDH2, have demonstrated roles. ALDH1A1 is highly expressed in the cytosol of DA neurons (Galter et al., 2003; Anderson et al., 2011b), and its gene expression is down-regulated in PD patients (Mandel et al., 2005). ALDH2 is a mitochondrial matrix protein constitutively expressed in a variety of tissues and cell types, including the brain (Goedde and Agarwal, 1990) and

PC12 cells (Robador et al., 2012). Both isozymes are thought to play critical roles in maintaining low intracellular levels of DOPAL (Maring et al., 1985; Galter et al., 2003; Marchitti et al., 2007).

MeHg has demonstrated effects on DA metabolism. The toxicant decreases the concentration of intracellular DOPAC (Bemis and Seegal, 1999; Dreiem et al., 2009), which may result from an observed decrease in MAO activity (Taylor and DiStefano, 1976; Chakrabarti et al., 1998; Beyrouy et al., 2006; Castoldi et al., 2006). MeHg could inhibit MAO by two potential mechanisms. Because MAO is localized to the outer mitochondrial membrane (Schnaitman et al., 1967), MeHg-induced loss of mitochondrial membrane potential (Bondy and McKee, 1991; Hare and Atchison, 1992; Limke and Atchison, 2002) could compromise enzyme activity. Additionally, several cysteine residues are required for proper MAO enzymatic function (Hubalek et al., 2003). MeHg has a high affinity for sulfhydryl groups (Hughes, 1957; Sanfeliu et al., 2003), and could bind these cysteine residue to impair MAO activity.

MeHg targeting of mitochondrial function and protein thiols to impair MAO activity might also contribute to inhibition of ALDH function. Mitochondrial-associated ALDH mediates the catabolism of DOPAL to DOPAC (Marchitti et al., 2007), and thus mitochondrial dysfunction induced by MeHg could impair ALDH enzymatic activity. Furthermore, the active site of ALDH contains two cysteine residues (Hempel et al., 1985), which MeHg could readily bind to inhibit enzymatic activity.

Impaired MAO or ALDH activity would be indicated by changes in the metabolomic profile of DA. Alterations in the ratios of DOPAC, DOPAL and DOPET would denote the level of enzymatic inhibition. While DA is predominately metabolized to DOPAC, the *reductive*

metabolic pathway has been proposed to compensate for DOPAL metabolism in the event of ALDH inhibition (Turner et al., 1974). Indeed, inhibition of the *oxidative pathway* decreases DOPAC formation and increases DOPET formation in PC12 cells (Lamensdorf et al., 2000b), indicating that when ALDH is blocked, a major portion of DOPAL is reduced by AR to DOPET. Therefore inhibition of MAO activity would be reflected as a decrease in both DOPAL and DOPAC, with a concomitant increase in DOPET, whereas inhibition of ALDH activity would be associated with a decrease in DOPAC and an increase in DOPAL and DOPET.

The goals of the present study were to 1) characterize the DA metabolomic profile following exposure to MeHg in undifferentiated PC12 cells, and 2) examine the specific contributions of direct and indirect ALDH inhibition to MeHg-impaired DA metabolism. To this end, the effects of MeHg on DA metabolism, ALDH activity, and mitochondrial function were compared with those of the reversible ALDH2 inhibitor daidzin (Keung and Vallee, 1993), and the reversible mitochondrial ETC Complex I inhibitor rotenone (Schuler and Casida, 2001).

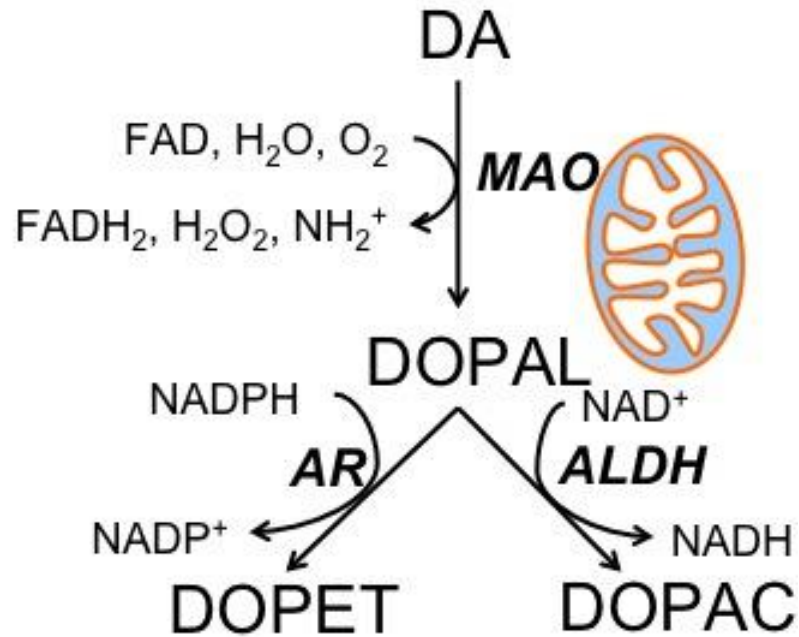


Figure 4.1. Diagram depicting DA metabolic pathways. First DA is deaminated to DOPAL by MAO. The majority of DA is degraded along the “oxidative pathway”, where DOPAL is oxidized to DOPAC by ALDH. A small portion of DOPAL is reduced by AR to form DOPET along a “reductive pathway”. MAO and ALDH are mitochondrial-associated enzymes. MAO is localized to the outer mitochondrial membrane, and ALDH is present in the mitochondrial matrix. Additionally, both enzymes rely on cofactors provided by the mitochondria, FAD is used by MAO and NAD is used by ALDH. (Adapted from Lamensdorf et al., 2000a)

4.2. Methods

4.2.1. Chemicals

MeHg (ICN Biochemicals), daidzin (Sigma), and rotenone (Sigma) were diluted from stock solutions in HBS. Drug solutions were diluted to final concentrations on the day of each experiment as described in General Methods Section 2.2.

4.2.2. Chemical treatment

PC12 cells were seeded at a density of $6-7 \times 10^5$ cells/mL in 6-well plates or XF24-well plates coated with poly-D-lysine 24-48 hr prior to treatment. To begin each experiment, culture medium was aspirated and replaced with HBS in the absence or presence of pharmacological and toxicant treatments. Cells were incubated at 37°C/5% CO₂ during treatment as described in General Methods Section 2.2.

4.2.3. Neurochemistry

At experiment termination, treatment medium was retained and acidified. Cells were rinsed, harvested, and pelleted by centrifugation. The content of DA and its metabolites in the treatment medium and cell pellet was determined by HPLC-ED as described in General Methods Section 2.3. Neurochemical concentrations were normalized to mL per sample for extracellular measurements or mg of protein for intracellular measurements as determined by the BCA protein assay (Sigma).

To measure DOPAL, a standard was synthesized as described in General Methods Section 2.3.2. Briefly, 750µL of 1.063mM phosphate-buffered DA was incubated at 37°C for

15 min. The reaction was started by adding 25 μ L MAO (10 U; BD Biosciences, San Jose, CA) to each of the two culture tubes and gently mixing. At 45min, a 50 μ L aliquot was withdrawn from the reaction and added to 450 μ L of ice-cold tissue buffer. Following centrifugation, supernatants were removed and placed into a fresh tube for HPLC-ED analysis of DA and DOPAL. Concentrations of DA were compared to 1ng standards of DA, and concentrations of DOPAL were determined by normalizing the DOPAL peak height to the amount of DA lost. DOPAL standards are unstable and degrade within a few days of synthesis. As such a fresh standard was synthesized each time measurements of DOPAL were made.

4.2.4. ALDH2 enzyme kinetics assay

To terminate the experiment, treatment medium was aspirated and replaced with 150 μ L homogenization buffer (0.1M Tris-HCl, 10mM DTT, 20% glycerol, and 1% Triton-X). Cells were scraped and pelleted by centrifugation at 13,000 *g* for 8 min at 4°C. Protein concentration of supernatant was determined by BCA protein assay (Sigma). ALDH2 enzyme activity was determined spectrophotometrically by monitoring the reductive reaction of NAD to NADH at 340 nm as described in General Methods Section 2.7. ALDH2 reaction rates were calculated as μ mole NADH per min per mg protein.

4.2.5. Mitochondrial bioenergetics

Following pharmacological and toxicant exposure, treatment medium was aspirated. Cells were washed once with XF24 RPMI Assay Medium and then incubated at 37°C/no CO₂ for 1 hr to allow medium temperature and pH to equilibrate before the first

measurements were made. The biosensor cartridge was hydrated overnight and injection ports were loaded with test compounds as described in General Methods Section 2.6. OCR was measured under basal conditions and following injection of test compounds using the XF24 Extracellular Flux Analyzer. Basal respiration, ATP generation, and spare respiration were calculated and compared between pharmacological and toxicant treatment groups.

4.2.6. NADH/NAD quantification

To terminate the experiment, treatment medium was aspirated and cells were pelleted by centrifugation. NAD and NADH were extracted and measured by spectrophotometry as described in General Methods Section 2.8. Absorbance was compared to NADH standards to calculate the concentration of total NAD, total NADH, and the ratio of NAD:NADH.

4.2.7. Statistical analysis

SigmaPlot® software version 12.0 (SysStat Software, Inc., Point Richmond, CA) was used to make statistical comparisons among groups using unpaired t-test, one-way ANOVA, or non-parametric alternatives as appropriate. If a significant difference was detected, *post hoc* between-group comparisons were performed using Tukey's test. Statistical significance was set at $p \leq 0.05$.

4.3. Results

4.3.1. MeHg impairs DA metabolism, shunting DA along an alternative metabolic pathway

As demonstrated in Figure 4.2A, treatment with 2 μ M MeHg for 60 min decreases the intracellular concentration of DOPAC, the primary DA metabolite ($p < 0.05$). Because MeHg, at this same concentration and time-point, also increases intracellular DA (Figure 3.5), the observation that MeHg impairs canonical DA metabolism, suggests that MeHg inhibits some process specific to DOPAC formation. Figures 4.2B-C illustrate that in contrast to the effect on DOPAC, treatment with 2 μ M MeHg for 60 min increases intracellular concentrations of DOPAL and DOPET ($p < 0.05$), the intermediate DA metabolite and alternative DA metabolic product, respectively.

Comparison of the DA metabolomic profile in control and MeHg-treated PC12 cells (Figure 4.3) revealed that treatment with 2 μ M MeHg for 60 min shifts the distribution of DA metabolites. Under basal conditions, DOPAC comprises 56% of total metabolites, while DOPAL and DOPET account for 31% and 13% respectively. Following exposure to MeHg, the concentration of DOPAC decreases to account for only 14.5% of the total metabolites, whereas DOPAL and DOPET concentrations increase to accounts for 53.5% and 32%, respectively. Additionally, MeHg significantly increases the total concentration of DA metabolites (i.e. DOPAC, DOPAL, and DOPET) from 257.9 ± 31.4 to 398.1 ± 40.2 ($p < 0.05$, HBS vs. MeHg).

These data together suggest that MeHg impairs DOPAC formation at the level of the second DA metabolic enzyme, ALDH. Inhibition of MAO activity would have been reflected as a decrease in both DOPAL and DOPAC formation. Based on these data additional experiments were designed to investigate whether MeHg directly or indirectly impairs

ALDH activity. Furthermore, given that changes in DOPAL directly correspond to changes in DOPET, only DOPET was analyzed in the remaining studies.

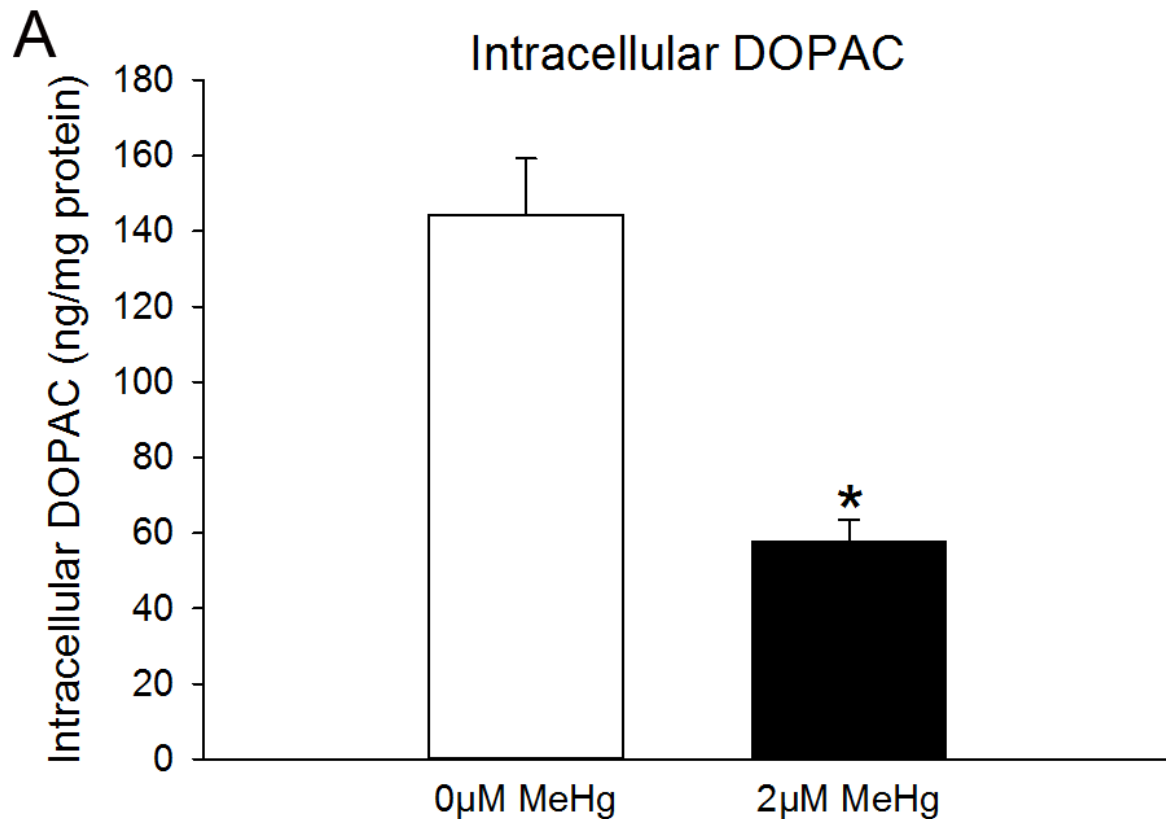
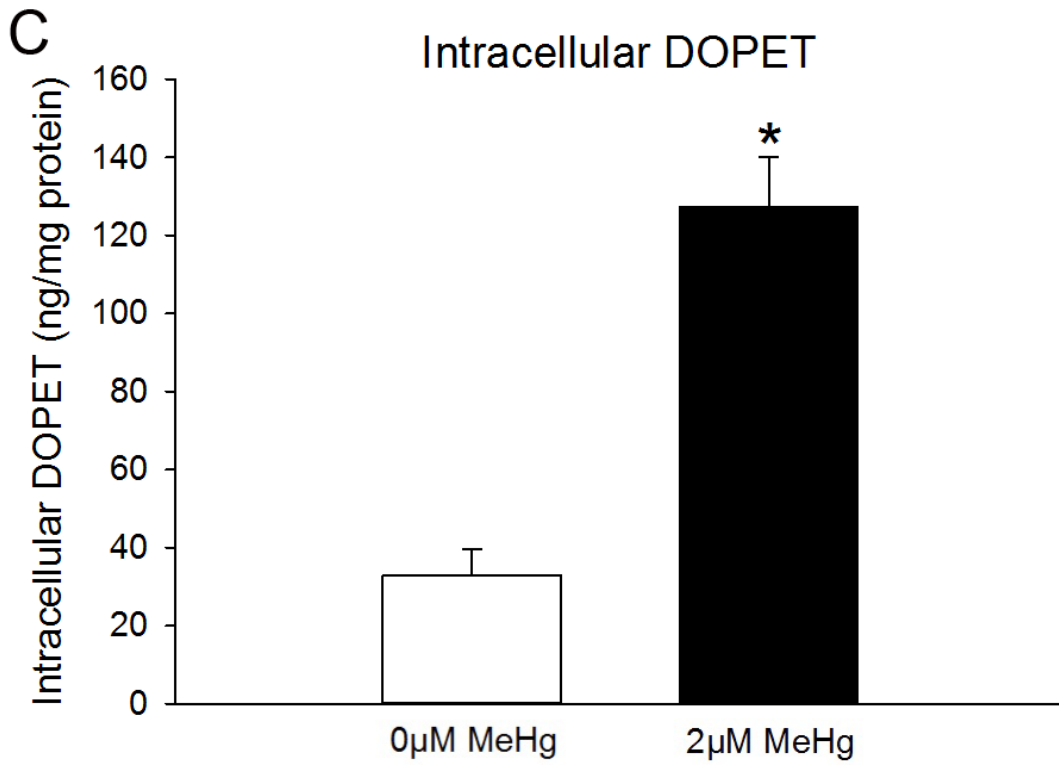
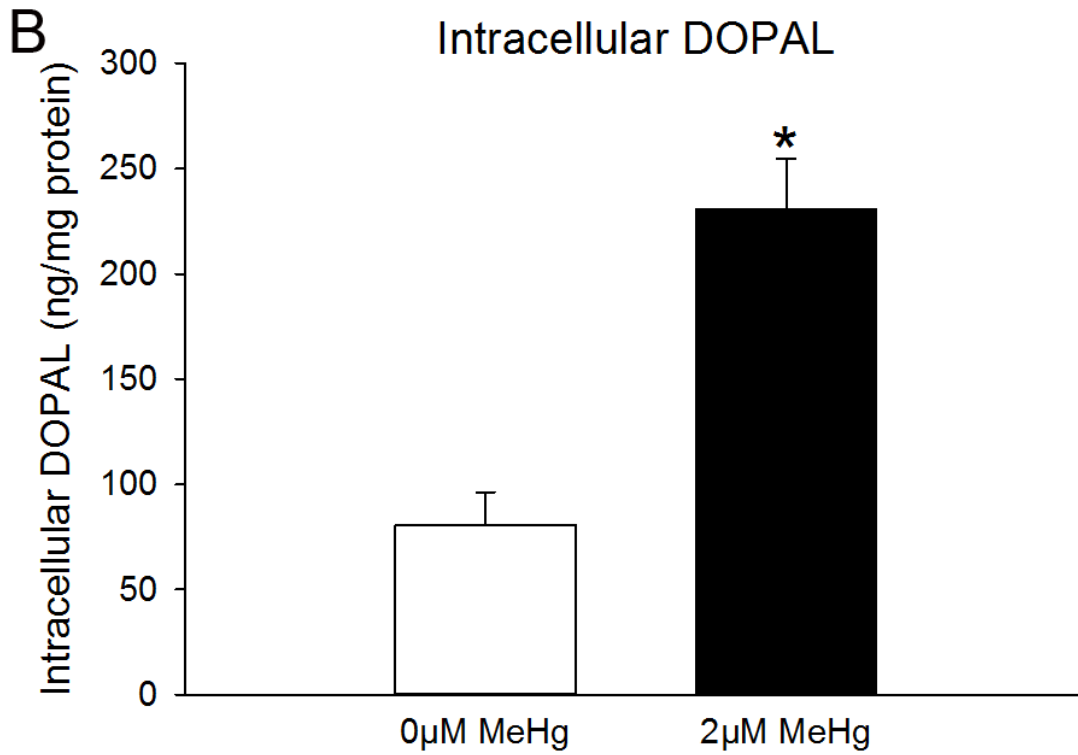


Figure 4.2. MeHg shunts DA metabolism along the reductive metabolic pathway. Intracellular concentrations of DOPAC (Panel A), DOPAL (Panel B), and DOPET (Panel C). Undifferentiated PC12 cells were treated with 0 μ M (white bars) or 2 μ M (black bars) MeHg in HBS for 60 min. The asterisk (*) indicates a value significantly different than 0 μ M MeHg ($p < 0.05$). Values are means + S.E.M. ($n = 3$, 3 replicates per n).

Figure 4.2 cont'd



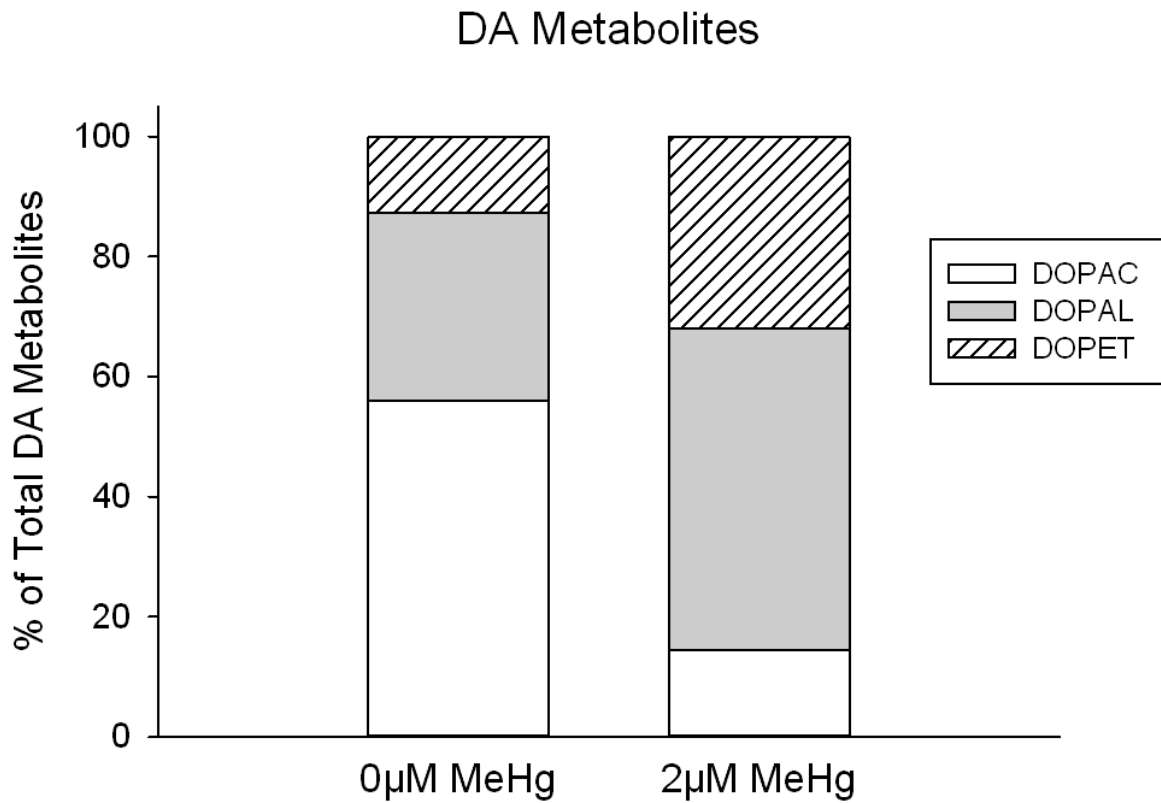


Figure 4.3. Percentage changes in the relative amounts of DA metabolites induced by MeHg. The DA metabolomic profile was expressed as the percentage of DOPAC (white), DOPAL (gray), or DOPET (hatched) as a proportion of all three metabolites in undifferentiated PC12 cells treated with 0µM and 2µM MeHg for 60min.

4.3.2. Selective inhibition of ALDH with daidzin impairs DA metabolism in a manner similar to MeHg

MeHg could impair ALDH activity directly by interacting with sulfhydryl groups present in the active site of the enzyme (Hempel et al., 1985). It could also indirectly decrease ALDH activity by decreasing availability of the ALDH cofactor, NAD, which is provided by Complex I of the mitochondrial ETC (Lamensdorf et al., 2000a; 2000b). In order to determine whether MeHg directly or indirectly inhibits ALDH activity, effects of MeHg on DA metabolism were compared to those of the specific ALDH2 inhibitor daidzin and the ETC Complex I inhibitor rotenone.

Rotenone alters DA metabolism in PC12 cells (Lamensdorf et al., 2000a). Treatment with 50nM rotenone for 15 min decreases the combined concentrations of intracellular and extracellular DOPAC, while increasing DOPET concentrations. Effects of the specific ALDH2 inhibitor daidzin (Keung and Vallee, 1998) on DA metabolism are less well characterized. Therefore preliminary concentration-response and time-course experiments were conducted to characterize how daidzin alters intracellular concentrations of DOPAC and DOPET. As demonstrated in Figure 4.4, treatment with daidzin for 45 min significantly increased DOPET formation in undifferentiated PC12 cells only at the highest concentration investigated, 20 μ M ($p < 0.05$). Intracellular DOPAC was not significantly altered by any concentration of daidzin. To examine time-course effects of daidzin, undifferentiated PC12 cells were exposed to 20 μ M daidzin for 0.75-24 hr (Figure 4.5). At all time points investigated, intracellular DOPAC was significantly decreased and intracellular DOPET was significantly increased ($p < 0.05$). Based on these results, treatment with 20 μ M daidzin for 45 min was selected for comparison with MeHg.

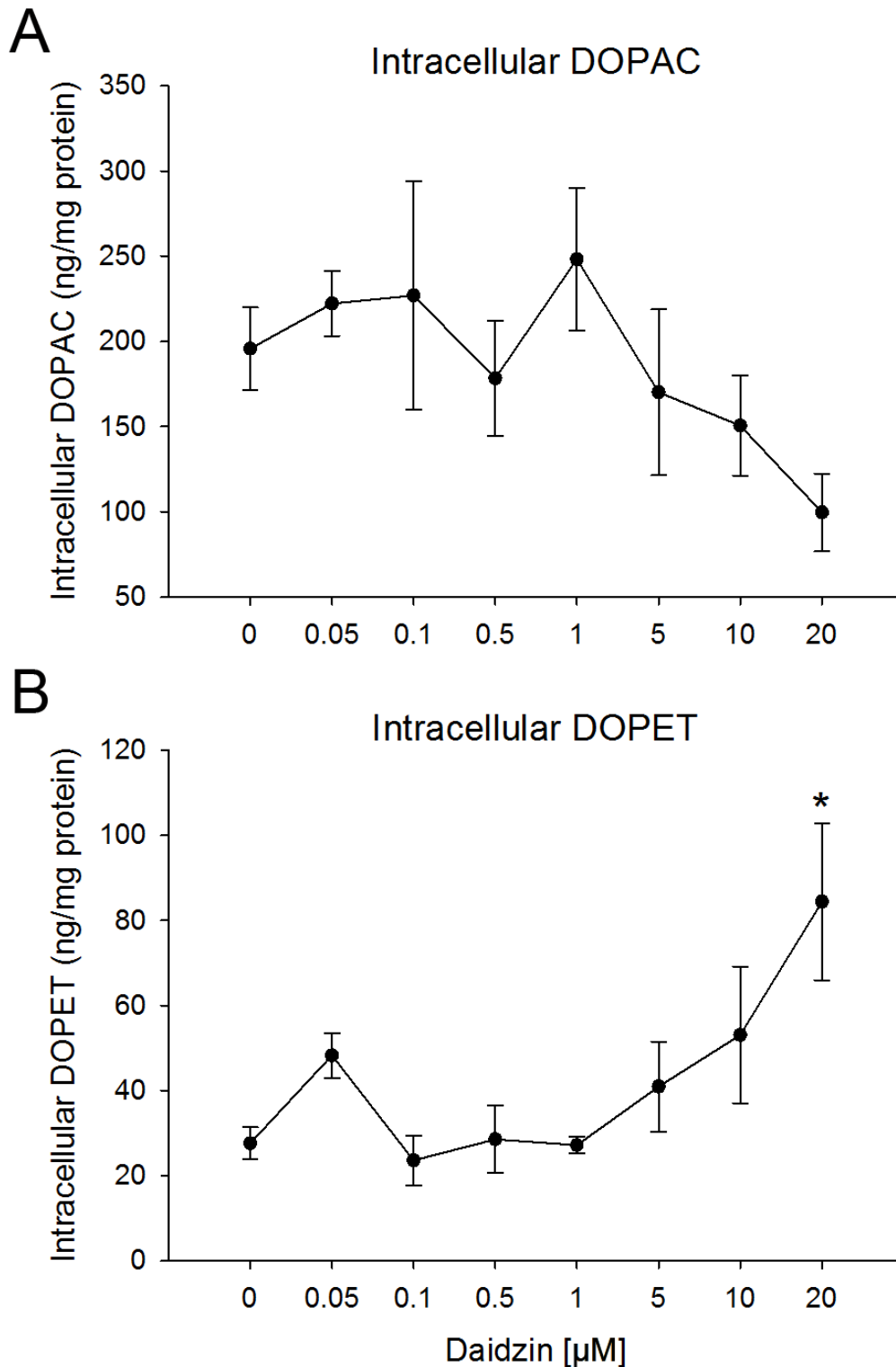


Figure 4.4. Concentration-response effects of the ALDH inhibitor daidzin on concentrations of intracellular metabolites. Undifferentiated PC12 cells were treated with 0-20 μ M daidzin for 45 min, and concentrations of DOPAC (Panel A) and DOPET (Panel B) were measured. The asterisk (*) indicates a value significantly different than control values ($p < 0.05$). Values are means \pm S.E.M. ($n = 1, 3$ replicates per n).

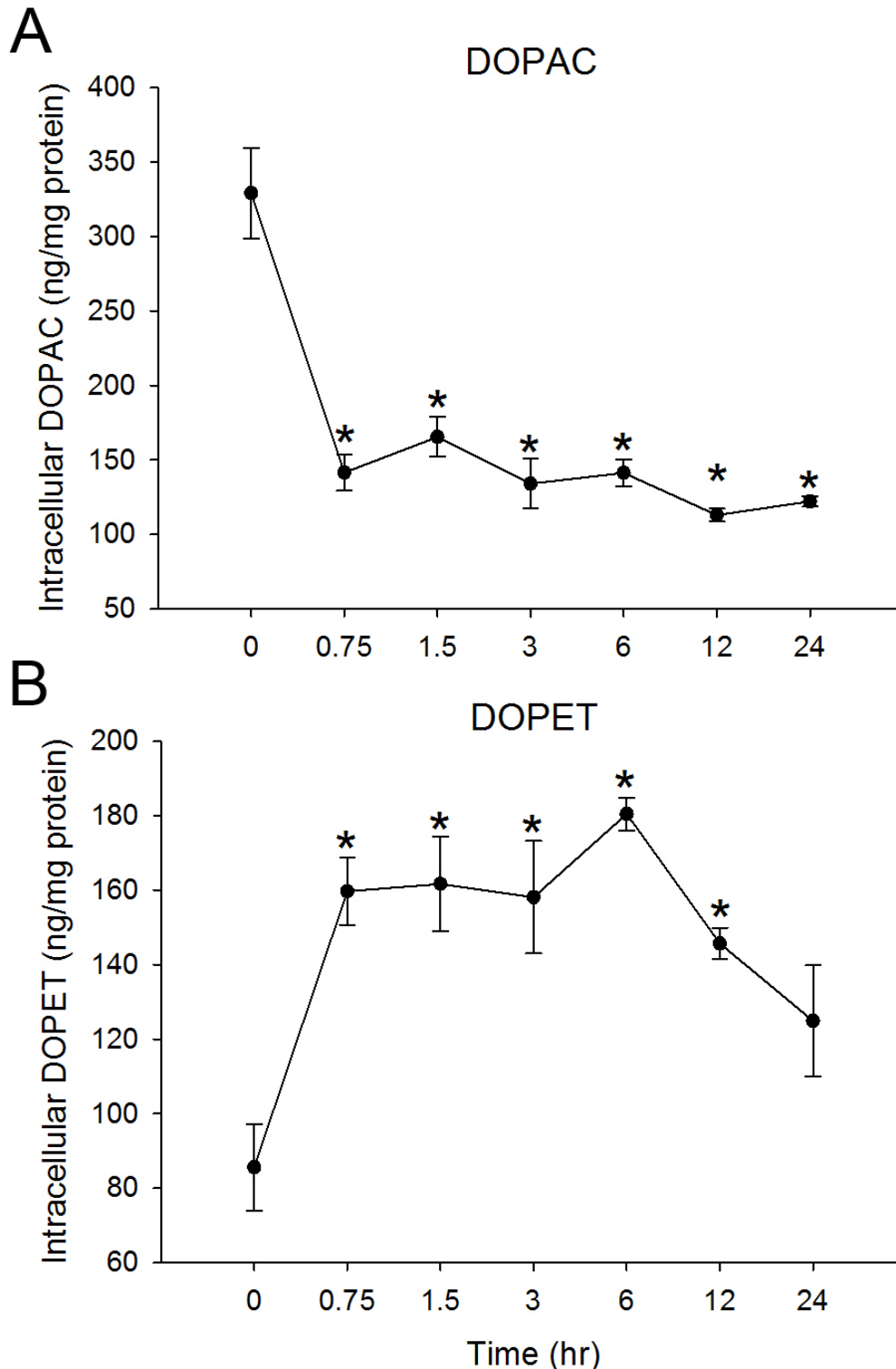


Figure 4.5. Time-course effects of the ALDH inhibitor daidzin on concentrations of intracellular metabolites. Undifferentiated PC12 cells were treated with 20 μ M daidzin for 0-24 hr, and concentrations of DOPAC (Panel A) and DOPET (Panel B) were measured. The asterisk (*) indicates a value significantly different than control values ($p < 0.05$). Values are means \pm S.E.M. ($n = 1, 3$ replicates per n).

4.3.3. Daidzin and rotenone impair DA metabolism in a manner that resembles MeHg

The comparative effects of MeHg, rotenone, and daidzin on intracellular DOPAC and DOPET concentrations are presented in Figure 4.6. Treatment with all three chemicals decreased intracellular DOPAC concentrations by approximately 60% as compared to cells treated with HBS ($p < 0.05$). MeHg and daidzin, but not rotenone, increased DOPET concentrations ($p < 0.05$). Furthermore, the increase induced by MeHg was more pronounced. While MeHg increased DOPET by over 300% as compared to HBS, daidzin only increased DOPET by ~200%. Rotenone did increase DOPET concentrations by ~100%, however this effect was not significantly different than HBS.

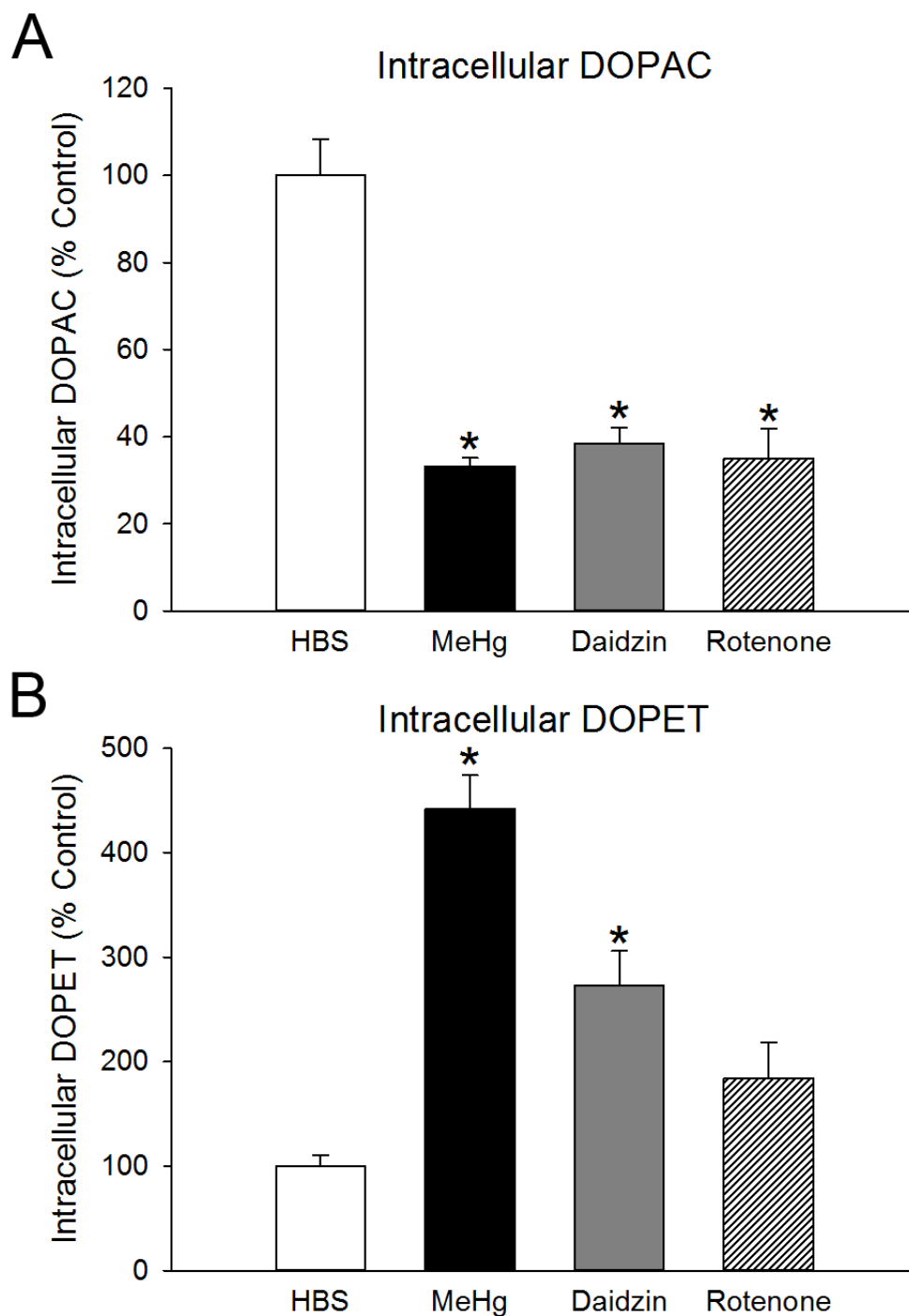


Figure 4.6. Comparative effects of MeHg, daidzin, and rotenone on concentrations of intracellular metabolites. Undifferentiated PC12 cells were treated with HBS for 60 min (white bars), 2 μ M MeHg for 60 min (black bars), 20 μ M daidzin for 45 min (gray bars), or 50nM rotenone for 15 min (hatched bars), and intracellular concentrations of DOPAC (Panel A) and DOPET (Panel B) were measured. The asterisk (*) indicates a value significantly different than HBS ($p < 0.05$). Values are means + S.E.M. ($n = 3$, 2-3 replicates per n).

4.3.4. ALDH activity is not directly altered by MeHg

To determine if MeHg has a direct effect on ALDH, enzymatic activity was measured as the production of NADH over time. ALDH uses NAD as a cofactor during substrate oxidation (Marchitti et al., 2008), and as a by-product, NADH is formed (Figure 4.1). NADH production was measured in PC12 cell lysate either following pre-treatment with or in the presence of HBS, 2 μ M MeHg, 20 μ M daidzin, or 50nM rotenone. Following pre-treatment, only rotenone increased NADH production (Figure 4.7A; $p < 0.05$). However when ALDH activity was measured in the presence of each chemical, daidzin decreased and rotenone increased NADH production (Figure 4.7B; $p < 0.05$). MeHg had no effect on NADH production under either experimental condition. In order to determine if MeHg impaired ALDH activity at higher concentrations, a concentration-response experiment was performed (Figure 4.8). NADH production was measured in the presence of 1-100 μ M MeHg. At no concentration did MeHg affect NADH production ($p > 0.05$).

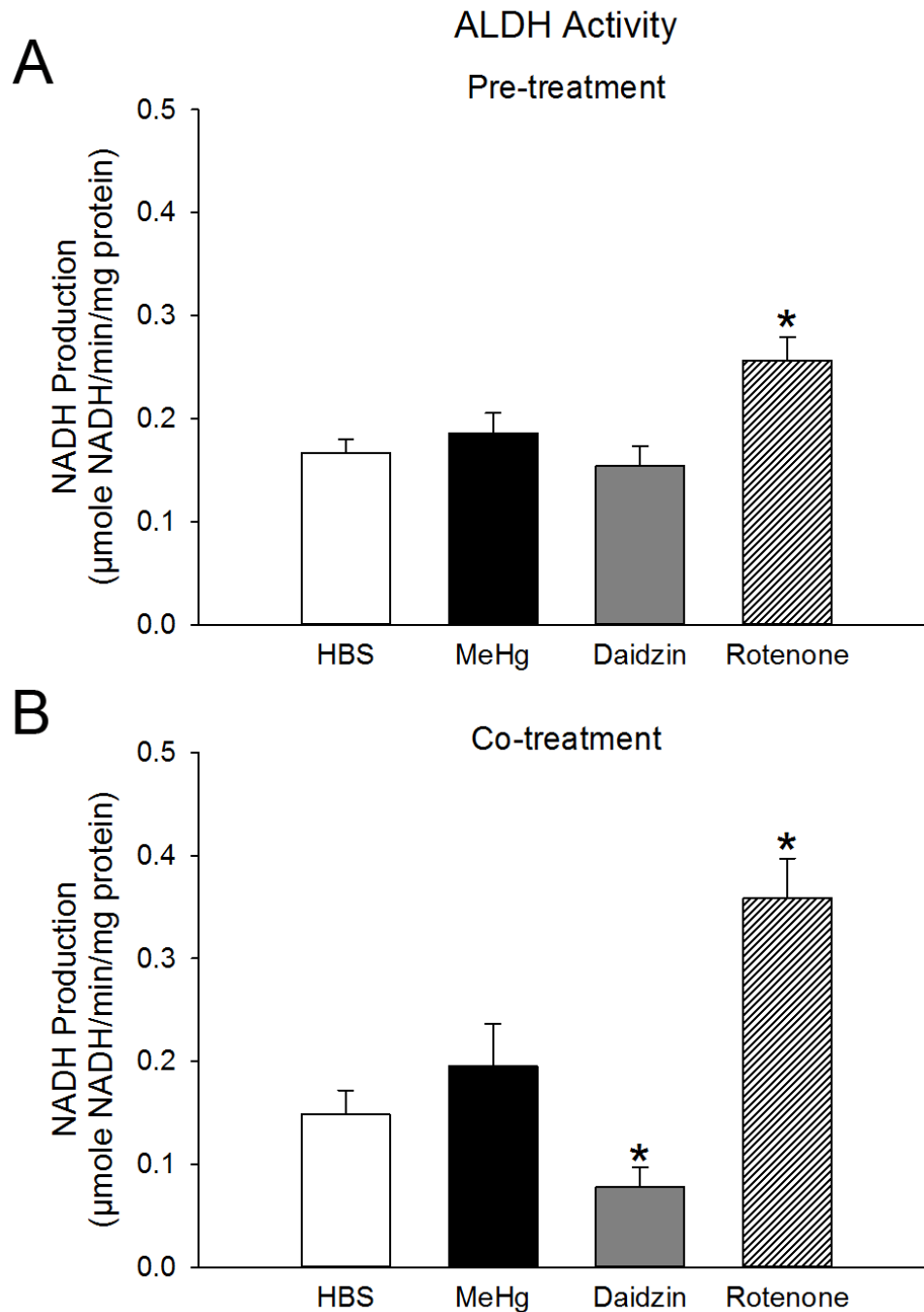


Figure 4.7. Comparative effects of MeHg, daidzin, and rotenone on ALDH activity. Panel A) Undifferentiated PC12 cells were treated with HBS for 60 min (white bars), 2µM MeHg for 60 min (black bars), 20µM daidzin for 45 min (gray bars), or 50nM rotenone for 15 min (hatched bars). Cells were then harvested and ALDH activity was measured in each treatment group. Drugs were not present during enzyme activity assay. Panel B) Undifferentiated PC12 cells were harvested and ALDH activity was measured in the presence of HBS (white bars), 2µM MeHg (black bars), 20µM daidzin (gray bars), or 50nM rotenone (hatched bars). The asterisk (*) indicates a value significantly different than HBS ($p < 0.05$). Values are means + S.E.M. ($n = 3$, 6 replicates per n).

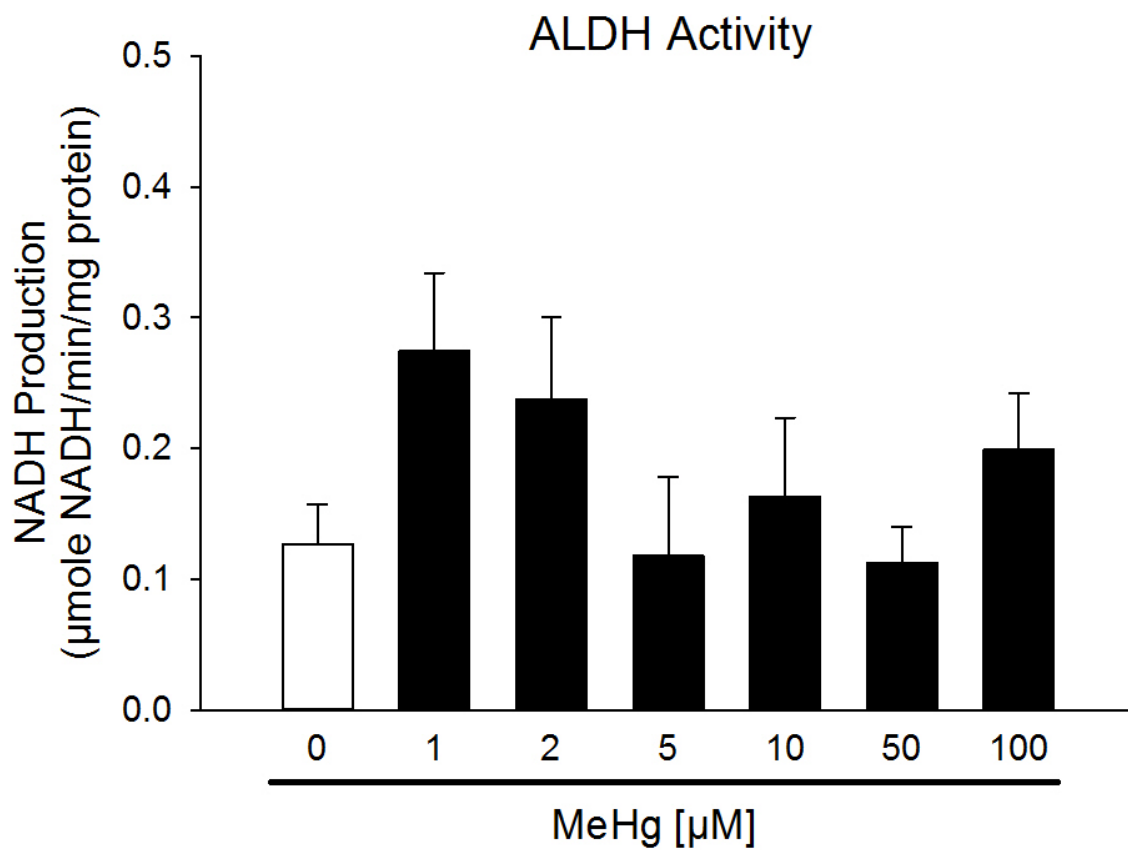


Figure 4.8. Concentration-response effects of MeHg on ALDH activity *ex vitro*. ALDH activity was measured in undifferentiated PC12 lysate in the presence of 0-100µM MeHg. Values are means + S.E.M. (n = 1, 6 replicates per n).

4.3.5. *MeHg impairs mitochondrial function and decreases availability of the ALDH cofactor NAD*

The indirect effects of MeHg on ALDH activity were investigated by measuring mitochondrial function and ALDH cofactor production. Mitochondrial respiration was measured in undifferentiated PC12 cells pre-treated with HBS for 60 min, 2 μ M MeHg for 60 min, 20 μ M daidzin for 45 min, or 50nM rotenone for 15 min. Following pre-treatment, OCR was measured under basal conditions and following treatment with 5mM pyruvate, 1 μ M oligomycin A, 2 μ M FCCP, and 1 μ M antimycin A. Treatment with these compounds is used to measure basal respiration, ATP generation, maximum respiration, and non-mitochondrial respiration, respectively. The effects of MeHg, daidzin, and rotenone on OCR is presented in Figure 4.9. The quantification of these effects revealed that MeHg attenuated basal and spare respiration, as well as ATP generation ($p < 0.05$). Rotenone only impaired spare respiration, and daidzin had no effect on mitochondrial function (Figure 4.10; $p < 0.05$).

Because Complex I of the mitochondrial ETC accepts electrons from NADH thereby forming NAD, and because ALDH uses NAD provided by Complex I, impaired mitochondrial respiration could detrimentally affect the production of NAD. In order to determine if MeHg alters the production of NAD, the amount of the coenzyme present in undifferentiated PC12 cells treated with either HBS or 2 μ M MeHg for 60 min was quantified. As illustrated in Figure 4.11, MeHg caused similar decreases in the amount of both NAD and NADH ($p < 0.05$) such that there was no change in the NAD/NADH ratio.

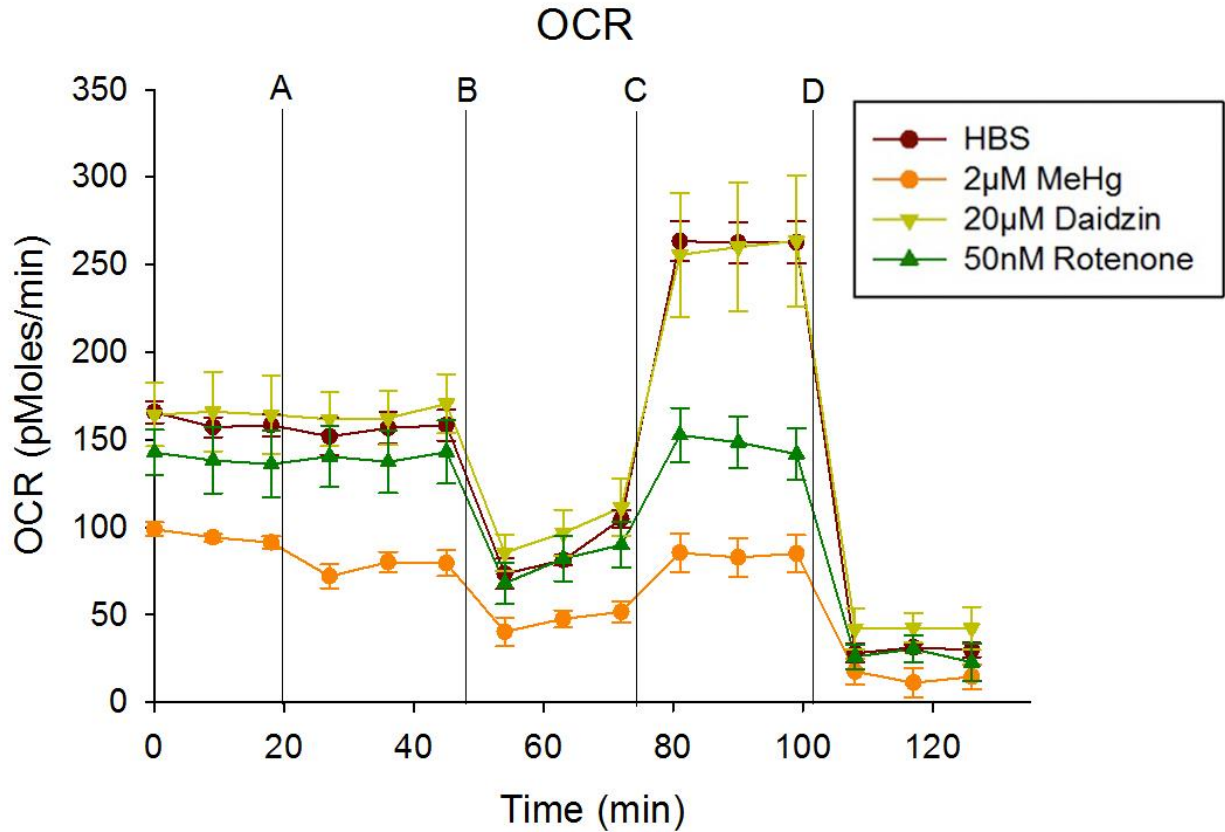


Figure 4.9. Comparative effects of MeHg, daidzin, and rotenone on mitochondrial bioenergetics. Undifferentiated PC12 cells were pretreated with HBS for 60 min (red), 2µM MeHg for 60 min (orange), 20µM daidzin for 45 min (yellow), or 50nM rotenone for 15 min (green). Following pre-treatment, OCR (pMoles/min) was measured under basal conditions and following injections of 5mM pyruvate (A), 1µM oligomycin (B), 2µM FCCP (C), and 1µM antimycin A (D). Values are means ± S.E.M. (n = 3, 4-5 replicates per n).

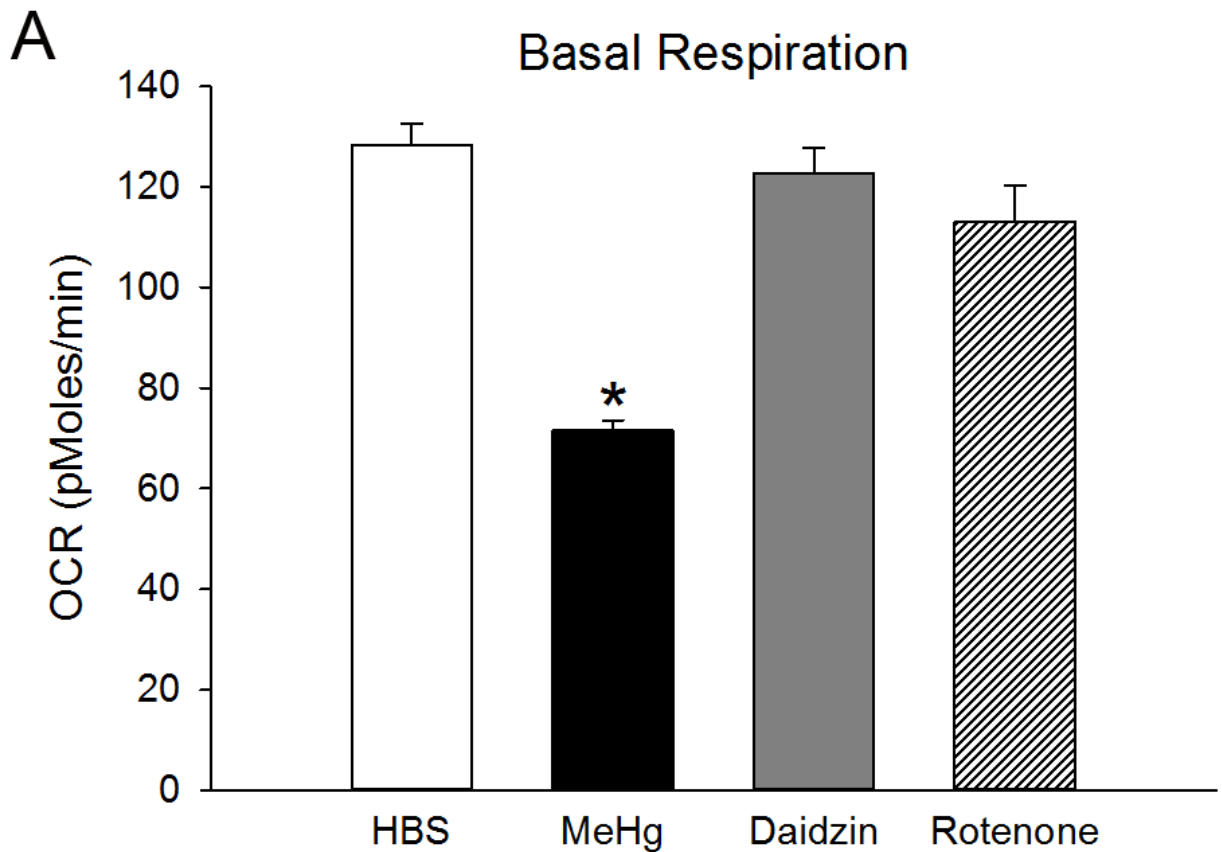
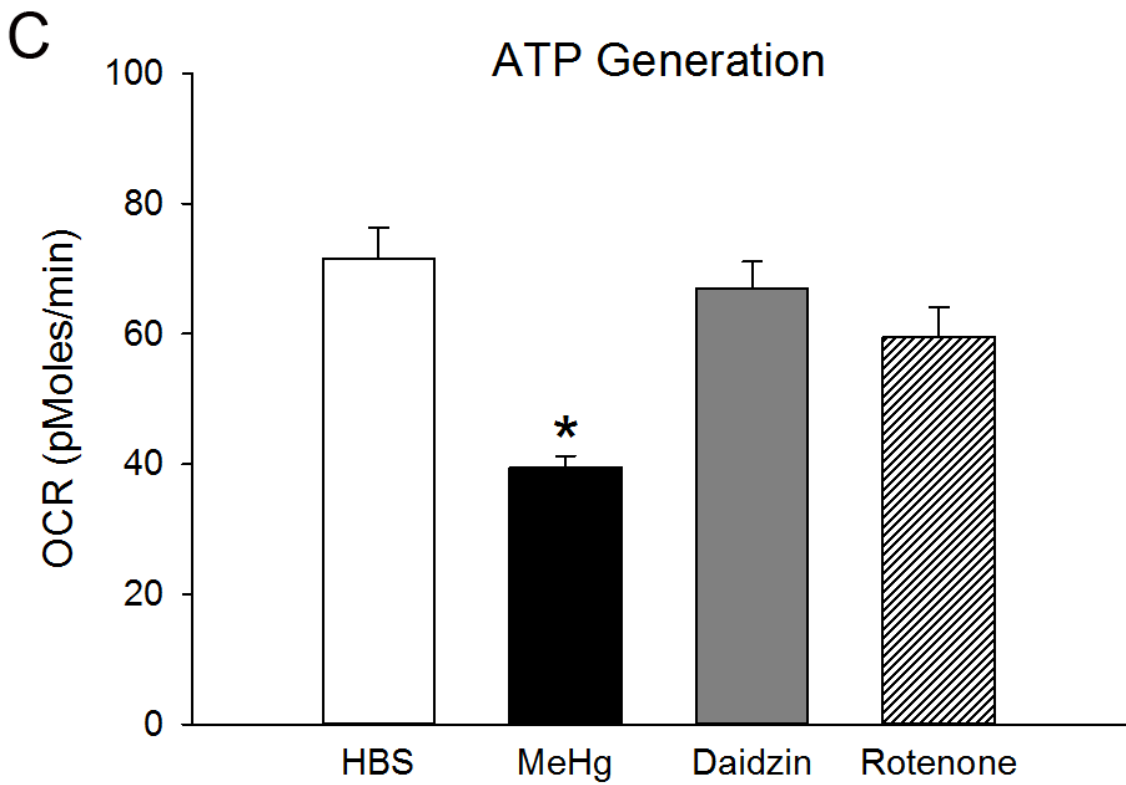
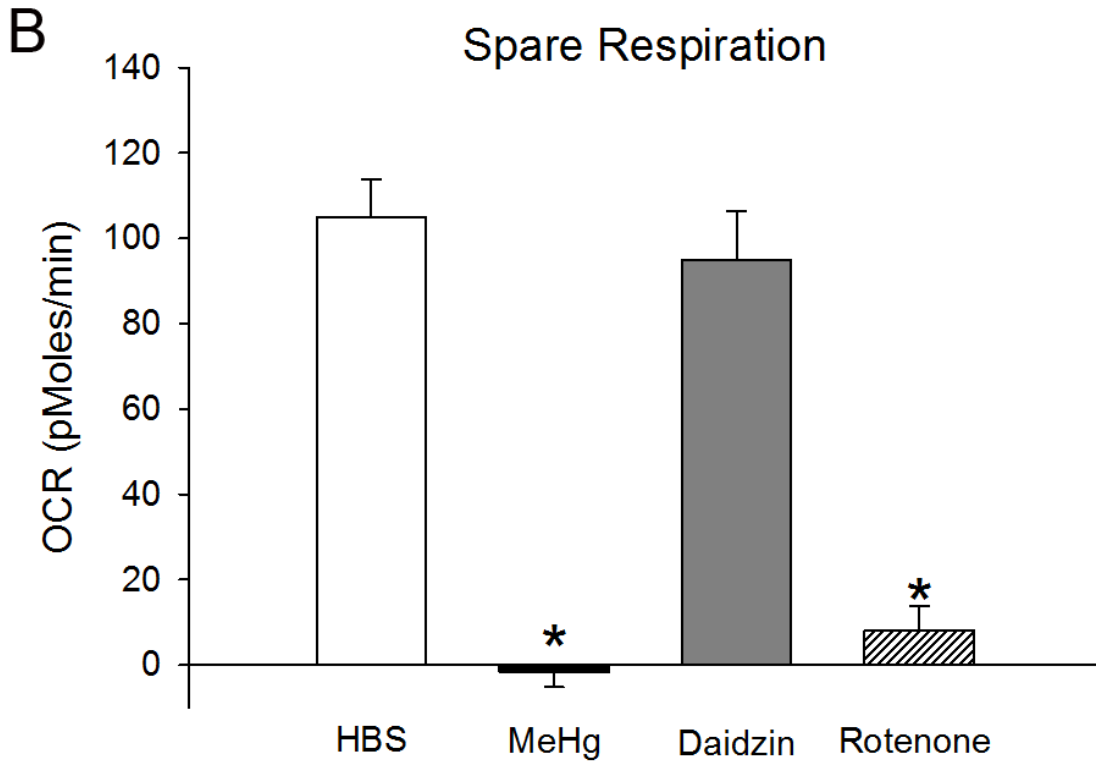


Figure 4.10. Quantification of changes in mitochondrial bioenergetics induced by MeHg, daidzin, or rotenone. Undifferentiated PC12 cells were treated with HBS for 60 min (white bars), 2 μ M MeHg for 60 min (black bars), 20 μ M daidzin for 45 min (gray bars), or 50nM rotenone for 15 min (hatched bars). Panel A) Basal respiration (OCR) was measured in the presence of 25mM glucose and 5mM pyruvate/2.5mM malate. Panel B) Spare respiration was calculated as the difference between maximum respiration (following treatment with 2 μ M FCCP) and basal respiration. Panel C) ATP generation was calculated as the difference between basal respiration and respiration following treatment with 1 μ M oligomycin A. The asterisk (*) indicates a value significantly different than HBS ($p < 0.05$). Values are means + S.E.M. ($n = 3, 4-5$ replicates per n).

Figure 4.10 cont'd



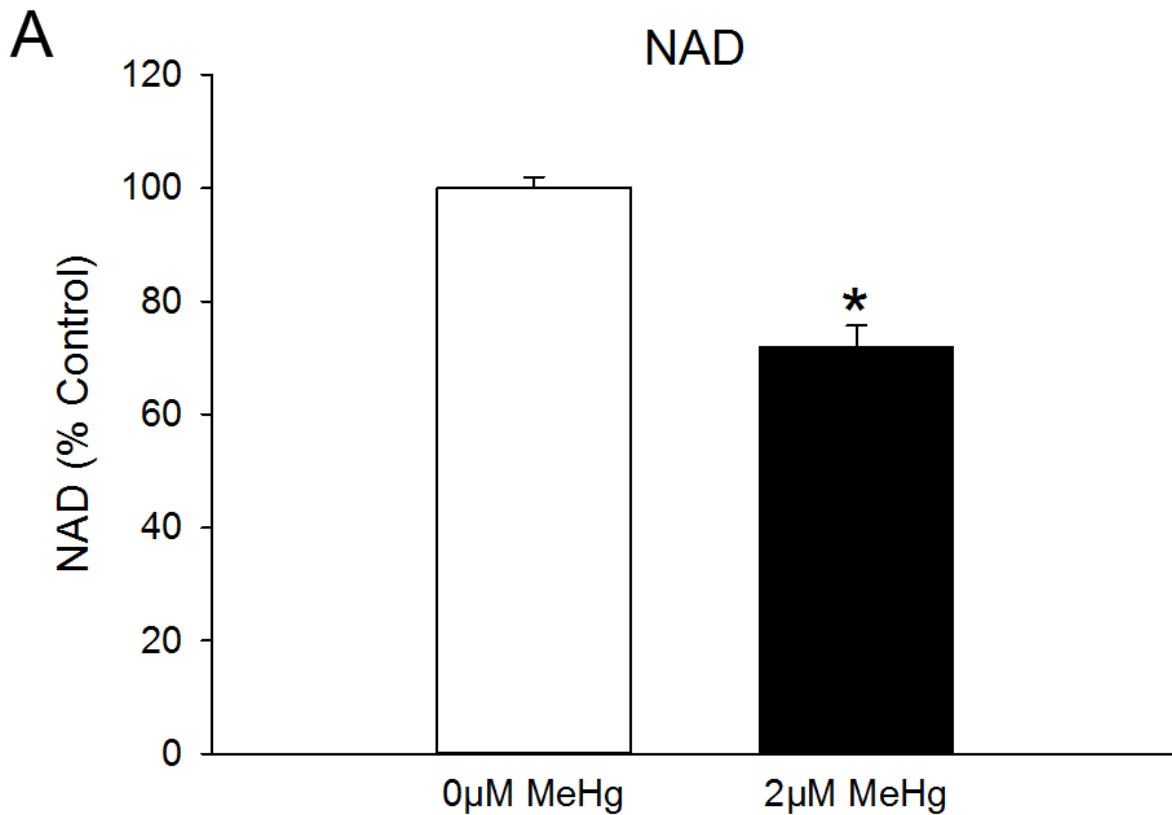
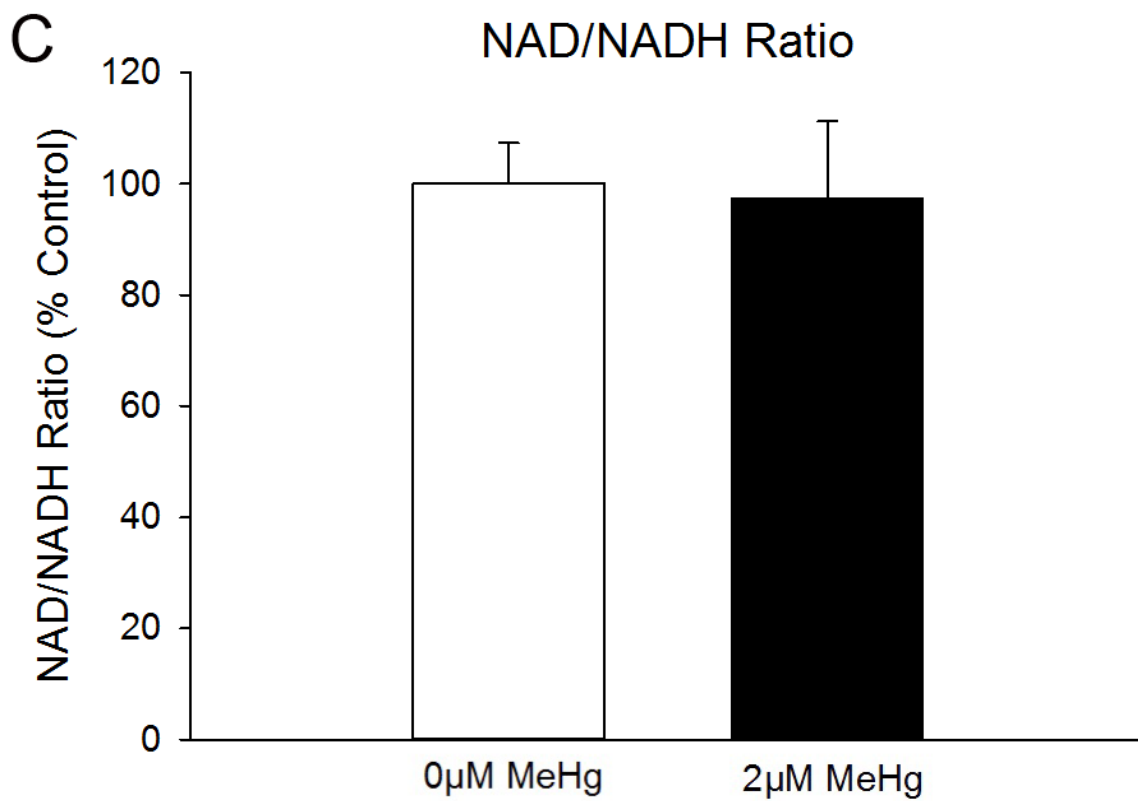
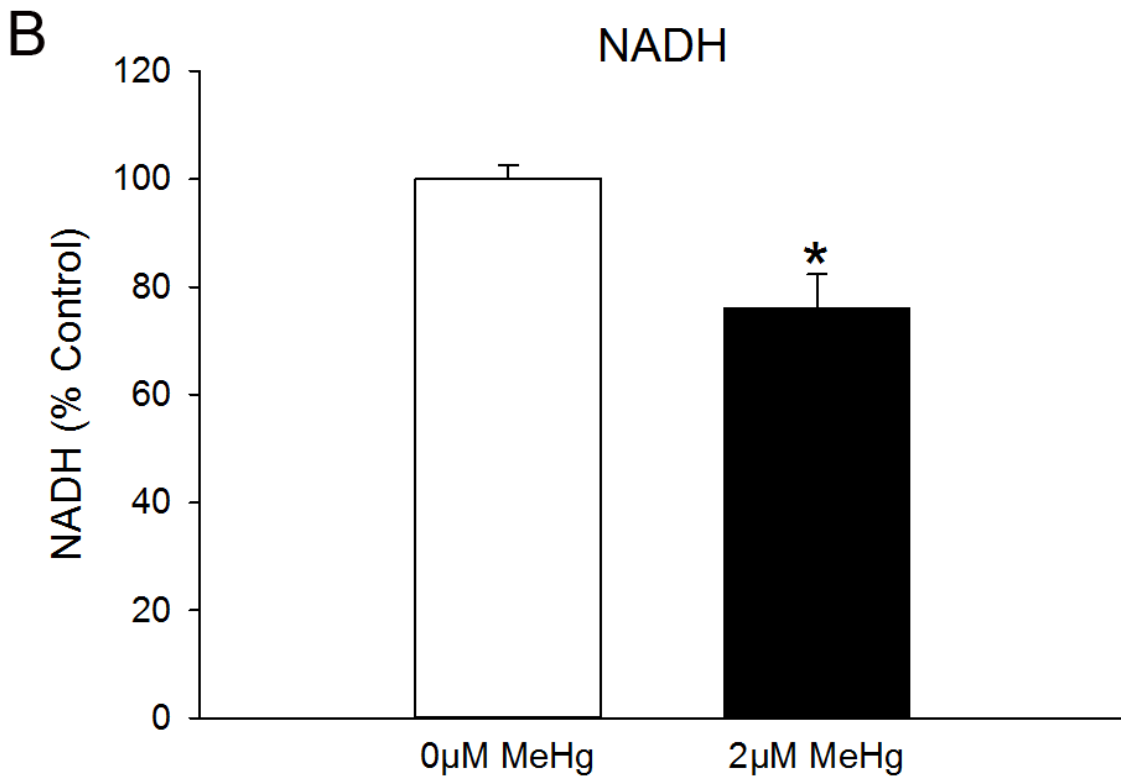


Figure 4.11. Effect of MeHg on the production of NAD(H). Undifferentiated PC12 cells were treated with 0µM (white bars) or 2µM (black bars) MeHg for 60 min, and then the amount of NAD (Panel A) and NADH (Panel B) were measured by spectrophotometry using an NAD/NADH Quantification Kit (Sigma). The ratio of NAD/NADH (Panel C) was calculated as (NAD-NADH)/NADH. The asterisk (*) indicates a value significantly different than 0µM MeHg ($p < 0.05$). Values are means + S.E.M. ($n = 4$, 4 replicates per n).

Figure 4.11 cont'd



4.4. Discussion

The present study provides evidence that MeHg impairs DA metabolism by indirectly inhibiting ALDH activity. These data are consistent with the following conclusions: 1) MeHg impairs conventional DA metabolism and shunts DA along an alternative metabolic pathway, 2) MeHg does not directly impair ALDH activity to alter DA metabolism, 3) mitochondrial dysfunction induced by MeHg decreases basal respiration, as well as ATP generation and reserve respiratory capacity, and 4) MeHg decreases availability of the enzyme cofactor NAD(H), which could indirectly impair ALDH activity.

4.4.1. The DA metabolomic profile induced by MeHg

MeHg inhibits DA metabolism. Previous reports demonstrate a concentration-dependent decrease in intracellular DOPAC in the striatum (Bemis and Seegal, 1999; Dreiem et al., 2009), and decreased striatal release of DOPAC (Faro et al., 2003; 2007). Results from the present study support and extend these findings. Intracellular DOPAC was significantly decreased by exposure to MeHg, and this effect was accompanied by a significant increase in intracellular concentrations of DOPAL and DOPET. Analysis of the percentage changes in these three metabolites reveals they are proportional; DOPAC decreases by approximately 60%, while DOPAL and DOPET increase by approximately 65% and 70% respectively.

These data suggest that MeHg impairs DA metabolism by inhibiting the oxidation of DOPAL to DOPAC. MAO is functional and its activity is intact because the concentration of DOPAL did not decrease. Conversely, the concentration of DOPAL increased, suggesting that ALDH activity is impaired. As a result, DOPAL metabolism shifts to the lower-affinity

reductive pathway mediated by AR, which enhances DOPET accumulation (Turner et al., 1974; Lamensdorf et al., 2000b).

The present analysis suggests that MeHg does not stimulate AR activity. DOPAL and DOPET increased in proportion to one another. If AR were stimulated, a profound increase in DOPET without a concomitant increase in DOPAL would be expected. Furthermore, while DOPET accumulation was moderately enhanced, this was expected as inhibition of the *oxidative pathway* has been previously demonstrated to increase DOPET formation (Lamensdorf et al., 2000b). However based on the present analysis, there is no conclusive evidence that MeHg does not stimulate AR, and further investigation would be needed to address this point.

The conclusion that MeHg inhibits ALDH is novel, however somewhat inconsistent with reports in the literature. Previous studies investigating the effects of MeHg on DA metabolism have primarily indicated that MeHg inhibits MAO activity (Taylor and DiStefano, 1976; Chakrabarti et al., 1998; Beyrouthy et al., 2006; Castoldi et al., 2006). In these studies MAO activity was measured in either whole or regional brain homogenates. Therefore the analysis of MAO activity in these studies was not specific to DA neurons, and the observed decrease in MAO activity in these studies could have been due to collective changes in multiple types of neurons.

It is also plausible that the lack of change in MAO activity observed presently is specific to the undifferentiated PC12 cell line. For example, expression of different MAO and ALDH isozymes in NSDA neurons could mediate alternative changes in the aberrant DA metabolomic profile induced by exposure to MeHg. Two isozymes of MAO, designated A and B, have been proposed based on substrate selectivity and inhibitor sensitivity (Cai et

al., 1998). MAO A has a higher affinity for DA, and is predominately found in rat catecholamine neurons and PC12 cells (Naoi et al., 1987; Jahng et al., 1997). However, in most species both forms can oxidize DA (O'Carroll et al., 1983), and in humans MAO B is primarily responsible for DA oxidation (Glover et al., 1977; Riederer and Jellinger, 1982). Similarly, two isozymes of ALDH, ALDH2 and ALDH1A1, can mediate DA metabolism (Marchitti et al., 2008). In PC12 cells, ALDH2 catalyzes the oxidation of DOPAL (Marchitti et al., 2007; Robador et al., 2012), whereas in NSDA neurons both ALDH2 and ALDH1A1 can participate (Galter et al., 2003; Anderson et al., 2011b). Given these differences, an investigation of the aberrant DA metabolomic profile induced by MeHg in NSDA neuronal cultures is warranted. However, the observed changes in DA metabolites suggest that mechanisms by which MeHg targets DA metabolism are more complex than previous assumed.

4.4.2. Comparative effects of MeHg, daidzin, and rotenone on DA metabolism

The observed neurochemical profile suggests that MeHg impairs ALDH activity, but does not provide evidence to distinguish between direct versus indirect effects. Directly, MeHg could bind cysteine residues present in the active site of the enzyme (Weiner and Wang, 1994). Indirectly, impaired mitochondrial respiration induced by MeHg could decrease availability of the ALDH cofactor NAD, which is produced when NADH donates electrons to Complex I of the ETC (Lamensdorf et al., 2000a). To identify direct or indirect mechanisms by which MeHg may target ALDH, the effect of the toxicant was compared with two other pharmacological inhibitors, daidzin and rotenone. Daidzin is a reversible, selective ALDH2 inhibitor (Keung and Vallee, 1993), and rotenone is a reversible inhibitor

of NADH:ubiquinone oxidoreducase (Complex I of the mitochondrial ETC; Schuler and Casida, 2001).

Rotenone and daidzin reduced the intracellular concentration of DOPAC to a similar extent as compare to MeHg. However the increase in DOPET induced by MeHg and daidzin was more pronounced than that induced by rotenone. These results suggest that all three compounds inhibit the *oxidative pathway* of DA metabolism; daidzin by directly inhibiting ALDH (Keung and Vallee, 1993), rotenone by decreasing availability of the ALDH cofactor NAD (Schuler and Casida, 2001), and MeHg by a yet to be elucidated mechanism. However, the three compounds stimulate the *reductive pathway* of DA metabolism to different degrees.

4.4.3. Evidence for a role of mitochondrial dysfunction rather than direct ALDH inhibition in MeHg-impaired DA metabolism

To investigate the direct effect of MeHg on ALDH, enzymatic activity was measured as the accumulation of NADH, a by-product of reactions catalyzed by ALDH (Guru and Shetty, 1990). The activity of ALDH was measured either following pre-treatment or in the presence of HBS, MeHg, daidzin, or rotenone. As expected, daidzin decreased NADH production, but only during co-treatment. Because daidzin is a reversible ALDH2 inhibitor, its presence is required to inhibit ALDH enzymatic activity. Rotenone increased NADH production. This observation was likely a false positive, resulting from the action of rotenone on NADH:ubiquinone oxidoreducase (Schuler and Casida, 2001). Inhibition of this enzyme complex by rotenone resulted in an artificially high accumulation of NADH in the enzyme assay. MeHg, however, had no observable effect on NADH production. This lack of

effect was demonstrated not only following pretreatment with 2 μ M for 60 min, but also in the presence of 1-100 μ M MeHg. Based on these results, it can be concluded that MeHg does not directly inhibit ALDH.

MeHg could indirectly inhibit ALDH activity by decreasing availability of its cofactor NAD. Mitochondrial dysfunction resulting in inhibition of the mitochondrial ETC and decreased respiration would contribute to decreased production of NAD. To investigate this hypothesis, mitochondrial respiration and NAD(H)⁺ were measured. In comparison to pre-treatment with daidzin and rotenone, MeHg not only decreased basal respiration and ATP generation, as demonstrated previously (Sone et al., 1977; Yee and Choi, 1994), but it also decreased spare respiratory capacity. Daidzin had no effect on mitochondrial function, as anticipated, and rotenone only impaired spare respiration. The observed effects of rotenone were less pronounced than expected, but likely resulted because rotenone is a reversible inhibitor.

Spare respiratory capacity is the ability of a cell to respond to an energy crisis (Nicholls et al., 2007). It is dependent upon increased usage of substrate supply and electron transport. Maintenance of an energy reserve is important in the face of oxidative stress (Vesce, 2005) or restriction of Complex I and/or II activity (Yadava and Nicholls, 2007; Choi et al., 2009). In cells with variable ATP requirements, such as neurons, spare respiratory capacity is a powerful diagnostic of cellular bioenergetics (Brand and Nicholls, 2011). Indeed, Nicholls et al., (2007) argue that the maintenance of some spare respiratory capacity is a major factor in survival of neurons.

The ability of MeHg to abolish completely spare respiratory capacity in undifferentiated PC12 cells is a novel finding with significant implications. These data

suggest that in the face of MeHg exposure, cells are operating at the upper limit of their bioenergetic capacity. As a result, they would be unable to combat subsequent oxidative stress and excitotoxicity induced by MeHg (Dreiem and Seegal, 2007; Franco et al., 2007; Mori et al., 2007; Liu et al., 2012). Abolition of spare respiratory capacity could be a critical early factor in the initiation of cell death (Nicholls et al., 2007).

These data are also indicative of impaired electron transport. The exact level at which MeHg impairs the ETC was not determined presently, however previous reports suggest that the toxicant inhibits both Complexes II and III (Sone et al., 1977; Yee and Choi, 1994; Mori et al., 2011). Inhibition at these positions along the respiratory chain would down-regulate the activity of Complex I (DiMauro and Schon, 2008; Cannino et al., 2012), and oxidation of NADH to NAD would diminish.

4.4.4. Consequences of decreased NAD(H) following MeHg exposure

Quantification of NAD(H) revealed a decrease in both total NAD and NADH, without altering their ratio. These data suggest that MeHg decreases the total amount of NAD(H) in either its oxidized or reduced form. This finding supports the conclusion that decreased availability of the ALDH cofactor contributes to the impairment of DA metabolism following exposure to MeHg.

Mitochondrial dysfunction induced by MeHg was hypothesized to contribute to the decreased availability of NAD. The present set of experiments does not provide conclusive evidence to support this hypothesis. Indeed, if MeHg did impair mitochondrial function to indirectly inhibit ALDH, the DA neurochemical profile would mimic that induced by rotenone. Instead MeHg increased the concentration of DOPET to a much greater extent

than did rotenone. Additionally, although MeHg profoundly impaired mitochondrial respiration, there is no evidence to correlate that dysfunction with the observed decrease in NAD. Lastly, because MeHg decreased the total amount of NAD(H), inhibition of the ETC, particularly Complex I, cannot completely account for the observed alterations in DA metabolism, as inhibition of Complex I would decrease the oxidation of NADH (Kang et al., 1997).

Yet unidentified intracellular factors must contribute to the observed decrease in NAD(H). Two possibilities are MeHg-induced inhibition of the citric acid cycle and/or activation of a protective metabolic network dedicated to the conversion of NADH to NADPH. The citric acid cycle is ubiquitous and comprises an essential series of chemical reactions responsible for generating cellular energy in aerobic organisms. Additionally, the cycle provides NADH, which can be used in numerous biochemical reactions, including the mitochondrial ETC. There is some evidence to suggest that MeHg inhibits the citric acid cycle. The formation of substrates for the cycle, including pyruvate, are increased in guinea pig cerebral cortical slices treated with 10-50 μ M MeHg (Fox et al., 1975). Furthermore MeHg is demonstrated to inhibit the activity of specific enzymes in the cycle, including succinate dehydrogenase (Yoshino et al., 1966) and malate dehydrogenase (Hamdy and Noyes, 1977). Resulting changes in substrate availability would regulate the activity of the citric acid cycle, and decrease production of NADH.

Another possible explanation for decreased availability of NAD(H) is conversion of NADH to NADPH. NADPH is an essential reducing agent, and contributes to antioxidant defense mechanisms by sustaining the activity of enzymes such as catalase, superoxide dismutase, and glutathione peroxidase (Minard, 2005). There is evidence to suggest that

under conditions of oxidative stress, NADH is converted to NADPH by a compensatory metabolic network involving NADH kinase and malic enzyme (Singh et al., 2008).

Activation of this pathway could potentially contribute to antioxidant defense strategies in the face of oxidative stress induced by MeHg (LeBel et al., 1990; Sarafian et al., 1994; Gatti et al., 2004). However, because MeHg inhibits many antioxidant enzymes, including glutathione peroxidase (Kaur et al., 2006; Franco et al., 2009) and catalase (Cuello et al., 2010), the actual protection offered by activation of this network could be negligible. It is unknown if and how NADPH levels are modulated following exposure to MeHg, however a potential increase in NADPH could contribute to AR stimulation and DOPET accumulation observed in these studies.

4.4.5. Potential biological effects of MeHg-impaired DA metabolism

The observation that MeHg increases DOPAL accumulation is of significant consequence. Increased production of DOPAL is one mechanism by which MeHg may exert toxicity in DA synthesizing cells. DOPAL has demonstrated toxic effects in DA neurons both *in vivo* and *in vitro*. Microinjections of DOPAL in the substantia nigra cause focal, generalized lesions associated with a loss of TH immunoreactivity and other phenotypic neuronal markers, as well as marked gliosis (Burke et al., 2003). In differentiated PC12 cells and striatal synaptosomes, exposure to micromolar concentrations of DOPAL increases the incidence of cell death (Mattammal et al., 1995).

In addition to increasing toxicity itself, DOPAL in combination with glucose deprivation and mitochondrial respiratory chain inhibition enhances toxicity (Lamensdorf et al., 2000a). Hence, inhibition of DOPAL oxidation potentiates toxicity induced by

metabolic stress and mitochondrial dysfunction. As demonstrated presently, MeHg impairs mitochondrial respiration and abolishes reserve respiratory capacity in cells. Therefore, the selective sensitivity of DA synthesizing cells to MeHg may result from a combination of the generalized molecular mechanism by which the toxicant exerts its effects and the distinct cellular environment created by the presence of DA and the enzymes necessary for its metabolism.

Furthermore, the finding that MeHg increases DOPAL activity as a result of indirect ALDH inhibition provides evidence in support of the hypothesis that exposure to MeHg contributes to the etiology of PD. A link between ALDH inhibition and PD has previously been established following occupational exposure to another environmental toxicant. Fitzmaurice et al. (2013) demonstrate that the fungicide benomyl causes concentration-dependent inhibition of ALDH, which is associated with decreased production of DOPAC in primary DA cultures and decreased VMAT positive neurons in zebrafish. In humans, occupational exposure to benomyl increases the incidence of PD by 67% (Fitzmaurice et al., 2013). Therefore environmental toxicants, including benomyl and MeHg, inhibit ALDH sufficiently to damage DA neurons and increase the risk of PD in exposed humans.

4.4.6. Summary

In conclusions, MeHg alters the DA metabolic profile in undifferentiated PC12 cells. Results suggest that ALDH activity is inhibited indirectly by mitochondrial dysfunction and decreased availability of the ALDH cofactor NAD. Consequences of impaired DA metabolism contribute to accumulation of the toxic DA metabolic intermediate, DOPAL. These data

provide evidence for a mechanism by which DA neurons may be selectively sensitive to the toxic effects of MeHg.

Chapter 5. The role of extracellular Ca^{2+} in MeHg-induced alterations in DA release and metabolism

5.1. Introduction

5.1.1. Neurotransmitter release and VGCCs

Extracellular Ca^{2+} influx through VGCCs is the primary event responsible for initiating synaptic transmission (Olivera et al., 1994; Dunlap et al., 1995). Once Ca^{2+} enters the cell, it binds the Ca^{2+} binding protein on the vesicle membrane, synaptotagmin, and activates proteins involved in vesicle docking and neurotransmitter release (Bommert et al., 1993; Elferink et al., 1993; Bajjalieh and Scheller, 1995; Catterall and Few, 2008). In the mammalian central nervous system, the P/Q-type VGCC plays the major role mediating vesicular exocytosis at most synapses (Sheng et al., 1998). However N- and L-type VGCCs have also been implicated in specific subsets of neurons, including inhibitory interneurons in the hippocampus (Poncer et al., 1997) and neuroendocrine cells (Yamada et al., 1996).

MeHg causes a concentration- and time-dependent increase in intracellular Ca^{2+} (Kauppinen et al., 1989). The first phase is slow, gradual, and mediated by the release of Ca^{2+} from intracellular stores (Hare and Atchison, 1995a; Limke et al., 2003). The second phase is rapid and occurs at a magnitude that overwhelms the cellular buffering capacity (Marty and Atchison, 1997). Removal of extracellular Ca^{2+} abolishes the second phase of intracellular Ca^{2+} elevation induced by MeHg, demonstrating a strict dependence on

extracellular Ca^{2+} (Denny et al., 1993). To date, the pathways mediating second phase Ca^{2+} influx have yet to be elucidated, however influx through L-, N-, or P/Q-type VGCCs has been implicated because their inhibition delays the time-to-onset (Marty and Atchison, 1997).

Effects of MeHg on VGCCs are well documented although somewhat enigmatic. Immediately following application, MeHg decreases VGCC-mediated $^{45}\text{Ca}^{2+}$ uptake in forebrain synaptosomes, and decreases specific binding of L- and N-type VGCC antagonists in PC12 cells (Shafer et al., 1990). Additionally, whole cell currents carried by Ba^{2+} , a Ca^{2+} surrogate, through L- and N-type VGCCs is rapidly and completely blocked by MeHg (Shafer and Atchison, 1991b). Based on these findings it has been predominantly concluded that MeHg interacts directly with channels to irreversibly block Ca^{2+} flux. However, MeHg does not reduce mean Ca^{2+} current amplitude when applied to the cytoplasmic side of the membrane (Shafer, 1998). One possible explanation for these paradoxical findings is that MeHg uses VGCCs to enter the cell, which competitively but temporarily blocks the channel. Once on the cytoplasmic side, the toxicant interacts with the channel to enhance extracellular Ca^{2+} influx. Delay of the second Ca^{2+} phase by VGCC inhibition supports this hypothesis (Marty and Atchison, 1997). In this instance, VGCC antagonism could actually delay the interaction of MeHg with target sites or delay its entry into the cell.

Because of the crucial role of Ca^{2+} influx through VGCCs in neurotransmitter release, it follows that extracellular Ca^{2+} influx induced by MeHg may act as a primary

mechanism mediating MeHg-induced DA release (Chapter 3). A role for extracellular Ca^{2+} in MeHg-induced catecholamine release has been documented (Gassó et al., 2000), however extracellular Ca^{2+} -independent DA release has also been described following MeHg exposure (Kalisch and Racz, 1996; Faro et al., 2002). As such, the present study sought to elucidate the role of extracellular Ca^{2+} and the potential contribution of VGCCs to MeHg-induced DA release.

5.1.2. Mitochondrial function and DA metabolism

Tight regulation of intracellular Ca^{2+} homeostasis is of critical importance because Ca^{2+} plays key roles in metabolic regulation and intracellular signaling cascades. Mitochondria are one of two essential Ca^{2+} buffering organelles responsible for maintaining a low concentration of intracellular Ca^{2+} (Blaustein, 1988; Meldolesi et al., 1992). Generally, a powerful stimulus of high intracellular Ca^{2+} is required for mitochondria to actively buffer Ca^{2+} from the cytosol into the mitochondrial matrix (Nicholls and Scott, 1980; Stockum et al., 2011). The Ca^{2+} uniporter mediates Ca^{2+} uptake (Pan et al., 2011), whereas the $\text{Na}^+/\text{Ca}^{2+}$ exchanger primarily mediates Ca^{2+} efflux (Deryabina et al., 2004). However Ca^{2+} can also be released from the mitochondria following reversal of the Ca^{2+} uniporter, collapse of the mitochondrial membrane potential, or opening of the mitochondrial permeability transition pore (Contreras et al., 2010; Assaly

et al., 2012; Roos et al., 2012). These pathological conditions occur as a result of Ca^{2+} overloading and indicate mitochondrial dysfunction, which can trigger apoptosis (Ravagnan et al., 2002; Jordan et al., 2003).

MeHg induces a mitochondrial state consistent with Ca^{2+} overloading (Roos et al., 2012). Respiration and ATP production are depressed (Kauppinen et al., 1989; Chapter 4; Gatti et al., 2004), Complexes II and III of the ETC are inhibited (Sone et al., 1977; Yee and Choi, 1996; Mori et al., 2011), and the mitochondrial membrane potential is dissipated (Bondy and McKee, 1991; Hare and Atchison, 1992; Limke and Atchison, 2002). Subsequent cell death is thought to result from opening of the mitochondrial permeability transition pore and release of pro-apoptotic factors, including apoptosis inducing factor (Fonfria et al., 2002; Limke and Atchison, 2002). MeHg affects mitochondrial Ca^{2+} regulation by at least two mechanisms. Directly, MeHg inhibits ETC respiratory proteins (Verity et al., 1975) and causes a loss of mitochondrial membrane potential (Bondy and McKee, 1991; Hare and Atchison, 1992; Limke and Atchison, 2002). Indirectly, MeHg-induced increase in intracellular Ca^{2+} initiates excessive uptake of Ca^{2+} by the mitochondria (Limke et al., 2003), ultimately depolarizing the inner mitochondrial membrane, inhibiting ATP production, and opening the mitochondrial permeability transition pore.

Considering that mitochondria play an essential role in buffering excessive intracellular Ca^{2+} (Blaustein, 1988; Meldolesi et al., 1992) and extracellular Ca^{2+} influx induced by MeHg contributes to deleteriously elevated intracellular Ca^{2+} (Denny et al.,

1993; Marty and Atchison, 1997), the role of MeHg-induced extracellular Ca^{2+} influx in mitochondrial dysfunction was investigated. Although removal of extracellular Ca^{2+} does not alter MeHg-induced ROS formation (Dreiem and Seegal, 2007), other aspects of mitochondrial function, including respiration and ATP production, have yet to be investigated. Since MeHg-impaired DA metabolism is due in part to mitochondrial dysfunction (Chapter 4), the role of extracellular Ca^{2+} in MeHg-impaired DA metabolism was also investigated.

The goals of the present study were to identify the contribution of extracellular Ca^{2+} to MeHg-induced changes in DA release, DA metabolism, and mitochondrial function.

5.2. Methods

5.2.1. Chemicals

The standard physiological saline used for extracellular solution was HBS, which contained (mM): 150 NaCl, 5 KCl, 2.4 CaCl_2 , 1.6 MgSO_4 , 20 HEPES, and 20 *d*-glucose (pH 7.3). In some experiments cells were treated in 0- Ca^{2+} HBS, which had the same composition as HBS with the following exceptions (mM): 0 CaCl_2 and 0.02 ethylene glycol tetraacetic acid.

MeHg (ICN Biochemicals), nimodipine (Sigma), and cadmium chloride (Cd^{2+} ; Sigma) were diluted from stock solutions in HBS or 0- Ca^{2+} HBS. Nimodipine was protected from light during preparation and experimentation. Drug solutions were diluted to final concentrations on the day of each experiment as described in General Methods Section 2.2.

5.2.2. Chemical treatment

PC12 cells were seeded at a density of $6-7 \times 10^5$ cells/mL in 6-well plates or XF24-well plates coated with poly-D-lysine 24-48 hr prior to treatment. To begin each experiment, culture medium was aspirated and replaced with HBS or 0-Ca^{2+} HBS in the absence or presence of pharmacological and toxicant treatments. Cells were incubated at $37^\circ\text{C}/5\%$ CO_2 during treatment as described in General Methods Section 2.2.

5.2.3. Neurochemistry

At experiment termination, treatment medium was retained and acidified. Cells were rinsed, harvested, and pelleted by centrifugation. The content of DA in the treatment medium and its metabolites in the cell pellet were determined by HPLC-ED as described in General Methods Section 2.3. Neurochemical concentrations were normalized to mL per sample for extracellular measurements or mg of protein for intracellular measurements as determined by the BCA protein assay (Sigma).

5.2.4. Mitochondrial bioenergetics

Following pharmacological and toxicant exposure, treatment medium was aspirated. Cells were washed once with XF24 RPMI Assay Medium and then incubated at $37^\circ\text{C}/\text{no CO}_2$ for 1 hr to allow medium temperature and pH to equilibrate before the first measurements were made. The biosensor cartridge was hydrated overnight and injection ports were loaded with test compounds as described in General Methods Section 2.6. OCR

was measured under basal conditions and following injection of test compounds using the XF24 Extracellular Flux Analyzer. Basal respiration, ATP generation, and spare respiration were calculated and compared between treatment groups.

5.2.5. Statistical analysis

SigmaPlot® software version 12.0 (SysStat Software, Inc., Point Richmond, CA) was used to make statistical comparisons among groups using unpaired t-test, one-, and two-way ANOVA, or non-parametric alternatives as appropriate. If a significant difference was detected, *post hoc* between-group comparisons were performed using Tukey's test. Statistical significance was set at $p \leq 0.05$.

5.3. Results

5.3.1. Spontaneous MeHg-mediated DA release is partially dependent upon the presence of extracellular Ca^{2+} , but not Ca^{2+} influx through VGCCs

DA is released from PC12 cells through Ca^{2+} -dependent exocytosis (Kishimoto et al., 2005). Because MeHg induces extracellular Ca^{2+} influx (Marty and Atchison, 1997), a role for extracellular Ca^{2+} in MeHg-mediated DA release from undifferentiated PC12 cells was evaluated by measuring extracellular DA concentrations after exposure to MeHg in a Ca^{2+} -free solution. As demonstrated previously (Chapter 3), in the presence of extracellular Ca^{2+} , treatment with 2 μ M MeHg for 60 min increased the concentration of extracellular DA (Figure 5.1A; $p < 0.05$). There was a slight non-significant decrease in spontaneous DA

release in cells incubated in Ca^{2+} -free HBS (Figure 5.1A, C; $p>0.05$). In the absence of extracellular Ca^{2+} , MeHg-induced DA release from PC12 cells was significantly attenuated as compared with HBS-treated cells ($p<0.05$). However, there was still a dramatic increase in DA released by MeHg in the absence of extracellular Ca^{2+} . When evaluated as the percentage change from medium control, DA release induced by MeHg in the absence of extracellular Ca^{2+} was not significantly different from DA released by MeHg in the presence of extracellular Ca^{2+} (Figure 5.1B; $p>0.05$).

VGCCs contribute to the perturbation of intracellular Ca^{2+} induced by MeHg (Hare and Atchison, 1995b; Marty and Atchison, 1997). Undifferentiated PC12 cells primarily express the L-type VGCC, and Ca^{2+} current through these channels is blocked by dihydropyridine antagonists, such as nimodipine (Kongsamut and Miller, 1986; Janigro et al., 1989; Avidor et al., 1994). Therefore experiments complementary to those evaluating MeHg-induced DA release in a Ca^{2+} -free buffer evaluated release following inhibition of VGCCs (Figure 5.2). Pretreatment with $2\mu\text{M}$ nimodipine, a selective L-type VGCC inhibitor, failed to attenuate DA release induced by $2\mu\text{M}$ MeHg for 60 min. Likewise, the nonspecific VGCC inhibitor Cd^{2+} ($200\mu\text{M}$) had no effect ($p>0.05$).

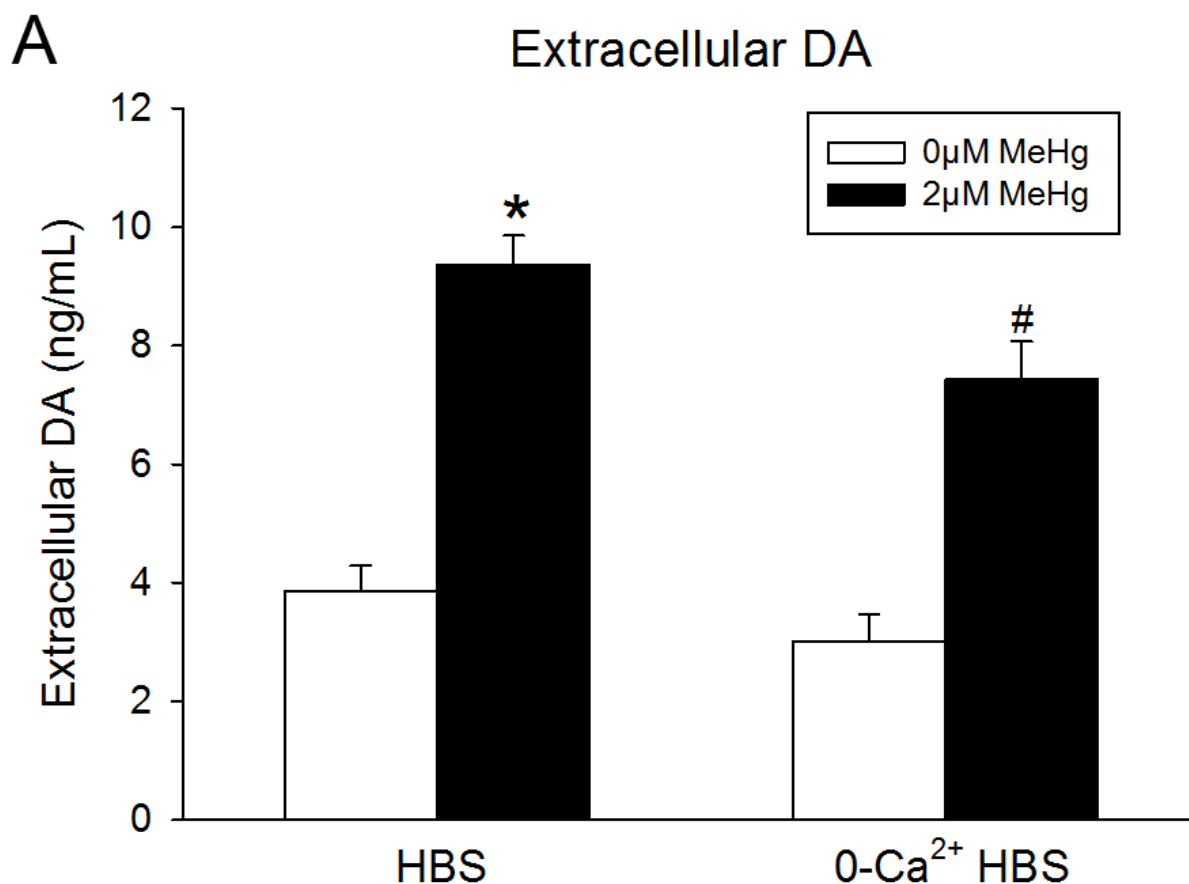
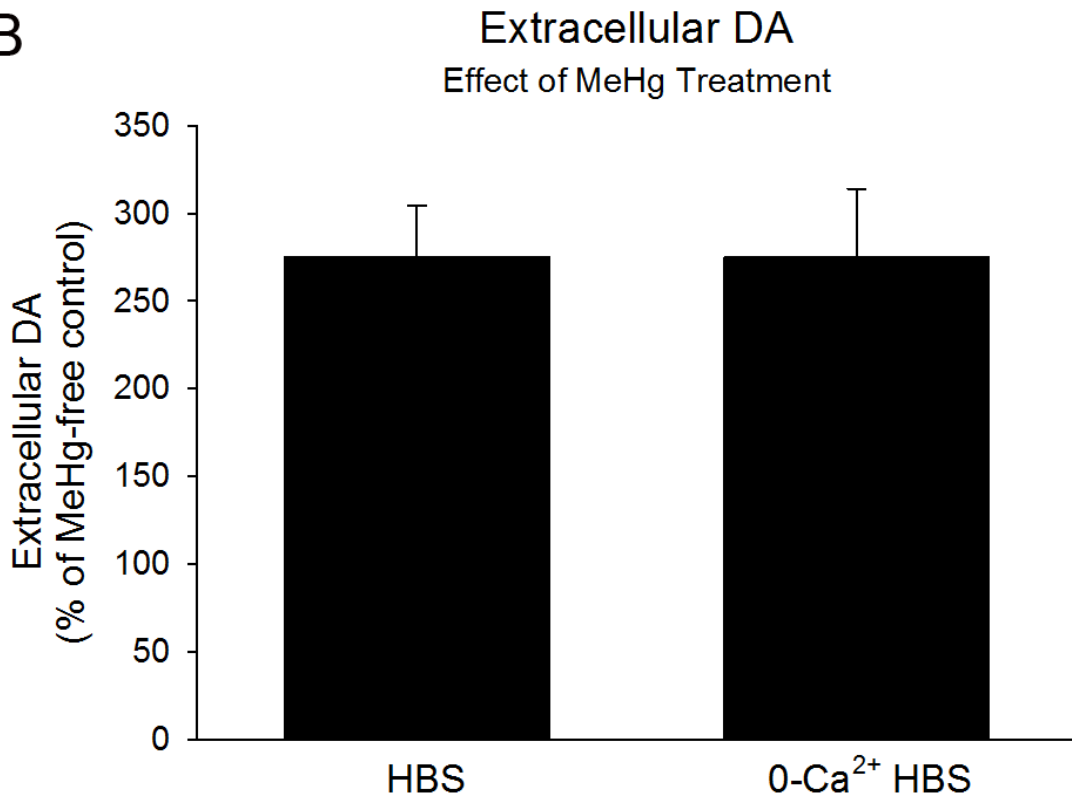


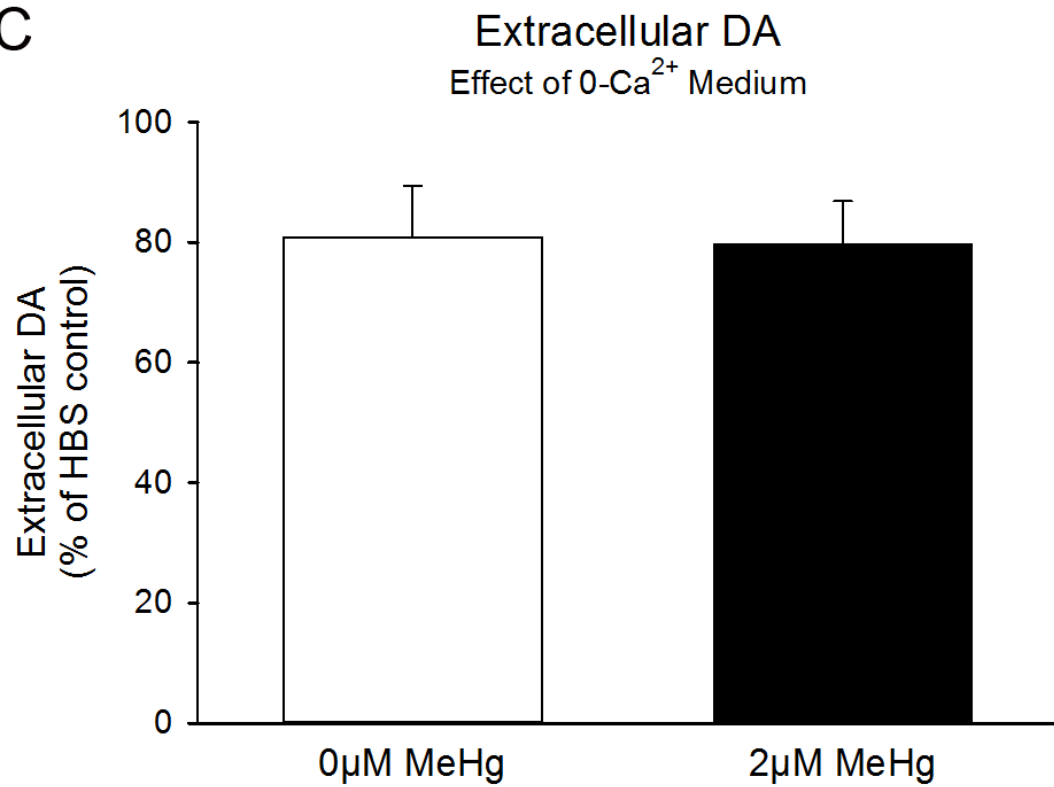
Figure 5.1. Extracellular Ca²⁺ does not contribute to MeHg-induced DA release. Undifferentiated PC12 cells were treated with 0µM (white bars) or 2µM (black bars) MeHg in the absence (0-Ca²⁺ HBS) or presence (HBS) of extracellular Ca²⁺ for 60 min. Panel A) Concentrations of extracellular DA. Panel B) The percentage change of extracellular DA after treatment with MeHg in cells treated with either HBS or 0-Ca²⁺ HBS. Panel C) The percentage reduction of extracellular DA by treatment with 0-Ca²⁺ HBS in cells treated with either 0µM or 2µM MeHg. The asterisk (*) indicates a value significantly different than HBS ($p \leq 0.05$). The hash (#) indicates a value significantly difference from both HBS-Control and HBS-MeHg ($p \leq 0.05$). Values are means + SEM ($n = 4$, 3 replicates per n).

Figure 5.1 cont'd

B



C



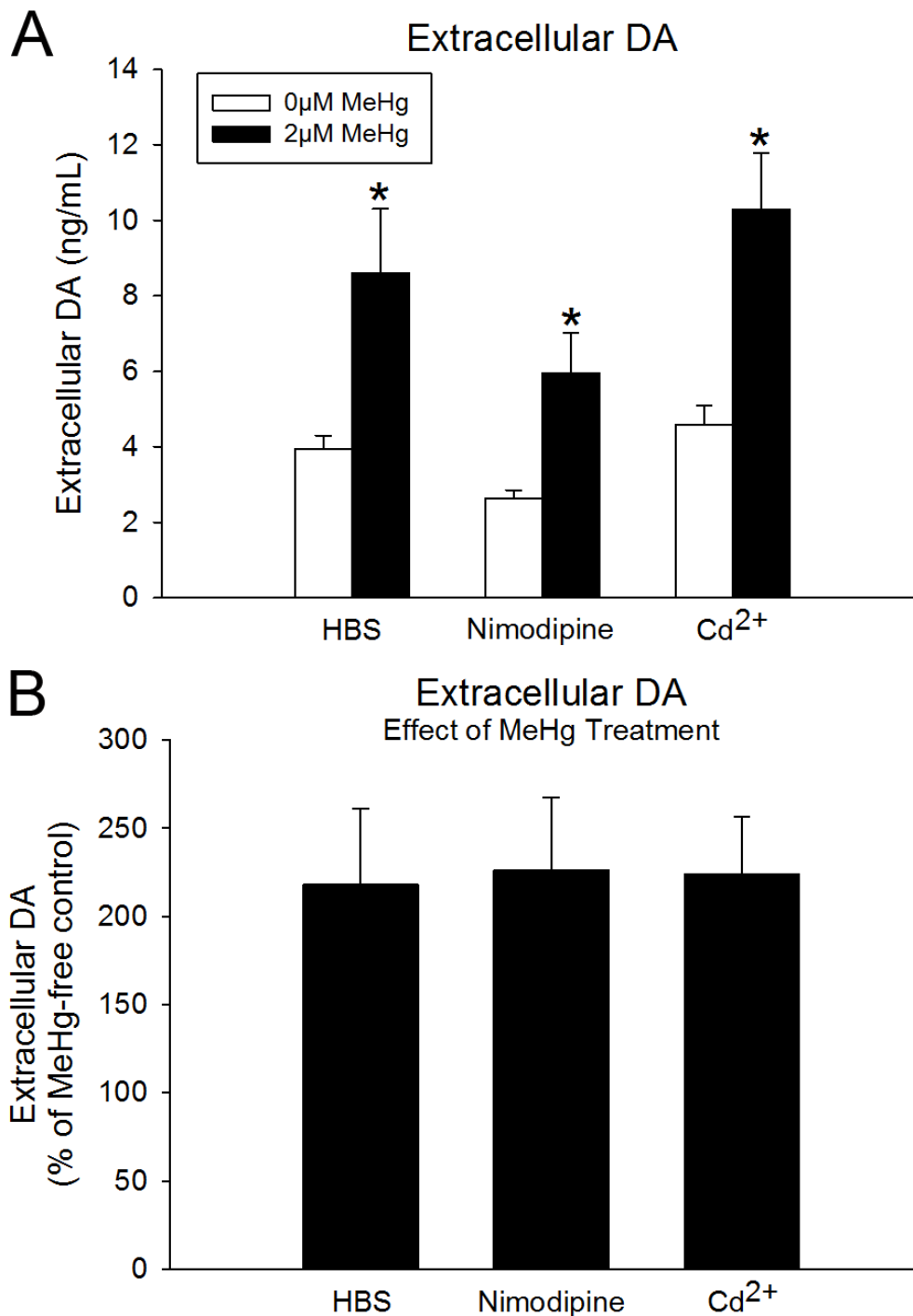


Figure 5.2. Spontaneous activation of VGCCs does not contribute to MeHg-induced DA release. Undifferentiated PC12 cells were treated with either 2µM nimodipine or 200µM Cd²⁺ in culture medium for 15min prior to co-treatment with 0µM (white bars) or 2µM (black bars) MeHg for 60 min. Panel A) Extracellular DA concentrations. Panel B) The percentage change of extracellular DA after treatment with MeHg in each treatment group. The asterisk (*) indicates a significant difference from HBS within treatment group ($p \leq 0.05$). Values are means + SEM ($n = 3$, 3 replicates per n).

5.3.2. *Extracellular Ca²⁺ stimulates mitochondrial bioenergetics, but does not contribute to MeHg-induced mitochondrial dysfunction or aberrant DA metabolism*

As demonstrated in Chapter 4, MeHg impairs both mitochondrial bioenergetics and DA metabolism. Results suggest MeHg may indirectly impair the oxidation of DOPAL to DOPAC by decreasing availability of the ALDH cofactor NAD, the majority of which is provided by Complex I of the mitochondrial ETC (Weiner and Wang, 1994). As such, MeHg-induced mitochondrial dysfunction is hypothesized to contribute to MeHg-impaired DA metabolism. To evaluate a role for extracellular Ca²⁺ in MeHg targeting of DA metabolism, parameters of mitochondrial bioenergetics and concentrations of intracellular DA metabolites were measured after exposure to MeHg in a Ca²⁺-free buffer. Mitochondrial respiration was measured in undifferentiated PC12 cells pre-treated with 2μM MeHg for 60 min in the absence or presence of extracellular Ca²⁺. Following pre-treatment, OCR was measured with the XF24 respirometer under basal conditions and following treatment with 5mM pyruvate, 1μM oligomycin A, 2μM FCCP, and 1μM antimycin A. Figure 5.3 depicts changes in OCR following treatment with these compounds. The quantification of these effects revealed that in the absence of extracellular Ca²⁺, basal respiration, spare respiratory capacity, and ATP generation were all enhanced (Figure 5.4; p<0.05). Treatment with 2μM MeHg for 60 min decreased all three parameters to a similar extent, regardless of the absence or presence of extracellular Ca²⁺ in the treatment medium (p<0.05).

In a complementary set of cultures, concentrations of DOPAC and DOPET were assessed following treatment with 2 μ M MeHg for 60 min in 0-Ca²⁺ HBS. MeHg decreased intracellular DOPAC and increased intracellular DOPET in undifferentiated PC12 cells, as previously observed (Chapter 4). Removal of extracellular Ca²⁺ from the treatment buffer did not alter the effect of MeHg on either metabolite (Figure 5.5; p>0.05).

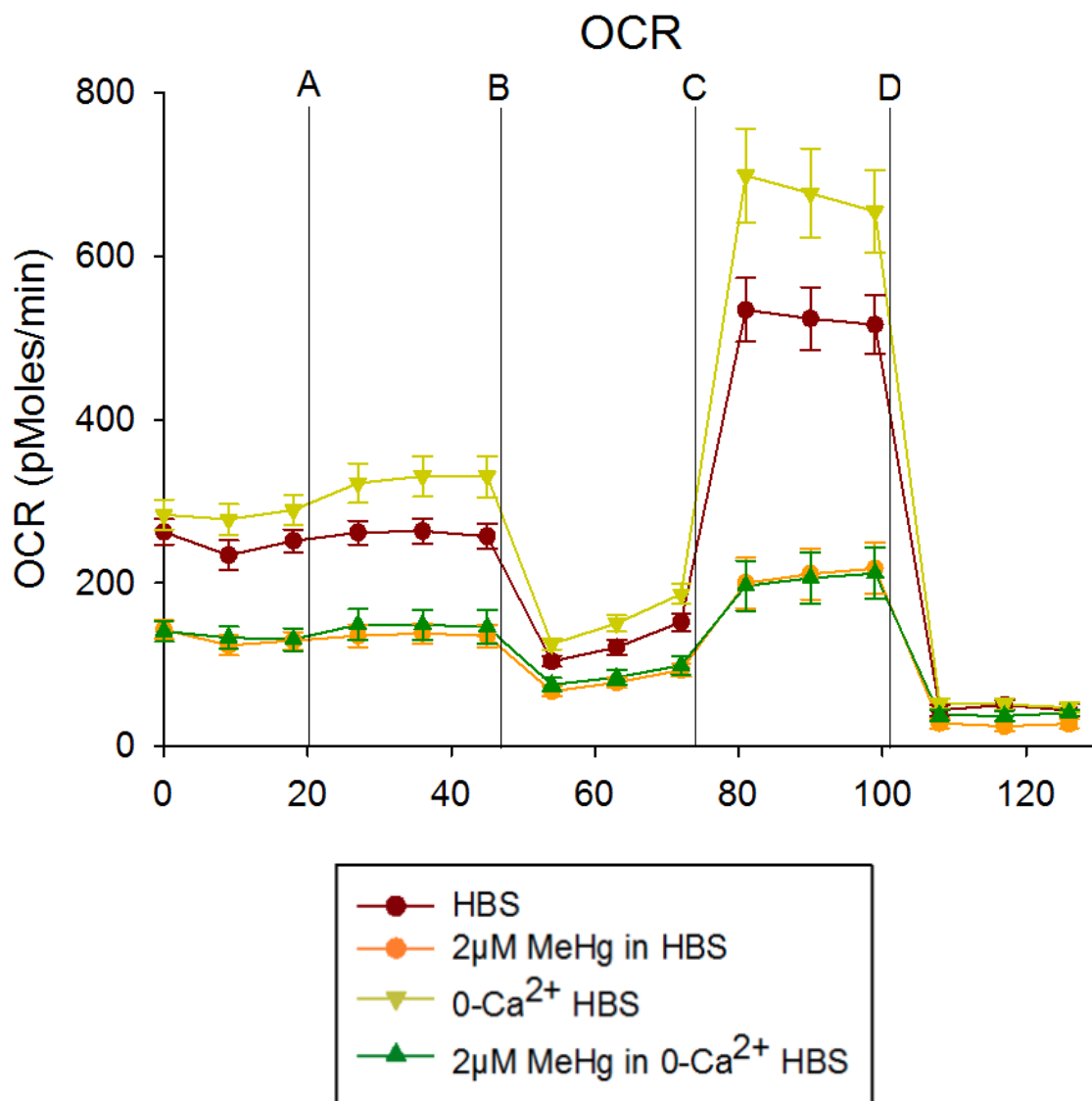


Figure 5.3. Changes in mitochondrial bioenergetics induced by MeHg in the absence or presence of extracellular Ca²⁺. Undifferentiated PC12 cells were pretreated for 60 min with 0µM MeHg in the absence (yellow) or presence (red) of extracellular Ca²⁺ or 2µM MeHg in the absence (green) or presence (orange) of extracellular Ca²⁺. Following pre-treatment, OCR (pMoles/min) was measured under basal conditions and following injections of 5mM pyruvate (A), 1µM oligomycin (B), 2µM FCCP (C), and 1µM antimycin A (D). Values are means ± S.E.M. (n = 3, 4-5 replicates per n).

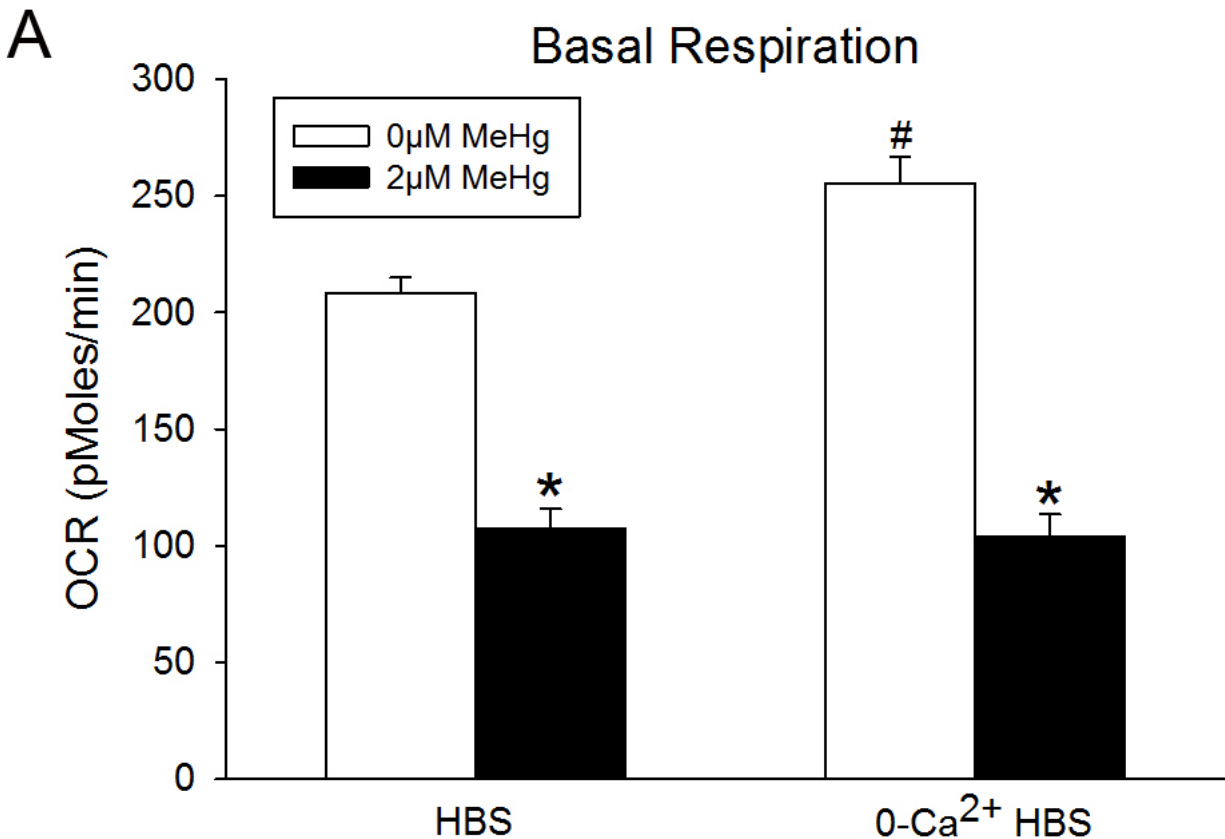
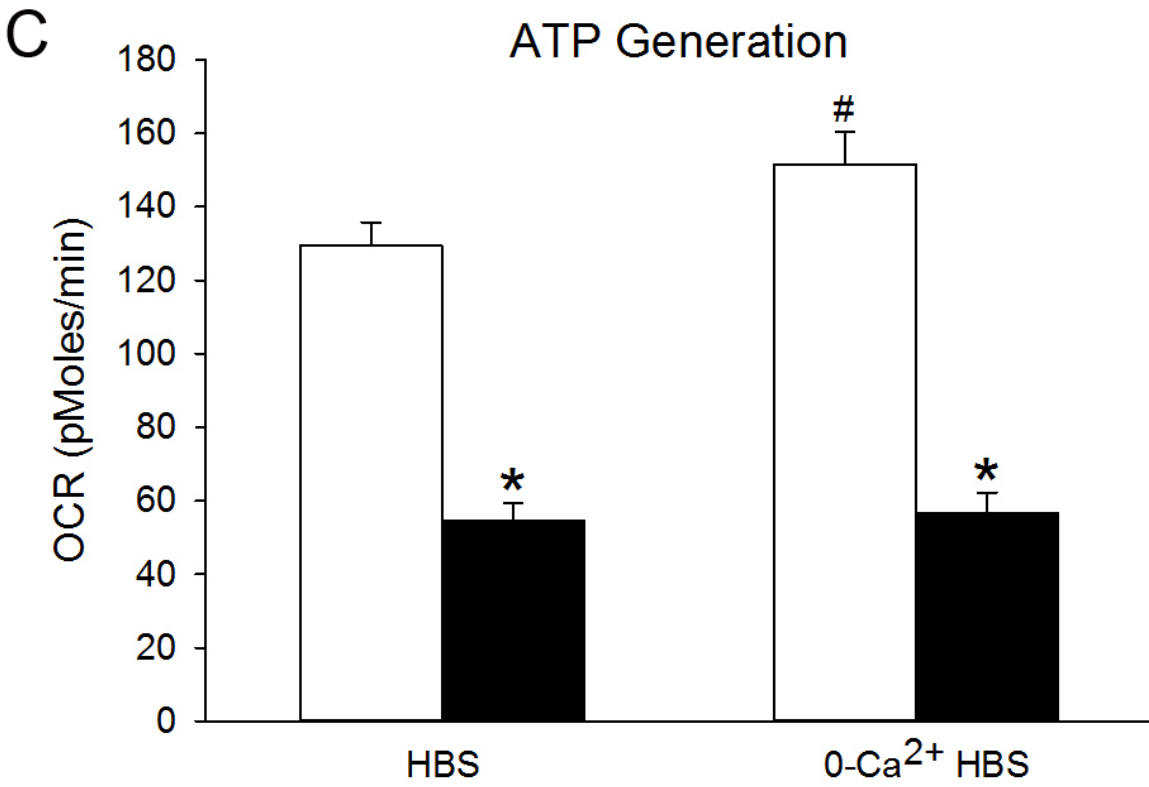
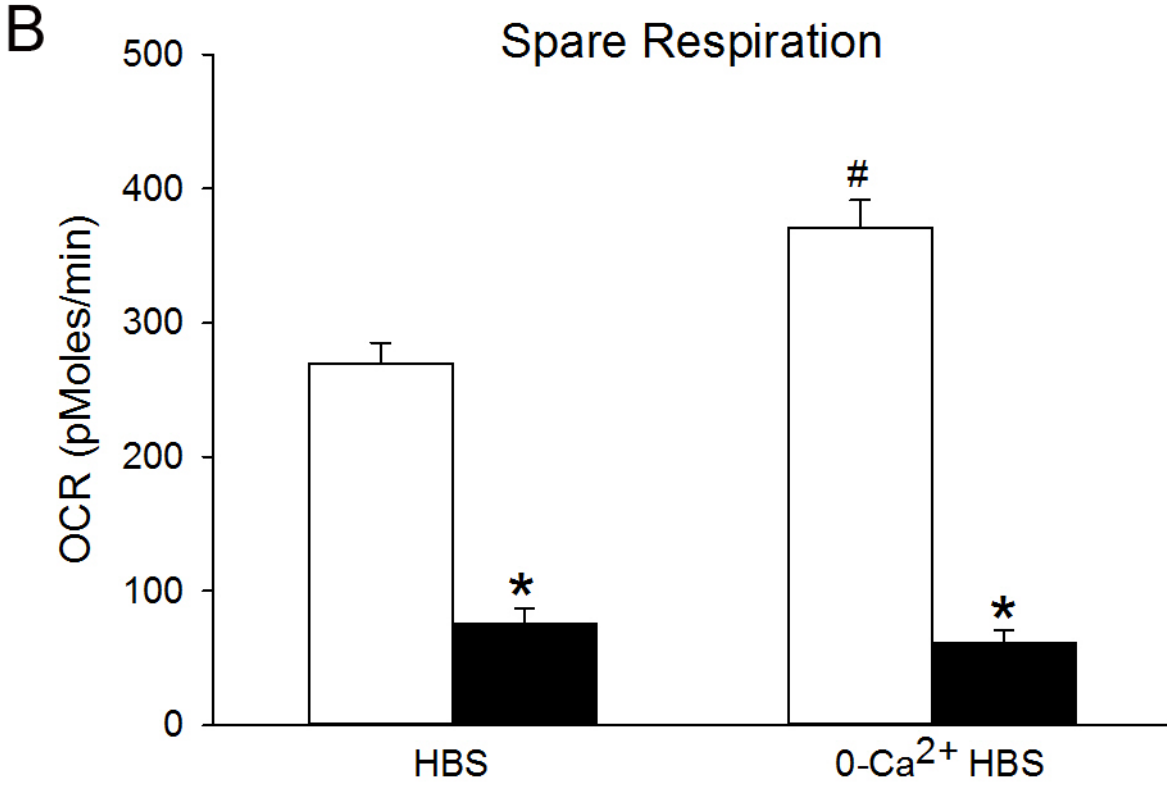


Figure 5.4. Quantification of changes in mitochondrial bioenergetics induced by MeHg in the absence or presence of extracellular Ca²⁺. Panel A) Basal respiration (OCR) was measured in the presence of 25mM glucose and 5mM pyruvate. Panel B) Spare respiration was calculated as the difference between maximum respiration (following treatment with 2µM FCCP) and basal respiration. Panel C) ATP generation was calculated as the difference between basal respiration and respiration following treatment with 1µM oligomycin A. The asterisk (*) indicates a value significantly different than vehicle control ($p < 0.05$). The hash (#) indicates a value significantly different than HBS-Control ($p \leq 0.05$). Values are means + S.E.M. ($n = 3, 4-5$ replicates per n).

Figure 5.4 cont'd



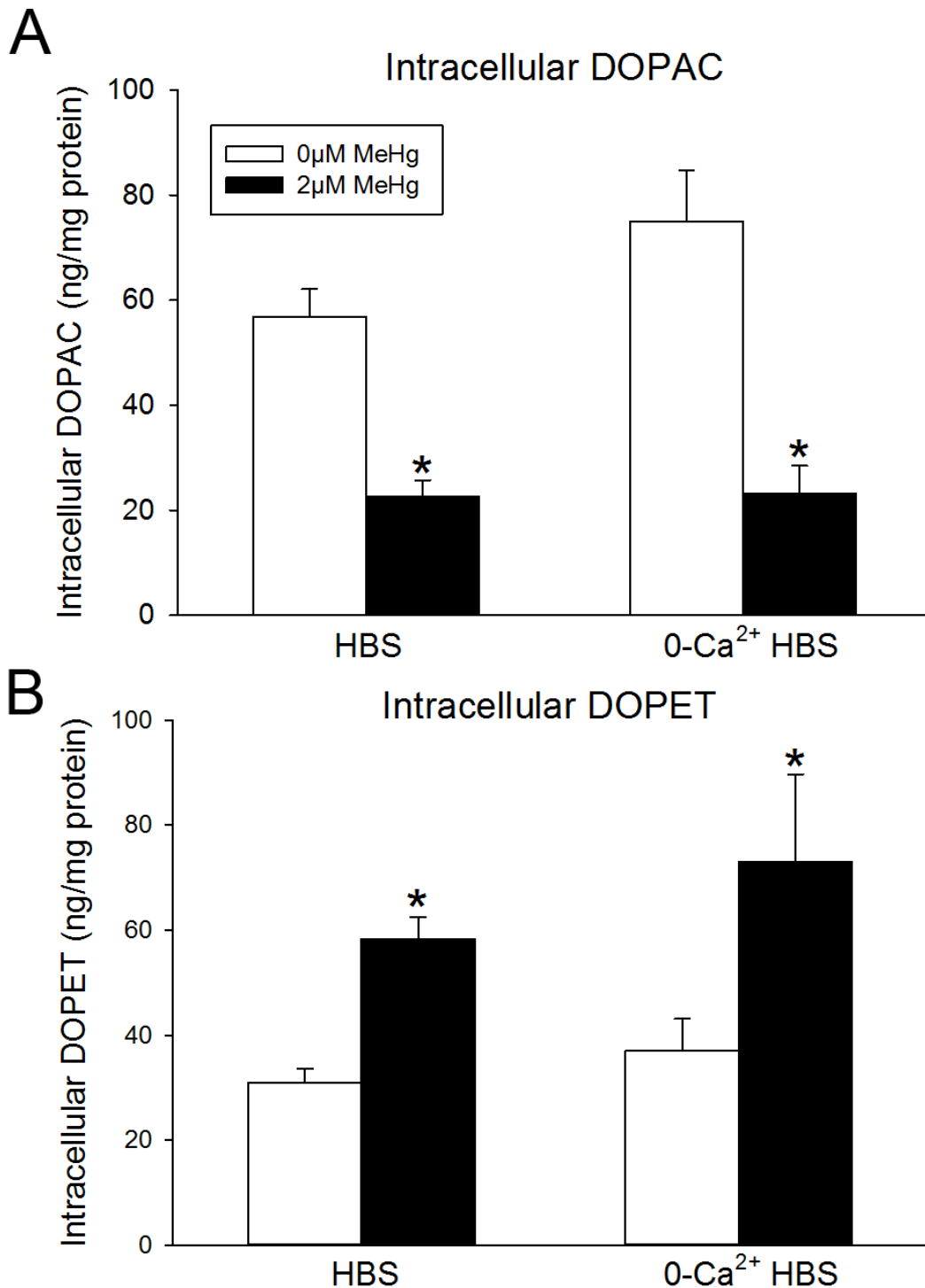


Figure 5.5. Effect of MeHg in the absence or presence of extracellular Ca²⁺ on concentrations of intracellular metabolites. Undifferentiated PC12 cells were treated with 0µM (white bars) or 2µM (black bars) MeHg in the absence (0- Ca²⁺ HBS) or presence (HBS) of extracellular Ca²⁺ for 60 min, and concentrations of DOPAC (Panel A) and DOPET (Panel B) were measured. The asterisk (*) indicates a value significantly different from vehicle medium ($p \leq 0.05$). Values are means + SEM ($n = 4$, 3 replicates per

5.4. Discussion

Ca^{2+} plays essential roles in many cellular functions including neurotransmitter release and intracellular signaling (Olivera et al., 1994; Dunlap et al., 1995). Because high concentrations of cytosolic Ca^{2+} can initiate cell death cascades, the concentration of intracellular Ca^{2+} must be tightly regulated (Kass and Orrenius, 1999). A non-physiologically high concentration of Ca^{2+} in the cytosol is a marker of pathology. MeHg increases the concentration of intracellular Ca^{2+} , which contributes to its toxicity (Kauppinen et al., 1989; Marty and Atchison, 1998). Both extracellular and intracellular sources of Ca^{2+} have been implicated in MeHg-induced elevation of intracellular Ca^{2+} (Denny et al., 1993; Marty and Atchison, 1997).

The present study sought to elucidate the role of extracellular Ca^{2+} as a primary mechanism mediating MeHg targeting of DA release and metabolism in PC12 cells, as well as impaired mitochondrial respiration and ATP generation induced by the toxicant. The principal findings from the present work are: 1) extracellular Ca^{2+} influx through VGCCs at rest does not contribute to either basal or MeHg-mediated DA release, 2) lack of extracellular Ca^{2+} enhances mitochondrial respiration and other parameters of bioenergetics including ATP generation and spare respiratory capacity, 3) mitochondrial dysfunction induced by MeHg is not dependent on extracellular Ca^{2+} , and 4) basal DA metabolism and changes induced by MeHg are not dependent upon the presence of extracellular Ca^{2+} .

5.4.1. Role of extracellular Ca²⁺ in spontaneous and MeHg-mediated DA release

Spontaneous basal DA release from PC12 cells was independent of extracellular Ca²⁺ because removal of Ca²⁺ from the extracellular medium, in the presence of a chelating agent, did not reduce the concentration of extracellular DA. Although DA release from PC12 cells is classically described as Ca²⁺-dependent (Greene and Rein, 1977a), the source of Ca²⁺ can be intracellular (Kishimoto et al., 2005). Therefore, spontaneous DA release from PC12 cells is most likely modulated by changes in cytosolic Ca²⁺ independent of extracellular Ca²⁺ influx.

MeHg induces a biphasic rise in intracellular Ca²⁺. Initially Ca²⁺ is released from intracellular stores followed by Ca²⁺ entry from the extracellular space (Marty and Atchison, 1997). Removal of Ca²⁺ from the medium attenuates the rise in extracellular DA following exposure to MeHg, demonstrating a partial dependence on extracellular Ca²⁺. This observation suggests that second phase Ca²⁺ influx following exposure to the toxicant contributes to DA release. However, further analysis of these data reveal that the contribution of extracellular Ca²⁺ is minimal; MeHg induced comparable increases in extracellular DA in the absence and presence of extracellular Ca²⁺.

These data are consistent with previous reports in the literature demonstrating that spontaneous DA release is diminished, but not abolished, in a Ca²⁺-free superfusate

(Kalisch and Racz, 1996). A large contribution of extracellular Ca^{2+} to the observed MeHg-induced DA release was not expected, considering that release was not evoked by depolarization in the present study. Rather, the phenomenon is more likely due to release of Ca^{2+} from intracellular stores that results during first phase Ca^{2+} influx following exposure to MeHg (Marty and Atchison, 1997). Alternatively, inhibition of the Na^+/K^+ ATPase by MeHg produces an increase in intracellular Ca^{2+} that could also contribute to DA release (Berg and Miles, 1979).

5.4.2. Role of VGCCs in spontaneous and MeHg-mediated DA release

Neurotransmitter release occurs in two phases, fast synchronous and slow asynchronous (Varma et al., 2003). The synchronous phase is driven by a precisely timed presynaptic Ca^{2+} current initiated by the arrival of an action potential, and this mediates a large, fast post-synaptic response (Llinas et al., 1981; Sabatini and Regehr, 1996). The asynchronous phase provides tonic neurotransmitter release at most synapses and results from residual Ca^{2+} remaining in the axon terminal after an action potential (Atluri and Regehr, 1998; Lu and Trussell, 2000). The observation that inhibition of VGCCs did not impair basal DA release in the present study is aligned with this hypothesis. Under physiological conditions spontaneous DA release in undifferentiated PC12 cells is primarily mediated by residual Ca^{2+} present in the cell, and not VGCC-mediated Ca^{2+} influx.

Treatment with nimodipine or Cd^{2+} did not attenuated MeHg-induced DA release. Hence, VGCCs do not contribute to catecholamine release induced by MeHg. These data support the conclusion that extracellular Ca^{2+} does not contribute to MeHg-induced neurotransmitter release. Although MeHg interacts with and impairs VGCC function (Shafer et al., 1990; Shafer and Atchison, 1991b; Sirois and Atchison, 2000; Hajela et al., 2003), there is little evidence to suggest MeHg is mediating extracellular Ca^{2+} influx through VGCCs. Instead, DA release induced by MeHg may result from the release of Ca^{2+} from intracellular stores. However it is also possible that there is an increase in Ca^{2+} influx, but the level of Ca^{2+} is not high enough to activate pathways responsible for vesicular release (Atchison, 1986; 1987).

5.4.3. Role of extracellular Ca^{2+} in mitochondrial bioenergetics and targeting by MeHg

The relationship between extracellular Ca^{2+} and mitochondrial respiration has only recently been established by one report in the literature. In an elegant study, Zhdanov et al. (2010) demonstrated a marked, transient activation of respiration in differentiated PC12 cells in response to depletion of extracellular Ca^{2+} . The authors established that depletion of extracellular Ca^{2+} with the chelator EGTA slightly decreased mitochondrial membrane potential, and decreased concentrations of Ca^{2+} in mitochondria and the cytosol. Furthermore treatment with the uncoupler FCCP increased the respiratory response to

EGTA by 80-90% (Zhdanov et al., 2010). In agreement, the present results support and extend these findings. While Zhdanov et al. reported an immediate, yet transient increase in oxygen consumption following exposure to EGTA, the present results suggest that sustained elevation of mitochondrial respiration can be induced by prolonged incubation in a Ca^{2+} -free solution. Additionally, the present work demonstrates that depletion of extracellular Ca^{2+} enhances other parameters of bioenergetics, including ATP generation and spare respiratory capacity.

In addition to establishing a prominent respiratory response to extracellular Ca^{2+} depletion, Zhdanov et al. (2010) also investigated pathways mediating the effect. The authors demonstrate dependence on extracellular Na^+ influx through VGCC, which activates mitochondrial $\text{Na}^+/\text{Ca}^{2+}$ exchange and causes the observed partial decrease in mitochondrial Ca^{2+} . The excessive exchange of Na^+ into the mitochondrial matrix would activate mitochondrial Na^+/H^+ exchange, and result in increased outward pumping of protons, electron transport, and oxygen consumption. In support of this model, the marked respiratory spike induced by EGTA was accompanied by acidification of the mitochondrial matrix, and inhibition of either the mitochondrial $\text{Na}^+/\text{Ca}^{2+}$ or Na^+/H^+ exchanger attenuated the response to extracellular Ca^{2+} depletion by ~50% (Zhdanov et al., 2010). Enhancement of ATP generation and spare respiratory capacity observed in the present study supports the general model proposed by these authors. Stimulated electron transport and respiration would activate the mitochondrial ATPase, and activation of

Na⁺/H⁺ exchange would provide the proton-motive force necessary for ATP synthesis. The spare respiratory capacity would result naturally from the galvanized system.

MeHg abolishes the activation of respiration induced by depletion of extracellular Ca²⁺. Although the underlying mechanism of this effect is not known, inhibition of VGCCs by MeHg (Shafer and Atchison, 1991b) could prevent Na⁺ influx. Furthermore, direct interaction of MeHg with the mitochondria would inhibit respiratory proteins (Verity et al., 1975) and dissipate the mitochondrial membrane potential (Bondy and McKee, 1991; Hare and Atchison, 1992; Limke and Atchison, 2002). As a result, even if Na⁺ influx occurred, cation exchange required for activation of respiration would be impeded as postulated by Zhdanov et al. (2010).

The observation that extracellular Ca²⁺ does not contribute to MeHg-induced mitochondrial dysfunction verifies other reports in the literature. ROS formation mediated by MeHg exposure is not affected by removal of extracellular Ca²⁺ (Dreiem and Seegal, 2007). These results support the conclusion that MeHg targeting of mitochondria is a primary event in cellular toxicity, and not secondary to perturbation of intracellular Ca²⁺ homeostasis. However because preventing the increase in intracellular Ca²⁺ can attenuate or delay cell toxicity (Marty and Atchison, 1998; Gassó et al., 2001), release of Ca²⁺ from intracellular stores could contribute to MeHg-induced mitochondrial damage.

5.4.4. Role of extracellular Ca²⁺ in basal and MeHg-impaired DA metabolism

Extracellular Ca²⁺ does not contribute to basal DA metabolism. To date, there are no reports investigating this relationship. Although the present conclusion was anticipated, a role for extracellular Ca²⁺ in DA metabolism may have been uncovered. Ca²⁺ could either directly or indirectly modify metabolism by interacting with MAO and/or ALDH. Ca²⁺ dependent phosphorylation or de-phosphorylation of these enzymes could regulate enzymatic activity. Indeed, protein kinase C, which can be activated by increased concentrations of Ca²⁺ (Farah and Sossin, 2012), translocates to the mitochondrial matrix and activates ALDH under conditions of oxidative stress (Churchill et al., 2009). However there is no demonstrated role for Ca²⁺-dependent phosphorylation or de-phosphorylation in MAO or ALDH regulation.

It is also possible that because the mitochondria play an integral role in both MAO and ALDH function (Schnaitman et al., 1967; Marchitti et al., 2008), changes in Ca²⁺ buffering induced by removing extracellular Ca²⁺ could alter enzyme function due to changes in mitochondrial membrane potential. While chelation of extracellular Ca²⁺ does alter mitochondrial membrane potential (Zhdanov et al., 2010), the magnitude of this decrease is only ~5mV. Therefore, it is likely that more substantial changes in mitochondrial function would be necessary to induce correlative changes in MAO or ALDH activity.

Extracellular Ca^{2+} does not contribute to altered DA metabolism induced by MeHg. Because MeHg-induced mitochondrial dysfunction was also unaltered by the absence of extracellular Ca^{2+} , these observations support the hypothesis that mitochondrial dysfunction is a primary mechanism responsible for MeHg-impaired DA metabolism. However, additional investigation is needed to confirm a relationship between the two factors, and to determine if Ca^{2+} released from intracellular stores contributes to changes in DA metabolism following exposure to MeHg.

5.4.5. Summary

The present work contributes to the understanding of MeHg targeting of DA homeostasis by establishing that extracellular Ca^{2+} does not play a role in either MeHg-induced DA release or MeHg-impaired DA metabolism. While removal of extracellular Ca^{2+} can stimulate mitochondrial respiration, MeHg targeting of the organelle abolishes this activation. Because MeHg increases intracellular Ca^{2+} by influx of extracellular Ca^{2+} , as well as release from intracellular stores, additional studies are needed to examine the contribution of intracellular Ca^{2+} to MeHg-induced DA release, and to determine if mitochondrial dysfunction or perturbation of intracellular Ca^{2+} homeostasis is a primary event in MeHg-impaired DA metabolism.

Chapter 6. The role of intracellular Ca^{2+} in MeHg-induced alterations in DA release and metabolism

6.1. Introduction

6.1.1. Regulation of intracellular Ca^{2+}

Free intracellular Ca^{2+} plays many important physiological roles in neurons, including protein cofactor, electric charge carrier, and diffusible intracellular messenger (Carafoli, 1987; Brini et al., 2013). The ability of Ca^{2+} to contribute to these processes results partly from its differential distribution across the plasma membrane. On the extracellular side, Ca^{2+} concentrations range from 1-2mM, whereas free cytosolic Ca^{2+} is maintained at $\sim 100\text{nM}$ (Kass and Orrenius, 1999). This distribution results in a steep electrochemical gradient that is maintained by a sophisticated network of transport and sequestration mechanisms that balance the elevation and diminution of cytosolic Ca^{2+} (Tsien and Tsien, 1990; Pozzan et al., 1994). Processes that increase intracellular Ca^{2+} include the influx of extracellular Ca^{2+} and the release of Ca^{2+} sequestered in organelles. Processes that reduce intracellular Ca^{2+} involve extrusion and sequestration.

The plasma membrane contains channels, transporters, and exchangers that mediate Ca^{2+} flux. Ca^{2+} enters excitable cells primarily through VGCCs, however ligand-gated channels permeable to Ca^{2+} , such as the nicotinic ACh receptor and the *N*-methyl-D-

aspartate receptor, also participate (Tsien and Tsien, 1990; Llinas et al., 1992; Denny and Atchison, 1996). Influx occurs readily and does not require energy input because Ca^{2+} diffuses down its concentration gradient. Extrusion pathways include the Ca^{2+} -ATPase and the $\text{Na}^+ / \text{Ca}^{2+}$ exchanger (Michaelis et al., 1987; Sanchez-Armass and Blaustein, 1987; Carafoli et al., 1996). Both of these processes require energy. The Ca^{2+} -ATPase uses ATP to pump Ca^{2+} against its gradient and out of the cell. The $\text{Na}^+ / \text{Ca}^{2+}$ exchanger uses energy associated with the influx of Na^+ down its gradient to drive Ca^{2+} efflux, but is also dependent upon ATP because the Na^+ / K^+ ATPase maintains the Na^+ gradient.

Intracellular Ca^{2+} buffering organelles are also responsible for maintaining Ca^{2+} homeostasis. The most prominent Ca^{2+} buffering organelles are the SER and the mitochondria (Somlyo et al., 1985; Richter and Kass, 1991; Pozzan et al., 1994). The SER is a high-affinity, low capacity sequestration site, and participates in Ca^{2+} buffering within a physiological range. A Ca^{2+} -ATPase present on the SER membrane transports Ca^{2+} from the cytosol into the lumen of the SER, whereas IP_3 receptors and Ca^{2+} -induced Ca^{2+} -release from ryanodine receptors mediate Ca^{2+} release from the SER (McPherson and Campbell, 1993; Pozzan et al., 1994). Mitochondria represent a low-affinity, high-capacity sequestration organelle, and require a powerful, pathologically high intracellular Ca^{2+} stimulus to begin buffering Ca^{2+} (Nicholls and Akerman, 1982). The Ca^{2+} uniporter is

responsible for the uptake of Ca^{2+} into the mitochondrial matrix, whereas release is accomplished by either reversal of the uniporter, $\text{Na}^+/\text{Ca}^{2+}$ exchanger, or opening of the mitochondrial permeability transition pore (Nicholls and Scott, 1980; Deryabina et al., 2004).

6.1.2. Effects of MeHg on intracellular Ca^{2+} homeostasis

MeHg disrupts intracellular Ca^{2+} homeostasis. This effect was first indicated by studies of the neuromuscular junction, which demonstrated an increase in spontaneous ACh release following application of MeHg (Atchison and Narahashi, 1982; Atchison, 1986). Imaging studies using the fluorophore fura-2 have confirmed that MeHg perturbs intracellular Ca^{2+} concentrations (Hare et al., 1993; Marty and Atchison, 1997).

MeHg induces a biphasic rise in intracellular Ca^{2+} , indicated by alterations in the ratio of fura-2 bound to intracellular Ca^{2+} . This has been observed in many cell types, including neuroblastoma cells (Hare et al., 1993; Hare and Atchison, 1995b), rat forebrain synaptosomes (Komulainen and Bondy, 1987; Denny et al., 1993), and rat cerebellar neurons (Sarafian et al., 1994; Marty and Atchison, 1997; Mundy and Freudenrich, 2000; Edwards et al., 2005). First, Ca^{2+} is released from intracellular stores. This produces a slow, gradual rise in cytosolic Ca^{2+} that is within the cellular buffering capacity (Marty and Atchison, 1997). A second Ca^{2+} phase follows whereby extracellular Ca^{2+} influx overwhelms the cellular buffering capacity, which contributes to the initiation of cytotoxic

events (Kass and Orrenius, 1999). Indeed, inhibition of VGCC channels not only delays the onset of MeHg-induced intracellular Ca^{2+} elevation, but also decreases the incidence of cell death in cerebellar granule cells (Marty and Atchison, 1998) and the appearance of neurological symptoms associated with MeHg intoxication in rats (Sakamoto et al., 1996).

6.1.3. Effects of MeHg on DA release and metabolism

Ca^{2+} plays an essential signaling role in vesicle docking and neurotransmitter release (Llinas et al., 1981; Sabatini and Regehr, 1996). While influx through VGCCs is the key event in depolarization-evoked vesicular exocytosis (Atluri and Regehr, 1998; Lu and Trussell, 2000), residual cytosolic Ca^{2+} can participate in spontaneous neurotransmitter release (Chapter 5; Tiernan et al., 2013). As demonstrated previously, spontaneous MeHg-induced DA release is dependent upon vesicular exocytosis (Chapter 3), and extracellular Ca^{2+} does not mediate this effect (Levesque and Atchison, 1987; 1988). Thus intracellular Ca^{2+} may be the key signaling mechanism responsible for MeHg-induced DA release.

Studies at the neuromuscular junction have characterized a role for intracellular Ca^{2+} in MeHg-induced ACh release (Levesque and Atchison, 1988). Specifically, agents that disrupt Ca^{2+} transport mechanisms in the mitochondria preclude MeHg from inducing ACh release, whereas agents that either disrupt Ca^{2+} buffering by the SER or Na^+ -dependent Ca^{2+} mobilization in the nerve terminal are ineffective (Levesque and Atchison, 1988). A role for intracellular Ca^{2+} in the spontaneous release of other neurotransmitters has yet to

be defined. Furthermore, because mitochondrial dysfunction contributes to ACh release (Tsien, 1981), and MeHg-impaired DA metabolism (Chapter 4), the relationships between intracellular Ca^{2+} , aberrant DA metabolism, and mitochondrial dysfunction were also investigated in the present study.

6.2. Methods

6.2.1. Chemicals

The standard physiological saline used for extracellular solution was HBS, which contained (mM): 150 NaCl, 5 KCl, 2.4 CaCl_2 , 1.6 MgSO_4 , 20 HEPES, and 20 *d*-glucose (pH 7.3). In some experiments cells were treated in 0- Ca^{2+} HBS, which had the same composition as HBS with the following exceptions (mM): 0 CaCl_2 and 0.02 ethylene glycol tetraacetic acid.

MeHg (ICN Biochemicals) and BAPTA/AM (Calbiochem) were diluted from stock solutions in HBS or 0- Ca^{2+} HBS. Drug solutions were diluted to final concentrations on the day of each experiment as described in General Methods Section 2.2.

6.2.2. Treatment for neurochemistry and mitochondrial bioenergetics

PC12 cells were seeded at a density of $6-7 \times 10^5$ cells/mL in 6-well plates or XF24-well plates coated with poly-D-lysine 24-48 hr prior to treatment. To begin each experiment, culture medium was aspirated and replaced with HBS in the absence or presence of 50 μM BAPTA/AM for 30 min, and then 0 μM or 2 μM MeHg in the absence or

presence of 50 μ M BAPTA/AM in HBS or 0-Ca²⁺ HBS for 60 min. Cells were incubated at 37°C/5% CO₂ during treatment as described in General Methods Section 2.2.

6.2.3. Neurochemistry

At experiment termination, treatment medium was retained and acidified. Cells were rinsed, harvested, and pelleted by centrifugation. The content of DA in the treatment medium and its metabolites in the cell pellet were determined by HPLC-ED as described in General Methods Section 2.3. Neurochemical concentrations were normalized to mL per sample for extracellular measurements or mg of protein for intracellular measurements as determined by the BCA protein assay (Sigma).

6.2.4. Mitochondrial bioenergetics

Following intracellular Ca²⁺ chelation and toxicant exposure, treatment medium was aspirated. Cells were washed once with XF24 RPMI Assay Medium and then incubated at 37°C/no CO₂ for 1 hr to allow medium temperature and pH to equilibrate before the first measurements were made. The biosensor cartridge was hydrated overnight and injection ports were loaded with test compounds as described in General Methods Section 2.6. OCR was measured under basal conditions and following injection of test compounds using the XF24 Extracellular Flux Analyzer. Basal respiration, ATP generation, and spare respiration were calculated and compared between treatment groups.

6.2.5. Measurement of fura-2 fluorescent change

PC12 cells were plated at 7×10^5 cells/mL on circular glass coverslips 24 hr prior to analysis. Cells were preloaded with $2 \mu\text{M}$ fura-2 in the presence of $50 \mu\text{M}$ BAPTA/AM. Following fura-2 loading and intracellular Ca^{2+} chelation, coverslips containing PC12 cells were mounted on an inverted microscope (Diaphot-TMD, Nikon, Toyko, Japan) and perfused with 0-Ca^{2+} HBS at 37°C . Digital fluorescent images were obtained using an IonOptix system (Milton, MA) and fura-2 fluorescence changes were monitored as described in General Methods Section 2.9.

6.2.6. Statistical analysis

SigmaPlot® software version 12.0 (SysStat Software, Inc., Point Richmond, CA) was used to make statistical comparisons among groups using unpaired t-test, one-, and two-way ANOVA, or non-parametric alternatives as appropriate. If a significant difference was detected, *post hoc* between-group comparisons were performed using Tukey's test. Statistical significance was set at $p \leq 0.05$.

6.3. Results

6.3.1. MeHg-induced DA release is dependent upon the presence of intracellular Ca^{2+}

BAPTA/AM is a selective intracellular Ca^{2+} chelator. The presence of an acetoxymethyl ester group (AM) allows the molecule to traverse biological membranes. Once inside the cell, the ester is cleaved by endogenous esterases, preventing BAPTA from

exiting the cell (Limke and Atchison, 2009). To investigate the role of intracellular Ca^{2+} in MeHg-induced DA release, undifferentiated PC12 cells were loaded with $50\mu\text{M}$ BAPTA/AM to chelate intracellular Ca^{2+} , and then treated with $2\mu\text{M}$ MeHg for 60 min. This experiment was performed in both the absence and presence of extracellular Ca^{2+} to assess the interplay between extracellular and intracellular Ca^{2+} pools.

The results of the present study shown in Figure 6.1 are consistent with previous results showing that $2\mu\text{M}$ MeHg increased DA release from undifferentiated PC12 cells (Chapter 3) and the removal of extracellular Ca^{2+} did not appreciably alter this effect (Chapter 4). In the presence of extracellular Ca^{2+} , pretreatment with BAPTA/AM did not alter basal DA release, but did attenuate MeHg-induced release (Figure 6.1; $p < 0.05$). In the absence of extracellular Ca^{2+} , a similar profile was observed. However, more stringent examination of the percentage change induced by MeHg in each treatment group demonstrated that only chelation of both extracellular and intracellular Ca^{2+} significantly diminished MeHg-induced DA release in undifferentiated PC12 cells ($p < 0.05$).

To confirm that BAPTA/AM attenuated the elevation in intracellular Ca^{2+} induced by MeHg, imaging studies were performed using single cell microfluorometry with the ratiometric Ca^{2+} indicating dye fura-2. In response to increasing Ca^{2+} concentrations, fura-2 shows a peak signal at 340nm and minimum signal at 380nm. The ratio of peak 340 signal/ peak 380 signal is an accurate assessment of the concentration of intracellular Ca^{2+}

(Marty and Atchison, 1997). In the absence of extracellular Ca^{2+} , the 340/380 fura-2 ratio increased gradually following application of $2\mu\text{M}$ MeHg (Figure 6.2), consistent with the first Ca^{2+} phase of MeHg exposure (Marty and Atchison, 1997). Preloading cells with $50\mu\text{M}$ BAPTA/AM for 30 min abolished this effect.

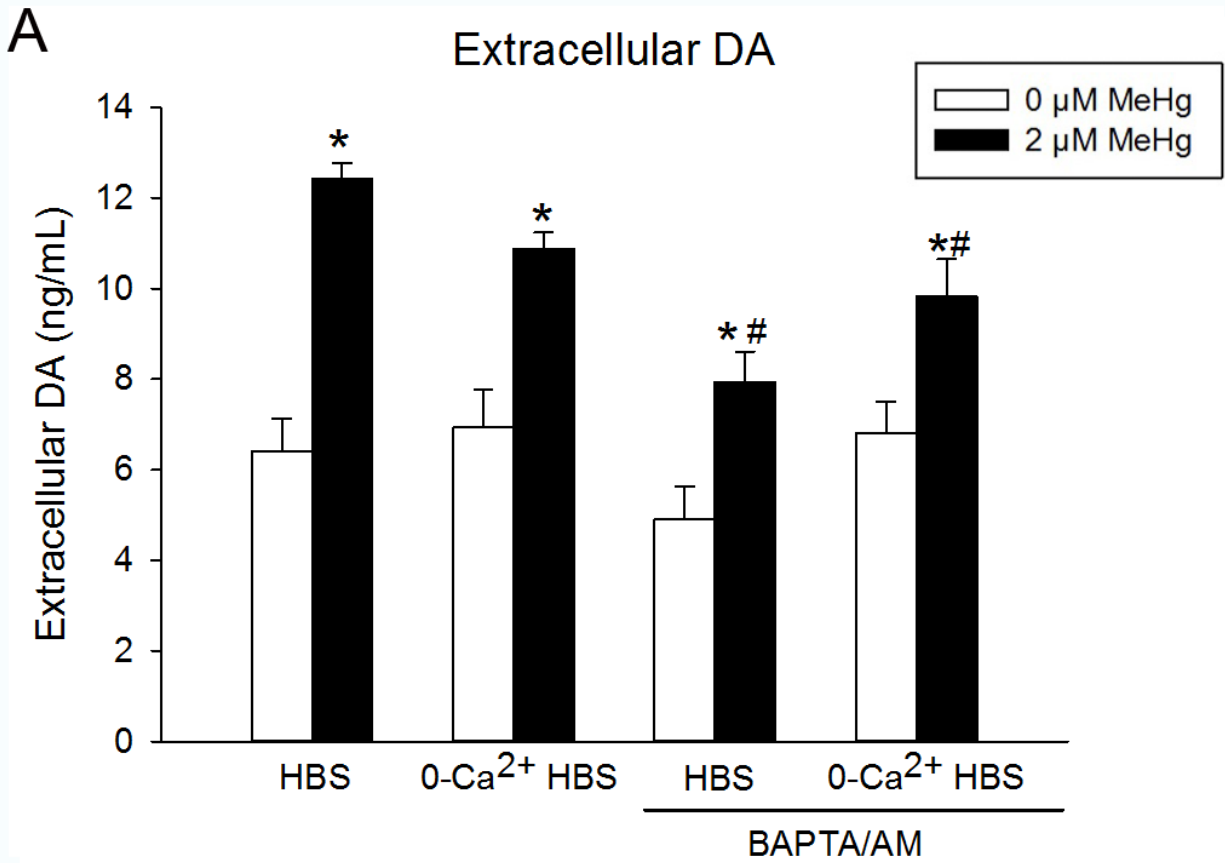
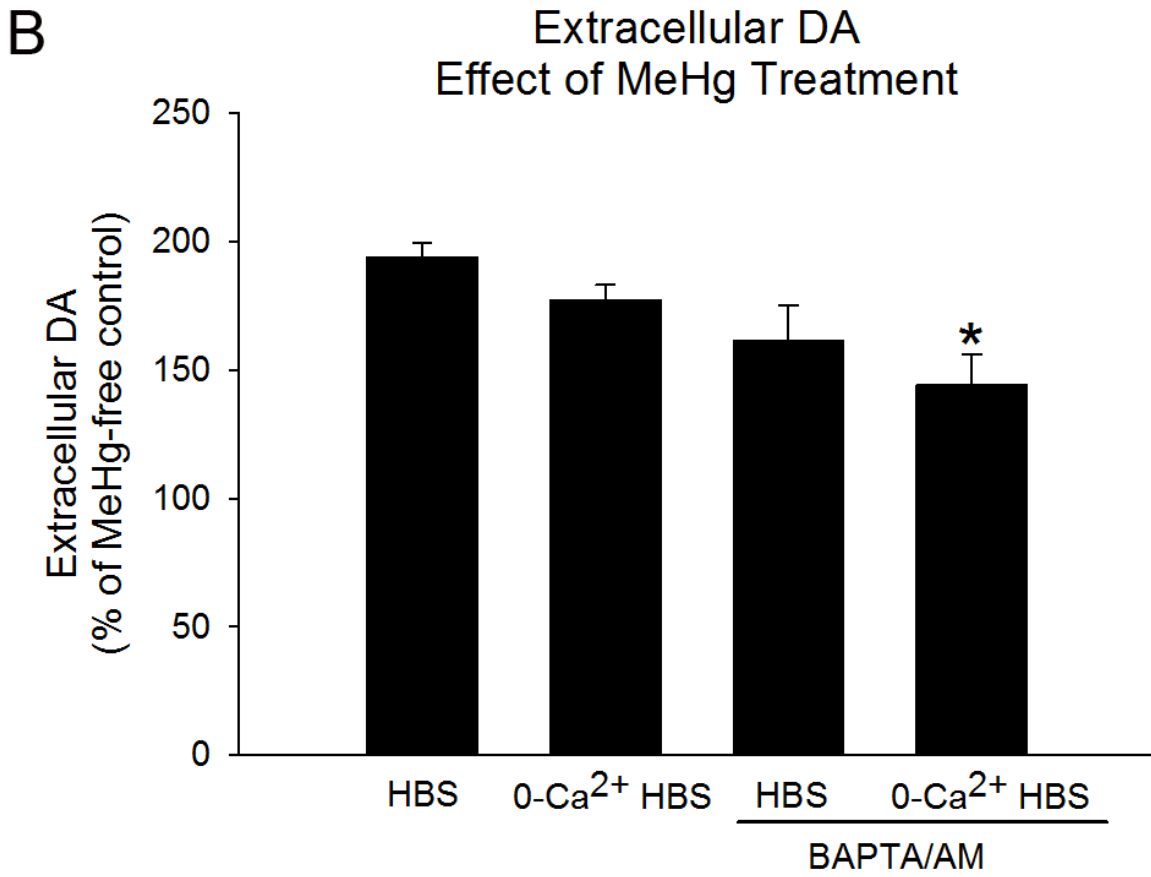


Figure 6.1. Intracellular Ca^{2+} partially contributes to MeHg-induced DA release.

Undifferentiated PC12 cells were treated with $50\mu\text{M}$ BAPTA/AM in HBS for 30min prior to co-treatment with $0\mu\text{M}$ (white bars) or $2\mu\text{M}$ (black bars) MeHg in the absence (Ca^{2+} -free HBS) or presence (HBS) of extracellular Ca^{2+} for 60 min. Panel A) Concentrations of extracellular DA. Panel B) The percentage change of extracellular DA after treatment with MeHg in cells treated with either HBS or Ca^{2+} -free HBS in the absence or presence of $50\mu\text{M}$ BAPTA/AM. The asterisk (*) indicates a value significantly different from HBS-Control ($p \leq 0.05$). The hash (#) indicates a value significantly difference from both HBS-Control and HBS-MeHg ($p \leq 0.05$). Values are means + SEM ($n = 4$, 3 replicates per n).

Figure 6.1 cont'd



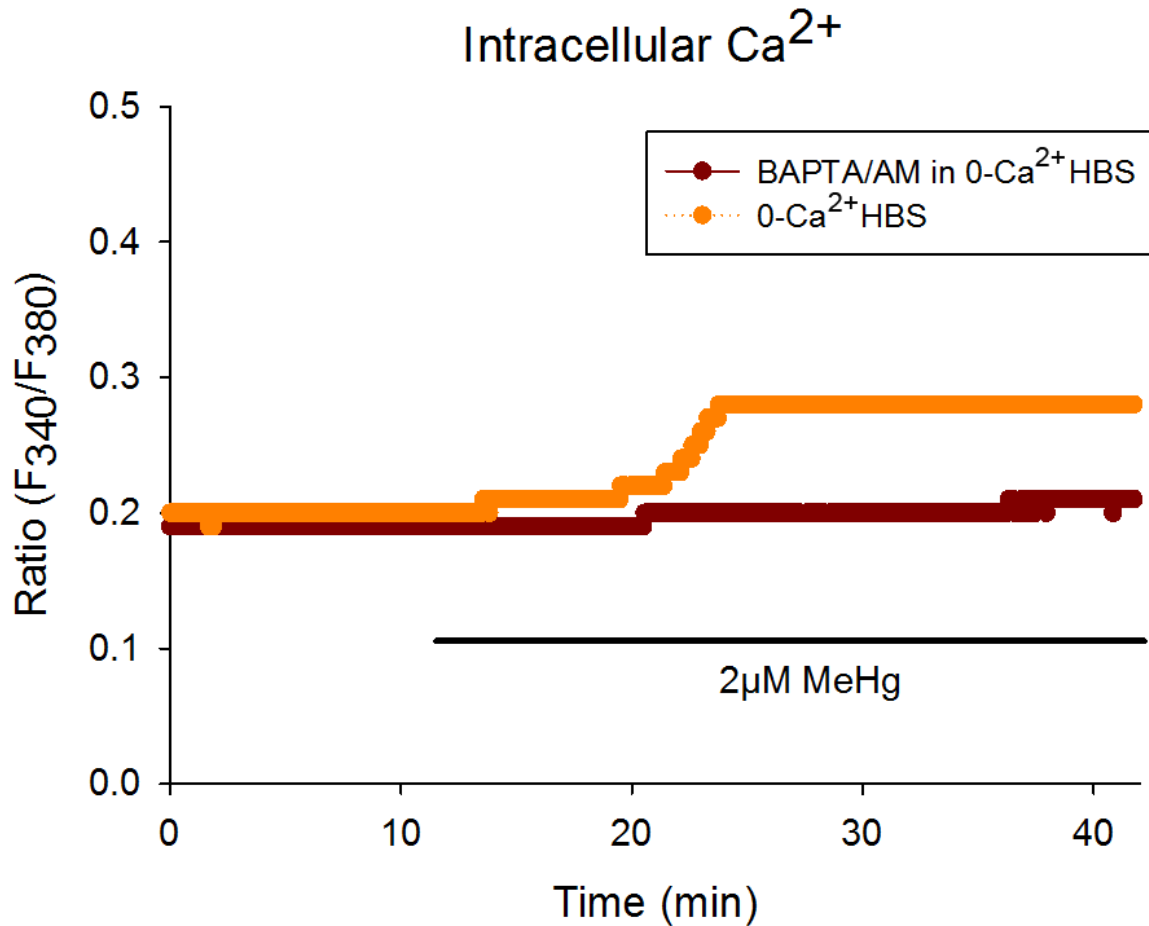


Figure 6.2. Representative traces showing changes in the ratio of fura-2 intensity. Undifferentiated PC12 cells were pre-incubated with 2µM fura-2/AM in absence (orange) or presence (red) of 50µM BAPTA/AM for 30 min. Following pre-incubation, cells were perfused with 0-Ca²⁺ HBS. 2µM MeHg was added where indicated. Pre-treatment with BAPTA/AM prevented the rise in fura-2 fluorescence intensity induced by MeHg. No second phase of MeHg-induced increase in fura-2 intensity was observed because all cells were perfused in the absence of extracellular Ca²⁺.

6.3.2. Intracellular Ca^{2+} is essential for the maintenance of mitochondria bioenergetics

To evaluate the contribution of different Ca^{2+} sources to mitochondrial dysfunction induced by MeHg, mitochondrial respiration was measured in undifferentiated PC12 cells treated with $2\mu\text{M}$ MeHg for 60 min in the absence or presence of intracellular and/or extracellular Ca^{2+} . Following toxicant treatment, OCR was measured with the XF24 respirometer under basal conditions and following treatment with 5mM pyruvate, $1\mu\text{M}$ oligomycin A, $2\mu\text{M}$ FCCP, and $1\mu\text{M}$ antimycin A. Figure 6.3 depicts changes in OCR following treatment with these compounds. Quantification of these changes (Figure 6.4) revealed an essential role for intracellular Ca^{2+} source in maintaining mitochondrial respiratory function. MeHg attenuated basal respiration, spare respiratory capacity, and ATP generation, as demonstrated previously (Chapter 4; $p < 0.05$). Chelation of extracellular Ca^{2+} alone was insufficient to reverse these effects (Chapter 5). However pre-treatment with BAPTA/AM caused marked decreases in basal respiration and ATP generation, and complete abolition of spare respiratory capacity ($p < 0.05$).

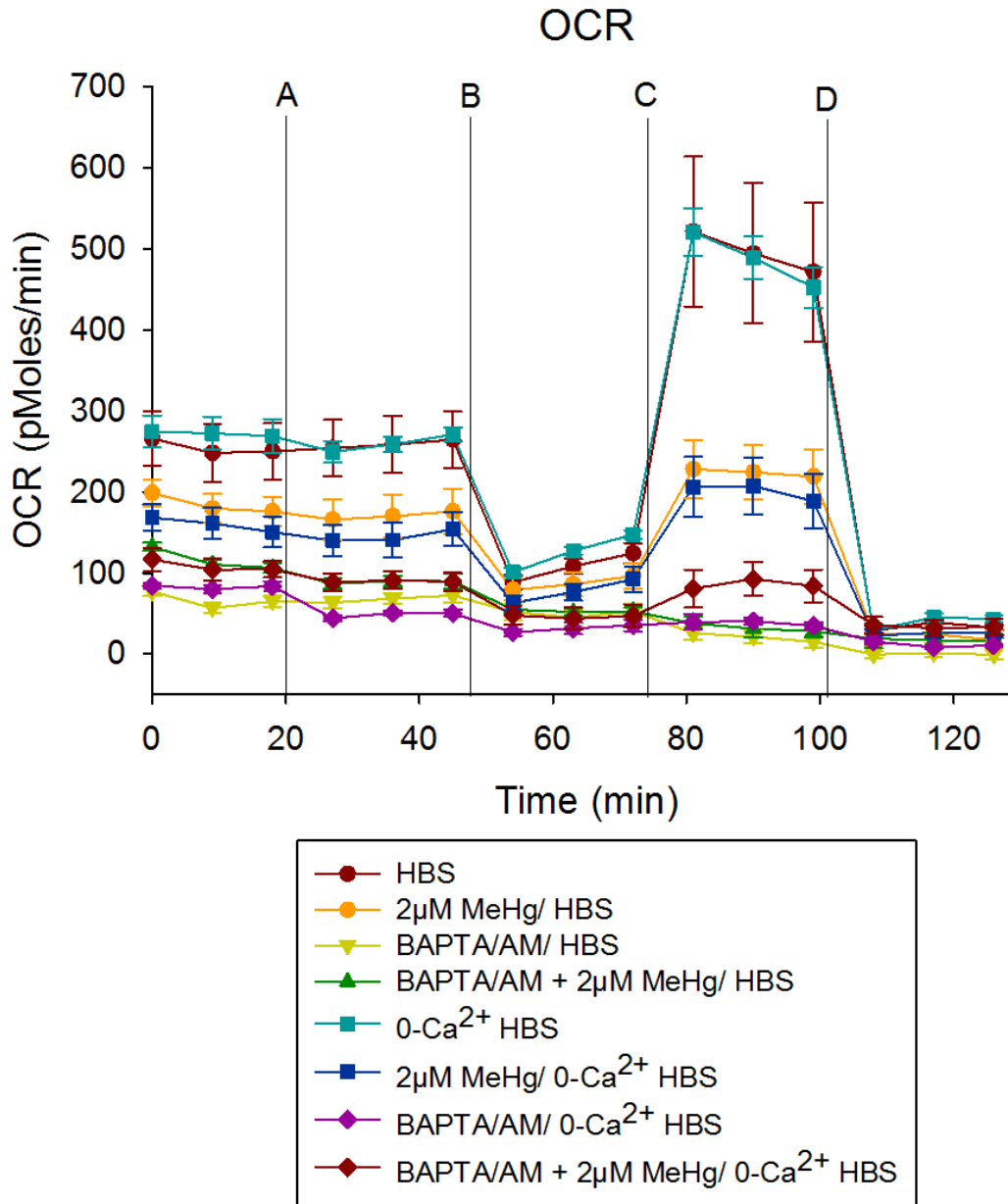


Figure 6.3. Changes in mitochondrial bioenergetics induced by MeHg in absence or presence of either intracellular or extracellular Ca²⁺. Undifferentiated PC12 cells were pretreated for 30 min in the absence or presence of 50µM BAPTA/AM in HBS followed by a 60 min with HBS (red circle), 2µM MeHg in HBS (orange circle), 50µM BAPTA/AM in HBS (yellow triangle), 2µM MeHg + 50µM BAPTA/AM in HBS (green triangle), 0-Ca²⁺ HBS (green square), 2µM MeHg in 0-Ca²⁺ HBS (blue square), 50µM BAPTA/AM in 0-Ca²⁺ HBS (purple diamond) or 2µM MeHg + 50µM BAPTA/AM in 0-Ca²⁺ HBS. Following pre-treatment, OCR (pMoles/min) was measured under basal conditions and following injections of 5mM pyruvate (A), 1µM oligomycin (B), 2µM FCCP (C), and 1µM antimycin A (D). Values are means ± S.E.M. (n = 3, 4-5 replicates per n).

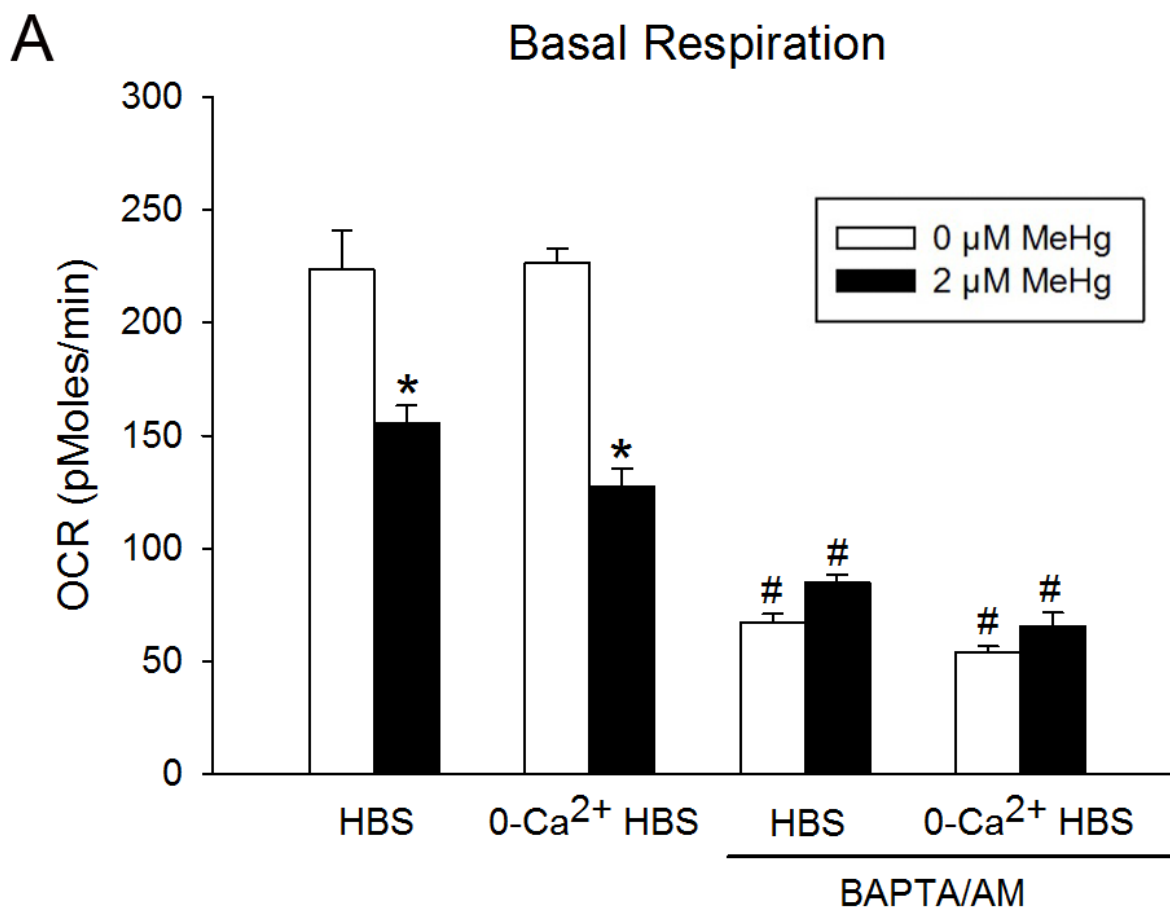
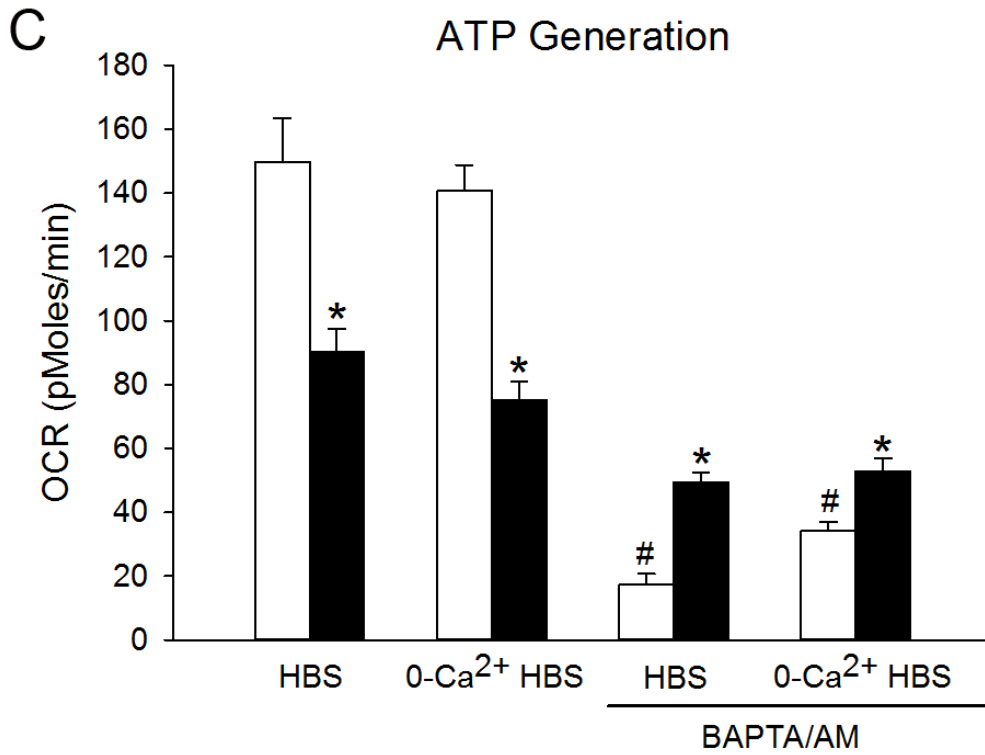
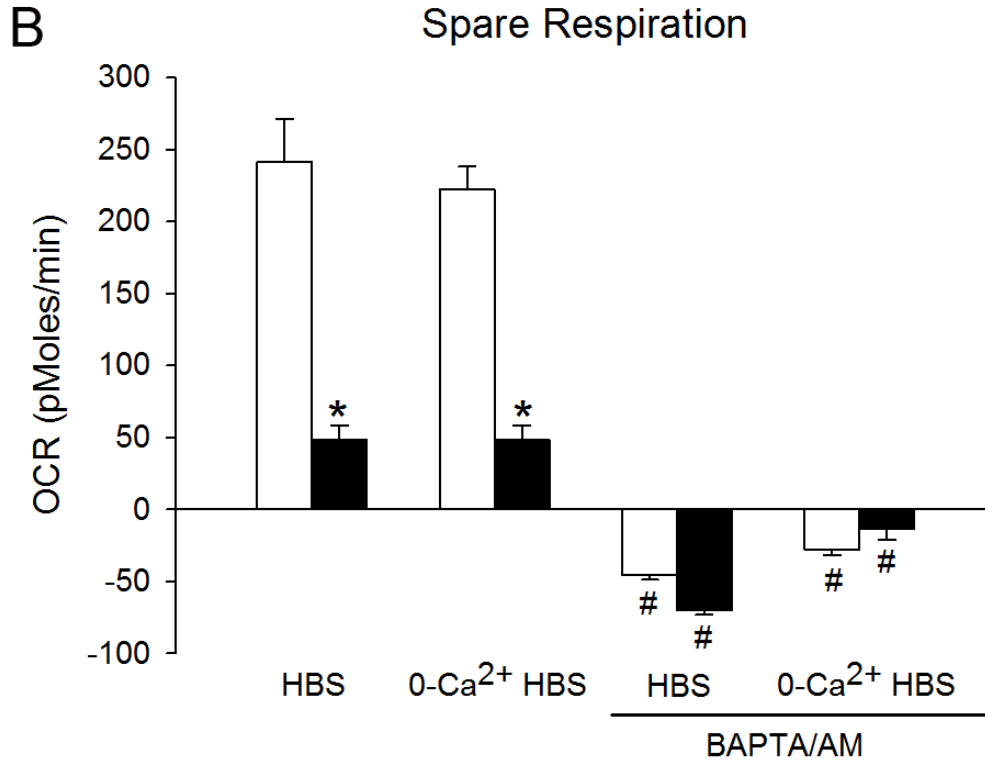


Figure 6.4. Quantification of changes in mitochondrial bioenergetics induced by MeHg in absence or presence of either intracellular or extracellular Ca^{2+} . Panel A) Basal respiration (OCR) was measured in the presence of 25mM glucose and 5mM pyruvate. Panel B) Spare respiration was calculated as the difference between maximum respiration (following treatment with 2 μM FCCP) and basal respiration. Panel C) ATP generation was calculated as the difference between basal respiration and respiration following treatment with 1 μM oligomycin A. The asterisk (*) indicates a value significantly different than vehicle control ($p < 0.05$). The hash (#) indicates a value significantly different than HBS-Control ($p \leq 0.05$). Values are means \pm S.E.M. ($n = 3, 4-5$ replicates per n).

Figure 6.4 cont'd



6.3.3. Aberrant DA metabolism induced by MeHg is not dependent upon intracellular Ca^{2+}

Chelating extracellular and/or intracellular Ca^{2+} had no effect on intracellular DOPAC formation (Figure 6.5). Concentrations of intracellular DOPET were markedly decreased by removal of intracellular Ca^{2+} ($p < 0.05$). Treatment with $2\mu\text{M}$ MeHg for 60 min significantly diminished DOPAC and increased DOPET formation regardless of the absence or presence of intracellular or extracellular Ca^{2+} ($p < 0.05$).

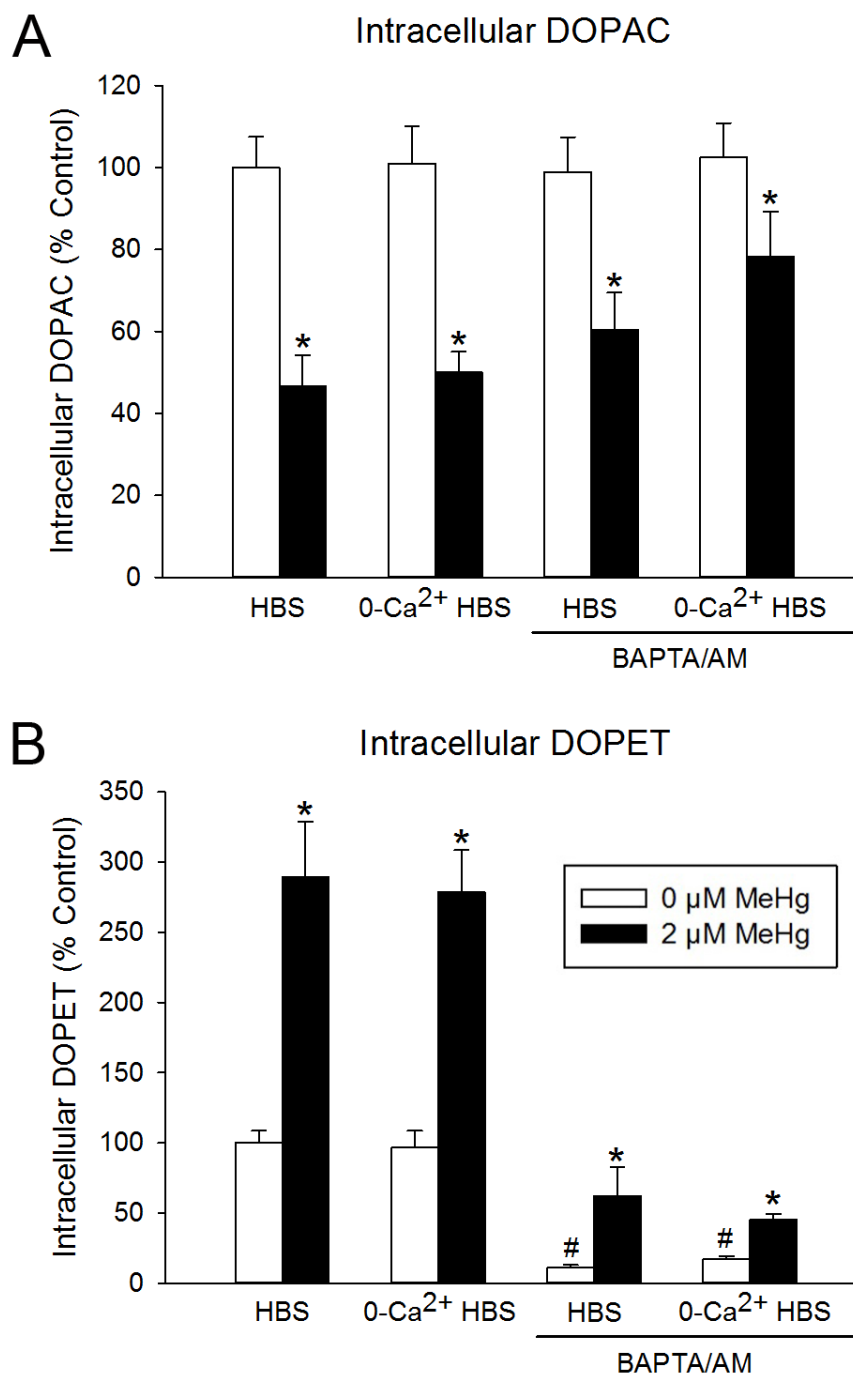


Figure 6.5. Effect of MeHg in the absence or presence of intracellular or extracellular Ca^{2+} on concentrations of intracellular metabolites. Undifferentiated PC12 cells were pre-treated with vehicle or 50 μM BAPTA/AM in HBS for 30 min prior to co-treatment with 0 μM (white bars) or 2 μM (black bars) MeHg in the absence (Ca^{2+} -free HBS) or presence (HBS) of extracellular Ca^{2+} for 60 min. Panel A) DOPAC and Panel B) DOPET. The asterisk (*) indicates a value significantly different from vehicle within treatment group ($p \leq 0.05$). The hash (#) indicates a value significantly different than 0 μM MeHg in HBS ($p \leq 0.05$). Values are means + SEM ($n = 4, 3$ replicates per n).

6.4. Discussion

MeHg targets both intracellular and extracellular pools of Ca^{2+} to disrupt cytosolic Ca^{2+} homeostasis (Chapter 3; Tiernan et al., 2013). Studies presented herein were designed to complement studies presented in Chapter 5, which demonstrated that extracellular Ca^{2+} does not mediate MeHg targeting of DA homeostasis or impaired mitochondrial bioenergetics. The present study sought to elucidate the role of intracellular Ca^{2+} as a primary mechanism in these effects. These data are consistent with the following conclusions: 1) intracellular Ca^{2+} at least in part mediates MeHg-induced DA release, 2) intracellular Ca^{2+} plays a crucial role in maintaining mitochondrial respiration and other parameters of bioenergetics including ATP generation and spare respiratory capacity, 3) the reductive pathway of DA metabolism, but not the oxidative pathway, is dependent upon the presence of intracellular Ca^{2+} , and 4) aberrant DA metabolism induced by MeHg is not dependent upon the presence of intracellular Ca^{2+} .

6.4.1. Role of intracellular Ca^{2+} in spontaneous and MeHg-mediated DA release

Chelating intracellular Ca^{2+} causes a small, non-significant decline in basal DA release, and in the absence of both intracellular and extracellular Ca^{2+} it is comparable to basal DA release. These data together suggest that tonic DA release from undifferentiated PC12 cells is Ca^{2+} independent. This conclusion is somewhat perplexing considering tonic

DA release from undifferentiated PC12 cells is dependent upon functional synaptic vesicles (Katz and Miledi, 1967; Bajjalieh and Scheller, 1995; Sudhof, 2012), and Ca^{2+} -dependent vesicular exocytosis plays a pivotal role in neurotransmitter release (Di Virgilio et al., 1984; Barrowman et al., 1986; Drapeau and Nachshen, 1988; Mochida et al., 1998; Parnas et al., 2000; Caldwell et al., 2013). However there is some evidence to support Ca^{2+} -independent vesicular exocytosis (Drapeau and Nachshen, 1988). Cytosolic acidification can stimulate DA release from striatal synaptosomes in the absence of extracellular Ca^{2+} (Mochida et al., 1998). Additionally, ACh release from cultured superior cervical ganglion neurons is stimulated following focal membrane depolarization with a hyperosmotic sucrose solution in a Ca^{2+} -free medium. This solution evoked release even when intracellular Ca^{2+} was chelated with BAPTA (Knight et al., 1989). In these studies, neurotransmitter release still required some stimulus to induced release, however secretion can be induced by endogenous factors independent of Ca^{2+} (Barrowman et al., 1986). For example, guanosine-5'-triphosphate analogs induce secretion from neutrophils in the absence of extracellular or intracellular Ca^{2+} (Atchison, 1986; Levesque and Atchison, 1987; 1988), suggesting that a G-protein-mediated secretory mechanism exists that is separate from Ca^{2+} -mediated exocytosis. The present data provide intriguing evidence for a Ca^{2+} -independent mechanism of vesicular exocytosis in undifferentiated PC12 cells and warrant further investigation.

MeHg-induced DA release is attenuated in the absence of intracellular Ca^{2+} , and this effect is most pronounced in the absence of both extracellular and intracellular Ca^{2+} . These results corroborate studies at the neuromuscular junction (Hare and Atchison, 1995a; Chetty et al., 1996) and suggest that MeHg-induced DA release is dependent upon an increase in free cytosolic Ca^{2+} . Furthermore, intracellular and extracellular Ca^{2+} pools work in concert to stimulate DA release following exposure to MeHg.

The source of intracellular Ca^{2+} responsible for MeHg-induced DA release is unknown but both the SER and the mitochondria could contribute to the elevation of intracellular Ca^{2+} induced by MeHg. In general, MeHg first stimulates Ca^{2+} release from an IP_3 -sensitive pool in the SER (Limke et al., 2003). This release activates mitochondrial Ca^{2+} uptake, and Ca^{2+} is initially buffered into the mitochondrial matrix (Levesque and Atchison, 1991; Limke et al., 2003). Following excessive accumulation of mitochondrial Ca^{2+} and dissipation of the mitochondrial membrane potential, Ca^{2+} is extruded from the mitochondrial matrix into the cytosol (Levesque and Atchison, 1991; Levesque et al., 1992).

Studies at the neuromuscular junction have identified mitochondria as the primary intracellular sequestration organelle responsible for MeHg-induced ACh release (Hare and Atchison, 1995a). However depending on the system, the contribution of each Ca^{2+} buffering organelle to MeHg-induced elevation in cytosolic Ca^{2+} is different. For example, in neuroblastoma cells an IP_3 -sensitive pool is the main contributor (Limke et al., 2003),

whereas in cerebellar granule cells it is the mitochondria (Denton, 2009; Glancy and Balaban, 2012; Pizzo et al., 2012). Therefore while both the SER and mitochondria likely participate to elevate intracellular Ca^{2+} following exposure to MeHg in undifferentiated PC12 cells, the magnitude of their contributions to MeHg-induced DA release has yet to be elucidated.

6.4.2. Role of intracellular Ca^{2+} in mitochondrial bioenergetics

Maintenance of intracellular Ca^{2+} homeostasis is essential for sustaining mitochondrial function. Chelating intracellular Ca^{2+} markedly diminishes respiration and ATP generation. These observations are aligned with a wealth of literature demonstrating the regulatory role of Ca^{2+} in ATP synthesis (Denton et al., 1972; Farah and Sossin, 2012). Indeed, Ca^{2+} activates at least three key enzymes that feed electrons in the ETC. Pyruvate dehydrogenase is stimulated when Ca^{2+} activates a phosphatase associated with the enzyme complex (Rutter and Denton, 1988; Mori et al., 2007; Jinsmaa et al., 2009), whereas isocitrate dehydrogenase, and α -ketoglutarate dehydrogenase are directly bound by Ca^{2+} , which increases affinity for their substrates (Yoshino et al., 1966; Hamdy and Noyes, 1977; Yamada and Huzel, 1985; Hubbard and McHugh, 1996; Fox et al., 2012). Furthermore the mitochondrial ATP synthase is responsive to changes in cytosolic Ca^{2+} , and Ca^{2+} readily binds the catalytic subunit of this enzyme (Schnaitman et al., 1967; Marchitti et al., 2008). Presently, buffering cytosolic Ca^{2+} would most likely cause the mitochondria to extrude

Ca²⁺ in an effort to maintain cytosolic Ca²⁺ levels. Loss of mitochondrial matrix Ca²⁺ would decrease activation of enzymes necessary for respiratory chain activity and ATP synthesis.

Effects of buffering cytosolic Ca²⁺ and the resulting diminution of mitochondrial function have implications for the present work. No conclusions can be made concerning the role of intracellular Ca²⁺ in MeHg-impaired mitochondrial dysfunction. Furthermore, it is surprising that cellular functions, including DA release and metabolism, were not more severely affected by the loss of mitochondrial respiration and ATP generation. Perhaps the short time-course of the present experimental paradigm precluded the run-down of energy reserves and initiation of cell death. However no conclusions can be made regarding these events, as no measurement were taken to investigate effects of BATPA/AM on mitochondrial membrane potential, opening of the mitochondrial permeability transition pore, or markers of cell death.

6.4.3. Role of intracellular Ca²⁺ in basal and MeHg-impaired DA metabolism

Intracellular DOPAC formation was not affected by buffering intracellular Ca²⁺ in the absence or presence of extracellular Ca²⁺. These data corroborate and extend results in Chapter 5 and suggest that canonical DA metabolism is independent of cytosolic Ca²⁺. Neither MAO nor ALDH are reported to require Ca²⁺ for enzymatic function. However because both enzymes are intimately associated with mitochondria (Petrash, 2004), the observation that DA metabolism proceeds in the face of a marked decrease in

mitochondrial respiration is confounding. One possible explanation is methodology. While neurochemistry can be measured from cell pellets harvested immediately after treatment, XF24 respirometry measurements are made during a time period of one to three hr following treatment. It is possible that mitochondrial dysfunction, as assessed using the XF24 respirometer, was not initiated until a time-point after neurochemical measurements were taken.

The reductive pathway of DA metabolism is dependent upon the presence of intracellular Ca^{2+} . DOPET formation was markedly reduced following treatment with BAPTA/AM. These data are novel in that a role for Ca^{2+} in AR function has yet to be established. There is some evidence to suggest that AR is a substrate for protein kinase C (Varma et al., 2003). Treatment with the protein kinase C stimulator bryostatin-1 directly increases phosphorylation of AR (Farah and Sossin, 2012), and because protein kinase C can be activated by Ca^{2+} (Mori et al., 2007; Jinsmaa et al., 2009), this represents one mechanism by which Ca^{2+} could modulate AR activity. Results presented herein are the first to demonstrate a direct effect of Ca^{2+} on DOPET formation.

Exposure to MeHg was still able to elicit an aberrant DA metabolomic profile, even in the absence of both extracellular and intracellular Ca^{2+} . These data suggest that MeHg-induced perturbation of intracellular Ca^{2+} homeostasis does not contribute to changes in DA metabolism mediated by the toxicant. The observation that intracellular Ca^{2+} is required for mitochondrial bioenergetics, but not DA metabolism, suggests that the DA

metabolomic profile induced by MeHg is not in response to mitochondrial dysfunction. Therefore ALDH inhibition and decreased availability of its cofactor NAD could be due to oxidative stress induced by MeHg (Yoshino et al., 1966; Hamdy and Noyes, 1977; Fox et al., 2012) or inhibition of enzymes in the citric acid cycle that ultimately down-regulate the amount of NAD(H) (Haycock, 1990).

6.4.4. Summary

The present work establishes a role for intracellular Ca^{2+} in MeHg-induced DA release, but suggests that aberrant DA metabolism induced by exposure to the toxicant is independent of altered intracellular Ca^{2+} homeostasis. Therefore, MeHg targets DA synthesizing cell by multiple mechanisms, including perturbation of intracellular Ca^{2+} homeostasis, impairment of mitochondrial function, and perhaps a yet to be elucidated mechanism responsible for inhibition of enzymes necessary for oxidative DA metabolism.

Chapter 7. General Discussion and Concluding Remarks

Methylmercury is a potent bioaccumulative neurotoxicant. Despite general cellular and molecular targets, certain neuronal populations are selectively susceptible to toxicity. The present dissertation characterizes MeHg-induced toxicity in DA-synthesizing cells. Results describe how perturbation of intracellular Ca^{2+} and mitochondrial dysfunction induced by exposure to MeHg alter DA neurochemistry, and identify potential disturbances that could contribute to heightened susceptibility of DA-synthesizing cells. A better understanding of DA neuronal targeting by MeHg elucidates how exposure to the environmental toxicant contributes to the etiology of PD.

7.1. Role of Ca^{2+} in MeHg-induced activation of DA synthesis

Results from pharmacological studies in this dissertation demonstrate that MeHg stimulates DA synthesis and vesicular exocytosis, but does not interact with the membrane DA transporter, to induce DA release. Furthermore, the primary event initiating these effects is an increase in intracellular Ca^{2+} .

Ca^{2+} contributes to DA synthesis by potentiating phosphorylation of TH (Daubner et al., 2011). TH enzymatic activity is modulated by phosphorylation and dephosphorylation events at critical Ser residues, including Ser19, -31, and -40 (Lehmann et al., 2006). Phosphorylation at Ser40 directly increases enzymatic activity, whereas phosphorylation at Ser19 and -31 indirectly activate TH via a hierarchical mechanism, which increases the rate of phosphorylation at Ser40 (Albert et al., 1984; Vulliet et al., 1985). A multitude of protein kinases have been linked to TH phosphorylation, including PKC (Yamauchi and

Fujisawa, 1981; Vulliet et al., 1984; Atluri and Regehr, 1998; Lu and Trussell, 2000) and CaM-MPK (Levesque and Atchison, 1987; 1988; Haavik et al., 1989), both of which phosphorylate TH as Ser19 and -40 via a Ca^{2+} dependent mechanism (Haavik et al., 1989).

Ca^{2+} has also been linked to dephosphorylation of TH. Two phosphatases, PP2A and PP2C account for 90% and 10%, respectively, of TH phosphatase activity (Wlodarchak et al., 2013). The effect of Ca^{2+} on PP2A activity in TH de-phosphorylation has not been investigated, however there is evidence to suggest its activity is regulated by Ca^{2+} (Bevilaqua et al., 2003). Specific investigation of PP2C has demonstrated that its activity is stimulated by certain divalent cations, including Mn^{2+} and Mg^{2+} , however Ca^{2+} inhibits its activity (Olivera et al., 1994; Dunlap et al., 1995)..

The ability of Ca^{2+} to facilitate phosphorylation and hinder de-phosphorylation indicates one potential mechanism by which MeHg stimulates DA synthesis. Western blot analysis of TH and pTH Ser40 in this dissertation demonstrate that MeHg increases phosphorylation of TH, without altering total protein. Phosphorylation is an acute regulatory mechanism, whereas protein synthesis provides chronic control. These data suggest that MeHg can regulate TH activity in an acute fashion, immediately following exposure. The precise role of Ca^{2+} has yet to be elucidated, however data presented herein support the hypothesis that MeHg stimulates TH phosphorylation via a Ca^{2+} -dependent mechanism. First, MeHg-mediated DA release is dependent upon the presence of intracellular Ca^{2+} . Secondly, *de novo* DA synthesis is necessary for MeHg-induced DA

release. Lastly, MeHg stimulates TH activity, as assessed by DOPA accumulation and Western blot. To investigate whether MeHg activates TH via a Ca^{2+} -dependent mechanism, future analysis could include quantification of pTH Ser40 (and possibly pTH Ser19) by Western blot, as well as changes in DOPA accumulation following exposure to MeHg under Ca^{2+} -free conditions.

7.2. Role of Ca^{2+} in MeHg-induced vesicular exocytosis

The present studies illustrate a role for vesicular exocytosis in MeHg-induced DA release. Moreover, MeHg mobilizes vesicular DA stores in a Ca^{2+} -dependent manner. Because MeHg was able to induce release in either the absence of extracellular Ca^{2+} or following inhibition of VGCC, extracellular Ca^{2+} does not appear to play an integral role. However, MeHg-induced DA release is attenuated in the absence of intracellular Ca^{2+} , and this effect is enhanced in the absence of extracellular Ca^{2+} . Taken together, these results suggest that release of Ca^{2+} from intracellular stores is the primary event mediating MeHg-induced vesicular DA release, and influx of extracellular Ca^{2+} plays a secondary role promoting release.

Ca^{2+} plays a ubiquitous role in vesicular exocytosis. Although neurotransmitter release is generally mediated by extracellular Ca^{2+} influx through VGCC (Atluri and Regehr, 1998; Lu and Trussell, 2000), intracellular Ca^{2+} can initiate exocytosis (Levesque and

Atchison, 1987; 1988). It follows that the elevation in intracellular Ca^{2+} induced by MeHg triggers release of DA-containing vesicles. However, this hypothesis is currently based on corollary data. Additional work is needed to demonstrate a direct effect of MeHg-induced intracellular Ca^{2+} elevation on vesicular DA release. Confocal imaging studies using the fluorescent membrane probe FM1-43 in combination with a Ca^{2+} indicating dye such as Fluo-4 would be able to visually and quantitatively illustrate a proximal and functional relationship between Ca^{2+} elevation and vesicular exocytosis.

7.3. Collaborative relationship between extracellular and intracellular Ca^{2+} pools

Studies investigating the source of Ca^{2+} that mediates MeHg-induced DA release suggest that release of Ca^{2+} from intracellular stores is the key event. At the neuromuscular junction, disruption of Ca^{2+} transport mechanisms into the mitochondria precluded MeHg from inducing Ca^{2+} release and subsequent ACh release (Levesque and Atchison, 1988).

Agents that disrupted Ca^{2+} buffering by the SER were ineffective (Limke et al., 2004). These data suggest that mitochondria, rather than SER, play the critical role in MeHg-induced ACh release. However, studies investigating the contributions of different intracellular pools to the elevation in cytosolic Ca^{2+} induced by MeHg suggest that alterations in Ca^{2+} handling are complex and differ depending on cell type.

MeHg initiates a cascade of events that culminates in elevated cytosolic Ca^{2+} (Bearss et al., 2001). In cerebellar granule cells (Hare and Atchison, 1995a) and neuroblastoma cells (Hare and Atchison, 1995a) at least part of this Ca^{2+} originates from the SER, however the magnitude of contribution differs. In some cell types, such as neuroblastoma cells, the SER supplies the majority of released intracellular Ca^{2+} . Treatment with the SER Ca^{2+} ATPase inhibitor thapsigargin depletes the SER Ca^{2+} content and reduces the amplitude of intracellular Ca^{2+} elevation by almost 70% (Bearss et al., 2001). In other cell types, such as cerebellar granule cells, the SER has a more limited storage capacity and treatment with thapsigargin, only reduces the amplitude of intracellular Ca^{2+} elevation by 30% (Limke et al., 2003). Mitochondria contribute the bulk of intracellular Ca^{2+} in these cell types. Prior depletion of mitochondrial Ca^{2+} with mitochondrial membrane depolarization reduces the amplitude of Ca^{2+} elevation by ~65% (Kass and Orrenius, 1999).

Neurons are constantly buffering large fluctuations of intracellular Ca^{2+} (Marty and Atchison, 1997), and as such have similar Ca^{2+} buffering systems in place. Because DA-synthesizing cells more closely resemble cerebellar granule cells, than neuroblastoma cells, it follows that Ca^{2+} handling would also be more similar in these cell types. Consequently, the intracellular Ca^{2+} pool responsible for MeHg-induced DA release is most likely the mitochondria. However, there are differences between DA-synthesizing cells and cerebellar granule cells. Experiments elucidating the source of intracellular Ca^{2+} that initiates MeHg-

induced DA release are necessary to confirm this hypothesis. Pharmacological manipulation of SER and mitochondrial Ca^{2+} pools in combination with Ca^{2+} imaging (i.e. fura-2 fluorescence changes) and neurochemistry could be used to evaluate sources of intracellular Ca^{2+} that trigger MeHg-induced DA release.

Buffering extracellular Ca^{2+} did not significantly attenuate MeHg-induced DA release, whereas buffering intracellular Ca^{2+} did. However the ability of intracellular Ca^{2+} to stimulate DA release was augmented by the presence of extracellular Ca^{2+} , because MeHg-induced DA release in the absence of both sources was the only condition that significantly attenuated the percentage change in extracellular DA induced by MeHg. These data suggest that different Ca^{2+} sources collaborate to stimulate neurotransmitter release.

Because VGCCs did not contribute to release in the present studies, other membrane channels permeable to Ca^{2+} or membrane depolarization could mediate extracellular Ca^{2+} influx. Certain subtypes of the glutamate *N*-methyl-D-aspartate receptor are permeable to Ca^{2+} , however evidence suggests that inhibition of these channels does not attenuate the elevation in intracellular Ca^{2+} induced by MeHg (Saito et al., 2003). Furthermore, PC12 cells do not express functional *N*-methyl-D-aspartate receptors (Patrick and Barchas, 1976), making it unlikely that these channels would contribute to extracellular Ca^{2+} influx in the present model. PC12 cells do, however, express nicotinic ACh receptors (Bondy and McKee, 1991). Although MeHg interacts with these channels to increase intracellular Ca^{2+}

in PC12 cells, evidence suggests that cellular effects mediated by this channel are related to an intracellular mechanism rather than Ca^{2+} entry (personal communication, Dr. William Atchison).

There may be a role for membrane depolarization in MeHg-induced DA release. MeHg depolarizes the plasma membrane (Limke et al., 2004). Furthermore, there is a temporal relationship between membrane depolarization and MeHg-induced mitochondrial dysfunction (Bemis and Seegal, 1999; Dreiem et al., 2009). Excessive accumulation of mitochondrial Ca^{2+} depletes ATP and inhibits its synthesis. Loss of ATP would inhibit plasma membrane transporters, including the Na^+/K^+ ATPase. Because this exchanger maintains the transmembrane potential, its inhibition would depolarize the plasma membrane, facilitating entry of extracellular Ca^{2+} . Thus release of Ca^{2+} from mitochondrial stores coincides with membrane depolarization and influx of extracellular Ca^{2+} . Together these events could initiate vesicular DA exocytosis.

7.4. Aberrant DA metabolism induced by MeHg

Previous studies have established that MeHg inhibits oxidative DA metabolism (Taylor and DiStefano, 1976; Chakrabarti et al., 1998; Beyrouty et al., 2006; Castoldi et al., 2006), however this is the first study to indicate that this inhibitory profile culminates in the up-regulation of the reductive DA metabolic pathway to form DOPET, and accumulation of the toxic intermediate DOPAL. The present results demonstrate that, in an intact system, MeHg inhibits DA metabolism at the level of ALDH, and not MAO as previously asserted

(Goedde and Agarwal, 1990). However there are other possible explanations. For example, the aberrant DA metabolomic profile induced by MeHg in undifferentiated PC12 cells could be a cell-type specific response, such that in other immortalized cell lines or primary cultures, MAO and not ALDH may be impaired.

Enzyme assays demonstrate that MeHg does not directly inhibit ALDH. PC12 cells only express the ALDH2 isoform, which is localized to the mitochondrial matrix (Marchitti et al., 2007). While ALDH2 plays an integral role in DA metabolism (Galter et al., 2003; Anderson et al., 2011b), another isoform ALDH1A1, localized to the cytosol, has been reported to catalyze DOPAL oxidation in NSDA neurons (Yoshino et al., 1966). Therefore it would be of interest to assess the potential contribution of ALDH1A1 to buffering DOPAL in NSDA neurons, and determine how MeHg interacts with this isoform *in vivo*. Perhaps different subcellular localizations or subtle differences in protein structure impart a contrasting interaction with MeHg that could influence NSDA neuronal susceptibility.

Based on neurochemical results, it was hypothesized that MeHg inhibits ALDH activity indirectly by decreasing availability of the ALDH cofactor NAD, and that inhibition of the respiratory chain by MeHg mediates decreased synthesis of NAD. While there is some evidence to support this hypothesis, there is also indication that it is incorrect. MeHg markedly inhibits both basal respiration and spare respiratory capacity. However chelating intracellular Ca^{2+} severely impairs mitochondrial respiration, but DA metabolism and impairment by MeHg proceed without hindrance. Thus the original hypothesis must be rejected; mitochondrial dysfunction does not decrease the availability of NAD or contribute to aberrant DA metabolism induced by MeHg.

Decreased availability of NAD could result from many deleterious circumstances. MeHg inhibits the activity of certain enzymes in the citric acid cycle, including succinate dehydrogenase (Hamdy and Noyes, 1977) and malate dehydrogenase (LeBel et al., 1990; Sarafian et al., 1994; Gatti et al., 2004). Inhibition of malate dehydrogenase, in particular, would decrease oxidation of NADH to NAD. Additionally, inhibition of certain citric acid cycle enzymes would down-regulate overall activity of the cycle and further decrease NADH oxidation.

Oxidative stress induced by MeHg (Singh et al., 2008) may also contribute to decreased NAD synthesis and impaired DA metabolism. There is evidence to suggest that under conditions of oxidative stress, NADH is converted to NADPH by a compensatory metabolic network involving NADH kinase and malic enzyme (Yee and Choi, 1996; Gatti et al., 2004; Cuello et al., 2010). Up-regulation of this network could account for the observed decrease in both NAD and NADH, however, it is unlikely that this pathway would provide a substantial defense against oxidative stress. NADPH is a cofactor for many endogenous antioxidant systems, including glutathione peroxidase and catalase, both of which are inhibited by MeHg (LeBel et al., 1990; Sarafian et al., 1994; Gatti et al., 2004).

Oxidative stress and the production of free radicals induced by MeHg (Jinsmaa et al., 2009) may also contribute to aberrant DA metabolism. Products of oxidative stress, 4-hydroxynonenal and malondialdehyde, significantly enhance DOPAL production in PC6-3 cells, a subline of the PC12 cell line (Franco et al., 2007; Mori et al., 2007; Grotto et al., 2011; Deng et al., 2012; Liu et al., 2012). Both compounds were found to inhibit DA metabolism and increase DOPAL production at low micromolar concentrations targeting the aldehyde oxidative and/or reductive pathways. Accumulation of these and other lipid peroxidation

products following MeHg exposure (Pearl et al., 2000) could contribute to DOPAL accumulation.

Additional analysis is needed to confirm the inhibitory effect of decreased NAD availability on ALDH activity, and to identify potential roles for citric acid cycle inhibition and/or oxidative stress in these processes. Attempts to reverse aberrant DA metabolism with NAD add-back proved futile because NAD(H) can stimulate TH activity and DA release (Minnema et al., 1989; Gassó et al., 2000; Yuan and Atchison, 2007), confounding an analysis of the metabolomic profile. Perhaps treatment with the NAD precursor nicotinamide would overcome these confounding variables. Studies investigating the roles of oxidative stress and citric acid cycle activity could include antioxidant treatment, citric acid cycle substrate addition, and isolated enzyme activity assays.

7.5. Pathways by which MeHg targets DA neurons

The present dissertation provides evidence for at least two pathways by which MeHg targets DA-synthesizing cells. A model depicting these mechanisms is illustrated in Figure 7.1. MeHg induces the release of Ca^{2+} from intracellular stores, including the mitochondria and SER, which elevates cytosolic Ca^{2+} . This event has two consequences: 1) activation of Ca^{2+} -dependent protein kinases, such as PKC and CaM-MPK, increases phosphorylation of TH at Ser19 and -40, which stimulates DA synthesis and increases the amount of cytosolic DA, and 2) Ca^{2+} -dependent vesicular exocytosis triggers release of stored DA. Newly synthesized DA may be packaged into vesicles and released, however, stimulation of DA synthesis may overwhelm the capacity of VMAT to package DA.

Remaining cytosolic DA would be partitioned for metabolism. A second primary event mediated by MeHg, that may involve oxidative stress, inhibits oxidative DA metabolism. This event shunts DOPAL along the reductive metabolic pathway, however because AR has a lower affinity for DOPAL, metabolism proceeds more slowly and the toxic intermediate accumulates.

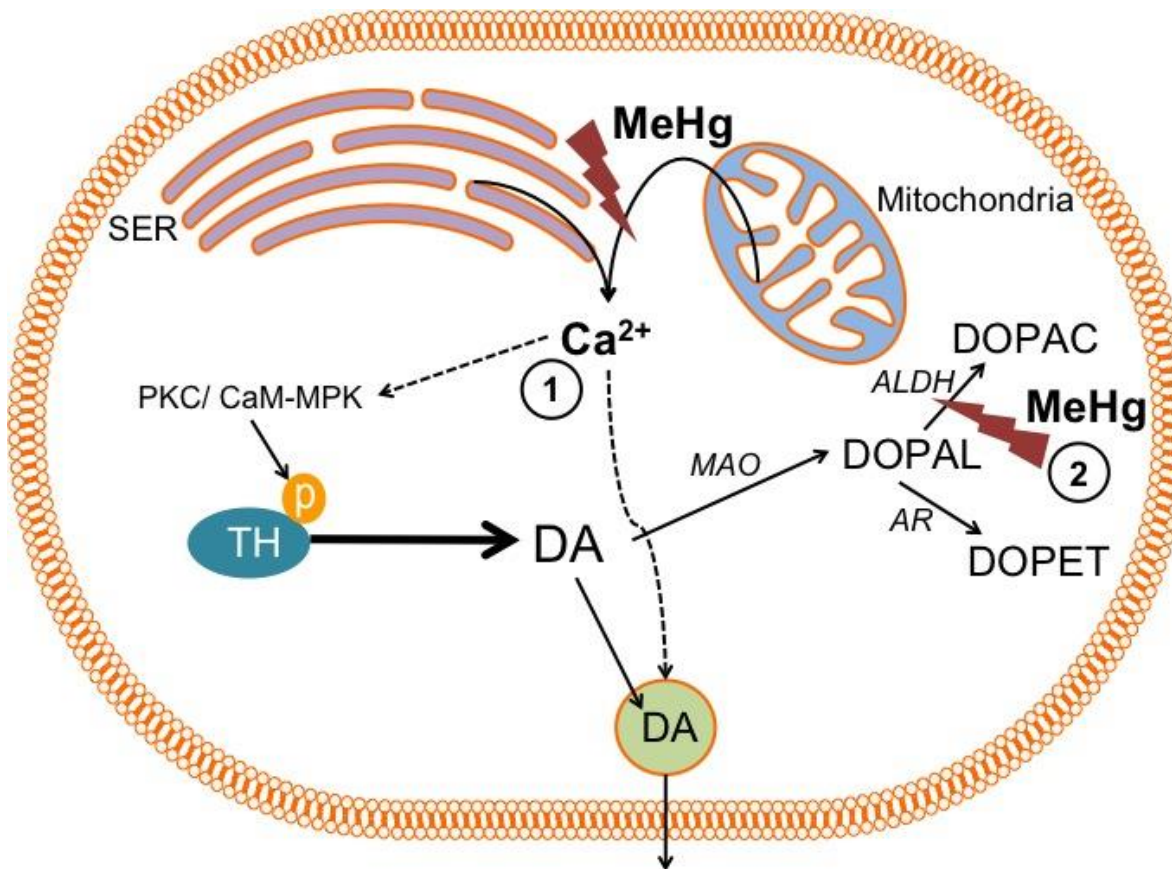


Figure 7.1. Proposed model identifying molecular targets of MeHg toxicity in DA-synthesizing cells. This dissertation has established at least two mechanisms by which MeHg alters DA homeostasis. 1) MeHg increases cytosolic Ca²⁺ primarily by causing release from intracellular stores. Elevated cytosolic Ca²⁺ activates protein kinases that phosphorylate TH and stimulate DA synthesis. Ca²⁺ in turn triggers vesicular exocytosis. 2) MeHg inhibits DA metabolism at the level of ALDH. The exact mechanism by which MeHg impairs ALDH activity remains unclear, however decreased availability of NAD is likely involved. Oxidative stress may also contribute. As a result of aberrant DA metabolism, a reductive DA metabolic pathway becomes active in response to elevated concentrations of the toxic intermediate DOPAL. MeHg, methylmercury; Ca²⁺, calcium; PKC, Ca²⁺/phospholipid dependent protein kinase; CaM-MPK, Ca²⁺/calmodulin-dependent multiprotein kinase; TH, tyrosine hydroxylase; DA, dopamine; MAO, monoamine oxidase; DOPAL, dihydroxyphenylacetaldehyde; ALDH, aldehyde dehydrogenase; DOPAC, dihydroxyphenylacetic acid; AR, aldehyde reductase; DOPET, dihydroxyphenylethanol; SER, smooth endoplasmic reticulum.

7.6. Factors influencing sensitivity of DA-synthesizing cells to MeHg

One of the goals of this dissertation was to identify mechanisms specific to DA neurons that would predispose them to MeHg toxicity. While MeHg-induced DA release, perturbation of intracellular Ca^{2+} homeostasis, and mitochondrial dysfunction certainly have deleterious consequences, these mechanisms are not specific to DA neurons. MeHg induces the release of many neurotransmitters, including NE, ACh, γ -aminobutyric acid, and glutamate (Roos et al., 2012). Similarly, Ca^{2+} dysregulation and mitochondrial dysfunction are ubiquitous mechanisms of action (Weiss et al., 2002; Weiss, 2011).

Accumulation of cytosolic DA and DOPAL would selectively and discretely heighten the sensitivity of DA neurons to MeHg toxicity. Non-vesicular DA has been described as an endogenous neurotoxin (Graham, 1978; Donaldson et al., 1982; Halliwell and Gutteridge, 1984; Stokes et al., 1999). It undergoes oxidation to form cytotoxic radicals and quinones either spontaneously or in the presence of transition metals, such as Mn^{2+} and Fe^{2+} (Akagawa et al., 2006). These oxidation events produce ROS and lipid peroxidation products (Kristal et al., 2001; Burke et al., 2003) that can severely damage cellular macromolecules.

DOPAL is 100-1000-fold more toxic than DA (500ng versus 20 μg ; Burke et al., 2003; 2003). While injections of exogenous DA or DOPAL each cause focal, non-specific lesions in the substantia nigra, DOPAL toxicity occurs at much lower concentrations (Mattammal et al., 1995). In striatal synaptosomes and differentiated PC12 cells, DOPAL neurotoxicity is attributed to uptake and accumulation in terminals by high-affinity DA transport (Anderson et al., 2011a), and in mesencephalic cultures, DOPAL causes specific, selective

damage to TH-immunoreactive neurons. Like DA, DOPAL oxidizes to produce quinones, which increases its likelihood to cross-link proteins (Li et al., 2001) and generate free radicals (Marchitti et al., 2007).

Accumulation of DA and particularly DOPAL following MeHg may be a critical endogenous event that triggers cell death in DA-synthesizing cells. Concentrations of DOPAL as low as 6 μ M can exert significant toxicity *in vitro* (Donaldson et al., 1982; Halliwell and Gutteridge, 1984; Li et al., 2001), well within the range observed presently. Future investigation concerning the contribution of DA and DOPAL oxidation products to MeHg-induced toxicity is of interest. Furthermore, because transition metals can increase the likelihood of both DA and DOPAL oxidation (Grace and Bunney, 1983), a better understanding of their interaction with MeHg would also be beneficial.

The L-type VGCC is another potential mechanism by which MeHg may exert selective susceptibility in DA neurons *in vivo*. While results in this dissertation suggest that MeHg does not interact with the L-type VGCC to induce DA release in PC12 cells, studies were only conducted while the channel was at rest; changes in MeHg-induced DA release were not assessed following VGCC activation. The L-type VGCC is essential for NSDA neuronal function and targeting by MeHg may be a critical event in discrete DA neurotoxicity.

Adult NSDA neurons maintain an autonomous rhythm, generating action potentials with a frequency of 2-4 Hz in the absence of synaptic input (Nedergaard et al., 1993; Bonci et al., 1998). Unlike most neurons that rely on monovalent cation channels to drive pacemaker activity, NSDA neurons engage somatodendritic L-type VGCCs (Chan et al., 2007) that contain the Cav1.3 pore-forming subunit (Koschak et al., 2001; Chan et al.,

2007). L-type VGCC with this subunit open at relatively hyperpolarized potentials (-50mV), and the influx of Ca^{2+} depolarized the cell to spike threshold (Sinnegger-Brauns et al., 2009). The Cav1.3 VGCC is rare, accounting for only ~10% of all L-type VGCCs in the brain (Surmeier, 2007), and is normally positioned near the synapse where it is only activated episodically. Sustained engagement of the Cav1.3 VGCC during pacemaking in NSDA neurons places a metabolic burden on these cells which is hypothesized to render them susceptible to degeneration in PD (Sirois and Atchison, 1996).

MeHg interacts with the L-type VGCC (Shafer and Atchison, 1991b; Shafer, 1998). Immediately following application, MeHg blocks whole cell currents carried by Ba^{2+} or Ca^{2+} through L-type VGCCs in PC12 cells (Denny et al., 1993; Marty and Atchison, 1997). However, L-type VGCC may also allow influx of extracellular Ca^{2+} during the second Ca^{2+} phase induced by MeHg (Marty and Atchison, 1997), as treatment with a L-type VGCC antagonist delays the time-to-onset of second phase influx (Tanner et al., 1999). Given these effects, a thorough analysis of the interaction between MeHg and Cav1.3 VGCCs in NSDA neurons may provide evidence of another mechanism by which MeHg selectively targets DA neurons.

7.7. Biological and clinical relevance to PD

Twin studies have demonstrated that environment contributes to the idiopathic form of PD. Concordance for monozygotic twins, although higher before age 51, is the same as that for dizygotic twins after the age of 51 (Monnet-Tschudi et al., 2006). The authors

discuss the possibility that heredity is not a major contributor in most cases of PD, and call for investigation of non-genetic risk factors. The data presented in this dissertation provide evidence that the environmental toxicant MeHg targets DA homeostasis, which alters neurochemistry and may contribute to DA neuronal degeneration. However work is still needed to establish the relationship between MeHg-induced changes in DA homeostasis and NSDA toxicity in PD.

Environmental exposure to MeHg could contribute to PD either through slow accumulation during long-term exposure to low concentrations, or exposure during a critical period during development (Choi et al., 1978). MeHg is a more potent neurotoxicant to the developing nervous system as compared to the adult nervous system (Amin-Zaki et al., 1978; Grandjean et al., 1997). Indeed, early life exposure to MeHg severely impairs neurobehavioral performance in several domains, including language, attention, memory, motor, and visuospatial function (McKeown-Eyssen and Ruedy, 1983; Davis et al., 1994; Weil et al., 2005). Adult exposure does not cause such pronounced deficits (Ngim and Devathasan, 1989; Wermuth et al., 2000; 2008; Petersen et al., 2008a; 2008b). Currently, a higher incidence of PD is only correlated with lifetime exposure to MeHg (Langston et al., 1999). However a mechanistic hypothesis suggests that early exposure to MeHg may reduce the number of neurons in vulnerable areas of the brain (e.g. the substantia nigra) below those needed to sustain function in the face of neuronal attrition associated with advanced aging (Klein and Westenberger, 2012). Few studies have investigated the effects of chronic, low-concentration MeHg exposure and its relevance to PD. A better understanding of how chronic, low-concentration exposure to MeHg induces oxidative stress and mitochondrial dysfunction, as well as dysregulation of DA homeostasis would

provide evidence to support current hypotheses about the impact of early life exposure to toxicants in neurodegenerative disease, and elucidate roles for exposure during a vulnerable period or exposure throughout one's lifetime.

Although genetic risk factors may not play the decisive role in the etiology of PD, their contribution is of significant importance. Moreover, understanding the interaction between genetic and environmental risk factors is essential in gaining a more complete understanding of how PD develops. To date, 28 distinct chromosomal regions have been associated with PD (Polymeropoulos et al., 1997), and MeHg exposure may be linked to at least three, parkin, DJ-1, and α -synuclein.

Mutations in the gene α -synuclein have been linked to autosomal dominant PD (Spillantini et al., 1998), however the protein also plays a role in idiopathic PD being a major component of Lewy bodies, abnormal aggregates of protein found in the substantia nigra of PD patients at autopsy (Piao et al., 2000). α -Synuclein is widely distributed throughout the brain (Xu et al., 2002), and as such mutations alone cannot account for the selective disturbances in DA neurons. Indeed, transfection of α -synuclein is toxic in DA-synthesizing neurons but not non-DA containing neurons (Betarbet et al., 2000; Giasson and Lee, 2000). Therefore α -synuclein-mediated toxicity depends on the synthesis of DA. α -Synuclein accumulation in Lewy bodies has been attributed to oxidative stress (Burke et al., 2003). It has been proposed that DOPAL and the generation of hydroxyl radicals associated with its oxidation trigger aggregation of α -synuclein in DA neurons (Li et al., 2001).

Data presented in this dissertation provides evidences for a mechanism by which MeHg may interact selectively with DA neurons to induce α -synuclein accumulation and associated toxicity. In a hypothetical scenario, MeHg exposure would interfere with ALDH-

mediated DA metabolism, leading to accumulation of DOPAL. Being a highly unstable intermediate, DOPAL would readily oxidize, and in the process produce a hydroxyl radical (Hashimoto et al., 1999; Xu et al., 2002). The associated oxidative stress would accelerate aggregation of α -synuclein in its toxic form selectively in DA neurons (Bonifati et al., 2003).

A similar situation could be envisioned for the PD-associated protein DJ-1 (Mitsumoto and Nakagawa, 2001; Mitsumoto et al., 2001). Although the exact function of DJ-1 is unknown, it is thought to monitor or buffer effects of excessive oxidative stress (Di Monte, 2003). Mutations in DJ-1 would compromise antioxidant function and increase susceptibility of DA neurons to oxidative stress (Shimura et al., 2000; Zhang et al., 2000). While there is currently no evidence linking MeHg exposure to mutations in DJ-1, a potential connection warrants further investigation. The production of free radicals associated with MeHg intoxication and aberrant DA metabolism could potentially have deleterious consequences in combination with a mutation in DJ-1.

Lastly, there is evidence to suggest that MeHg interacts with the protein parkin in DA neurons. Parkin is a component of the multiprotein E3 ubiquitin ligase complex (Sherman and Goldberg, 2001), which in turn is part of the ubiquitin-proteasome system that targets misfolded proteins for degradation (Kitada et al., 1998; Mizuno et al., 2001). Loss of function mutations in the gene that encodes parkin cause autosomal recessive juvenile PD (Martinez-Finley et al., 2013). Mutations would abolish its E3 ligase activity and result in the accumulation of misfolded parkin substrates. A recent study has reported that early-life exposure to MeHg exacerbates the loss of DA neurons associated with parkin knockout in *C. elegans*. Evidence suggests that mercury accumulates more readily in parkin

knockout worms, and cell death might be due to an inability to mount an antioxidant defense against MeHg toxicity as compared to wildtype counterparts. Future studies investigating the relationship between MeHg-impaired DA metabolism and oxidative stress in the face of parkin mutations would contribute greatly to the understanding of gene/environment interactions.

7.8. Concluding Remarks

MeHg is a bioaccumulative environmental neurotoxicant that preferentially targets discrete regions of the brain, including the NSDA system. Results presented in this dissertation describe the deleterious consequences of MeHg exposure in DA-synthesizing cells. Aberrant DA homeostasis can be attributed to multiple primary mechanisms of action, one of which is intracellular Ca^{2+} dysregulation. While some observed effects could be generalized to other systems, others are specific to DA neurons. These results begin to explain why DA neurons are selectively susceptible to MeHg neurotoxicity. Furthermore, MeHg exposure may be a critical environmental risk factor for PD, and the present findings provide evidence for mechanisms by which MeHg targets DA-synthesizing cells. Future analysis on MeHg neurotoxicity in DA neuronal population *in vivo* and studies elucidating the interaction between MeHg and certain genetic risk factors of PD would provide a more complete understanding of how MeHg exposure induces cytotoxicity in DA neurons.

REFERENCES

REFERENCES

- Akagawa M, Ishii Y, Ishii T, Shibata T, Yotsu-Yamashita M, Suyama K, Uchida K (2006) Metal-catalyzed oxidation of protein-bound dopamine. *Biochemistry* 45:15120–15128.
- Albert KA, Helmer-Matyjek E, Nairn AC, Müller TH, Haycock JW, Greene LA, Goldstein M, Greengard P (1984) Calcium/phospholipid-dependent protein kinase (protein kinase C) phosphorylates and activates tyrosine hydroxylase. *Proc Natl Acad Sci U S A* 81:7713–7717.
- Amenta F, Cavalotta D, Del Valle ME, Mancini M, Sabbatini M, Torres JM, Vega JA (1994) Calbindin D-28k immunoreactivity in the rat cerebellar cortex: age-related changes. *Neurosci Lett* 178:131–134.
- Amin-Zaki L, Majeed MA, Clarkson TW, Greenwood MR (1978) Methylmercury poisoning in Iraqi children: clinical observations over two years. *Brit Med J* 1:613–616.
- Anderson DG, Mariappan SVS, Buettner GR, Doorn JA (2011a) Oxidation of 3,4-Dihydroxyphenylacetaldehyde, a toxic dopaminergic metabolite, to a semiquinone radical and an ortho-quinone. *J Biol Chem* 286:26978–26986.
- Anderson DW, Schray RC, Duester G, Schneider JS (2011b) Functional significance of aldehyde dehydrogenase ALDH1A1 to the nigrostriatal dopamine system. *Brain Res* 1408:81–87.
- Assaly R, de Tassigny AD, Paradis S, Jacquin S, Berdeaux A, Morin D (2012) Oxidative stress, mitochondrial permeability transition pore opening and cell death during hypoxia-reoxygenation in adult cardiomyocytes. *Eur J Pharmacol* 675:6–14.
- Atchison WD (1986) Extracellular calcium-dependent and -independent effects of methylmercury on spontaneous and potassium-evoked release of acetylcholine at the neuromuscular junction. *J Pharm Exper Ther* 237:672–680.
- Atchison WD (1987) Effects of activation of sodium and calcium entry on spontaneous release of acetylcholine induced by methylmercury. *J Pharm Exper Ther* 241:131–139.
- Atchison WD, Clark AW, Narahashi T (1984) Presynaptic effects of methylmercury at the mammalian neuromuscular junction. In: *Cellular and Molecular Neurotoxicity* (Narahashi T, ed), pp 23–42. Raven Pr.
- Atchison WD, Hare MF (1994) Mechanisms of methylmercury-induced neurotoxicity. *FASEB J* 8:622–629.
- Atchison WD, Narahashi T (1982) Methylmercury-induced depression of neuromuscular transmission in the rat. *NeuroToxicology* 3:37–50.

- Atluri PP, Regehr WG (1998) Delayed release of neurotransmitter from cerebellar granule cells. *J Neurosci* 18:8214–8227.
- Avidor B, Avidor T, Schwartz L, De Jongh KS, Atlas D (1994) Cardiac L-type Ca^{2+} channel triggers transmitter release in PC12 cells. *FEBS Lett* 342:209–213.
- Badoyannis HC, Sharma SC, Sabban EL (1991) The differential effects of cell density and NGF on the expression of tyrosine hydroxylase and dopamine β -hydroxylase in PC12 cells. *Brain Res Mol Brain Res* 11:79–87.
- Bajjalieh SM, Scheller RH (1995) The biochemistry of neurotransmitter secretion. *J Biol Chem* 270:1971–1974.
- Bakir F, Damluji SF, Amin-Zaki L, Murtadha M, Khalidi A, al-Rawi NY, Tikriti S, Dahahir HI, Clarkson TW, Smith JC, Doherty RA (1973) Methylmercury poisoning in Iraq. *Science* 181:230–241.
- Barrowman MM, Cockcroft S, Gomperts BD (1986) Two roles for guanine nucleotides in the stimulus-secretion sequence of neutrophils. *Nature* 319:504–507.
- Bartolome J, Whitmore WL, Seidler FJ, Slotkin TA (1984) Exposure to methylmercury in utero: effects on biochemical development of catecholamine neurotransmitter systems. *Life Sci* 35:657–670.
- Bauerfeind R, Régnier-Vigouroux A, Flatmark T, Huttner WB (1993) Selective storage of acetylcholine, but not catecholamines, in neuroendocrine synaptic-like microvesicles of early endosomal origin. *Neuron* 11:105–121.
- Bemis JC, Seegal RF (1999) Polychlorinated biphenyls and methylmercury act synergistically to reduce rat brain dopamine content in vitro. *Environ Health Perspect* 107:879–885.
- Berg GG, Miles EF (1979) Mechanisms of inhibition of active transport ATPases by mercurials. *Chem Biol Inter* 27:199–219.
- Betarbet R, Sherer TB, MacKenzie G, Garcia-Osuna M, Panov AV, Greenamyre JT (2000) Chronic systemic pesticide exposure reproduces features of Parkinson's disease. *Nat Neurosci* 3:1301–1306.
- Bevilaqua L, Cammarota M, Dickson PW, Sim ATR, Dunkley PR (2003) Role of protein phosphatase 2C from bovine adrenal chromaffin cells in the dephosphorylation of phospho-serine 40 tyrosine hydroxylase. *J Neurochem* 85:1368–1373.
- Bevilaqua LRM (2001) Phosphorylation of Ser19 alters the conformation of tyrosine hydroxylase to increase the rate of phosphorylation of Ser40. *J Biol Chem* 276:40411–40416.

- Beyrouty P, Stamler CJ, Liu J-N, Loua KM, Kubow S, Chan HM (2006) Effects of prenatal methylmercury exposure on brain monoamine oxidase activity and neurobehaviour of rats. *Neurotoxicol Teratol* 28:251–259.
- Bhan A, Sarkar NN (2005) Mercury in the environment: effect on health and reproduction. *Rev Environ Health* 20:39–56.
- Björklund A, Dunnett SB (2007) Dopamine neuron systems in the brain: an update. *Trends Neurosci* 30:194–202.
- Blaschko H (1942) The activity of *l*(-)-dopa decarboxylase. *J Physiol (Lond.)* 101:337–349.
- Blaustein MP (1988) Calcium transport and buffering in neurons. *Trends Neurosci* 11:438–443.
- Bommert K, Charlton MP, DeBello WM, Chin GJ, Betz H, Augustine GJ (1993) Inhibition of neurotransmitter release by C2-domain peptides implicates synaptotagmin in exocytosis. *Nature* 363:163–165.
- Bonci A, Grillner P, Mercuri NB, Bernardi G (1998) L-Type calcium channels mediate a slow excitatory synaptic transmission in rat midbrain dopaminergic neurons. *J Neurosci* 18:6693–6703.
- Bondy SC, McKee M (1991) Disruption of the potential across the synaptosomal plasma membrane and mitochondria by neurotoxic agents. *Toxicol Lett* 58:13–21.
- Bonifati V, Rizzu P, van Baren MJ, Schaap O, Breedveld GJ, Krieger E, Dekker MCJ, Squitieri F, Ibanez P, Joosse M, van Dongen JW, Vanacore N, van Swieten JC, Brice A, Meco G, van Duijn CM, Oostra BA, Heutink P (2003) Mutations in the DJ-1 gene associated with autosomal recessive early-onset parkinsonism. *Science* 299:256–259.
- Bonnet JJ, Benmansour S, Amejdki-Chab N, Costentin J (1994) Effect of CH₃HgCl and several transition metals on the dopamine neuronal carrier; peculiar behaviour of Zn²⁺. *Eur J Pharmacol* 266:87–97.
- Brand MD, Nicholls DG (2011) Assessing mitochondrial dysfunction in cells. *Biochem J* 435:297–312.
- Brini M, Cali T, Ottolini D, Carafoli E (2013) Intracellular calcium homeostasis and signaling. *Met Ions Life Sci* 12:119–168.
- Brodie BB, Costa E, Dlabac A, Neff NH, Smookler HH (1966) Application of steady state kinetics to the estimation of synthesis rate and turnover time of tissue catecholamines. *J Pharmacol Exp Ther* 154:493–498.
- Brooks PJ, Theruvathu JA (2005) DNA adducts from acetaldehyde: implications for alcohol-related carcinogenesis. *Alcohol* 35:187–193.

- Brüss M, Pörzgen P, Bryan-Lluka LJ, Bönisch H (1997) The rat norepinephrine transporter: molecular cloning from PC12 cells and functional expression. *Brain Res Mol Brain Res* 52:257–262.
- Buck KJ, Amara SG (1995) Structural domains of catecholamine transporter chimeras involved in selective inhibition by antidepressants and psychomotor stimulants. *Mol Pharmacol* 48:1030–1037.
- Burke WJ, Li SW, Williams EA, Nonneman R, Zahm DS (2003) 3,4-Dihydroxyphenylacetaldehyde is the toxic dopamine metabolite in vivo: implications for Parkinson's disease pathogenesis. *Brain Res* 989:205–213.
- Cai J, Yang J, Jones DP (1998) Mitochondrial control of apoptosis: the role of cytochrome c. *Biochim Biophys Acta* 1366:139–149.
- Caldwell L, Harries P, Sydlik S, Schwiening CJ (2013) Presynaptic pH and vesicle fusion in *Drosophila* larvae neurons. *Synapse* 00:000-000.
- Cannino G, El-Khoury R, Pirinen M, Hutz B, Rustin P, Jacobs HT, Dufour E (2012) Glucose modulates respiratory complex I activity in response to acute mitochondrial dysfunction. *J Biol Chem* 287:38729–38740.
- Carafoli E (1987) Intracellular calcium homeostasis. *Annu Rev Biochem* 56:395–433.
- Carafoli E, Garcia-Martin E, Guerini D (1996) The plasma membrane calcium pump: recent developments and future perspectives. *Experientia* 52:1091–1100.
- Carlsson A, Davis JN, Kehr W, Lindqvist M, Atack CV (1972) Simultaneous measurement of tyrosine and tryptophan hydroxylase activities in brain in vivo using an inhibitor of the aromatic amino acid decarboxylase. *Naunyn Schmiedebergs Arch Pharmacol* 275:153–168.
- Castoldi AF, Barni S, Turin I, Gandini C, Manzo L (2000) Early acute necrosis, delayed apoptosis and cytoskeletal breakdown in cultured cerebellar granule neurons exposed to methylmercury. *J Neurosci Res* 59:775–787.
- Castoldi AF, Blandini F, Randine G, Samuele A, Manzo L, Coccini T (2006) Brain monoaminergic neurotransmission parameters in weanling rats after perinatal exposure to methylmercury and 2,2',4,4',5,5'-hexachlorobiphenyl (PCB153). *Brain Res* 1112:91–98.
- Castoldi AF, Coccini T, Ceccatelli S, Manzo L (2001) Neurotoxicity and molecular effects of methylmercury. *Brain Res Bull* 55:197–203.
- Catterall WA, Few AP (2008) Calcium channel regulation and presynaptic plasticity. *Neuron* 59:882–901.

- Chakrabarti SK, Loua KM, Bai C, Durham H, Panisset JC (1998) Modulation of monoamine oxidase activity in different brain regions and platelets following exposure of rats to methylmercury. *Neurotoxicol Teratol* 20:161–168.
- Chamley JH, Mark GE, Campbell GR, Burnstock G (1972) Sympathetic ganglia in culture. I. Neurons. *Z Zellforsch Mikrosk Anat* 135:287–314.
- Chan CS, Guzman JN, Ilijic E, Mercer JN, Rick C, Tkatch T, Meredith GE, Surmeier DJ (2007) “Rejuvenation” protects neurons in mouse models of Parkinson’s disease. *Nature* 447:1081–1086.
- Chen T, Yang W, Li Y, Chen X, Xu S (2011) Mono-(2-ethylhexyl) phthalate impairs neurodevelopment: inhibition of proliferation and promotion of differentiation in PC12 cells. *Toxicol Lett* 201:34–41.
- Chetty CS, Rajanna S, Hall E, Yallapragada PR, Rajanna B (1996) In vitro and in vivo effects of lead, methyl mercury and mercury on inositol 1,4,5-trisphosphate and 1,3,4,5-tetrakisphosphate receptor bindings in rat brain. *Toxicol Lett* 87:11–17.
- Chio KS, Tappel AL (1969) Inactivation of ribonuclease and other enzymes by peroxidizing lipids and by malonaldehyde. *Biochemistry* 8:2827–2832.
- Choi BH, Lapham LW, Amin-Zaki L, Saleem T (1978) Abnormal neuronal migration, deranged cerebral cortical organization, and diffuse white matter astrocytosis of human fetal brain: a major effect of methylmercury poisoning in utero. *J Neuropathol Exp Neurol* 37:719–733.
- Choi SW, Gerencser AA, Nicholls DG (2009) Bioenergetic analysis of isolated cerebrocortical nerve terminals on a microgram scale: spare respiratory capacity and stochastic mitochondrial failure. *J Neurochem* 109:1179–1191.
- Choksi NY, Kodavanti PR, Tilson HA, Booth RG (1997) Effects of polychlorinated biphenyls (PCBs) on brain tyrosine hydroxylase activity and dopamine synthesis in rats. *Fundam Appl Toxicol* 39:76–80.
- Churchill EN, Disatnik MH, Mochly-Rosen D (2009) Time-dependent and ethanol-induced cardiac protection from ischemia mediated by mitochondrial translocation of ϵ PKC and activation of aldehyde dehydrogenase 2. *J Mol Cell Cardio* 46:278–284.
- Clarkson TW (1998) Human toxicology of mercury. *J Trace Elem Exper Med* 11:303–317.
- Collins MA, Neafsey EJ (2002) Potential neurotoxic “agents provocateurs” in Parkinson’s disease. *Neurotoxicol Teratol* 24:571–577
- Contreras L, Drago I, Zampese E, Pozzan T (2010) Mitochondria: The calcium connection. *BBA - Bioenergetics* 1797:607–618.

- Cuello S, Goya L, Madrid Y, Campuzano S, Pedrero M, Bravo L, Cámara C, Ramos S (2010) Molecular mechanisms of methylmercury-induced cell death in human HepG2 cells. *Food Chem Toxicol* 48:1405–1411.
- Daubner SC, Lauriano C, Haycock JW, Fitzpatrick PF (1992) Site-directed mutagenesis of serine 40 of rat tyrosine hydroxylase. Effects of dopamine and cAMP-dependent phosphorylation on enzyme activity. *J Biol Chem* 267:12639–12646.
- Daubner SC, Le T, Wang S (2011) Tyrosine hydroxylase and regulation of dopamine synthesis. *Arch Biochem Biophys* 508:1–12.
- Dauer W, Przedborski S (2003) Parkinson's Disease - Mechanisms and Models. *Neuron* 39:21–21.
- Davis LE, Kornfeld M, Mooney HS, Fiedler KJ, Haaland KY, Orrison WW, Cernichiari E, Clarkson TW (1994) Methylmercury poisoning: long-term clinical, radiological, toxicological, and pathological studies of an affected family. *Ann Neurol* 35:680–688.
- Deng Y, Xu Z-F, Liu W, Xu B, Yang H-B, Wei Y-G (2012) Riluzole-triggered GSH synthesis via activation of glutamate transporters to antagonize methylmercury-induced oxidative stress in rat cerebral cortex. *Oxid Med Cell Longev* 2012:534705.
- Denny MF, Atchison WD (1996) Mercurial-induced alterations in neuronal divalent cation homeostasis. *NeuroToxicology* 17:47–61.
- Denny MF, Hare MF, Atchison WD (1993) Methylmercury alters intrasynaptosomal concentrations of endogenous polyvalent cations. *Toxicol Appl Pharmacol* 122:222–232.
- Denton RM (2009) Regulation of mitochondrial dehydrogenases by calcium ions. *Biochim Biophys Acta* 1787:1309–1316.
- Denton RMR, Randle PJP, Martin BRB (1972) Stimulation by calcium ions of pyruvate dehydrogenase phosphate phosphatase. *Biochem J* 128:161–163.
- Deryabina YI, Isakova EP, Zvyagilskaya RA (2004) Mitochondrial calcium transport systems: properties, regulation, and taxonomic features. *Biochemistry (Mosc)* 69:91–102.
- Di Monte DA (2003) The environment and Parkinson's disease: is the nigrostriatal system preferentially targeted by neurotoxins? *Lancet Neurol* 2:531–538.
- Di Virgilio F, Lew DP, Pozzan T (1984) Protein kinase C activation of physiological processes in human neutrophils at vanishingly small cytosolic Ca²⁺ levels. *Nature* 310:691–693.
- Dichter MA, Tischler AS, Greene LA (1977) Nerve growth factor-induced increase in

- electrical excitability and acetylcholine sensitivity of a rat pheochromocytoma cell line. *Nature* 268:501–504.
- DiMauro S, Schon EA (2008) Mitochondrial disorders in the nervous system. *Annu Rev Neurosci* 31:91–123.
- Dobrowsky RT, Kamibayashi C, Mumby MC, Hannun YA (1993) Ceramide activates heterotrimeric protein phosphatase 2A. *J Biol Chem* 268:15523–15530.
- Donaldson J, McGregor D, LaBella F (1982) Manganese neurotoxicity: a model for free radical mediated neurodegeneration? *Can J Physiol Pharmacol* 60:1398–1405.
- Drapeau PP, Nachshen DAD (1988) Effects of lowering extracellular and cytosolic pH on calcium fluxes, cytosolic calcium levels, and transmitter release in presynaptic nerve terminals isolated from rat brain. *J Gen Physiol* 91:305–315.
- Dreiem A, Gertz CC, Seegal RF (2005) The effects of methylmercury on mitochondrial function and reactive oxygen species formation in rat striatal synaptosomes are age-dependent. *Toxicol Sci* 87:156–162.
- Dreiem A, Seegal RF (2007) Methylmercury-induced changes in mitochondrial function in striatal synaptosomes are calcium-dependent and ROS-independent. *NeuroToxicology* 28:720–726.
- Dreiem A, Shan M, Okoniewski RJ, Sanchez-Morrissey S, Seegal RF (2009) Methylmercury inhibits dopaminergic function in rat pup synaptosomes in an age-dependent manner. *Neurotoxicol Teratol* 31:312–317.
- Drukarch B, Jongenelen CA, Schepens E, Langeveld CH, Stoof JC (1996) Glutathione is involved in the granular storage of dopamine in rat PC12 pheochromocytoma cells: implications for the pathogenesis of Parkinson's disease. *J Neurosci* 16:6038–6045.
- Duncan RJ, Sourkes TL (1974) Some enzymic aspects of the production of oxidized or reduced metabolites of catecholamines and 5-hydroxytryptamine by brain tissues. *J Neurochem* 22:663–669.
- Dunkley PR, Bobrovskaya L, Graham ME, Nagy-Felsobuki von EI, Dickson PWP (2004) Tyrosine hydroxylase phosphorylation: regulation and consequences. *J Neurochem* 91:1025–1043.
- Dunlap K, Luebke JI, Turner TJ (1995) Exocytotic Ca^{2+} channels in mammalian central neurons. *Trends Neurosci* 18:89–98.
- Edwards JR, Marty MS, Atchison WD (2005) Comparative sensitivity of rat cerebellar neurons to dysregulation of divalent cation homeostasis and cytotoxicity caused by methylmercury. *Toxicol Appl Pharmacol* 208:222–232.

- Eisenhofer G (2004) Catecholamine Metabolism: A Contemporary View with Implications for Physiology and Medicine. *Pharmacol Rev* 56:331–349.
- Elferink LA, Peterson MR, Scheller RH (1993) A role for synaptotagmin (p65) in regulated exocytosis. *Cell* 72:153–159.
- Elsworth JD, Roth RH (1997) Dopamine synthesis, uptake, metabolism, and receptors: relevance to gene therapy of Parkinson's disease. *Exp Neurol* 144:6–6.
- EPA (2001) Water Quality Criterion for the Protection of Human Health: ... US EPA Office of Science and Technology, Office of Water. Available at: http://water.epa.gov/scitech/swguidance/standards/criteria/aqlife/methylmercury/upload/2009_01_15_criteria_methylmercury_mercury-criterion.pdf.
- Erickson JD, Eiden LE, Hoffman BJ (1992) Expression cloning of a reserpine-sensitive vesicular monoamine transporter. *Proc Natl Acad Sci U S A* 89:10993–10997.
- Esterbauer H, Zollner H, Scholz N (1975) Reaction of glutathione with conjugated carbonyls. *Z Naturforsch C* 30:466–473.
- Eto K (1997) Pathology of Minamata Disease. *Toxicol Path* 25:614–623.
- Fahn S (2003) Description of Parkinson's disease as a clinical syndrome. *Ann N Y Acad Sci* 991:1–14.
- Farah CA, Sossin WS (2012) The role of C2 domains in PKC signaling. In: *Advances in Experimental Medicine and Biology*, pp 663–683 *Adv Exp Med Biol*. Dordrecht: Springer, Netherlands.
- Faro LRF, Do Nascimento JLM, Alfonso M, Durán R (1998) Acute administration of methylmercury changes in vivo dopamine release from rat striatum. *Bull Environ Contam Toxicol* 60:632–638.
- Faro LRF, Do Nascimento JLM, Alfonso M, Durán R (2002) Mechanism of action of methylmercury on in vivo striatal dopamine release. Possible involvement of dopamine transporter. *Neurochem Int* 40:455–465.
- Faro LRF, Do Nascimento JLM, San José JM, Alfonso M, Durán R (2000) Intra-striatal administration of methylmercury increases in vivo dopamine release. *Neurochem Res* 25:225–229.
- Faro LRF, Durán R, Do Nascimento JLM, Alfonso M, Picanço-Diniz CW (1997) Effects of methyl mercury on the in vivo release of dopamine and its acidic metabolites DOPAC and HVA from striatum of rats. *Ecotoxicol Environ Saf* 38:95–98.
- Faro LRF, Durán R, Do Nascimento JLM, Perez-Vences D, Alfonso M (2003) Effects of successive intra-striatal methylmercury administrations on dopaminergic system.

Ecotoxicol Environ Saf 55:173–177.

- Faro LRF, Rodrigues KJA, Santana MB, Vidal L, Alfonso M, Durán R (2007) Comparative effects of organic and inorganic mercury on in vivo dopamine release in freely moving rats. *Braz J Med Biol Res* 40:1361–1365.
- Feng Z, Hu W, Tang M-S (2004) Trans-4-hydroxy-2-nonenal inhibits nucleotide excision repair in human cells: a possible mechanism for lipid peroxidation-induced carcinogenesis. *Proc Natl Acad Sci U S A* 101:8598–8602.
- Fitzmaurice AG, Rhodes SL, Lulla A, Murphy NP, Lam HA, O'Donnell KC, Barnhill L, Casida JE, Cockburn M, Sagasti A, Stahl MC, Maidment NT, Ritz B, Bronstein JM (2013) Aldehyde dehydrogenase inhibition as a pathogenic mechanism in Parkinson disease. *Proc Natl Acad Sci U S A* 110:636–641.
- Fonfria E, Dare E, Benelli M, Suñol C, Ceccatelli S (2002) Translocation of apoptosis-inducing factor in cerebellar granule cells exposed to neurotoxic agents inducing oxidative stress. *Eur J Neurosci* 16:2013–2016.
- Fornai F, Lenzi P, Lazzeri G, Ferrucci M, Fulceri F, Giorgi FS, Falleni A, Ruggieri S, Paparelli A (2007) Fine ultrastructure and biochemistry of PC12 cells: A comparative approach to understand neurotoxicity. *Brain Res* 1129:174–190.
- Fox DA, Grandjean P, de Groot D, Paule MG (2012) Developmental origins of adult diseases and neurotoxicity: epidemiological and experimental studies. *NeuroToxicology* 33:810–816.
- Fox JH, Patel-Mandlik K, Cohen MM (1975) Comparative effects of organic and inorganic mercury on brain slice respiration and metabolism. *J Neurochem* 24:757–762.
- Franco JL, Braga HC, Stringari J, Missau FC, Posser T, Mendes BG, Leal RB, Santos ARS, Dafre AL, Pizzolatti MG, Farina M (2007) Mercurial-induced hydrogen peroxide generation in mouse brain mitochondria: protective effects of quercetin. *Chem Res Toxicol* 20:1919–1926.
- Franco JL, Posser T, Dunkley PR, Dickson PW, Mattos JJ, Martins R, Bainy ACD, Marques MR, Dafre AL, Farina M (2009) Methylmercury neurotoxicity is associated with inhibition of the antioxidant enzyme glutathione peroxidase. *Free Radical Biol Med* 47:449–457.
- Friedrich U, Bönisch H (1986) The neuronal noradrenaline transport system of PC-12 cells: kinetic analysis of the interaction between noradrenaline, Na⁺ and Cl⁻ in transport. *Naunyn Schmiedebergs Arch Pharmacol* 333:246–252.
- Fukuda Y, Ushijima K, Kitano T, Sakamoto M, Futatsuka M (1999) An analysis of subjective complaints in a population living in a methylmercury-polluted area. *Environ Res* 81:100–107.

- Galter D, Buervenich S, Carmine A, Anvret M, Olson L (2003) ALDH1 mRNA: presence in human dopamine neurons and decreases in substantia nigra in Parkinson's disease and in the ventral tegmental area in schizophrenia. *Neurobiol Dis* 14:637–647.
- Gassó S, Cristòfol RM, Selema G, Rosa R, Rodríguez-Farré E, Sanfeliu C (2001) Antioxidant compounds and Ca²⁺ pathway blockers differentially protect against methylmercury and mercuric chloride neurotoxicity. *J Neurosci Res* 66:135–145.
- Gassó S, Suñol C, Sanfeliu C, Rodríguez-Farré E, Cristòfol R (2000) Pharmacological characterization of the effects of methylmercury and mercuric chloride on spontaneous noradrenaline release from rat hippocampal slices. *Life Sci* 27:1219–1231.
- Gatti R, Belletti S, Uggeri J, Vettori MV, Mutti A, Scandroglio R, Orlandini G (2004) Methylmercury cytotoxicity in PC12 cells is mediated by primary glutathione depletion independent of excess reactive oxygen species generation. *Toxicology* 204:175–185.
- Giasson BIB, Lee VMV (2000) A new link between pesticides and Parkinson's disease. *Nat Neurosci* 3:1227–1228.
- Glancy B, Balaban RS (2012) Role of mitochondrial Ca²⁺ in the regulation of cellular energetics. *Biochemistry* 51:2959–2973.
- Glover V, Sandler M, Owen F, Riley GJ (1977) Dopamine is a monoamine oxidase B substrate in man. *Nature* 265:80–81.
- Goedde HW, Agarwal DP (1990) Pharmacogenetics of aldehyde dehydrogenase (ALDH). *Pharmacol Ther* 45:345–371.
- Grace AA, Bunney BS (1983) Intracellular and extracellular electrophysiology of nigral dopaminergic neurons--2. Action potential generating mechanisms and morphological correlates. *Neuroscience* 10:317–331.
- Graham DG (1978) Oxidative pathways for catecholamines in the genesis of neuromelanin and cytotoxic quinones. *Mol Pharmacol* 14:633–643.
- Graham DG, Tiffany SM, Bell WR, Gutknecht WF (1978) Autoxidation versus covalent binding of quinones as the mechanism of toxicity of dopamine, 6-hydroxydopamine, and related compounds toward C1300 neuroblastoma cells in vitro. *Mol Pharmacol* 14:644–653.
- Grandjean P, Weihe P, White RF, Debes F, Araki S, Yokoyama K, Murata K, Sørensen N, Dahl R, Jørgensen PJ (1997) Cognitive deficit in 7-year-old children with prenatal exposure to methylmercury. *Neurotoxicol Teratol* 19:417–428.
- Graybiel AM (1990) The basal ganglia and the initiation of movement. *Rev Neurol (Paris)* 146:570–574.

- Greene LA, Rein G (1977a) Release, storage and uptake of catecholamines by a clonal cell line of nerve growth factor (NGF) responsive pheochromocytoma cells. *Brain Res* 129:247–263.
- Greene LA, Rein G (1977b) Synthesis, storage and release of acetylcholine by a noradrenergic pheochromocytoma cell line. *Nature* 268:349–351.
- Greene LA, Rein G (1978) Short-term regulation of catecholamine biosynthesis in a nerve growth factor responsive clonal line of rat pheochromocytoma cells. *J Neurochem* 30:549–555.
- Greene LA, Tischler AS (1976) Establishment of a noradrenergic clonal line of rat adrenal pheochromocytoma cells which respond to nerve growth factor. *Proc Natl Acad Sci U S A* 73:2424–2428.
- Grotto D, Valentini J, Serpeloni JM, Monteiro PAP, Latorraca EF, de Oliveira RS, Antunes LMG, Garcia SC, Barbosa FJ (2011) Evaluation of toxic effects of a diet containing fish contaminated with methylmercury in rats mimicking the exposure in the Amazon riverside population. *Environ Res* 111:1074–1082.
- Gu H, Wall SC, Rudnick G (1994) Stable expression of biogenic amine transporters reveals differences in inhibitor sensitivity, kinetics, and ion dependence. *J Biol Chem* 269:7124–7130.
- Guru SC, Shetty KT (1990) Methodological aspects of aldehyde dehydrogenase assay by spectrophotometric technique. *Alcohol* 7:397–401.
- Haavik J, Schelling DL, Campbell DG, Andersson KK, Flatmark T, Cohen P (1989) Identification of protein phosphatase 2A as the major tyrosine hydroxylase phosphatase in adrenal medulla and corpus striatum: evidence from the effects of okadaic acid. *FEBS Lett* 251:36–42.
- Hajela RK, Peng S, Atchison WD (2003) Comparative effects of methylmercury and Hg²⁺ on human neuronal N- and R-type high-voltage activated calcium channels transiently expressed in human embryonic kidney 293 Cells. *J Pharmacol Exp Ther* 306:1129–1136.
- Halling J, Petersen MS, Damkier P, Nielsen F, Grandjean P, Weihe P, Lundgren S, Lundblad MS, Broesen K (2005) Polymorphism of CYP2D6, CYP2C19, CYP2C9 and CYP2C8 in the Faroese population. *Eur J Clin Pharmacol* 61:491–497.
- Halling J, Petersen MS, Grandjean P, Weihe P, Broesen K (2008) Genetic predisposition to Parkinson's disease: CYP2D6 and HFE in the Faroe Islands. *Pharmacogenet Genom* 18:209–212.
- Halliwell B, Gutteridge JM (1984) Oxygen toxicity, oxygen radicals, transition metals and disease. *Biochem J* 219:1–14.

- Hamdy MK, Noyes OR (1977) Effect of mercury on NADH and the protective role of oxalacetate. *Bull Environ Contam Toxicol* 17:112–120.
- Hare MF, Atchison WD (1992) Comparative action of methylmercury and divalent inorganic mercury on nerve terminal and intraterminal mitochondrial membrane potentials. *J Pharmacol Exp Ther* 261:166–172.
- Hare MF, Atchison WD (1995a) Methylmercury mobilizes Ca⁺⁺ from intracellular stores sensitive to inositol 1,4,5-trisphosphate in NG108-15 cells. *J Pharmacol Exp Ther* 272:1016–1023.
- Hare MF, Atchison WD (1995b) Nifedipine and tetrodotoxin delay the onset of methylmercury-induced increase in [Ca²⁺]_i in NG108-15 cells. *Toxicol Appl Pharmacol* 135:299–307.
- Hare MF, McGinnis KM, Atchison WD (1993) Methylmercury increases intracellular concentrations of Ca⁺⁺ and heavy metals in NG108-15 cells. *J Pharmacol Exp Ther* 266:1626–1635.
- Harris JE, Roth RH (1971) Potassium-induced acceleration of catecholamine biosynthesis in brain slices. I. A study of the mechanism of action. *Mol Pharmacol* 7:593–604.
- Hashimoto M, Hsu LJ, Xia Y, Takeda A, Sisk A, Sundsmo M, Masliah E (1999) Oxidative stress induces amyloid-like aggregate formation of NACP/alpha-synuclein in vitro. *Neuroreport* 10:717–721.
- Haxton J, Lindsay DG, Hislop JS, Salmon L, Dixon EJ, Evans WH, Reid JR, Hewitt CJ, Jeffries DF (1979) Duplicate diet study on fishing communities in the United Kingdom: mercury exposure in a "critical group". *Environ Res* 18:351–368.
- Haycock JW (1990) Phosphorylation of tyrosine hydroxylase in situ at serine 8, 19, 31, and 40. *J Biol Chem* 265:11682–11691.
- Hempel J, Kaiser R, Jörnvall H (1985) Mitochondrial aldehyde dehydrogenase from human liver. Primary structure, differences in relation to the cytosolic enzyme, and functional correlations. *Eur J Biochem* 153:13–28.
- Hillman D, Chen S, Aung TT, Cherksey B, Sugimori M, Llinas RR (1991) Localization of P-type calcium channels in the central nervous system. *Proc Natl Acad Sci U S A* 88:7076–7080.
- Hornykiewicz O (1966) Dopamine (3-hydroxytyramine) and brain function. *Pharmacol Rev* 18:925–964.
- Hubalek FF, Pohl JJ, Edmondson DED (2003) Structural comparison of human monoamine oxidases A and B: mass spectrometry monitoring of cysteine reactivities. *J Biol Chem* 278:28612–28618.

- Hubbard MJ, McHugh NJ (1996) Mitochondrial ATP synthase F₁- β -subunit is a calcium-binding protein. *FEBS Lett* 391:323–329.
- Hughes WL (1957) A physicochemical rationale for the biological activity of mercury and its compounds. *Ann N Y Acad Sci* 65:454–460.
- Hunter D, Bomford RR, Russell DS (1940) Poisoning by methyl mercury compounds. *Q J Med* 9:193–226.
- Hunter D, Russell DS (1954) Focal cerebral and cerebellar atrophy in a human subject due to organic mercury compounds. *J Neurol Neurosurg Psych* 17:235–241.
- Inoue Y, Saijoh K, Sumino K (1988) Action of mercurials on activity of partially purified soluble protein kinase C from mice brain. *Pharmacol Toxicol* 62:278–281.
- InSug O, Datar S, Koch CJ, Shapiro IM, Shenker BJB (1997) Mercuric compounds inhibit human monocyte function by inducing apoptosis: evidence for formation of reactive oxygen species, development of mitochondrial membrane permeability transition and loss of reductive reserve. *Toxicology* 124:211–224.
- Jahng JW, Houpt TA, Wessel TC, Chen K, Shih JC, Joh TH (1997) Localization of monoamine oxidase A and B mRNA in the rat brain by in situ hybridization. *Synapse* 25:30–36.
- Janigro D, Maccaferri G, Meldolesi J (1989) Calcium channels in undifferentiated PC12 rat pheochromocytoma cells. *FEBS Letters* 255:398–400.
- Jinsmaa Y, Florang VR, Rees JN, Anderson DG, Strack S, Doorn JA (2009) Products of oxidative stress inhibit aldehyde oxidation and reduction pathways in dopamine catabolism yielding elevated levels of a reactive intermediate. *Chem Res Toxicol* 22:835–841.
- Johnson RG, Scarpa A (1979) Protonmotive force and catecholamine transport in isolated chromaffin granules. *J Biol Chem* 254:3750–3760.
- Jordan J, Cena V, Prehn JHM (2003) Mitochondrial control of neuron death and its role in neurodegenerative disorders. *J Physiol Biochem* 59:129–141.
- Kadowaki K, McGowan E, Mock G, Chandler S, Emson PC (1993) Distribution of calcium binding protein mRNAs in rat cerebellar cortex. *Neurosci Lett* 153:80–84.
- Kalisch BE, Racz WJ (1996) The effects of methylmercury on endogenous dopamine efflux from mouse striatal slices. *Toxicol Lett* 89:43–49.
- Kalyanaraman B, Felix CC, Sealy RC (1985) Semiquinone anion radicals of catechol(amine)s, catechol estrogens, and their metal ion complexes. *Environ Health Perspect* 64:185–198.
- Kang DD, Miyako KK, Kuribayashi FF, Hasegawa EE, Mitsumoto AA, Nagano TT, Takeshige

- KK (1997) Changes of energy metabolism induced by 1-methyl-4-phenylpyridinium (MPP⁺)-related compounds in rat pheochromocytoma PC12 cells. *Arch Biochem Biophys* 337:6–6.
- Kass GE, Orrenius S (1999) Calcium signaling and cytotoxicity. *Environ Health Perspect* 107 Suppl 1:25–35.
- Katz B, Miledi R (1967) The timing of calcium action during neuromuscular transmission. *J Physiol (Lond.)* 189:535–544.
- Kauppinen RA, Komulainen H, Taipale H (1989) Cellular mechanisms underlying the increase in cytosolic free calcium concentration induced by methylmercury in cerebrocortical synaptosomes from guinea pig. *J Pharmacol Exp Ther* 248:1248–1254.
- Kaur P, Aschner M, Syversen T (2006) Glutathione modulation influences methyl mercury induced neurotoxicity in primary cell cultures of neurons and astrocytes. *NeuroToxicology* 27:492–500.
- Kawamura M, Eisenhofer G, Kopin IJ, Kador PF, Lee YS, Fujisawa S, Sato S (2002) Aldose reductase: an aldehyde scavenging enzyme in the intraneuronal metabolism of norepinephrine in human sympathetic ganglia. *Auton Neurosci* 96:131–139.
- Keung WM, Vallee BL (1993) Daidzin: a potent, selective inhibitor of human mitochondrial aldehyde dehydrogenase. *Proc Natl Acad Sci U S A* 90:1247–1251.
- Keung WM, Vallee BL (1998) Daidzin and its antidipsotropic analogs inhibit serotonin and dopamine metabolism in isolated mitochondria. *Proc Natl Acad Sci U S A* 95:2198–2203.
- Kilty JEJ, Lorang DD, Amara SGS (1991) Cloning and expression of a cocaine-sensitive rat dopamine transporter. *Science* 254:578–579.
- Kishimoto T, Liu TT, Hatakeyama H, Nemoto T, Takahashi N, Kasai H (2005) Sequential compound exocytosis of large dense-core vesicles in PC12 cells studied with TEPIQ (two-photon extracellular polar-tracer imaging-based quantification) analysis. *J Physiol (Lond.)* 568:905–915.
- Kitada T, Asakawa S, Hattori N, Matsumine H, Yamamura Y, Minoshima S, Yokochi M, Mizuno Y, Shimizu N (1998) Mutations in the parkin gene cause autosomal recessive juvenile parkinsonism. *Nature* 392:605–608.
- Kittner B, Bräutigam M, Herken H (1987) PC12 cells: a model system for studying drug effects on dopamine synthesis and release. *Arch Int Pharmacodyn Ther* 286:181–194.
- Klein C, Westenberger A (2012) Genetics of Parkinson's Disease. *Cold Spring Harbor Perspectives in Medicine*. 2:1-15.

- Knight DE, Grafenstein Von H, Athayde CM (1989) Calcium-dependent and calcium-independent exocytosis. *Trends Neurosci* 12:451–458.
- Komulainen H, Bondy SC (1987) Increased free intrasynaptosomal Ca^{2+} by neurotoxic organometals: distinctive mechanisms. *Toxicol Appl Pharmacol* 88:77–86.
- Komulainen H, Tuomisto J (1985) ^3H -dopamine uptake and ^3H -haloperidol binding in striatum after administration of methyl mercury to rats. *Arch Toxicol* 57:268–271.
- Komulainen HH, Tuomisto JJ (1982) Effects of heavy metals on monoamine uptake and release in brain synaptosomes and blood platelets. *Neurobehav Toxicol Teratol* 4:647–649.
- Kongsamut S, Miller RJ (1986) Nerve growth factor modulates the drug sensitivity of neurotransmitter release from PC-12 cells. *Proc Natl Acad Sci U S A* 83:2243–2247.
- Kopin IJ (1964) Storage and metabolism of catecholamines: the role of monoamine oxidase. *Pharmacol Rev* 16:179–191.
- Kopin IJ (1968) Biosynthesis and metabolism of catecholamines. *Anesthesiology* 29:654–660.
- Koschak A, Reimer D, Huber I, Grabner M, Glossmann H, Engel J, Striessnig J (2001) $\alpha 1\text{D}$ (Cav1.3) subunits can form l-type Ca^{2+} channels activating at negative voltages. *J Biol Chem* 276:22100–22106.
- Kristal BS, Conway AD, Brown AM, Jain JC, Ulluci PA, Li SW, Burke WJ (2001) Selective dopaminergic vulnerability: 3,4-dihydroxyphenylacetaldehyde targets mitochondria. *Free Rad Biol Med* 30:924–931.
- Kumagai T, Kawamoto Y, Nakamura Y, Hatayama I, Satoh K, Osawa T, Uchida K (2000) 4-hydroxy-2-nonenal, the end product of lipid peroxidation, is a specific inducer of cyclooxygenase-2 gene expression. *Biochem Biophys Res Comm* 273:437–441.
- Kumer SC, Vrana KE (1996) Intricate regulation of tyrosine hydroxylase activity and gene expression. *J Neurochem* 67:443–462.
- Kung MP, Kostyniak PJ, Olson JR, Sansone FM, Nickerson PA, Malone MA, Ziembiec N, Roth JA (1989) Cell specific enzyme markers as indicators of neurotoxicity: effects of acute exposure to methylmercury. *NeuroToxicology* 10:41–52.
- Kunimoto M (1994) Methylmercury induces apoptosis of rat cerebellar neurons in primary culture. *Biochem Biophys Res Comm* 204:310–317.
- Lacinová LL (2005) Voltage-dependent calcium channels. *Gen Physiol Biophys* 24 Suppl 1:1–78.

- Lamensdorf I, Eisenhofer G, Harvey-White J, Hayakawa Y, Kirk K, Kopin IJ (2000a) Metabolic stress in PC12 cells induces the formation of the endogenous dopaminergic neurotoxin, 3,4-dihydroxyphenylacetaldehyde. *J Neurosci Res* 60:552–558.
- Lamensdorf I, Eisenhofer G, Harvey-White J, Nechustan A, Kirk K, Kopin IJ (2000b) 3,4-Dihydroxyphenylacetaldehyde potentiates the toxic effects of metabolic stress in PC12 cells. *Brain Res* 868:191–201.
- Landrigan PJ, Sonawane B, Butler RN, Trasande L, Callan R, Droller D (2005) Early environmental origins of neurodegenerative disease in later life. *Environ Health Perspect* 113:1230–1233.
- Langston JW, Forno LS, Tetrud J, Reeves AG, Kaplan JA, Karluk D (1999) Evidence of active nerve cell degeneration in the substantia nigra of humans years after 1-methyl-4-phenyl-1,2,3,6-tetrahydropyridine exposure. *Ann Neurol* 46:598–605.
- LaVoie MJ, Hastings TG (1999) Dopamine quinone formation and protein modification associated with the striatal neurotoxicity of methamphetamine: evidence against a role for extracellular dopamine. *J Neurosci* 19:1484–1491.
- LaVoie MJ, Hastings TG (2002) Peroxynitrite- and nitrite-induced oxidation of dopamine: implications for nitric oxide in dopaminergic cell loss. *J Neurochem* 73:2546–2554.
- Le Moal M, Simon H (1991) Mesocorticolimbic dopaminergic network: functional and regulatory roles. *Physiol Rev* 71:155–234.
- LeBel CP, Ali SF, McKee M, Bondy SC (1990) Organometal-induced increases in oxygen reactive species: the potential of 2',7'-dichlorofluorescein diacetate as an index of neurotoxic damage. *Toxicol Appl Pharmacol* 104:17–24.
- Lehmann IT, Bobrovskaya L, Gordon SL, Dunkley PR, Dickson PW (2006) Differential regulation of the human tyrosine hydroxylase isoforms via hierarchical phosphorylation. *J Biol Chem* 281:17644–17651.
- Leonarduzzi G, Robbesyn F, Poli G (2004) Signaling kinases modulated by 4-hydroxynonenal. *Free Rad Biol Med* 37:1694–1702.
- Leslie SW, Woodward JJ, Wilcox RE (1985) Correlation of rates of calcium entry and endogenous dopamine release in mouse striatal synaptosomes. *Brain Res* 325:99–105.
- Levesque P, Atchison WD (1987) Interactions of mitochondrial inhibitors with methylmercury on spontaneous quantal release of acetylcholine. *Toxicol Appl Pharmacol* 87:315–324.
- Levesque P, Atchison WD (1988) Effect of alteration of nerve terminal Ca^{2+} regulation on increased spontaneous quantal release of acetylcholine by methyl mercury. *Toxicol Appl Pharmacol* 94:55–65.

- Levesque P, Atchison WD (1991) Disruption of brain mitochondrial calcium sequestration by methylmercury. *J Pharmacol Exp Ther* 256:236–242.
- Levesque P, Hare MF, Atchison WD (1992) Inhibition of mitochondrial Ca^{2+} release diminishes the effectiveness of methyl mercury to release acetylcholine from synaptosomes. *Toxicol Appl Pharmacol* 115:11–20.
- Leviel V (2011) Dopamine release mediated by the dopamine transporter, facts and consequences. *J Neurochem* 118:475–489.
- Levitt M, Spector S, Sjoerdsma A, Udenfriend S (1965) Elucidation of the rate-limiting step in norepinephrine biosynthesis in the perfused guinea-pig heart. *J Pharmacol Exp Ther* 148:1–8.
- Lévay G, Bodell WJ (1993) Detection of dopamine--DNA adducts: potential role in Parkinson's disease. *Carcinogenesis* 14:1241–1245.
- Li SW, Lin TS, Minteer S, Burke WJ (2001) 3,4-Dihydroxyphenylacetaldehyde and hydrogen peroxide generate a hydroxyl radical: possible role in Parkinson's disease pathogenesis. *Brain Res Mol Brain Res* 93:1–7.
- Limke TL, Atchison WD (2002) Acute exposure to methylmercury opens the mitochondrial permeability transition pore in rat cerebellar granule cells. *Toxicol Appl Pharmacol* 178:52–61.
- Limke TL, Atchison WD (2009) Application of single-cell microfluorimetry to mechanistic toxicology. *Curr Protoc Toxicol*. Chapter Unit 12-15.
- Limke TL, Heidemann SR, Atchison WD (2004) Disruption of intraneuronal divalent cation regulation by methylmercury: are specific targets involved in altered neuronal development and cytotoxicity in methylmercury poisoning? *NeuroToxicology* 25:741–760.
- Limke TL, Otero-Montanez JKL, Atchison WD (2003) Evidence for interactions between intracellular calcium stores during methylmercury-induced intracellular calcium dysregulation in rat cerebellar granule neurons. *J Pharmacol Exp Ther* 304:949–958.
- Liu TT, Kishimoto T, Hatakeyama H, Nemoto T, Takahashi N, Kasai H (2005) Exocytosis and endocytosis of small vesicles in PC12 cells studied with TEPIQ (two-photon extracellular polar-tracer imaging-based quantification) analysis. *J Physiol* 568:917–929.
- Liu W, Xu Z, Deng Y, Xu B, Yang H, Wei Y, Feng S (2012) Excitotoxicity and oxidative damages induced by methylmercury in rat cerebral cortex and the protective effects of tea polyphenols. *Environ Toxicol*.
- Llinas R, Steinberg IZ, Walton K (1981) Relationship between presynaptic calcium current

- and postsynaptic potential in squid giant synapse. *Biophysical Journal* 33:323–351.
- Llinas R, Sugimori M, Silver RB (1992) Microdomains of high calcium concentration in a presynaptic terminal. *Science* 256:677–679.
- Lookingland KJ, Moore KE (2005) Chapter VIII Functional neuroanatomy of hypothalamic dopaminergic neuroendocrine systems. *Handbook of Chemical Neuroanatomy* 21:435–523.
- Lorang D, Amara SG, Simerly RBR (1994) Cell-type-specific expression of catecholamine transporters in the rat brain. *J Neurosci* 14:4903–4914.
- Lu T, Trussell LO (2000) Inhibitory transmission mediated by asynchronous transmitter release. *Neuron* 26:683–694.
- Mahata M, Zhang K, Gayen JR, Nandi S, Brar BK, Ghosh S, Mahapatra NR, Taupenot L, O'Connor DT, Mahata SK (2011) Catecholamine biosynthesis and secretion: physiological and pharmacological effects of secretin. *Cell Tissue Res* 345:87–102.
- Mains RE, Patterson PH (1973) Primary cultures of dissociated sympathetic neurons. I. Establishment of long-term growth in culture and studies of differentiated properties. *J Cell Biol* 59:329–345.
- Malagelada C, Greene LA (2011) PC12 cells as a model for parkinson's disease research. In: *Parkinson's Disease: Molecular and therapeutic insights from model systems* (Nass R, Przedborski S, eds), pp 375–387. Academic Press, Amsterdam.
- Mandel S, Grunblatt E, Riederer P, Amariglio N, Jacob-Hirsch J, Rechavi G, Youdim MBH (2005) Gene expression profiling of sporadic Parkinson's disease substantia nigra pars compacta reveals impairment of ubiquitin-proteasome subunits, SKP1A, aldehyde dehydrogenase, and chaperone HSC-70. *Ann N Y Acad Sci* 1053:356–375.
- Marchitti SA, Brocker C, Stagos D, Vasiliou V (2008) Non-P450 aldehyde oxidizing enzymes: the aldehyde dehydrogenase superfamily. *Expert Opin Drug Metab Toxicol* 4:697–720.
- Marchitti SA, Deitrich RA, Vasiliou V (2007) Neurotoxicity and metabolism of the catecholamine-derived 3,4-dihydroxyphenylacetaldehyde and 3,4-dihydroxyphenylglycolaldehyde: the role of aldehyde dehydrogenase. *Pharmacol Rev* 59:125–150.
- Maring JA, Deitrich RA, Little R (1985) Partial purification and properties of human brain aldehyde dehydrogenases. *J Neurochem* 45:1903–1910.
- Mariussen E, Fonnum F (2001) The effect of polychlorinated biphenyls on the high affinity uptake of the neurotransmitters, dopamine, serotonin, glutamate and GABA, into rat brain synaptosomes. *Toxicology* 159:11–21.

- Marroquin LD, Hynes J, Dykens JA, Jamieson JD, Will Y (2007) Circumventing the crabtree effect: replacing media glucose with galactose increases susceptibility of HepG2 cells to mitochondrial toxicants. *Toxicol Sci* 97:539–547.
- Martinez-Finley EJ, Chakraborty S, Slaughter JC, Aschner M (2013) Early-life exposure to methylmercury in wildtype and pdr-1/parkin knockout *C. elegans*. *Neurochem Res* 38:1543-1552.
- Marty MS, Atchison WD (1997) Pathways mediating Ca^{2+} entry in rat cerebellar granule cells following in vitro exposure to methylmercury. *Toxicol Appl Pharmacol* 147:319–330.
- Marty MS, Atchison WD (1998) Elevations of intracellular Ca^{2+} as a probable contributor to decreased viability in cerebellar granule cells following acute exposure to methylmercury. *Toxicol Appl Pharmacol* 150:8–8.
- Mattammal MB, Haring JH, Chung HD, Raghu G, Strong R (1995) An endogenous dopaminergic neurotoxin: implication for Parkinson's disease. *Neurodegeneration* 4:271–281.
- McKay SJ, Reynolds JN, Racz WJ (1986) Effects of mercury compounds on the spontaneous and potassium-evoked release of [^3H]dopamine from mouse striatal slices. *Can J Physiol Pharmacol* 64:1507–1514.
- McKeown-Eyssen GE, Ruedy J (1983) Methyl mercury exposure in northern Quebec. I. Neurologic findings in adults. *Am J Epidemiol* 118:461–469.
- McPherson PS, Campbell KP (1993) Characterization of the major brain form of the ryanodine receptor/ Ca^{2+} release channel. *J Biol Chem* 268:19785–19790.
- Meiser J, Weindl D, Hiller K (2013) Complexity of dopamine metabolism. *Cell Commun Signal* 11:34.
- Meldolesi J, Villa A, Podini P, Clementi E, Zacchetti D, D'Andrea P, Lorenzon P, Grohovaz F (1992) Intracellular Ca^{2+} stores in neurons. Identification and functional aspects. *J Physiol (Paris)* 86:23–30.
- Michaelis ML, Kitos TE, Nunley EW, Lecluyse E, Michaelis EK (1987) Characteristics of Mg^{2+} -dependent, ATP-activated Ca^{2+} transport in synaptic and microsomal membranes and in permeabilized synaptosomes. *J Biol Chem* 262:4182–4189.
- Milman N, a Steig T, Koefoed P, Pedersen P, Fenger K, Nielsen FC (2005) Frequency of the hemochromatosis HFE mutations C282Y, H63D, and S65C in blood donors in the Faroe Islands. *Ann Hematol* 84:146–149.

- Minard KI (2005) Sources of NADPH in yeast vary with carbon source. *J Biol Chem* 280:39890–39896.
- Minnema DJ, Cooper GP, Greenland RD (1989) Effects of methylmercury on neurotransmitter release from rat brain synaptosomes. *Toxicol Appl Pharmacol* 99:510–521.
- Missale C, Nash SR, Robinson SW, Jaber M, Caron MG (1998) Dopamine receptors: from structure to function. *Physiol Rev* 78:189–225.
- Mitsumoto A, Nakagawa Y (2001) DJ-1 is an indicator for endogenous reactive oxygen species elicited by endotoxin. *Free Radic Res* 35:885–893.
- Mitsumoto A, Nakagawa Y, Takeuchi A, Okawa K, Iwamatsu A, Takanezawa Y (2001) Oxidized forms of peroxiredoxins and DJ-1 on two-dimensional gels increased in response to sublethal levels of paraquat. *Free Radic Res* 35:301–310.
- Mizuno Y, Hattori N, Mori H, Suzuki T, Tanaka K (2001) Parkin and Parkinson's disease. *Curr Opin Neurol* 14:477–482.
- Mochida S, Yokoyama CT, Kim DK, Itoh K, Catterall WA (1998) Evidence for a voltage-dependent enhancement of neurotransmitter release mediated via the synaptic protein interaction site of N-type Ca²⁺ channels. *Proc Natl Acad Sci U S A* 95:14523–14528.
- Monnet-Tschudi F, Zurich M, Boschat C, Corbaz A, Honegger P (2006) Involvement of environmental mercury and lead in the etiology of neurodegenerative diseases. *Rev Environ Health* 21:105–117.
- Monsma FJ, Mahan LC, McVittie LD, Gerfen CR, Sibley DR (1990) Molecular cloning and expression of a D1 dopamine receptor linked to adenylyl cyclase activation. *Proc Natl Acad Sci U S A* 87:6723–6727.
- Morel FMM, Kraepiel AML, Amyot M (1998) The chemical cycle and bioaccumulation of mercury. *Ann Rev Ecol Sys*:543–566.
- Mori N, Yasutake A, Hirayama K (2007) Comparative study of activities in reactive oxygen species production/defense system in mitochondria of rat brain and liver, and their susceptibility to methylmercury toxicity. *Arch Toxicol* 81:769–776.
- Mori N, Yasutake A, Marumoto M, Hirayama K (2011) Methylmercury inhibits electron transport chain activity and induces cytochrome c release in cerebellum mitochondria. *Toxicol Sci* 36:253–259.
- Mundy WR, Freudenrich TM (2000) Sensitivity of immature neurons in culture to metal-induced changes in reactive oxygen species and intracellular free calcium. *NeuroToxicology* 21:1135–1144.

- Møller-Madsen B (1994) Localization of mercury in CNS of the rat. An autometallographic study. *Pharmacol Toxicol* 75 Suppl 1:1–41.
- Nadkarni DV, Sayre LM (1995) Structural definition of early lysine and histidine adduction chemistry of 4-hydroxynonenal. *Chem Res Toxicol* 8:284–291.
- Nagatsu T (2004) Progress in monoamine oxidase (MAO) research in relation to genetic engineering. *NeuroToxicology* 25:11–20.
- Nair V, Cooper CS, Vietti DE, Turner GA (1986) The chemistry of lipid peroxidation metabolites: crosslinking reactions of malondialdehyde. *Lipids* 21:6–10.
- Naoi M, Suzuki H, Takahashi T, Shibahara K, Nagatsu T (1987) Ganglioside GM1 causes expression of type B monoamine oxidase in a rat clonal pheochromocytoma cell line, PC12h. *J Neurochem* 49:1602–1605.
- Neal AP, Yuan Y, Atchison WD (2010) Allethrin differentially modulates voltage-gated calcium channel subtypes in rat PC12 cells. *Toxicol Sci* 116:604–613.
- Nedergaard S, Flatman JA, Engberg I (1993) Nifedipine- and ω -conotoxin-sensitive Ca^{2+} conductances in guinea-pig substantia nigra pars compacta neurones. *J Physiol (Lond.)* 466:727–747.
- Ngim CH, Devathasan G (1989) Epidemiologic study on the association between body burden mercury level and idiopathic Parkinson's disease. *Neuroepidemiology* 8:128–141.
- Nicholls D, Akerman K (1982) Mitochondrial calcium transport. *Biochim Biophys Acta* 683:57–88.
- Nicholls DG, Johnson-Cadwell L, Vesce S, Jekabsons M, Yadava N (2007) Bioenergetics of mitochondria in cultured neurons and their role in glutamate excitotoxicity. *J Neurosci Res* 85:3206–3212.
- Nicholls DG, Scott ID (1980) The regulation of brain mitochondrial calcium-ion transport. The role of ATP in the discrimination between kinetic and membrane-potential-dependent calcium-ion efflux mechanisms. *Biochem J* 186:833–839.
- Nierenberg DW, Nordgren RE, Chang MB, Siegler RW, Blayney MB, Hochberg F, Toribara TY, Cernichiari E, Clarkson T (1998) Delayed cerebellar disease and death after accidental exposure to dimethylmercury. *N Engl J Med* 338:1672–1676.
- Nilsson GE, Tottmar O (1987) Biogenic aldehydes in brain: on their preparation and reactions with rat brain tissue. *J Neurochem* 48:1566–1572.
- Nowycky MC, Roth RH (1978) Dopaminergic neurons: role of presynaptic receptors in the regulation of transmitter biosynthesis. *Prog Neuro-Psychopharmacol* 2:139–158.

- O'Carroll AM, Fowler CJ, Phillips JP, Tobbia I, Tipton KF (1983) The deamination of dopamine by human brain monoamine oxidase. Specificity for the two enzyme forms in seven brain regions. *Naunyn Schmiedebergs Arch Pharmacol* 322:198–202.
- Olivera BM, Miljanich GP, Ramachandran J, Adams ME (1994) Calcium channel diversity and neurotransmitter release: the ω -conotoxins and ω -agatoxins. *Annu Rev Biochem* 63:823–867.
- Omata S, Hirakawa E, Daimon Y, Uchiyama M, Nakashita H, Horigome T, Sugano I, Sugano H (1982) Methylmercury-induced changes in the activities of neurotransmitter enzymes in nervous tissues of the rat. *Arch Toxicol* 51:285–294.
- Onali P, Olanas MC, Gessa GL (1985) Characterization of dopamine receptors mediating inhibition of adenylate cyclase activity in rat striatum. *Mol Pharmacol* 28:138–145.
- Ostrerova N, Petrucelli L, Farrer M, Mehta N, Choi P, Hardy J, Wolozin B (1999) α -Synuclein shares physical and functional homology with 14-3-3 proteins. *J Neurosci* 19:5782–5791.
- Oxender DL, Christensen HN (1963) Distinct mediating systems for the transport of neutral amino acids by the Ehrlich cell. *J Biol Chem* 238:3686–3699.
- Pan S, Ryu S-Y, Sheu S-S (2011) Distinctive characteristics and functions of multiple mitochondrial Ca^{2+} influx mechanisms. *Sci China Life Sci* 54:763–769.
- Pappas SS, Kennedy T, Goudreau JL, Lookingland KJ (2011) Opioid-mediated regulation of A11 diencephalospinal dopamine neurons: Pharmacological evidence of activation by morphine. *Neuropharmacology* 61:614–621.
- Parnas H, Segel L, Dudel J, Parnas I (2000) Autoreceptors, membrane potential and the regulation of transmitter release. *Trends Neurosci* 23:9–9.
- Parran DK, Mundy WR, Barone S (2001) Effects of methylmercury and mercuric chloride on differentiation and cell viability in PC12 cells. *Toxicol Sci* 59:278–290.
- Patrick RL, Barchas JD (1976) Dopamine synthesis in rat brain striatal synaptosomes. II. Dibutyryl cyclic adenosine 3':5'-monophosphoric acid and 6-methyltetrahydropterine-induced synthesis increases without an increase in endogenous dopamine release. *J Pharmacol Exp Ther* 197:97–104.
- Pearl SM, Antion MD, Stanwood GD, Jaumotte JD, Kapatos G, Zigmond MJ (2000) Effects of NADH on dopamine release in rat striatum. *Synapse* 36:95–101.
- Peng XM (2005) α -Synuclein activation of protein phosphatase 2A reduces tyrosine hydroxylase phosphorylation in dopaminergic cells. *J Cell Sci* 118:3523–3530.
- Petersen MS, Halling J, Bech S, Wermuth L, Weihe P, Nielsen F, Jørgensen PJ, Budtz-

- Jørgensen E, Grandjean P (2008a) Impact of dietary exposure to food contaminants on the risk of Parkinson's disease. *NeuroToxicology* 29:584–590.
- Petersen MS, Weihe P, Choi A, Grandjean P (2008b) Increased prenatal exposure to methylmercury does not affect the risk of Parkinson's disease. *NeuroToxicology* 29:591–595.
- Petrash JM (2004) All in the family: aldose reductase and closely related aldo-keto reductases. *Cell Molec Life Sci* 61:737–749.
- Piao YS, Wakabayashi K, Hayashi S, Yoshimoto M, Takahashi H (2000) Aggregation of alpha-synuclein/NACP in the neuronal and glial cells in diffuse Lewy body disease: a survey of six patients. *Clin Neuropathol* 19:163–169.
- Pizzo P, Drago I, Filadi R, Pozzan T (2012) Mitochondrial Ca²⁺ homeostasis: mechanism, role, and tissue specificities. *Pflugers Arch - Eur J Physiol* 464:3–17.
- Plummer MR, Logothetis DE, Hess P (1989) Elementary properties and pharmacological sensitivities of calcium channels in mammalian peripheral neurons. *Neuron* 2:1453–1463.
- Polymeropoulos MH et al. (1997) Mutation in the alpha-synuclein gene identified in families with Parkinson's disease. *Science* 276:2045–2047.
- Poncer JC, McKinney RA, Gahwiler BH, Thompson SM (1997) Either N- or P-type calcium channels mediate GABA release at distinct hippocampal inhibitory synapses. *Neuron* 18:463–472.
- Pozzan T, Rizzuto R, Volpe P, Meldolesi J (1994) Molecular and cellular physiology of intracellular calcium stores. *Physiol Rev* 74:595–636.
- Rajanna B, Hobson M (1985) Influence of mercury on uptake of [³H]dopamine and [³H]norepinephrine by rat brain synaptosomes. *Toxicol Lett* 27:7–14.
- Ramsey AJ, Fitzpatrick PF (1998) Effects of phosphorylation of serine 40 of tyrosine hydroxylase on binding of catecholamines: evidence for a novel regulatory mechanism. *Biochemistry* 37:8980–8986.
- Randall A, Tsien RW (1995) Pharmacological dissection of multiple types of Ca²⁺ channel currents in rat cerebellar granule neurons. *J Neurosci* 15:2995–3012.
- Ravagnan L, Roumier T, Kroemer G (2002) Mitochondria, the killer organelles and their weapons. *J Cell Physiol* 192:131–137.
- Reber B, Porzig H, Becker C, Reuter H (1990) Depolarization-induced changes of free intracellular Ca²⁺ concentration and of [³H] dopamine release in undifferentiated and

- differentiated PC12 cells. *Neurochem Int* 17:197–203.
- Rees JN, Florang VR, Eckert LL, Doorn JA (2009) Protein reactivity of 3,4-dihydroxyphenylacetaldehyde, a toxic dopamine metabolite, is dependent on both the aldehyde and the catechol. *Chem Res Toxicol* 22:1256–1263.
- Ribeiro P, Wang Y, Citron BA, Kaufman S (1992) Regulation of recombinant rat tyrosine hydroxylase by dopamine. *Proc Natl Acad Sci U S A* 89:9593–9597.
- Richter C, Kass GE (1991) Oxidative stress in mitochondria: its relationship to cellular Ca^{2+} homeostasis, cell death, proliferation, and differentiation. *Chemico-Biological Interactions* 77:1–23.
- Riederer P, Jellinger K (1982) Morphological and biochemical changes in the aging brain: pathophysiological and possible therapeutic consequences. *Exp Brain Res Suppl* 5:158–166.
- Ritchie AK (1979) Catecholamine secretion in a rat pheochromocytoma cell line: two pathways for calcium entry. *J Physiol (Lond.)* 286:541–561.
- Robador PA, Seyedi N, Chan NYK, Koda K, Levi R (2012) Aldehyde dehydrogenase type 2 activation by adenosine and histamine inhibits ischemic norepinephrine release in cardiac sympathetic neurons: mediation by protein kinase C. *J Pharmacol Exp Ther* 343:97–105.
- Rodríguez-Enríquez S, Juárez O, Rodríguez-Zavala JS, Moreno-Sánchez R (2001) Multisite control of the Crabtree effect in ascites hepatoma cells. *Eur J Biochem* 268:2512–2519.
- Roos D, Seeger R, Puntel R, Vargas Barbosa N (2012) Role of calcium and mitochondria in MeHg-mediated cytotoxicity. *J Biomed Biotech* 2012:1–15.
- Rossignol R (2004) Energy substrate modulates mitochondrial structure and oxidative capacity in cancer cells. *Cancer Res* 64:985–993.
- Royo M, Fitzpatrick PF, Daubner SC (2005) Mutation of regulatory serines of rat tyrosine hydroxylase to glutamate: effects on enzyme stability and activity. *Arch Biochem Biophys* 434:266–274.
- Rubin RP (1970) The role of calcium in the release of neurotransmitter substances and hormones. *Pharmacol Rev* 22:389–428.
- Rudnick G (1998) Bioenergetics of neurotransmitter transport. *J Bioenerg Biomembr* 30:173–185.
- Rutter GA, Denton RM (1988) Regulation of NAD^{+} -linked isocitrate dehydrogenase and 2-oxoglutarate dehydrogenase by Ca^{2+} ions within toluene-permeabilized rat heart

- mitochondria. Interactions with regulation by adenine nucleotides and NADH/NAD⁺ ratios. *Biochem J* 252:181–189.
- Sabatini BL, Regehr WG (1996) Timing of neurotransmission at fast synapses in the mammalian brain. *Nature* 384:170–172.
- Saito Y, Tsuzuki K, Yamada N, Okado H, Miwa A, Goto F, Ozawa S (2003) Transfer of NMDAR2 cDNAs increases endogenous NMDAR1 protein and induces expression of functional NMDA receptors in PC12 cells. *Brain Res Mol Brain Res* 110:159–168.
- Sakamoto M, Ikegami N, Nakano A (1996) Protective effects of Ca²⁺ channel blockers against methyl mercury toxicity. *Pharmacol Toxicol* 78:193–199.
- Salinas M, Diaz R, Abraham NG, Ruiz de Galarreta CM, Cuadrado A (2003) Nerve growth factor protects against 6-hydroxydopamine-induced oxidative stress by increasing expression of heme oxygenase-1 in a phosphatidylinositol 3-kinase-dependent manner. *J Biol Chem* 278:13898–13904.
- Sanchez-Armass S, Blaustein MP (1987) Role of sodium-calcium exchange in regulation of intracellular calcium in nerve terminals. *Am J Physiol* 252:C595–C603.
- Sanfeliu C, Sebastià J, Cristòfol R, Rodríguez-Farré E (2003) Neurotoxicity of organomercurial compounds. *Neurotox Res* 5:283–305.
- Sarafian TA (1993) Methyl mercury increases intracellular Ca²⁺ and inositol phosphate levels in cultured cerebellar granule neurons. *J Neurochem* 61:648–657.
- Sarafian TA, Vartavarian L, Kane DJ, Bredesen DE, Verity MA (1994) bcl-2 expression decreases methyl mercury-induced free-radical generation and cell killing in a neural cell line. *Toxicol Lett* 74:149–155.
- Schmitz Y, Benoit-Marand M, Gonon F, Sulzer D (2003) Presynaptic regulation of dopaminergic neurotransmission. *J Neurochem* 87:273–289.
- Schnaitman C, Erwin VG, Greenawalt JW (1967) The submitochondrial localization of monoamine oxidase. An enzymatic marker for the outer membrane of rat liver mitochondria. *J Cell Biol* 32:719–735.
- Schuldiner S, Liu Y, Edwards RH (1993) Reserpine binding to a vesicular amine transporter expressed in Chinese hamster ovary fibroblasts. *J Biol Chem* 268:29–34.
- Schuler F, Casida JE (2001) Functional coupling of PSST and ND1 subunits in NADH:ubiquinone oxidoreductase established by photoaffinity labeling. *BBA - Bioenergetics* 1506:79–87.
- Shafer TJ (1998) Effects of Cd²⁺, Pb²⁺ and CH₃Hg⁺ on high voltage-activated calcium

- currents in pheochromocytoma (PC12) cells: potency, reversibility, interactions with extracellular Ca²⁺ and mechanisms of block. *Toxicol Lett* 99:207–221.
- Shafer TJ, Atchison WD (1991a) Transmitter, ion channel and receptor properties of pheochromocytoma (PC12) cells: a model for neurotoxicological studies. *NeuroToxicology* 12:473–492.
- Shafer TJ, Atchison WD (1991b) Methylmercury blocks N- and L-type Ca⁺⁺ channels in nerve growth factor-differentiated pheochromocytoma (PC12) cells. *J Pharmacol Exp Ther* 258:149–157.
- Shafer TJ, Contreras ML, Atchison WD (1990) Characterization of interactions of methylmercury with Ca²⁺ channels in synaptosomes and pheochromocytoma cells: radiotracer flux and binding studies. *Mol Pharmacol* 38:102–113.
- Sharma RP, Aldous CN, Farr CH (1982) Methylmercury induced alterations in brain amine syntheses in rats. *Toxicol Lett* 13:195–201.
- Sheng ZH, Westenbroek RE, Catterall WA (1998) Physical link and functional coupling of presynaptic calcium channels and the synaptic vesicle docking/fusion machinery. *J Bioenerg Biomembr* 30:335–345.
- Sherman MY, Goldberg AL (2001) Cellular defenses against unfolded proteins: a cell biologist thinks about neurodegenerative diseases. *Neuron* 29:15–32.
- Shih JC, Chen K, Ridd MJ (1999) Monoamine oxidase: from genes to behavior. *Annu Rev Neurosci* 22:197–217.
- Shimada S, Kitayama S, Lin CL, Patel A, Nanthakumar E, Gregor P, Kuhar M, Uhl G (1991) Cloning and expression of a cocaine-sensitive dopamine transporter complementary DNA. *Science* 254:576–578.
- Shimoke K, Chiba H (2001) Nerve growth factor prevents 1-methyl-4-phenyl-1,2,3,6-tetrahydropyridine-induced cell death via the Akt pathway by suppressing caspase-3-like activity using PC12 cells: relevance to therapeutical application for Parkinson's disease. *J Neurosci Res* 63:402–409.
- Shimura H, Hattori N, Kubo SI, Mizuno Y, Asakawa S, Minoshima S, Shimizu N, Iwai K, Chiba T, Tanaka K, Suzuki T (2000) Familial Parkinson disease gene product, parkin, is a ubiquitin-protein ligase. *Nat Genet* 25:302–305.
- Singh R, Lemire J, Mailloux RJ, Appanna VD (2008) A Novel Strategy Involved Anti-Oxidative Defense: The conversion of NADH into NADPH by a metabolic network. *PLoS ONE* 3:e2682.
- Sinnesger-Brauns MJ, Huber IG, Koschak A, Wild C, Obermair GJ, Einzinger U, Hoda JC, Sartori SB, Striessnig J (2009) Expression and 1,4-Dihydropyridine-Binding Properties

- of Brain L-Type Calcium Channel Isoforms. *Mol Pharmacol* 75:407–414.
- Sirois JE, Atchison WD (1996) Effects of mercurials on ligand- and voltage-gated ion channels: a review. *NeuroToxicology* 17:63–84.
- Sirois JE, Atchison WD (2000) Methylmercury affects multiple subtypes of calcium channels in rat cerebellar granule cells. *Toxicol Appl Pharmacol* 167:1–11.
- Somlyo AP, Bond M, Somlyo AV (1985) Calcium content of mitochondria and endoplasmic reticulum in liver frozen rapidly in vivo. *Nature* 314:622–625.
- Sone N, Larsstuvold MK, Kagawa Y (1977) Effect of methyl mercury on phosphorylation, transport, and oxidation in mammalian mitochondria. *J Biol Chem* 82:859–868.
- Spanagel R, Weiss F (1999) The dopamine hypothesis of reward: past and current status. *Trends Neurosci* 22:521–527.
- Spector S, Sjoerdsma A, Udenfriend S (1965) Blockade of endogenous norepinephrine synthesis by alpha-methyl-tyrosine, an inhibitor of tyrosine hydroxylase. *J Pharmacol Exp Ther* 147:86–95.
- Spillantini MG, Crowther RA, Jakes R, Hasegawa M, Goedert M (1998) α -Synuclein in filamentous inclusions of Lewy bodies from Parkinson's disease and dementia with lewy bodies. *Proc Natl Acad Sci U S A* 95:6469–6473.
- Stockum von S, Basso E, Petronilli V, Sabatelli P, Forte MA, Bernardi P (2011) Properties of Ca^{2+} transport in mitochondria of *Drosophila melanogaster*. *J Biol Chem* 286:41163–41170.
- Stokes AH, Hastings TG, Vrana KE (1999) Cytotoxic and genotoxic potential of dopamine. *J Neurosci Res* 55:659–665.
- Streit J, Lux HD (1987) Voltage dependent calcium currents in PC12 growth cones and cells during NGF-induced cell growth. *Pflugers Arch - Eur J Physiol* 408:634–641.
- Sudhof TC (2012) Calcium Control of Neurotransmitter Release. *Cold Spring Harbor Perspect Biol* 4:a011353–a011353.
- Sulzer D, Chen TK, Lau YY, Kristensen H, Rayport S, Ewing A (1995) Amphetamine redistributes dopamine from synaptic vesicles to the cytosol and promotes reverse transport. *J Neurosci* 15:4102–4108.
- Surmeier DJ (2007) Calcium, ageing, and neuronal vulnerability in Parkinson's disease. *Lancet Neurol* 6:6–6.
- Takahashi M, Tsukui H, Hatanaka H (1985) Neuronal differentiation of Ca^{2+} channel by nerve growth factor. *Brain Res* 341:381–384.

- Takeuchi T, Morikawa N, Matsumoto H, Shiraishi Y (1962) A pathological study of Minamata disease in Japan. *Acta Neuropathologica* 2:40–57.
- Tanaka O, Sakagami H, Kondo H (1995) Localization of mRNAs of voltage-dependent Ca²⁺-channels: four subtypes of alpha 1- and beta-subunits in developing and mature rat brain. *Brain Res Mol Brain Res* 30:1–16.
- Tank AW, Ham L, Curella P (1986) Induction of tyrosine hydroxylase by cyclic AMP and glucocorticoids in a rat pheochromocytoma cell line: effect of the inducing agents alone or in combination on the enzyme levels and rate of synthesis of tyrosine hydroxylase. *Mol Pharmacol* 30:486–496.
- Tanner CM, Ottman R, Goldman SM, Ellenberg J, Chan P, Mayeux R, Langston JW (1999) Parkinson disease in twins: an etiologic study. *JAMA* 281:341–346.
- Taylor LL, DiStefano V (1976) Effects of methylmercury on brain biogenic amines in the developing rat pup. *Toxicol Appl Pharmacol* 38:489–497.
- Taylor SC, Shaw SM, Peers C (2000) Mitochondrial Inhibitors Evoke Catecholamine Release from Pheochromocytoma Cells. *Biochem Biophys Res Comm* 273:17–21.
- Tewalt S, Bragg LJ, Finkleman R (2001) Mercury in U.S. coal—abundance, distribution, and modes of occurrence. *USGS Fact Sheet*: 1–4.
- Thomas B, Beal MF (2007) Parkinson's disease. *Hum Mol Gen* 16:R183–R194.
- Tiernan CT, Edwin EA, Goudreau JL, Atchison WD, Lookingland KJ (2013) The role of de novo catecholamine synthesis in mediating methylmercury induced vesicular dopamine release from rat pheochromocytoma (PC12) cells. *Toxicol Sci* 133:125–132.
- Torres GE, Gainetdinov RR, Caron MG (2003) Plasma membrane monoamine transporters: structure, regulation and function. *Nat Rev Neurosci* 4:13–25.
- Tsien RW, Tsien RY (1990) Calcium channels, stores, and oscillations. *Annu Rev Cell Biol* 6:715–760.
- Tsien RY (1981) A non-disruptive technique for loading calcium buffers and indicators into cells. *Nature* 290:527–528.
- Turner AJ, Illingworth JA, Tipton KF (1974) Simulation of biogenic amine metabolism in the brain. *Biochem J* 144:353–360.
- Turner MD, Marsh DO, Smith JC, Inglis JB, Clarkson TW, Rubio CE, Chiriboga J, Chiriboga CC (1980) Methylmercury in populations eating large quantities of marine fish. *Arch Environ Health* 35:367–378.
- Usdin TBT, Mezey EE, Chen CC, Brownstein MJM, Hoffman BJB (1991) Cloning of the

- cocaine-sensitive bovine dopamine transporter. *Proc Natl Acad Sci U S A* 88:11168–11171.
- Usonicz MM, Porzig H, Becker C, Reuter H (1990) Differential expression by nerve growth factor of two types of Ca^{2+} channels in rat pheochromocytoma cell lines. *J Physiol (Lond.)* 426:95–116.
- Valciukas JA, Levin SM, Nicholson WJ, Selikoff IJ (1986) Neurobehavioral assessment of Mohawk Indians for subclinical indications of methyl mercury neurotoxicity. *Arch Environ Health* 41:269–272.
- VanDuyn N, Settivari R, Wong G, Nass R (2010) SKN-1/Nrf2 inhibits dopamine neuron degeneration in a *Caenorhabditis elegans* model of methylmercury toxicity. *Toxicol Sci* 118:613–624.
- Varma T, Liu S-Q, West M, Thongboonkerd V, Ruvolo PP, May WS, Bhatnagar A (2003) Protein kinase C-dependent phosphorylation and mitochondrial translocation of aldose reductase. *FEBS Letters* 534:175–179.
- Verity MA, Brown WJ, Cheung M (1975) Organic mercurial encephalopathy: in vivo and in vitro effects of methyl mercury on synaptosomal respiration. *J Neurochem* 25:759–766.
- Vesce S (2005) Acute glutathione depletion restricts mitochondrial ATP export in cerebellar granule neurons. *J Biol Chem* 280:38720–38728.
- Vulliet PR, Woodgett JR, Cohen P (1984) Phosphorylation of tyrosine hydroxylase by calmodulin-dependent multiprotein kinase. *J Biol Chem* 259:13680–13683.
- Vulliet PRP, Woodgett JRJ, Ferrari SS, Hardie DGD (1985) Characterization of the sites phosphorylated on tyrosine hydroxylase by Ca^{2+} and phospholipid-dependent protein kinase, calmodulin-dependent multiprotein kinase and cyclic AMP-dependent protein kinase. *FEBS Lett* 182:335–339.
- Wagner JA (1985) Structure of catecholamine secretory vesicles from PC12 cells. *J Neurochem* 45:1244–1253.
- Weil MM, Bressler JJ, Parsons PP, Bolla KK, Glass TT, Schwartz BB (2005) Blood mercury levels and neurobehavioral function. *JAMA* 293:1875–1882.
- Weiner H, Wang X (1994) Aldehyde dehydrogenase and acetaldehyde metabolism. *Alcohol Alcohol Suppl* 2:141–145.
- Weiss B (2011) Lead, manganese, and methylmercury as risk factors for neurobehavioral impairment in advanced age. *Internatl J Alz Dis* 2011:1–11.
- Weiss B, Clarkson TW, Simon W (2002) Silent latency periods in methylmercury poisoning and in neurodegenerative disease. *Environ Health Perspect* 110 Suppl 5:851–854.

- Wermuth L, Bech S, Skaalum Petersen M, Joensen P, Weihe P, Grandjean P (2008) Prevalence and incidence of Parkinson's disease in the Faroe Islands. *Acta Neurol Scand* 118:126–131.
- Wermuth L, Joensen P, Bünger N, Jeune B (1997) High prevalence of Parkinson's disease in the Faroe Islands. *Neurology* 49:426–432.
- Wermuth L, Weitzel-Mudersbach von P, Jeune B (2000) A two-fold difference in the age-adjusted prevalences of Parkinson's disease between the island of Als and the Faroe Islands. *Eur J Neurol* 7:655–660.
- WHO (1990) Environmental Health Criteria 101 Methylmercury. Geneva: World Health Organization.
- Wlodarchak N, Guo F, Satyshur KA, Jiang L, Jeffrey PD, Sun T, Stanevich V, Mumby MC, Xing Y (2013) Structure of the Ca²⁺-dependent PP2A heterotrimer and insights into Cdc6 dephosphorylation. *Cell Res* 23:931–946.
- Xu J, Kao S-Y, Lee FJS, Song W, Jin L-W, Yankner BA (2002) Dopamine-dependent neurotoxicity of alpha-synuclein: a mechanism for selective neurodegeneration in Parkinson disease. *Nat Med* 8:600–606.
- Yadava N, Nicholls DG (2007) Spare respiratory capacity rather than oxidative stress regulates glutamate excitotoxicity after partial respiratory inhibition of mitochondrial complex I with rotenone. *J Neurosci* 27:7310–7317.
- Yamada EWE, Huzel NJN (1985) Ca²⁺-binding properties of a unique ATPase inhibitor protein isolated from mitochondria of bovine heart and rat skeletal muscle. *Cell Calcium* 6:469–479.
- Yamada H, Yamamoto A, Takahashi M, Michibata H, Kumon H, Moriyama Y (1996) The L-type Ca²⁺ channel is involved in microvesicle-mediated glutamate exocytosis from rat pinealocytes. *J Pineal Res* 21:165–174.
- Yamauchi T, Fujisawa H (1981) Tyrosine 3-monooxygenase is phosphorylated by Ca²⁺-, calmodulin-dependent protein kinase, followed by activation by activator protein. *Biochem Biophys Res Comm* 100:807–813.
- Yee S, Choi BH (1994) Methylmercury poisoning induces oxidative stress in the mouse brain. *Exp Mol Pathol* 60:188–196.
- Yee S, Choi BH (1996) Oxidative stress in neurotoxic effects of methylmercury poisoning. *NeuroToxicology* 17:17–26.
- Yoshino Y, Mozai T, Nakao K (1966) Biochemical changes in the brain in rats poisoned with an alkylmercury compound, with special reference to the inhibition of protein synthesis

- in brain cortex slices. *J Neurochem* 13:1223–1230.
- Youdim M, Heldman E, Pollard HB, Fleming P, McHugh E (1986) Contrasting monoamine oxidase activity and tyramine induced catecholamine release in PC12 and chromaffin cells. *Neuroscience* 19:1311–1318.
- Youdim MBH, Edmondson D, Tipton KF (2006) The therapeutic potential of monoamine oxidase inhibitors. *Nat Rev Neurosci* 7:295–309.
- Yuan W, Guo J, Li X, Zou Z, Chen G, Sun J, Wang T, Lu D (2009) Hydrogen peroxide induces the activation of the phospholipase C- 1 survival pathway in PC12 cells: protective role in apoptosis. *Acta Biochim Biophys Sinica* 41:625–630.
- Yuan Y, Atchison WD (2007) Methylmercury-induced increase of intracellular Ca^{2+} increases spontaneous synaptic current frequency in rat cerebellar slices. *Mol Pharmacol* 71:1109–1121.
- Zhang Y, Gao J, Chung KK, Huang H, Dawson VL, Dawson TM (2000) Parkin functions as an E2-dependent ubiquitin- protein ligase and promotes the degradation of the synaptic vesicle-associated protein, CDCrel-1. *Proc Natl Acad Sci U S A* 97:13354–13359.
- Zhdanov AV, Ward MW, Taylor CT, Souslova EA, Chudakov DM, Prehn JHM, Papkovsky DB (2010) Extracellular calcium depletion transiently elevates oxygen consumption in neurosecretory PC12 cells through activation of mitochondrial Na^+/Ca^{2+} exchange. *Biochim Biophys Acta* 1797:1627–1637.
- Zhu J, Hexum TD (1992) Characterization of cocaine-sensitive dopamine uptake in PC12 cells. *Neurochem Int* 21:521–526.
- Zimmer B, Schildknecht S, Kuegler PB, Tanavde V, Kadereit S, Leist M (2011) Sensitivity of dopaminergic neuron differentiation from stem cells to chronic low-dose methylmercury exposure. *Toxicol Sci* 121:357–367.